

İSTANBUL TECHNICAL UNIVERSITY ★ INSTITUTE OF SCIENCE AND TECHNOLOGY

***IN SITU* COPPER (I) FORMATION IN ATOM TRANSFER RADICAL
POLYMERIZATION**

Ph.D. Thesis by

Hümeyra MERT BALABAN, M.Sc.

Department: Polymer Science and Technology

Programme: Polymer Science and Technology

JUNE 2007

***IN SITU* COPPER (I) FORMATION IN ATOM TRANSFER RADICAL
POLYMERIZATION**

**Ph.D. Thesis by
Hümeyra MERT BALABAN, M.Sc.**

(515032005)

Date of submission : 26 March 2007

Date of defence examination: 14 June 2007

Supervisor (Chairman): Prof. Dr. Gürkan HIZAL

Members of the Examining Committee: Prof. Dr. Yusuf YAĞCI (I.T.U.)

Prof. Dr. Duygu AVCI (B.U.)

Prof. Dr. Niyazi BIÇAK (I.T.U.)

Asi. Prof. A. Ersin ACAR (B.U.)

JUNE 2007

İSTANBUL TEKNİK ÜNİVERSİTESİ ★ FEN BİLİMLERİ ENSTİTÜSÜ

**ATOM TRANSFER RADİKAL POLİMERİZASYON'DA *İN SİTU*
BAKIR (I) OLUŞUMU**

DOKTORA TEZİ

Y. Kim. Hümeysra MERT BALABAN

(515032005)

Tezin Enstitüye Verildiği Tarih : 26 Mart 2007

Tezin Savunulduğu Tarih : 14 Haziran 2007

Tez Danışmanı : Prof. Dr. Gürkan HIZAL

Diğer Jüri Üyeleri : Prof. Dr. Yusuf YAĞCI (İTÜ)

Prof. Dr. Duygu AVCI (BÜ)

Prof. Dr. Niyazi BIÇAK (İTÜ)

Yrd. Doç. Dr. A. Ersin ACAR (BÜ)

HAZİRAN 2007

ACKNOWLEDGEMENTS

It is a great pleasure to express my most sincere thanks to my supervisor Prof. Dr. Gürkan HIZAL for his supervision during my graduate career. I am very thankful for his invaluable comments and guidance throughout the preparation of this thesis. His suggestions will be treasured in my life.

My sincere appreciation goes to Prof. Dr. Ümit Tunca for helpful discussions and comments throughout this study. I would also like to thank Prof. Dr. Yusuf YAĞCI who is the coordinator of research group of my doctoral fellowship supported by TÜBİTAK and a member of graduate committee for suggestions about science and life.

I would like to thank TÜBİTAK – BDP Programme for financial support through a doctoral fellowship.

I would like to extend my sincere gratitude to Prof. Dr. Krzysztof Matyjaszewski for sharing his deep knowledge with me and giving me a nice project during my stay in Pittsburgh, USA. I would like to thank Dr. Nicolay V. Tsarevsky and Dr. Joanna Pietrasik for their support and friendship that made my Carnegie Mellon days enjoyable.

I am thankful to Prof. Dr. Filip E. Du PREZ from Ghent University, Belgium for MALDI-TOF measurements and comments.

I would especially like to thank my friend Dr. Tuba ERDOĞAN BEDRİ for her invaluable friendship and support that made coming to lab interesting everyday. I also would like to thank our group members and friends, especially Sermin ARAS and Aydan DAĞ; working with you was a pleasure for me.

I would like to express my sincere thanks to my husband Mehmet BALABAN for his love and making my life outside the lab enjoyable and unforgettable. I would like to dedicate this thesis to him for his endless support, patience, and understanding throughout the preparation of this thesis.

I would like to thank my dear parents Battal-Necla MERT, my brother Recep MERT and my sister Ayşe GÜLLÜ for their unconditional love. I also dedicate this thesis to my family to thank them for their support and advice that have helped me get through all obstacles in my life.

June 2007

Hümeysra MERT BALABAN

TABLE of CONTENTS

LIST of ABBREVIATIONS	vii
LIST of TABLES	ix
LIST of FIGURES	x
LIST of SYMBOLS	xv
SUMMARY	xvi
ÖZET	xx
1. INTRODUCTION	1
2. THEORETICAL PART	4
2.1. Conventional Free Radical Polymerization (FRP) versus Controlled/"Living" Radical Polymerization (LRP)	4
2.1.1. Persistent radical effect (PRE)	5
2.1.2. Reversible activation-deactivation process in LRP	5
2.1.3. Prerequisites of LRP	6
2.1.4. Characteristics of LRP	7
2.1.5. Various types of LRP methods	9
2.2. Atom Transfer Radical Addition (ATRA)	10
2.3. Atom Transfer Radical Polymerization (ATRP)	12
2.3.1. Basic components of ATRP	12
2.3.1.1. Monomers	13
2.3.1.2. Initiator	14
2.3.1.3. Transition metals and ligands	16
2.3.1.4. Deactivator	19
2.3.1.5. Solvents	20
2.3.1.6. Temperature and reaction time	20
2.3.2. Kinetics and mechanism of ATRP	21
2.3.2.1. Molecular weight distribution ($MWD = M_w/M_n$)	22
2.3.2.2. Molecular weight	23
2.3.3. Procedures for initiation of an ATRP reaction	24
2.3.3.1. Normal initiation	24
2.3.3.2. Reverse ATRP	25
2.3.3.3. Simultaneous reverse & normal initiation ATRP (SR&NI)	26
2.3.3.4. ATRP via <i>in situ</i> copper (I) formation or activator generated via electron transfer ATRP (AGET)	27

2.3.3.5. Macroinitiator technique and halogen exchange	32
2.3.4. Controlled composition, and topology via ATRP	34
2.3.4.1. Homopolymers	34
2.3.4.2. Block copolymers	35
2.3.4.3. Star polymers	36
2.4. Oxidative Polymerization of Phenols	37
2.4.1. Mechanism	39
2.4.2. Metal catalyst systems for oxidative coupling polymerization	40
2.5. Sulfur Chemistry	41
2.5.1. Oxidation of thiols	42
2.5.2. Sulfur containing polymers	43
2.5.3. Application of thiol-disulfide interchange in ATRP	44
2.6. Catalyst Residue in Products Prepared via ATRP	47
2.6.1. Postpolymerization methods	47
2.6.2. Solid supported ATRP	48
2.6.2.1. Solid phase ATRP	48
2.6.2.2. Solid supported catalyst via physical adsorption	50
2.6.2.3. Solid supported catalyst via covalent bonding	51
2.6.3. Recoverable homogeneous catalyst	56
2.6.3.1. Liquid liquid biphasic systems	56
2.6.3.2. Use of precipitons	58
2.6.3.3. Soluble linear or hyperbranched polymer supported catalyst	59
2.6.3.4. Hybrid catalyst systems	61
3. EXPERIMENTAL WORK	63
3.1. Materials and Chemicals	63
3.1.1. Monomers	63
3.1.2. Solvents	63
3.1.3. Other chemicals	64
3.2. Equipment	65
3.2.1. Gel permeation chromatography (GPC)	65
3.2.2. Gas chromatography (GC)	66
3.2.3. UV-Visible (UV-VIS) spectrophotometer	66
3.2.4. Nuclear magnetic resonance spectroscopy (NMR)	66
3.2.5. Matrixassisted laser desorption/ionization time-of-flight (MALDI-TOF) Mass Spectrometer	66
3.2.6. Atomic absorption spectrometer	66
3.3. Synthetic Procedures	67

3.3.1. UV–VIS monitoring of <i>in situ</i> copper (I) formation via electron transfer from fructose	67
3.3.2. General procedure for the kinetic studies of ATRP of St (or <i>n</i> BA) catalyzed by Cu(II)/PMDETA/reducing agent (RA)	67
3.3.3. General procedure for the kinetic studies of ATRP of St catalyzed by Cu(II)/PMDETA/PhSNa in the presence of definite amount of air	68
3.3.4. UV–VIS monitoring of <i>in situ</i> Cu (I) formation via electron transfer from PhSNa	68
3.3.5. General procedure for the kinetic studies of ATRP of MMA catalyzed by Cu(II)/PMDETA/PhSNa (or <i>p</i> -methoxythiophenol) in the presence of definite amount of air	68
3.3.6. Block copolymerization and chain extension polymerizations	69
3.3.6.1. Preparation of linear homo- and block co-polymers via ATRP	69
3.3.6.2. Preparation of star homo- and block co-polymers via ATRP	73
3.3.6.3. Preparation of linear homo- and block co-polymers via ATRP in the presence of limited amount of air	74
3.3.6.4. Preparation of linear homo- and block co-polymers via ATRP using PhONa as reducing agent	76
3.3.7. General procedure for the kinetic studies of ATRP of St catalyzed by silica gel supported CuCl ₂ /PMDETA	77
3.3.8. General procedure for the catalyst reuse	78
3.3.9. UV–VIS monitoring of <i>in situ</i> copper (I) formation via electron transfer from sodium phenoxide	78
4. RESULTS and DISCUSSION	79
4.1. Fructose as a Reducing Agent for <i>in situ</i> Generation of Copper(I) Species via Electron Transfer Reaction in ATRP of Styrene (St)	79
4.1.1. UV-VIS monitoring of copper (II) complex consumption and copper (I) complex formation	80
4.1.2. Effect of fructose concentration on ATRP of St	81
4.1.3. ATRP of St applying different initiator/catalyst systems	82
4.1.4. ATRP of <i>n</i> -butyl acrylate	84
4.2. Ascorbic acid as a RA for <i>in situ</i> Generation of Cu (I) Species in ATRP of St	86
4.2.1. The effect of PMDETA concentration on ATRP of St	87
4.3. Fructose Versus Ascorbic Acid as a RA in ATRP of St	89
4.4. Phenol Derivatives as RA for <i>in situ</i> Generation of Copper (I) Species in ATRP of St	92

4.5. Thiophenol Derivatives as a RA for <i>in situ</i> Generation of Cu(I) Species via Electron Transfer Reaction in ATRP of St in the Presence of Limited Amount of Air	96
4.5.1. Effect of PhSNa on ATRP of St	96
4.5.2. <i>p</i> -methoxythiophenol versus sodium thiophenolate as a RA	98
4.5.3. Comparison of different initiator/catalyst systems	100
4.5.4. Dependence of propagation rate on temperature	102
4.5.5. UV-VIS monitoring of Cu(II) complex consumption	103
4.5.6. ATRP of methyl methacrylate (MMA)	106
4.6. Chain Extension and Block (Co)Polymerization	107
4.6.1. Characterization of linear PS macroinitiator synthesized via ATRP under inert atmosphere using fructose as a RA	108
4.6.2. Preparation of linear PS- <i>b</i> -PMMA copolymer	110
4.6.3. Characterization of linear PS-Br macroinitiator and PS- <i>b</i> -PMMA copolymer synthesized via ATRP using <i>p</i> -methoxyphenol as a RA	116
4.6.4. Star block copolymer synthesis under inert atmosphere	118
4.6.4.1. Synthesis of octafunctional initiator 5,11,17,23,29,35,41,47-octa- <i>tert</i> -butyl-49,50,51,52,53,54,55,56-octakis(2-bromopropionyloxy)calix[8]arene (1)	118
4.6.4.2. Preparation of octa-arm PS stars	120
4.6.4.3. Preparation of octa-arm PS- <i>b</i> -PMMA stars	122
4.6.5. Characterization of PS macroinitiator and PS- <i>b</i> -PMMA copolymers synthesized via ATRP in the presence of definite amount of air	124
4.6.5.1. Chain extension polymerization	124
4.6.5.2. Block copolymerization : normal ATRP versus ATRP via <i>in situ</i> copper (I) formation	125
4.7. Air- Stable and Recoverable Catalyst for ATRP of St	133
4.7.1. UV-VIS monitoring of Cu(II) complex consumption	137
4.7.2. Synthesis of PS macroinitiator and chain extension polymerization	138
4.7.3. Catalyst reuse	140
5. CONCLUSIONS	143
REFERENCES	145
AUTOBIOGRAPHY	174

LIST of ABBREVIATIONS

FRP	: Free Radical Polymerization
ATRP	: Atom Transfer Radical Polymerization
NMP	: Nitroxide Mediated Radical Polymerization
LRP	: Controlled/“Living” Radical Polymerization
RAFT	: Reversible Addition-Fragmentation Chain Transfer Polymerization
ATRA	: Atom Transfer Radical Addition
St	: Styrene
MMA	: Methyl Methacrylate
MA	: Methyl Acrylate
PS	: Polystyrene
PMMA	: Poly(methyl methacrylate)
PBA	: Poly(butyl acrylate)
Bipy	: 2,2'-Bipyridine
PMDETA	: <i>N,N,N',N'',N'''</i> -Pentamethyldiethylenetriamine
TMEDA	: <i>N,N,N',N'</i> -Tetramethylethylenediamine
HMTETA	: <i>N,N,N',N'',N''',N'''</i> -Hexamethyltriethylenetetraamine
Me₆-TREN	: Tris[2-(dimethylamino)ethyl]amine
dNbpy	: 4,4'-di(5-nonyl)-2,2'- bipyridine
phen	: 1,10-phenanthroline
NPrPMI	: <i>N</i> -propyl-(2-pyridyl)methanimine
tpy	: 2,2':6',2''-terpyridine
tNtpy	: 4,4',4''-tris(5-nonyl)- 2,2':6',2''-terpyridine
BPMOA	: <i>N,N</i> -bis(2-pyridylmethyl)octylamine
TPMA	: tris[(2-pyridyl)methyl]amine
Me₄CYCLAM	: 1,4,8,11-tetraaza-1,4,8,11-tetramethylcyclotetradecane
AIBN	: 2, 2'-azobisisobutyronitrile
SR&NI	: Simultaneous reverse & normal initiation
AGET	: Activator generated via electron transfer
DPPH	: Diphenylpicrylhydrazyl
DMP	: 2,6-dimethylphenol
PPO	: Poly(phenyleneoxide)
1-PECI	: 1-chloro-1-phenylethane
EiBr	: Ethyl-2-bromoisobutyrate
ARGET	: Activators regenerated by electron transfer
TPEN	: <i>N,N,N',N'</i> - tetra[(2-pyridyl)methyl]ethylenediamine
TBA	: Tributylamine
TEA	: Triethylamine
HEA	: 2-hydroxy ethylacrylate
HEMA	: 2-hydroxyethyl methacrylate
MWD	: Molecular weight distribution
ROMP	: Ring-Opening Metathesis Polymerization
DPQ	: 3,3',5,5'-tetramethyl-4,4'-diphenone
BDE	: Bond Dissociation Energy

Fe(Oct)₃	: Iron (III) Octanoate
Fe(CN)₆³⁻	: Iron (III) Hexacyanate
UV	: Ultra Violet
FeCl₃	: Iron (III) Chloride
PBu₃	: Tributyl Phosphine
MeOH	: Methanol
HCSNMe₂	: N,N-dimethylthioformamide
DTT	: Dithiothreitol
DMF	: Dimethyl Formamide
Me₂CO₃	: Alkali Metal Carbonate
PNIPAM	: Poly(<i>N</i> -isopropylacrylamide)
NIPAAM	: <i>N</i> -isopropylacrylamide
PMPC	: Poly (2-methacryloyloxyethyl phosphorylcholine)
NaOH	: Sodium Hydroxide
Na₂S	: Sodium Sulfide
Boc	: <i>tert</i> -butyloxycarbonyl
THF	: Tetrahydrofuran
DMAEMA	: 2-(dimethylamino)ethyl methacrylate
PDMAEMA	: Poly(2-(dimethylamino)ethyl methacrylate)
TEDETA	: Tetraethyldiethylenetriamine
DiPA	: Di(2-picolyl)amine
PEG	: Poly(ethylene glycol)
ICP	: Inductively Coupled Plasma
PE	: Polyethylene
HPEI	: Hyperbranched Polyethylenimine
CaH₂	: Calcium Hydride
<i>n</i>-BA	: <i>n</i> -Butyl Acrylate
EC	: Ethylene Carbonate
MBP	: Methyl-2-bromopropionate
GPC	: Gel Permeation Chromatography
GC	: Gas Chromatography
UV-VIS	: Ultraviolet-Visible
¹H-NMR	: Proton Nuclear Magnetic Resonance Spectroscopy
MALDI-TOF	: Matrixassisted Laser Desorption / Ionization Time – Of - Flight
PTFE	: Poly(tetrafluoroethylene)
SG	: Silica Gel
AgTFA	: Silver Trifluoroacetate
DP_n	: Degree of Polymerization
PRE	: Persistent Radical Effect
Sn(EH)₂	: Stannous (II) Ethylhexanoate
AIBN	: 2,2'-azobisisobutyronitrile
<i>M</i>_{n,theo}	: Theoretical molecular weight

LIST of TABLES

	<u>Page No</u>
Table 4.1 Characteristics of linear homo- and block co-polymers prepared via ATRP using fructose as a RA	111
Table 4.2 Characteristics of linear homo- and block co-polymers prepared via ATRP using ascorbic acid as a RA.....	115
Table 4.3 Characteristics of linear homo- and block co-polymers prepared via ATRP using <i>p</i> -methoxyphenol as a RA.....	117
Table 4.4 Characteristics of linear homo- and block co-polymers prepared via ATRP using <i>p</i> -methoxy thiophenol as a RA.....	129
Table 4.5 Characteristics of Linear Homo and Block (Co)polymers prepared via ATRP using PhSNa as a RA.....	132

LIST of FIGURES

	<u>Page No</u>
Figure 2.1 : Effect of slow initiation, transfer, termination and exchange on kinetics	8
Figure 2.2 : Effect of slow initiation, transfer, termination and exchange on molecular weights.....	9
Figure 2.3 : Solid-phase ATRP. (A) Introducing initiator moieties; (B) 1, solid phase ATRP and 2, separation and purification; (C) cleaving the linkers and polymer harvesting.....	49
Figure 4.1 : Time dependence of UV–VIS spectra of $\text{CuCl}_2/\text{PMDETA}/\text{fructose}$ mixture in water; $[\text{CuCl}_2]_0 = 2.18 \times 10^{-4} \text{ M}$; $[\text{CuCl}_2]_0/[\text{PMDETA}]_0/[\text{fructose}]_0 = 1/10/0.5$. room temperature; (a) $t = 0 \text{ min}$; (b) $t = 5 \text{ min}$. at 85°C ; (c) $t = 15 \text{ min}$. at 85°C ; (d) $t = 30 \text{ min}$. at 85°C ; (e) $t = 80 \text{ min}$. at 85°C ; (f) $t = 140 \text{ min}$ at 85°C	80
Figure 4.2 : The first-order kinetic plot ATRP of St in bulk at 110°C using fructose as a RA. $[\text{St}]_0 = 7.73 \text{ M}$; $[\text{St}]_0 : [1\text{-PECl}]_0 : [\text{CuCl}_2]_0 : [\text{PMDETA}]_0 : [\text{Fructose}]_0 = 100 : 1 : 0.5 : 1 : 0.125$ (or 0.250).....	81
Figure 4.3 : The dependence of M_n , and M_w/M_n , upon monomer conversion for ATRP of St in bulk at 110°C (Experimental conditions such as in Fig. 4.2).....	82
Figure 4.4 : The first-order kinetic plot for ATRP of St in toluene (50/50, v/v) at 110°C using fructose as a RA. Initiator: EiBr (\blacktriangle) or MBP (\blacksquare); $[\text{St}]_0 = 3.96 \text{ M}$; $[\text{St}]_0 : [\text{Initiator}]_0 : [\text{CuCl}_2]_0 : [\text{PMDETA}]_0 : [\text{Fructose}]_0 = 30 : 1 : 0.5 : 1 : 0.05$	83
Figure 4.5 : The dependence of M_n , and M_w/M_n , upon monomer conversion for ATRP of St in solution at 110°C (Experimental conditions such as in Fig. 4.4).....	84
Figure 4.6 : The first-order kinetic plot for ATRP of nBA in EC (10/1, v/v) at 70°C using fructose as a RA. Copper salt: CuBr_2 (\blacktriangle) or CuCl_2 (\star); $[\text{BA}]_0 = 5.73 \text{ M}$; $[\text{n-BA}]_0 : [\text{Initiator}]_0 : [\text{CuBr}_2]_0 : [\text{PMDETA}]_0 : [\text{Fructose}]_0 = 100 : 1 : 0.25 : 0.5 : 0.5$	85
Figure 4.7 : The dependence of M_n , and M_w/M_n , upon monomer conversion for ATRP of nBA at 70°C in EC (Experimental conditions as in Fig. 4.6).....	85
Figure 4.8 : The first-order kinetic plot ATRP of St in bulk at 110°C using ascorbic acid as a RA. $[\text{St}]_0 = 7.73 \text{ M}$; $[\text{St}]_0 : [1\text{-PECl}]_0 : [\text{CuCl}_2]_0 : [\text{PMDETA}]_0 : [\text{Ascorbic acid}]_0 = 100 : 1 : 0.5 : 1 : 0.125$ (or 0.250).....	86

Figure 4.9	: The dependence of M_n , and M_w/M_n , upon monomer conversion for ATRP of St at 110 °C in bulk (Experimental conditions as in Fig. 4.8).....	87
Figure 4.10	: The first-order kinetic plot ATRP of St in bulk at 110 °C using ascorbic acid as a RA. $[St]_0 : [1-PECl]_0 : [CuCl_2]_0 : [PMDETA]_0 : [Ascorbic\ acid]_0 = 100 : 1 : 0.5 : X : 0.125$. (▲): $[St]_0 = 7.73\text{ M}$; (■): $[St]_0 = 7.26\text{ M}$	88
Figure 4.11	: The dependence of M_n , and M_w/M_n , upon monomer conversion for ATRP of St at 110 °C in bulk (Experimental conditions as in Fig. 4.10).....	89
Figure 4.12	: The first-order kinetic plot ATRP of St in bulk at 110 °C using ascorbic acid as a RA. $[St]_0 = 7.73\text{ M}$; $[St]_0 : [1-PECl]_0 : [CuCl_2]_0 : [PMDETA]_0 : [Fructose\ or\ Ascorbic\ acid]_0 = 100 : 1 : 0.5 : 1 : 0.25$	91
Figure 4.13	: The dependence of M_n , and M_w/M_n , upon monomer conversion for ATRP of St at 110 °C in bulk (Experimental conditions as in Fig. 4.12).....	91
Figure 4.14	: Time dependence of $\ln([M]_0/[M])$ for the bulk polymerization of St at 110 °C using <i>p</i> -methoxyphenol as a RA. $[St]_0 : [1-PECl]_0 : [CuCl_2]_0 : [PMDETA] : [p\text{-methoxyphenol}] = 100 : 1 : 0,5 : X : 3$. (■): $[St]_0 = 7.26\text{ M}$; (★): $[St]_0 = 7.13\text{ M}$	92
Figure 4.15	: The dependence of M_n , and M_w/M_n , upon monomer conversion for ATRP of St at 110 °C in bulk (Experimental conditions as in Fig. 4.14).....	93
Figure 4.16	: Time dependence of $\ln([M]_0/[M])$ for the bulk polymerization of St at 110°C; $[St]_0 = 6\text{ mol. L}^{-1}$ $[St]_0 : [1-PECl]_0 : [PMDETA]_0 : [CuCl_2]_0 : [p\text{-tert-butylphenol}]_0 = 100 : 1 : 5 : 0,5 : 0,25$	94
Figure 4.17	: Dependence of M_n and M_w/M_n versus percent conversion for the bulk polymerization of St at 110°C (Experimental conditions as in Fig. 4.16).....	94
Figure 4.18	: Time dependence of $\ln([M]_0/[M])$ for the bulk polymerization of St at 110°C; $[M]_0 = 6\text{ mol. L}^{-1}$ $[St]_0 : [1-PECl]_0 : [PMDETA]_0 : [CuCl_2]_0 : [Dihydroquinone]_0 = 100 : 1 : 5 : 0,5 : 0,75$	95
Figure 4.19	: Dependence of M_n and M_w/M_n versus percent conversion for the bulk polymerization of St at 110°C. (Experimental conditions as in Fig. 4.18).....	95
Figure 4.20	: Time dependence of $\ln([M]_0/[M])$ for the polymerization of St at 110 °C in the presence of various amounts of PhSNa. $[St]_0 = 7.26\text{ mol.L}^{-1}$ $[St]_0 : [1-PECl]_0 : [CuCl_2]_0 : [PMDETA]_0 : [PhSNa]_0 = 100 : 1 : 0.5 : 5 : X$. (X = ■ : 0.25; ● : 0.5; ★ : 0.75; ▲ : 1; □ : 3).....	97
Figure 4.21	: Dependence of M_n and M_w/M_n vs. percent conversion for the bulk polymerization of St at 110°C. $M_{n,theo}$ (—). (Experimental conditions as in Figure 4.20).....	98

Figure 4.22	: Time dependence of $\ln([M]_0/[M])$ for the polymerization of St at 110°C. $[St]_0$: $[1-PECl]_0$: $[CuCl_2]_0$: $[PMDETA]_0$: $[PhSNa \text{ or } p\text{-methoxythiophenol}]_0 = 100 : 1 : 0.5 : 5 : 1.5$; $[St]_0 = 7.26 \text{ mol.L}^{-1}$	99
Figure 4.23	: Dependence of M_n and M_w/M_n vs. conversion % for the bulk polymerization of St at 110°C. $M_{n,theo}(—)$. (Experimental conditions as in Figure 4.22).....	100
Figure 4.24	: Time dependence of $\ln([M]_0/[M])$ for the ATRP of St at 110°C. $[St]_0$: $[Initiator]_0$: $[CuX_2]_0$: $[PMDETA]_0$: $[PhSNa]_0 = 100 : 1 : 0.5 : 5 : 0.75$. $[St]_0 = 7.26 \text{ mol.L}^{-1}$	101
Figure 4.25	: Dependence of M_n and M_w/M_n versus percent conversion for the bulk polymerization of St at 110°C. $M_{n,theo}(—)$ (Experimental conditions as in Figure 4.24).....	101
Figure 4.26	: Time dependence of $\ln([M]_0/[M])$ for the ATRP of St at different temperatures. $[St]_0 = 7.26 \text{ mol.L}^{-1}$ $[St]_0$: $[1-PECl]_0$: $[CuCl_2]_0$: $[PMDETA]_0$: $[PhSNa]_0 = 100 : 1 : 0.5 : 5 : 0.75$	102
Figure 4.27	: Arrhenius plot for the ATRP of St. $[St]_0 = 7.26 \text{ mol.L}^{-1}$; $[St]_0$: $[1-PECl]_0$: $[CuCl_2]_0$: $[PMDETA]_0$: $[PhSNa] = 100 : 1 : 0.5 : 5 : 0.75$	103
Figure 4.28	: UV–VIS spectra of $CuCl_2/PMDETA/PhSNa$ system in DMF; $[CuCl_2] = 2.18 \times 10^{-4} \text{ M}$; $[CuCl_2]$: $[PMDETA]$: $[PhSNa] = 1 : 10 : 1.5$	104
Figure 4.29	: The first-order kinetic plots for ATRP of MMA in toluene (1/1, v/v) at 90 °C. $[MMA]_0$: $[EtBr]_0$: $[CuCl_2]_0$: $[PMDETA]_0$: $[PhSNa \text{ or } p\text{-methoxythiophenol}]_0 = 100 : 1 : 0.5 : 5 : 0.75$; $[MMA]_0 = 4.58 \text{ mol.L}^{-1}$	106
Figure 4.30	: Dependence of M_n and M_w/M_n vs. conversion % for the bulk polymerization of MMA at 110°C (Experimental conditions as in Figure 4.29).....	107
Figure 4.31	: MALDI-TOF mass spectrum of linear PS-Br macroinitiator; $[St]_0 = 3.96 \text{ M}$; $[St]_0/[EtBr]_0/[CuBr_2]_0/[PMDETA]_0/[Fructose]_0 = 50/1/0.5/1/0.05$; at 110 °C. In the inset, a detail of the MALDI-TOF mass spectrum is given. Matrix, dithranol; cationating agent, AgTFA.....	109
Figure 4.32	: Comparison of experimental and theoretical isotope distribution of ions formed in the MALDI process.....	110
Figure 4.33	: GPC traces of (a) linear PS-Br macroinitiator (H2) and (b) linear PS- <i>b</i> -PMMA (H3).....	112
Figure 4.34	: GPC traces of (a) linear PS-Br macroinitiator (H2) and (b) linear PS- <i>b</i> -PMMA (H4).....	113
Figure 4.35	: GPC traces of (a) linear PS-Br macroinitiator (H2) and (b) linear PS- <i>b</i> -PMMA (H5).....	113
Figure 4.36	: GPC traces of (a) linear PS-Br macroinitiator (H6) and (b) linear PS- <i>b</i> -PMMA (H7).....	114
Figure 4.37	: GPC traces of (a) linear PS-Br macroinitiator (H6), and (b) PS- <i>b</i> -PMMA (H8).....	116
Figure 4.38	: GPC traces of (a) linear PS-Br macroinitiator (H9), and (b) PS- <i>b</i> -PMMA (H10).....	117

Figure 4.39	: GPC traces of (a) linear PS-Br macroinitiator (H9), and (b) PS- <i>b</i> -PMMA (H11).....	118
Figure 4.40	: Synthesis of 5,11,17,23,29,35,41,47-Octa- <i>tert</i> -butyl-49,50,51,52,53,54,55,56-Octakis-(2-bromopropionyloxy)calix[8]arene, (1).....	119
Figure 4.41	: The ¹ H-NMR spectrum of the initiator, (1), 5,11,17,23,29,35,41,47-Octa- <i>tert</i> -butyl-49,50,51,52,53,54,55,56-Octakis-(2-bromopropionyloxy)calix[8]arene in CDCl ₃	120
Figure 4.42	: The ¹ H-NMR spectrum of Octa-arm PS Macroinitiator (H12) in CDCl ₃ , 110 °C.....	121
Figure 4.43	: GPC traces of octa-arm star PS-Br (M_n , NMR = 23850) obtained using [M]/[1] of 3000 (a) before (H12) and (b) after (H13) hydrolysis of the ester function.....	122
Figure 4.44	: GPC traces of octa-arm PS-Br star macroinitiator (H12) (a), and octa-arm star PS- <i>b</i> -PMMA (H14) (b).....	123
Figure 4.45	: The ¹ H-NMR spectrum of Octa-arm PS- <i>b</i> -PMMA (H14) in CDCl ₃	124
Figure 4.46	: GPC traces of PS macroinitiator (H15), (a), and the chain-extended polymer (H16).....	125
Figure 4.47	: The ¹ H-NMR spectrum of PS-Br (H17) macroinitiator in CDCl ₃	127
Figure 4.48	: MALDI-TOF spectra of PS-Br (H17) (M_n = 2800, M_w/M_n = 1.17).....	128
Figure 4.49	: GPC traces of PS macroinitiator (H17) (M_n = 2800, M_w/M_n = 1.17 at 18 % conversion), (a), and the related PS- <i>b</i> -PMMA copolymers (H19-22).....	130
Figure 4.50	: GPC traces of PS macroinitiator (H17) (M_n = 2800, M_w/M_n = 1.17 at 18 % conversion), (a), and the related PS- <i>b</i> -PMMA copolymer (H18).....	131
Figure 4.51	: GPC traces of PS macroinitiator (H23) (M_n = 2100, M_w/M_n = 1.12 at 40 % conversion), (a), and the PS- <i>b</i> -PMMA block copolymers (H24-27).....	133
Figure 4.52	: First-order kinetic plot for the polymerization of St catalyzed by SG- CuCl ₂ /PMDETA at 110 °C; [St] ₀ = 6.8 M; [St] ₀ /[1-PECL] ₀ /[CuCl ₂]/[PMDETA]/[PhONa] = 100/1/0.5/10/0.75; silica gel / CuCl ₂ = 10 (w/w).....	134
Figure 4.53	: The dependences of molecular weights and polydispersities on monomer conversion in the polymerization of St catalyzed by SG-CuCl ₂ /PMDETA at 110 °C $M_{n,theo}$ (—). (Experimental conditions as in Fig. 4.52).....	135
Figure 4.54	: UV-VIS spectra of (1) [CuCl ₂] = 1.09 x 10 ⁻³ M, [CuCl ₂]:[PMDETA]:[PhONa] = 1: 10: 3 in acetonitrile, at room temperature, t= 0; (2) t= 30 min at 80 °C; (3) t= 50 min at 80 °C; (4) t= 80 min at 80 °C.....	138
Figure 4.55	: GPC traces of PS macroinitiator (H28) (M_n = 2000, M_w/M_n = 1.27 at 20 % conversion), (a), and the chain-extended polymer (M_n = 15000, M_w/M_n = 1.18 at 22 % conversion) (H29), (b). See text for experimental conditions.....	140

Figure 4.56	: First-order kinetic plot for the polymerization of St catalyzed by recycled SG-CuCl ₂ /PMDETA at 110 °C; [St] ₀ = 6.8 M; silica gel/CuCl ₂ = 10 (w/w). [St] ₀ /[1-PECl] ₀ /[CuCl ₂]/[PMDETA]/[PhONa] = 100 / 1/ 0.5 / 2.5 / 0.75.....	142
Figure 4.57	: The dependences of M_n and M_w/M_n on monomer conversion in the polymerization of St catalyzed by recycled SG-CuCl ₂ /PMDETA at 110 °C $M_{n,theo}$ (—). (Experimental conditions as in Fig. 4.56).....	142

LIST of SYMBOLS

k_{act}	: Pseudo-first-order activation rate constant
k_{deact}	: Pseudo-first-order deactivation rate constant
k_t	: Rate constant of termination
k_p	: Rate constant of propagation
k_p^{app}	: Apparent rate constant of propagation
k_i	: Rate constant of initiation
k_{ox}	: Rate constant of oxidation
M	: Monomer
X\cdot	: Persistent Radical
P\cdot	: Propagating radical
R_p	: Rate of polymerization
T	: Time
Mtⁿ	: Transition metal in the oxidation state n
L	: Ligand
X	: (Pseudo)halogen
R-X	: Alkyl halide
Cs	: Chain transfer constant
P_n\cdot	: Propagating species
k_{ai}	: Rate constant of association
k_{di}	: Rate constant of dissociation
M_n	: The number average molecular weight
M_w	: The weight average molecular weight
M_w/M_n	: The molecular weight distribution
f	: Function
f	: Initiation efficiency
I-I	: Free radical initiator
PhOH	: Phenol
PhSNa	: Sodium thiophenolate
ArOH	: Phenol derivative
RSH	: Thiol
RSSR	: Disulfide
PhSH	: Thiophenol
Conv	: Conversion
RT	: Room temperature
PhONa	: Sodium phenoxide
λ	: Wavelength
$M_{\text{n,theo}}$: Theoretical molecular weight
E_a^{app}	: Apparent activation energy
Cys-SH	: Cysteine
In	: Initiator
RA	: Reducing agent
I₀	: Initial molar concentration of the initiator

IN SITU COPPER (I) FORMATION IN ATOM TRANSFER RADICAL POLYMERIZATION

SUMMARY

There has been a conspicuous growth in the development of controlled / “living” radical polymerization (LRP) techniques in the last decade. Several LRP processes have been extensively developed in the past decades, including nitroxide-mediated polymerization (NMP), reversible addition-fragmentation chain transfer polymerization (RAFT), and atom transfer radical polymerization (ATRP). Among these LRP techniques, ATRP is perhaps the most promising method because of catalytic nature and its synthetic versatility. In ATRP, a transition metal complex plays a crucial role in the establishment of a dynamic reversible activation/deactivation equilibrium. A number of transition metal complexes, including complexes based on early, middle, and late transition metals, have been investigated and developed as efficient ATRP catalysts. Among them copper catalyzed ATRP in conjunction with alkyl halide initiator and amine ligand, received more interest.

Major disadvantages of ATRP are high cost and easy oxidation of metal salt in lower oxidation state. These can be overcome by *in situ* Cu (I) generation via an electron transfer from a reducing agent (RA) to a more stable higher oxidation state metal salt (Figure 1).

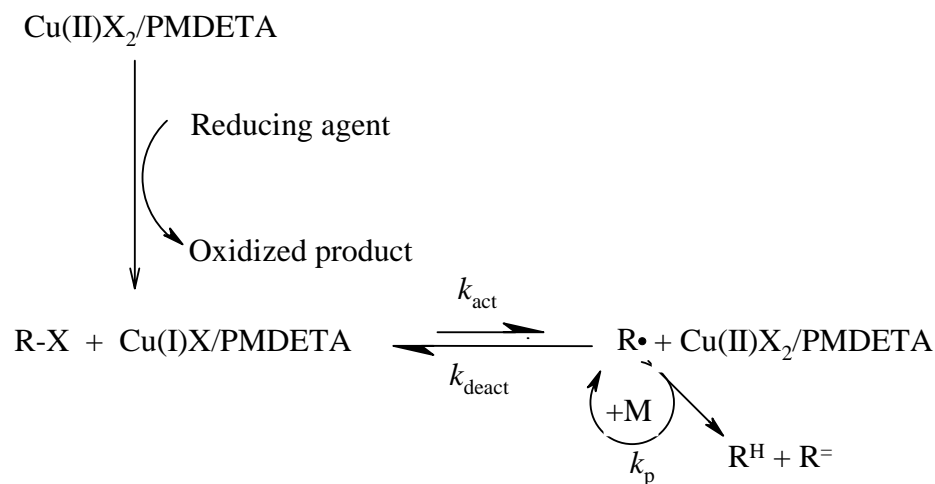


Figure 1: ATRP via *In Situ* Copper (I) Formation.

This approach is different than the normal ATRP in two respects:

(i) In this system, reactive Cu (I) species are formed *in situ* via redox process between Cu(II) and reducing agents (RA). Therefore, the small concentration of Cu (I) promotes the low concentration of transient radicals, in addition, the initial presence of Cu (II) (persistent radical) facilitates the deactivation process and thus suppresses undesirable radical-radical coupling reaction.

(ii) The unavoidable oxidation of catalyst or the oxygen induced polymerization by the diffused oxygen as it was reported in normal ATRP does not play detrimental role in this system.

In this regard firstly, ATRP of styrene (St) was carried out in the presence of fructose as a reducing agent (RA) for Cu(II)/ *N,N,N',N'',N''*-pentamethyldiethylenetriamine (PMDETA) complex by using either 1-chloro-1-phenyl ethane (1-PECl), ethyl-2-bromoisobutyrate (EiBr) or methyl-2-bromopropionate (MBP) as an initiator (In) and (PMDETA) as ligand at 110 °C. Kinetic experiments were carried out to reveal the effect of fructose concentration on ATRP of St. Moreover, to demonstrate the universality and simplicity of new catalytic system different reducing agents (RA) were used such as ascorbic acid, *p*-methoxyphenol, *p*-tert-butylphenol, dihydroquinone.

Secondly, we used thiophenol derivatives as a reducing agent for Cu(II)/PMDETA complex in ATRP of St. A plausible mechanism of Cu (I) generation in the CuX₂/PMDETA mediated LRP using thiophenol derivative is given in Figure 2. ATRP of St was carried out in the presence of thiophenol derivative such as sodium thiophenolate (PhSNa) or *p*-methoxythiophenol as a reducing agent for Cu(II)/PMDETA complex by using either 1-PECl or EiBr as an initiator and PMDETA as ligand at 110 °C. Kinetic experiments were carried out to reveal the effect of PhSNa concentration on ATRP of St. Furthermore, ATRP of methyl methacrylate (MMA) catalyzed by Cu(II)/ PMDETA/*p*-methoxythiophenol or PhSNa was also investigated.

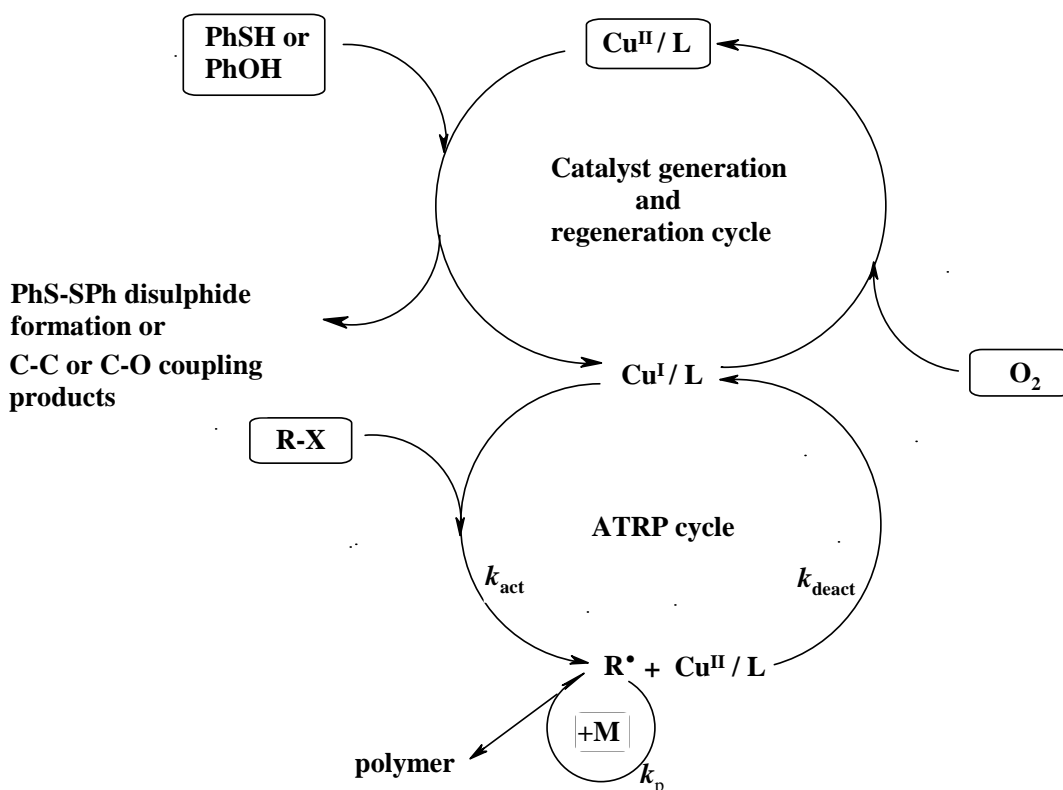


Figure 2: Proposed Mechanism of ATRP Employing Thiophenol or Phenol Derivatives as a Reducing Agent.

Thirdly, this technique was successfully applied for the preparation of homopolymers (linear and star type polystyrene (PS)) and corresponding block copolymers (PS-*b*-PMMA) (Figure 3 and 4). Thus obtained polymers were characterized using gel permeation chromatography (GPC), ^1H NMR, and matrix assisted laser desorption/ionization time-of-flight (MALDI-TOF) measurements.

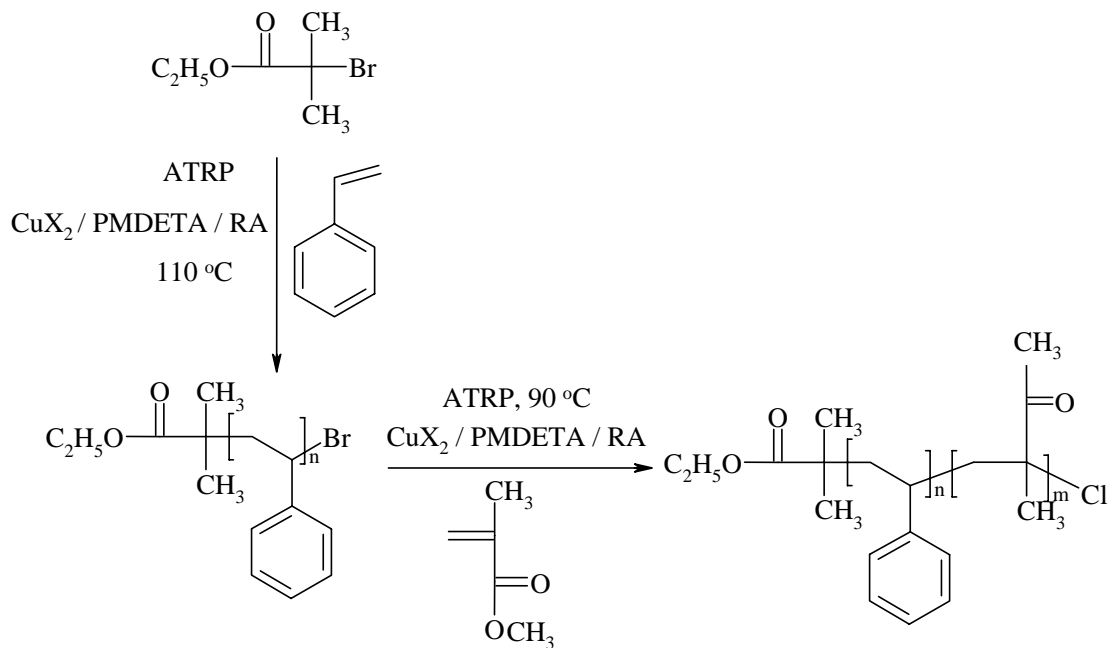


Figure 3: Block Copolymerization by ATRP via *In Situ* Copper (I) Formation.

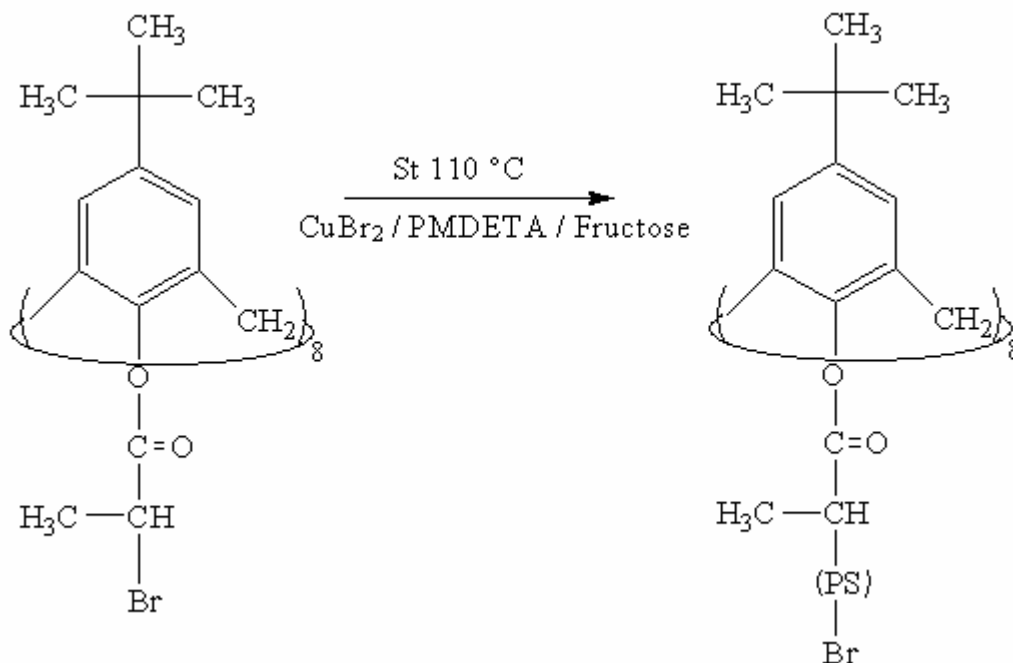


Figure 4: Star Homopolymer Precursor Synthesized by ATRP via *In Situ* Copper (I) Formation.

As taken into a consideration, another major challenge facing ATRP is the removal and recycling of the catalyst. Despite the growing interest in heterogeneous polymerization catalysis, the majority of the polymerization catalysts used industrially are single-use entities that are left in the polymer product. Recoverable and recyclable polymerization catalysts have not reached the industrial utility of single-use catalysts because the catalyst and product separation have not become economical. The successful development of recyclable transition metal polymerization catalysts must take a rational design approach, hence academic and industrial researchers need to further expand the fundamental science and engineering of recyclable polymerization catalysis to gain an understanding of critical parameters that allow the design of economically viable, recoverable solid polymerization catalysts. Unfortunately, the rapid development of ATRP over the past 10 years has not resulted in its wide spread industrial practice. Numerous reports regarding the immobilization of transition metal ATRP catalysts, in attempts to increase its applicability, have extended the fundamentals of recyclable polymerization catalysis. However, for industrial viability, more research is required in the area of how immobilization methodology and support structure affect the catalyst polymerization performance, regeneration, and recyclability.

In the last part, we demonstrated the preparation of an oxidatively stable silica gel supported heterogeneous catalyst and its application for the benefits of the catalyst separation and recycling process in ATRP. ATRP of St was conducted using the silica gel supported $\text{CuCl}_2/\text{PMDETA}$ complex as catalyst. Silica gel was chosen as support, mainly, for two reasons. First, the heterogeneous catalyst technique is the most practical way for catalyst separation. Second, the supported catalyst used in this study is simply prepared by the adsorption of Cu(II) /amine complex on to silica surface (Figure 5).

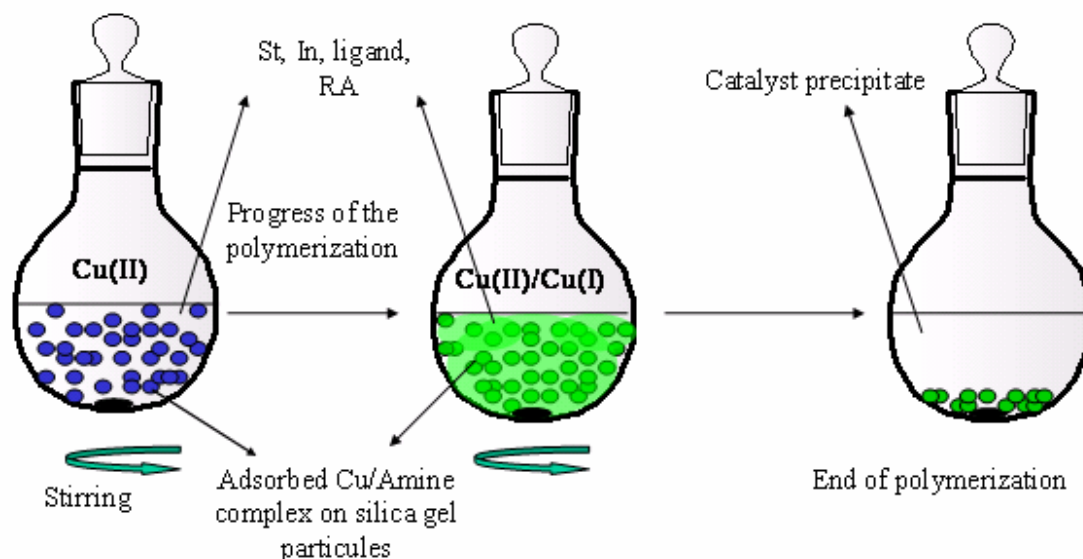


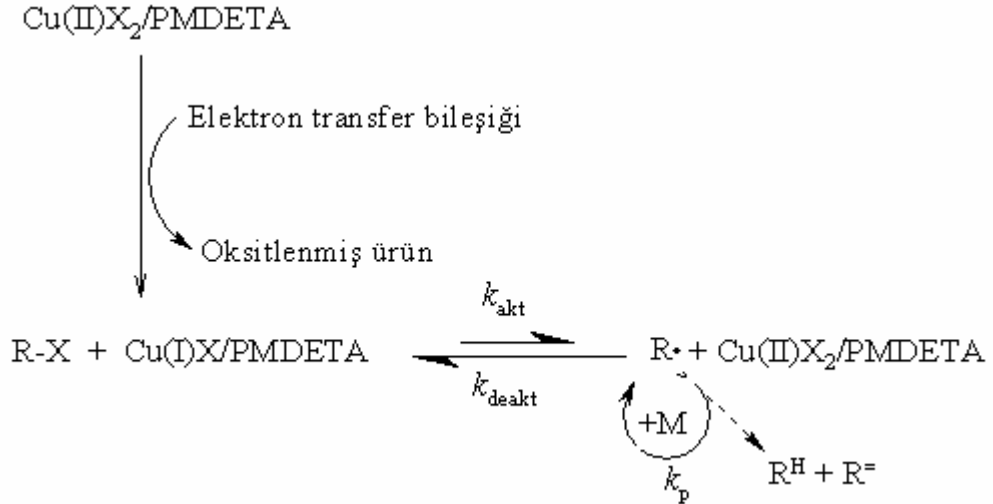
Figure 5: Air Stable Recovable Catalyst in ATRP.

ATOM TRANSFER RADİKAL POLİMERİZASYON'DA *İN SITU* BAKIR (I) OLUŞUMU

ÖZET

Son yıllar kontrollü/ “yaşayan” radikal polimerizasyonlarının (LRP) gelişiminde büyük ilerlemelere tanıklık etmiştir. Nitroksit ortamlı radikal polimerizasyonu (NMP), tersinir eklenme ayrılma zincir transferi polimerizasyonu (RAFT) ve atom transfer radikal polimerizasyonu (ATRP) yakın dönemde bir çok akademik araştırmaya konu olmuş LRP yöntemlerindendirler. Bu yöntemler içinde katalitik yapısı ve uygulama kolaylığı dolayısıyla en çok umut vaad eden yöntem ATRP’dir. ATRP’de dinamik tersinir aktivasyon/deaktivasyon dengesinin kurulmasında geçiş metal komplekslerinin önemli bir yeri vardır. İlk, orta ve son geçiş metallerini içeren bir çok geçiş metal kompleksi geliştirilmiş ve etkin ATRP katalizleri olarak kullanımları araştırılmıştır. Bunlar içinden alkil halojenür başlatıcılı (RX), amin ligandlı ve bakır (Cu) katalizli ATRP en çok ilgiyi çekmiştir.

Yüksek maliyetli ve kolaylıkla oksitlenebilen düşük oksidasyon basamağındaki metal tuzları katalizliğinde gerçekleşmesi ATRP’nin en büyük dezavantajlarından. Bu dezavantaj kararlı ve yüksek oksidasyon basamağındaki geçiş metal tuzunun (Cu (II)) elektron transfer bileşikleriyle (RA) indirgenmesi sonucu düşük oksidasyon basamağındaki geçiş metal tuzunun reaksiyon ortamında oluşturulmasına dayanan *in situ* Cu (I) oluşumu metoduyla ortadan kaldırılabilir (Şekil 1).



Şekil 1: ATRP’de *In Situ* Bakır (I) Oluşumu.

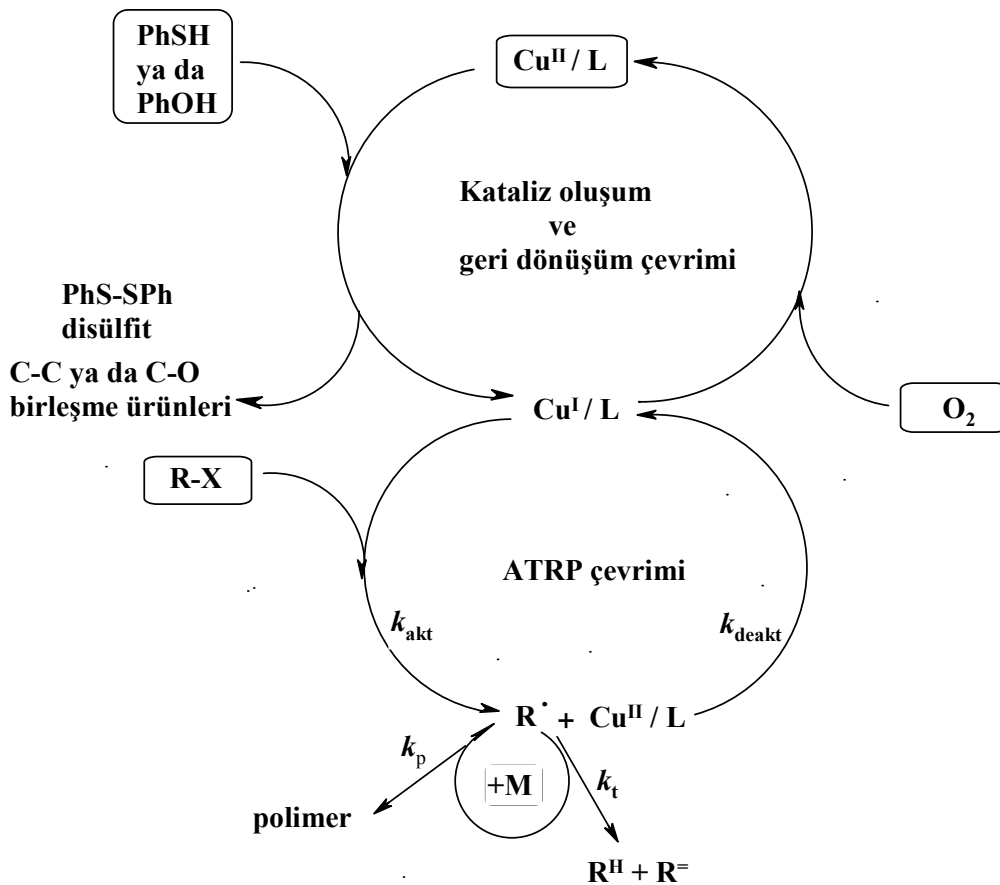
Bu yaklaşım iki açıdan normal ATRP’den farklıdır:

(i) Bu sistemde, aktif Cu (I) türleri elektron transfer bileşikleri ve Cu (II) arasındaki redoks reaksiyonu sonucunda *in situ* oluşmaktadır. Az miktardaki Cu (I) radikal konsantrasyonunun düşük olmasını sağlar. Ayrıca reaksiyonun başında ortamda Cu(II)’nin olması (kararlı radikal etkisi (PRE)) deaktivasyon prosesini daha da

etkinleştirerek istenmeyen radikal radikal sonlanma reaksiyonlarının önlenmesini sağlar.

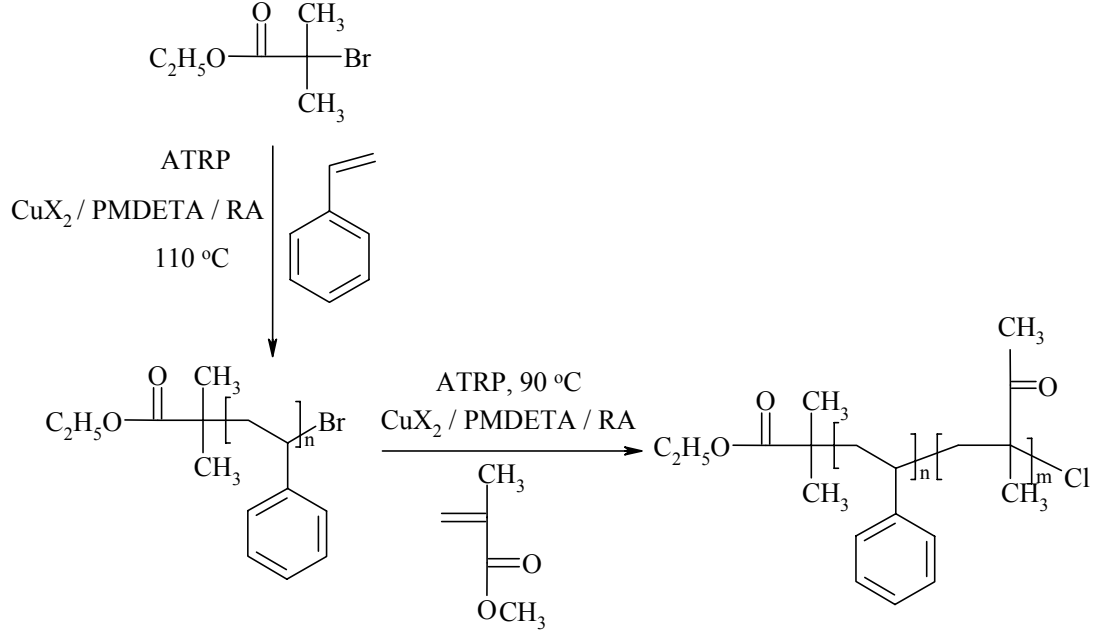
(ii) Katalizin istenmeyen oksidasyonu ve difüze olan oksijenin başlattığı polimerizasyon normal ATRP'deki kadar önemli bir rol oynamaz Bu çalışmada ilk olarak stirenin (St) ATRP'si Cu(II)/ *N,N,N',N'',N''*-pentametildietilentriamin (PMDETA) kompleksi için elektron transfer bileşiği (RA) olarak fruktoz, başlatıcı (In) olarak 1-kloro-1-feniletan (1-PECl) ya da etil-2-bromoizobütirat (EiBr) ya da metil-2-bromopropiyonat (MBP), ligand olarak PMDETA kullanılarak 110 °C'de gerçekleştirildi. Fruktoz konsantrasyonunun stirenin ATRP'si üzerine etkisi incelendi. Bu yeni kataliz sisteminin kolaylığını ve uygulanabilirliğini kanıtlamak için askorbik asit, *p*-metoksifenol, *p-ter*-bütilfenol, dihidrokinon gibi farklı bileşikler elektron transfer bileşiği olarak kullanıldı.

İkinci olarak tiyofenol türevlerinin stirenin ATRP'sinde Cu(II)/PMDETA kompleksi için elektron transfer bileşiği olarak kullanımı gösterildi. Tiyofenol türevleri ve belirli miktarda hava varlığında gerçekleşen ATRP için öngördüğümüz mekanizma Şekil 2'de görülmektedir. Bu bölümde stirenin ATRP'si elektron transfer bileşiği olarak sodyum tiyofenolat (PhSNa), *p*-metoksitiyofenol gibi tiyofenol türevleri, başlatıcı olarak 1-PECl ya da EiBr, ligand olarak PMDETA kullanılarak belirli miktarda hava varlığında 110 °C'de gerçekleştirildi. PhSNa konsantrasyonunun polimerizasyon kinetiği üzerine etkisi incelendi. Bunun yanında metil metakrilatın (MMA) Cu(II)/PMDETA/ *p*-metoksitiyofenol ya da PhSNa katalizli ATRP'si de incelendi.

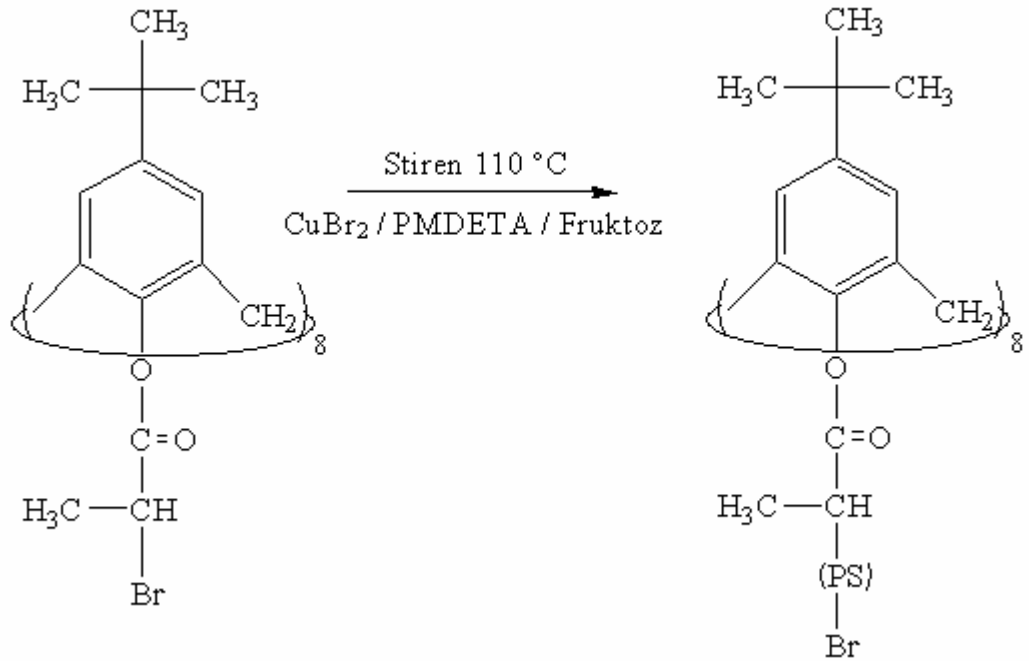


Şekil 2: Oksijen Varlığındaki ATRP'de İn Situ Bakır (I) Oluşumu.

Üçüncü olarak ATRP’de *in situ* Cu (I) oluşumu tekniğiyle homopolimerler hazırlandı (lineer ve yıldız tipli polistiren (PS)) ve bu homopolimerlerin makrobaşılatıcı olarak kullanılmasıyla PS-PMMA blok kopolimerleri başarıyla sentezlendi (Şekil 3 ve 4). Elde edilen homo- ve blok ko-polimerler jel geçirgenlik kromatografisi (GPC), ^1H NMR ve kütle spektroskopisi (MALDI-TOF) ölçümleriyle karakterize edildi.



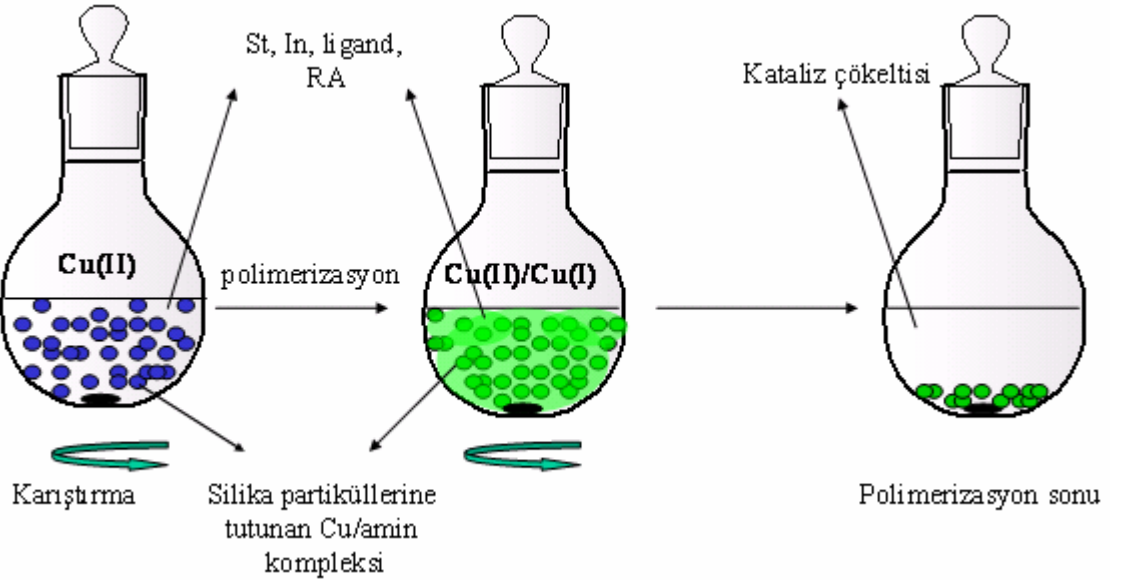
Şekil 3: ATRP’de *În Situ* Bakır (I) Oluşumu Yöntemiyle Blok Kopolimer Sentezi.



Şekil 4: ATRP’de *În Situ* Bakır (I) Oluşumu Yöntemiyle Yıldız Tipli Homopolimer Makrobaşılatıcısının Sentezi.

ATRP'nin bir diğer dezavantajı ise katalizin polimerden uzaklaştırılması ve geri kazanımıdır. Heterojen polimerizasyon katalizlerine artan ilgiye rağmen endüstriyel olarak kullanılan polimerizasyon katalizlerinin çoğu polimerik ürün içerisinde bırakılan tek kullanımlık katalizlerdir. Kataliz ve ürün ayırımı ekonomik olmadığı için, yenilenebilir polimerizasyon katalizlerinin endüstriyel kullanımı; tek kullanımlık katalizlerin kullanımı kadar yaygınlaşamamıştır. Yenilenebilir geçiş metal polimerizasyon katalizlerinin gelişimine rasyonel bir bakış açısıyla yaklaşıldığında ekonomik açıdan uygun, yenilenebilir kataliz dizaynına olanak sağlayacak kritik parametrelerin anlaşılması için akademik ve endüstriyel alandaki araştırmacıların temel bilim ve mühendislik alanındaki araştırmaları daha da genişletmeleri gerektiği görülmektedir. Malesef ATRP'nin geçen 10 yıldaki hızlı gelişimi endüstriyel kullanımının yaygınlaşmasıyla sonuçlanmamıştır. Destekli geçiş metal ATRP katalizinin kullanılabilirliğini artırmak için yapılan bir çok yayın yenilenebilir polimerizasyon katalizlerinin temelini güçlendirmiştir. Fakat endüstriyel kullanım için destekleme metodunun ve destek yapısının katalizin performansını, yenilenmesini ve yeniden kullanılmasını nasıl etkilediği konularında daha çok araştırma yapılması gerekmektedir.

Bu bağlamda son bölümde, havaya dayanıklı silika jel destekli heterojen kataliz hazırlandı ve ATRP'de kullanıldı. Geri kazanılmış kataliz tekrar kullanıldı ve aktivitesini önemli ölçüde koruduğu gözlemlendi. Destek olarak silika jeli seçilmesinin iki temel nedeni vardır. Bunlardan ilki, heterojen kataliz tekniğinin kataliz ayırımı için en pratik yol olması, ikincisi ise bu çalışmada kullanılan destekli katalizin, Cu(II)/amin kompleksinin silikaya fiziksel adsorpsiyonu sonucu kolaylıkla hazırlanabilmesidir (Şekil 5).



Şekil 5: ATRP'de Havaya Dayanıklı Yenilenebilir Destekli Kataliz Kullanımı.

1. INTRODUCTION

Polymers are widely used in all walks of human life and play a vital role in shaping modern man's activities to be as sophisticated and comfortable as they are today. The advances in science and technology made in recent decades owe much to the development of polymer science. The synthesis and design of new polymeric materials to achieve specific physical properties and specialized applications, and the attempt to find interesting applications involving advanced structures and architectures, are in continuous and parallel development in the area of polymer science. However, it is essential now that, after the initial period of discovery and investigation of fundamental polymerization principles, new or advanced technologies are pursued by an intensive search to ensure that the materials reach their fullest potential. As the performance requirements of polymeric materials become more demanding, the ability to control architecture, i.e. the physical properties of polymers through the polymerization process, becomes increasingly important. A thorough understanding of numerous structure-property relationships has helped us to design polymers that are tailored for specific applications. Depending on particular needs, polymeric materials have to satisfy certain requirements in terms of their processability, durability, resistance to environment, cost effectiveness, mechanical performance, and so on. New applications and modern technologies have required the preparation of tailor-made macromolecules with precisely controlled dimensions, molecular weight distributions (MWD), microstructures (sequences, tacticities), and terminal functionalities. Novel phenomena and properties can be observed for well-defined polymers and copolymers. These include mechanical, electrical, optical, surface and other properties. To achieve such a goal, polymer chemists have a variety of synthetic processes to choose from and can often fine-tune reactions with very high selectivity when planning a particular synthesis. However, each method has its strengths and its weaknesses, and often requires high-purity reagents and special conditions. For example, radical polymerization is industrially the most widespread method to

produce polymeric materials. This is due to its tolerance to protic compounds such as water, a high reaction rate, convenient temperature range and very minimal requirements for purification of monomers, solvents. Furthermore, radical polymerizations can be carried out in bulk in solution, aqueous suspension, emulsion, dispersion. The major drawback of conventional radical polymerization is the lack of control over polymer structure. Due to slow initiation fast propagation, and subsequent transfer or termination, polymers with high molecular weight and broad molecular weight distribution are generally produced. These features are reflected in the physical and mechanical properties of the produced polymers [1].

Living polymerization is free from side reactions such as termination and chain transfer and can thus generate polymers of well-defined architectures and molecular weights. However, ionic polymerization is limited to a handful of monomers; it also requires very stringent drying, exclusion of moisture, and also very low temperatures.

The recent development of the living (or controlled/“living”) radical polymerization (LRP) opened up a new and versatile route to the synthesis of well-defined, polymers with narrow MWD and various possible architectures. Among them atom transfer radical polymerization (ATRP) is the most convenient and useful method to synthesize polymers with well-controlled molecular weight and molecular weight distribution from a wide range of monomers [2, 3]. The advantages of ATRP, in comparison with other LRP processes, include the large range of available monomers and (macro)initiators, the simplicity of reaction setup, and the ability to conduct the process over a large range of temperatures, solvents, and dispersed media. However, ATRP has some limitations. Since ATRP is initiated by a redox reaction between an initiator with a radically transferable atom or group and a catalyst complex comprising a transition metal compound in a lower oxidation state, the transition metal complexes can be easily oxidized to a higher oxidation state. Therefore, to obtain consistent results, special handling procedures are required, and the preformed catalysts must be stored under an inert atmosphere. Oxygen or other oxidants should be removed from the system prior to addition of the catalyst in the lower oxidation state; therefore, the process of catalyst complex handling can be challenging [4-6].

Another limitation of ATRP, is the presence of catalyst that is not bound to the end of the chain, as it is in coordination polymerization, with substoichiometric amounts

with respect to the initiator. Nevertheless, it is typically used at concentrations ranging from 0.1 to 1 mol % with respect to the monomer and therefore needs to be removed from the final polymer. There have been several attempts to remove and recycle the catalyst efficiently by extraction, precipitation, immobilization, or by using biphasic systems [5, 7-10]. However, there is always some loss of polymerization control in biphasic systems or added cost associated with catalyst preparation.

This thesis focused on the eliminating the limitations facing normal ATRP via *in situ* copper (I) formation method. This method employing oxidatively stable catalyst precursors can potentially allow the more facile preparation, storage, and shipment of ATRP catalyst systems.

2. THEORETICAL PART

2.1 Conventional Free Radical Polymerization (FRP) versus Controlled/"Living" Radical Polymerization (LRP)

Conventional free radical polymerization (FRP) is probably the most important commercial process leading to high molar mass polymers. This is due to the large variety of monomers which can be polymerized and copolymerized radically and to the relatively simple experimental conditions which require the absence of oxygen but which can be carried out in the presence of water, e.g., as in suspension or emulsion polymerizations, and within a convenient temperature range, typically -20 to 200 °C [1]. The only disadvantage to FRP is the poor control over macromolecular structures of synthesized polymers. This includes the relatively broad molecular weight distribution ($MWD = M_w/M_n$ where M_n is number average molecular weight, and M_w is weight average molecular weight of the polymer), and also the practical impossibility to synthesize block copolymers, and other advanced structures. Thus, it has always been desirable to prepare, by a free radical mechanism, well-defined block and graft copolymers, stars, combs and many other materials (2.1) under mild conditions from a larger range of monomers than available for ionic living polymerization [11]. Controlled/"living" (LRP) radical processes have been recently developed which allow for both control over molar masses and for complex architectures (2.2) under simpler reaction conditions than are appropriate for ionic processes [11, 12].

Compositions



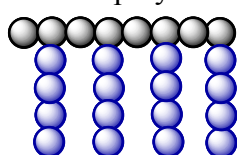
Block copolymers



Statistical copolymers



Graft copolymers

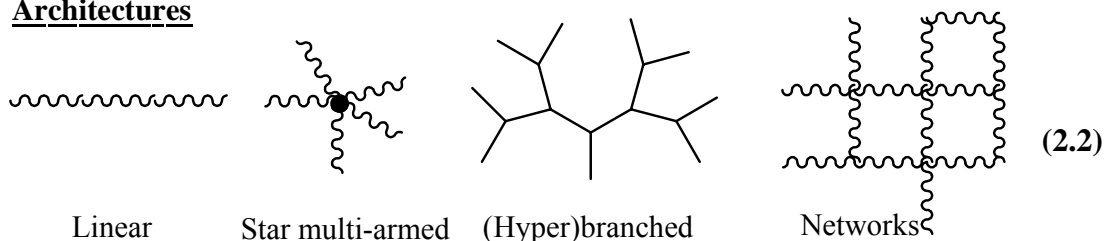


Gradient copolymers



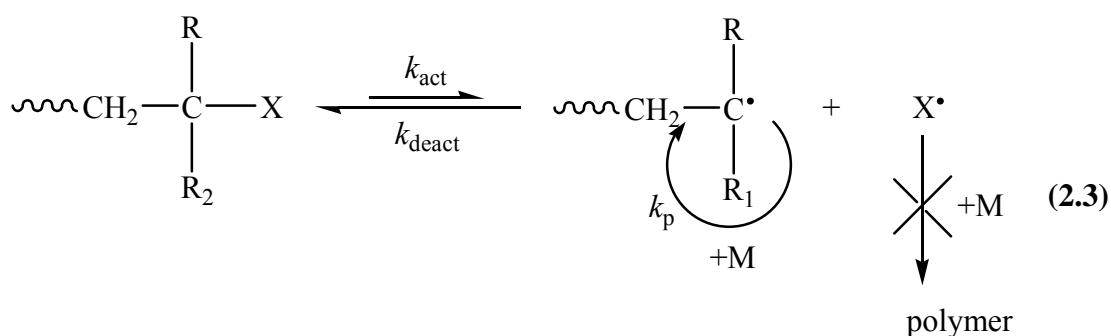
(2.1)

Architectures



2.1.1 Persistent Radical Effect (PRE)

It was first theorized by Otsu et al. [13] that minimization of the bimolecular termination events would occur if the propagating radical species could be controlled. It was postulated that reversible dissociation of a polymer chain end (dormant species) into a transient radical species and a persistent radical species would generate the controlled polymerization (2.3).



The persistent radical is a stable radical that is incapable of initiating polymerization. However, this persistent radical can easily couple unstable propagating radicals to reform the dormant species. The transient species formed from the dissociation reaction is short-lived unstable radical that can undergo propagation reactions with monomer molecules with a rate constant of k_p . The slow dissociation reaction would limit the concentration of transient radicals present in the reaction, thereby minimizing the probability of bimolecular termination. The fast recombination would limit the amount of monomer units incorporated during each monomer addition cycle to approximately one (i.e., $k_p \leq k_{\text{deact}}$). The dissociation would need to be facile enough so that there would be many monomer addition cycles and chain growth would occur until all monomer is consumed [14, 15].

2.1.2 Reversible Activation-Deactivation Process in LRP

Reversible activation- deactivation process based on persistent radical effect forms the basis of LRP (2.4). The dormant (endcapped) chain P-X is supposed to be

activated to the polymer radical P^\bullet by thermal, photochemical, and/or chemical stimuli. In the presence of monomer M , P^\bullet will undergo propagation until it is deactivated back to $P-X$. In practically important systems, it usually holds that $[P^\bullet]/[P-X] < 10^{-5}$, meaning that a living chain spends most of its polymerization time in the dormant state. LRP is accordingly defined as the radical polymerization that is structurally (and kinetically in many cases) controlled by the work of living chains.



If a living chain experiences the activation–deactivation cycles frequently enough over a period of polymerization time, all living chains will have a nearly equal chance to grow, yielding a narrow MWD product.

LRP is distinguished also from truly living systems like anionic living polymerization by the existence of bimolecular, chain transfer and all the other elementary reactions involved in FRP. While it clearly limits the degree of structural control attainable, this feature of LRP provides a variety of unique polymerization systems that are particularly interesting from the viewpoint of polymerization kinetics. Given the rate constants of all the elementary reactions, including those of the activation and deactivation reactions, and details of experimental conditions such as the concentrations of reactants and temperature, one will be able to stimulate the whole process of a LRP run and predict the characteristics of the polymer produced, quite accurately in principle. This, in turn, indicates the feasibility of optimizing experimental conditions for the highest optional performance. The demerit of termination and other side reactions would be minimized in a well designed LRP run.

2.1.3 Prerequisites of LRP

LRP requires all chains to begin growing (reversibly via exchange reactions) at the same time and retain functionalities until the very end of the reaction. This is in contrast to FRP where all chains terminate and initiation is never completed, even when all monomer is consumed. Therefore, three basic prerequisites for LRP are

- (i) Initiation should be completed at low monomer conversions,

- (ii) Relatively low molecular weight (degree of polymerization (DP_n) < 1000) should be targeted to avoid transfer effects. This requires high concentration of growing chains (for example $>10^{-2}$ M for bulk polymerization),
- (iii) Concentration of propagating radicals ($[P\bullet] < 10^{-7}$ M) should be sufficiently low to enable growth of chains to sufficiently high molecular weight, before they terminate.

The mismatch between concentration of growing chains and propagating chains (10^{-2} M \gg 10^{-7} M) can be achieved by the exchange reactions between high concentration of growing chains in the dormant state and the minute amounts of propagating radicals.

2.1.4 Characteristics of LRP

Ideally, LRP systems lead to polymers with DP_n predetermined by the ratio of the concentrations of consumed monomer to the introduced initiator (2.5),

$$DP_n = \Delta[M]/[I]_0 \quad (2.5)$$

MWD close to Poisson distribution (2.6),

$$DP_w/DP_n \approx 1 + 1/DP_n \quad (2.6)$$

and with all chains end-functionalized. Experimentally the best way to evaluate such systems is to follow the kinetics of polymerization and the evolution of molecular weights, MWD and functionalities with conversion. Well controlled systems should provide :

- (i) linear kinetic plots in semilogarithmic coordinates ($\ln ([M]_0/[M])$ vs. time), if the polymerization is first order with respect to monomer concentration (2.7) and (2.8); acceleration on such plots may indicate slow initiation whereas deceleration may indicate termination or deactivation of the catalyst,

$$R_p = \frac{-d[M]}{dt} = k_p [P\bullet] [M] \quad (2.7)$$

$$\ln \frac{[M]_0}{[M]} = k_p [P^\bullet] t = k_p^{app} t \quad (2.8)$$

- (ii) linear evolution of molecular weights with conversion (2.9); molecular weights lower than predicted by $\Delta[M]/[I]_0$ ratios indicate transfer, molecular weights higher than predicted by $\Delta[M]/[I]_0$ indicate inefficient initiation or chain coupling (at most twice higher than predicted molecular weights can be formed by bimolecular radical coupling),

$$DP_n = \frac{M_n}{M_0} = \frac{\Delta[M]}{[I]_0} = \frac{[M]_0}{[I]_0} \times (\text{conversion}) \quad (2.9)$$

- (iii) MWD should decrease with conversion for systems with slow initiation and slow exchange; MWD increase with conversion when the contribution of chain breaking reactions become significant,
- (iv) end functionalities are not affected by slow initiation and exchange but they are reduced when chain breaking reactions become important.

Typical dependences for LRP systems and corresponding deviations are illustrated schematically in Figure 2.1 and 2.2.

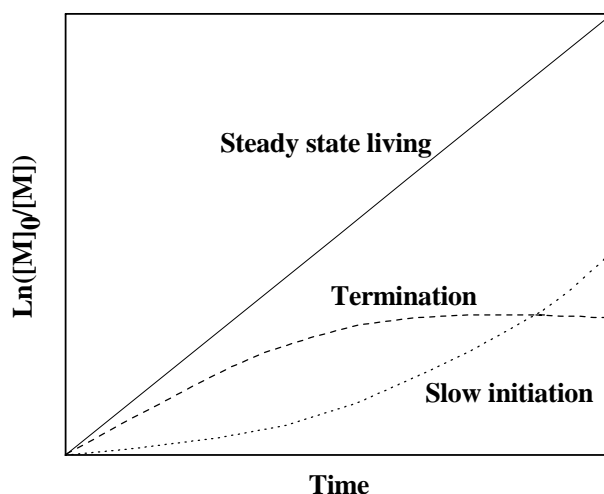


Figure 2.1: Effect of Slow Initiation, Transfer, Termination and Exchange on Kinetics.

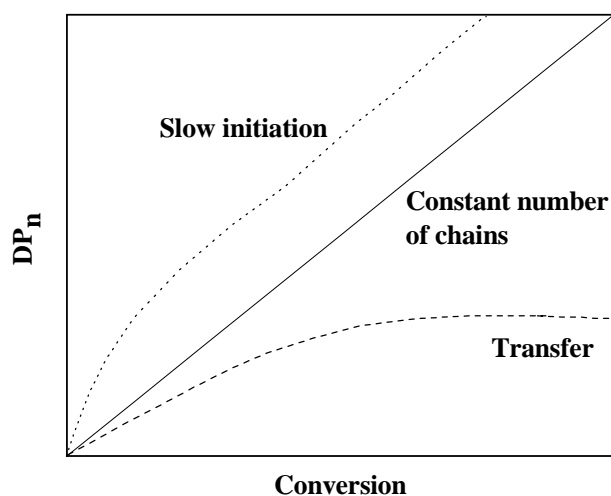


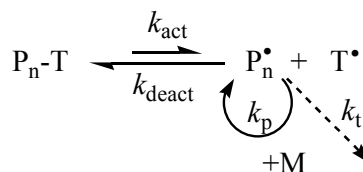
Figure 2.2: Effect of Slow Initiation, Transfer, Termination and Exchange on Molecular Weights.

2.1.5 Various Types of LRP Methods

A number of LRP methods have been developed and the three most promising are: stable free radical polymerization (SFRP), most commonly nitroxide mediated polymerization (NMP) [16, 17], but may also include organometallic species [18] ((2.10), 1); transition-metal-catalyzed atom transfer radical polymerization (ATRP) [2, 3] ((2.10), 2); and degenerative transfer with alkyl iodides [19], methacrylate macromonomers [20], and dithioesters via reversible addition fragmentation chain transfer (RAFT) polymerization [21, 22] ((2.10), 3). Significant progress has been reported in each LRP system over the past decade. However, ATRP will receive detailed consideration in this work (controlled living radical polymerizations).

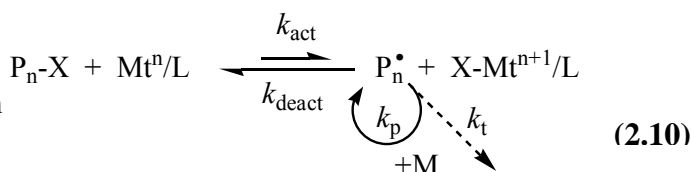
1) SFRP or NMP

Thermal dissociation of dormant species (k_{act}) provides a low concentration of radicals



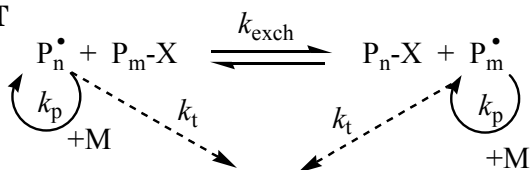
2) ATRP

Transition metal activation (k_{act}) of a dormant species with a radically transferable atom



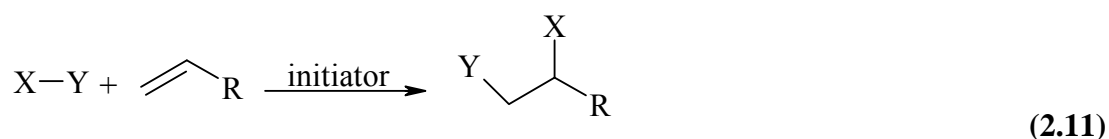
3) Degenerative Transfer or RAFT

Majority of chains are dormant species that participate in transfer reactions (k_{exch}) with a low concentration of active radicals



2.2 Atom Transfer Radical Addition (ATRA)

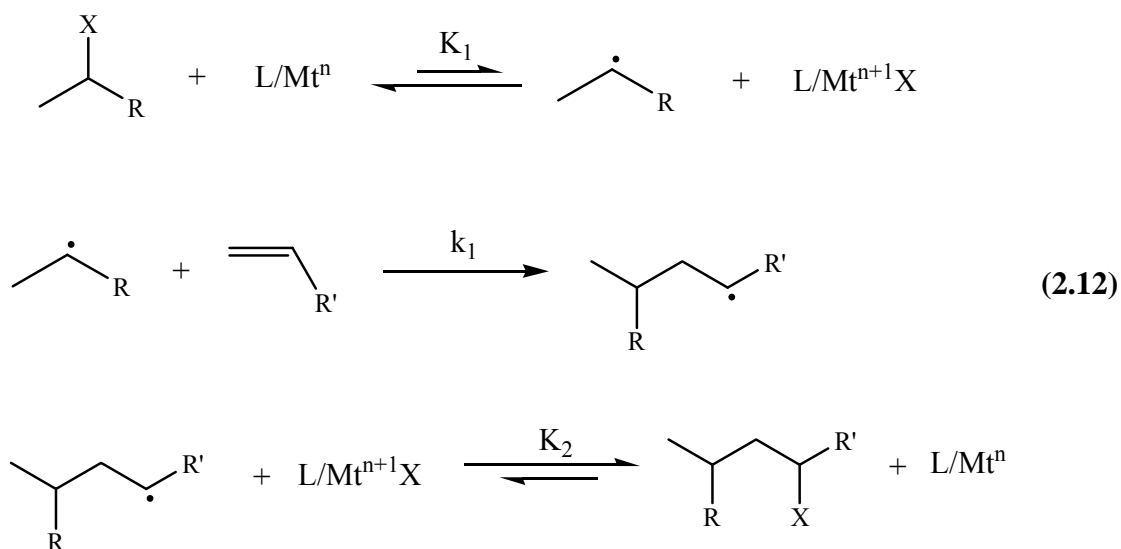
One of the fundamental reactions in organic chemistry involves the addition of a reagent XY across a carbon carbon double (or triple) bond through a radical process [23, 24]. This reaction was first reported in the early 1940s in which the halogenated methanes were directly added to olefinic double bonds [25, 26]. This reaction became known as the atom transfer radical addition (ATRA) or Kharasch addition, in honor of its discoverer, and it is generally accepted to occur via a free-radical mechanism [27, 28] as illustrated in (2.11).



X= H, halogen

Y= carbon, heteroatom

In ATRA a metal catalyst, usually a complex of a copper (I) halide and 2,2'-bipyridyl [29, 23, 30-32] (although Ni, [33] Pd, [34] Ru, [35] Fe, [36] and other metals [37] have been used as well), undergoes a one-electron oxidation with concomitant abstraction of a halogen atom from a substrate. Reaction mechanism is depicted in (2.12), where X is halogen, Mt^n is transition metal in the oxidation state n, L is ligand.



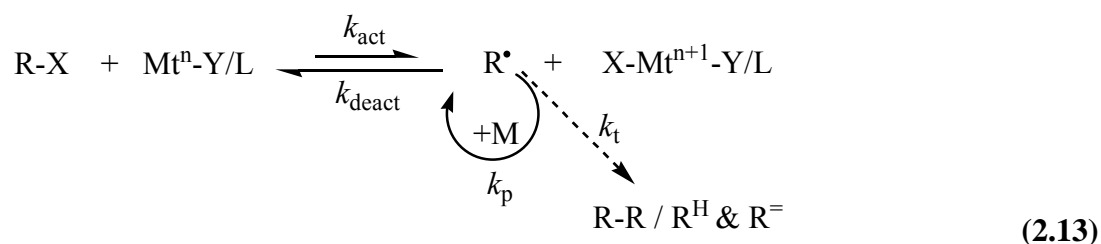
This reaction generates an organic radical and a copper (II) complex. One requirement for the reaction to occur is that substituents must be present on the organic halide that will stabilize the resultant radical. The resultant organic radical can add to an unsaturated compound in an inter- or intramolecular fashion, or it can abstract the halogen atom from the copper (II) complex and revert back to the original dormant organic halide species. The copper (I) complex is reformed, completing the catalytic cycle. The radical may also react with another radical, but because the concentration of propagating radicals is very small, the contribution from termination reactions to the products formed is minimal.

The substrates for this reaction are typically chosen such that if addition occurs, then the newly formed radical is much less stabilized relative to the initial radical and will essentially react irreversibly with the copper(II) complex to form an inactive alkyl halide product ($K_2 \gg K_1$). Therefore, in ATRA usually only one addition step occurs.

Atom transfer radical addition can be extended to atom transfer radical polymerization (ATRP) if the conditions can be modified such that more than one addition step is possible. Thus, if the radical species in (2.12) before and after addition of the unsaturated substrate possess comparable stabilization, then the activation-addition-deactivation cycle will repeat until all of the unsaturated substrate present is consumed. This process results in a chain-growth polymerization.

2.3 Atom Transfer Radical Polymerization (ATRP)

In 1995, a new class of controlled/“living” radical polymerization (LRP) method based on ATRA was reported independently by the groups of Sawamoto [2] and Matyjaszewski [3] : atom transfer radical polymerization (ATRP). A general reaction scheme for ATRP is shown in (2.13) [38-48].



Mtⁿ : Cu, Ru, Fe, Ni, etc. in the oxidation state n

Y : complexing ligand or counterion

X : (pseudo)halogen

L : ligand

M : vinyl monomer

In ATRP, homolytic cleavage of the alkyl (pseudo)halogen bond (R-X) by a transition metal complex in the lower oxidation state (Mtⁿ-Y/ligand) generates an alkyl radical (R•) and a transition metal complex in the higher oxidation state (X-Mtⁿ⁺¹-Y/ligand). The formed radicals can initiate the polymerization by adding across the double bond of a vinyl monomer, propagate, terminate by either coupling or disproportionation, or be reversibly deactivated by the transition metal complex in the higher oxidation state. The formation of radicals during the ATRP process is reversible. Polymerization systems utilizing this concept have been developed using Cu^I [3, 39, 49-52], Ni^{II} [53, 54], Ru^{II}/ Al(OR)₃, [2, 55] and Fe^{II} [56, 57] complexes to catalyze the radical-forming equilibrium.

2.3.1 Basic Components of ATRP

As a multicomponent system, ATRP is composed of vinyl monomer, an initiator with a transferable (pseudo)halogen, and a catalyst (composed of a transition metal species with any suitable ligand). Sometimes an additive is used. For a successful ATRP, other factors, such as solvent and temperature, must also be taken into consideration.

2.3.1.1 Monomers

Due to a number of factors, the ATRP of each type of monomer requires a specific set of conditions. Each monomer possesses an intrinsic radical propagation rate, so the concentration of propagating radicals and the rate of radical deactivation may need to be adjusted to maintain polymerization control. How such adjustments should be made is monomer specific as well. For the polymerization of each monomer, the corresponding alkyl halide end group will possess its own unique redox potential. Therefore, in combination with the same metal catalyst, each end group will exhibit a different atom transfer equilibrium constant, deactivation rate constant, and corresponding concentration of propagating radicals.

A variety of monomers have been successfully polymerized using ATRP. Typical monomers include styrenes, (meth)acrylates, (meth)acrylamides, and acrylonitrile, which contain substituents that can stabilize the propagating radicals [38, 58]. Ethylene, α -olefins, vinyl chloride and vinyl acetate give non-stabilized, reactive radicals; therefore the currently used catalyst systems are not sufficient to polymerize these monomers although copolymerization is sometimes successful [59].

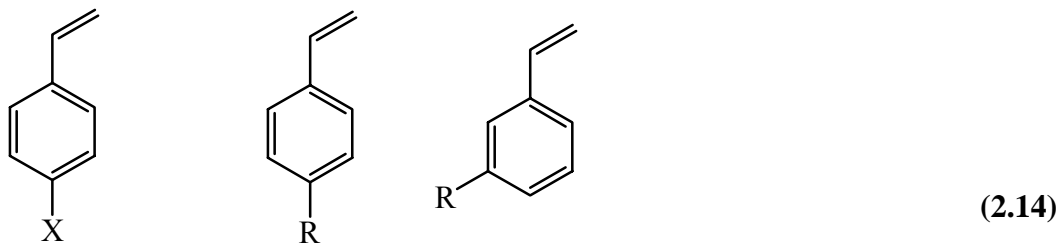
Styrenes (St):

Styrene ATRP has been reported for the copper [3, 39, 49-51, 60] and iron [57] catalyst systems; thus far the majority of work has been performed using the copper-based system.

In styrene ATRP, polymerizations are conducted at 110 °C for bromide-mediated polymerization and 130 °C for chloride-mediated polymerization. The corresponding 1-phenylethyl halide is usually used as the initiator; however, a wide variety of compounds have been used successfully as initiators for copper-mediated styrene ATRP, [49, 50] such as benzylic halides, allylic halides, α -bromoesters, polyhalogenated alkanes, and arenesulfonyl chlorides. Solvents may be used for styrene ATRP, but the stability of the halide end group displays a pronounced solvent dependence as demonstrated by model studies using 1-phenylethyl bromide [61]. Therefore, non-polar solvents are recommended for styrene ATRP.

Well-defined polystyrenes can be prepared within the molecular weight range of 1000 to 90 000. In the region from 1000 to 30 000 the MWD (M_w/M_n) are narrower than 1.10, and above 30 000 the MWD fall within the range of 1.10 to 1.50. A wide

range of styrene derivatives were polymerized in a controlled fashion using this method (2.14), [62].



Halogens

Alkyls

X = F, Cl, Br

R = CH₃, CF₃, *tert*-butyl

Methyl methacrylate (MMA) :

Methyl methacrylate (MMA) ATRP has been reported for the copper, [49, 52, 63, 64] ruthenium/aluminum alkoxide, [2, 55] iron, [56, 57] and nickel [53, 54] catalyst systems. The radical propagation rate for MMA ($k_p = 1.6 \times 10^3 \text{ M}^{-1} \text{ s}^{-1}$ at 90 °C) [65, 66] is greater than that for styrene ($k_p = 8.95 \times 10^2 \text{ M}^{-1} \text{ s}^{-1}$ at 90 °C), [65, 67] so it is important to keep the concentration of propagating radicals low by adjusting the atom transfer equilibrium. The best initiators for MMA ATRP are *p*-toluenesulfonyl chloride, benzhydryl chloride, and dialkyl-2-bromo-2-methylmalonates because with these initiators the apparent rate constant of initiation is larger than that of propagation.

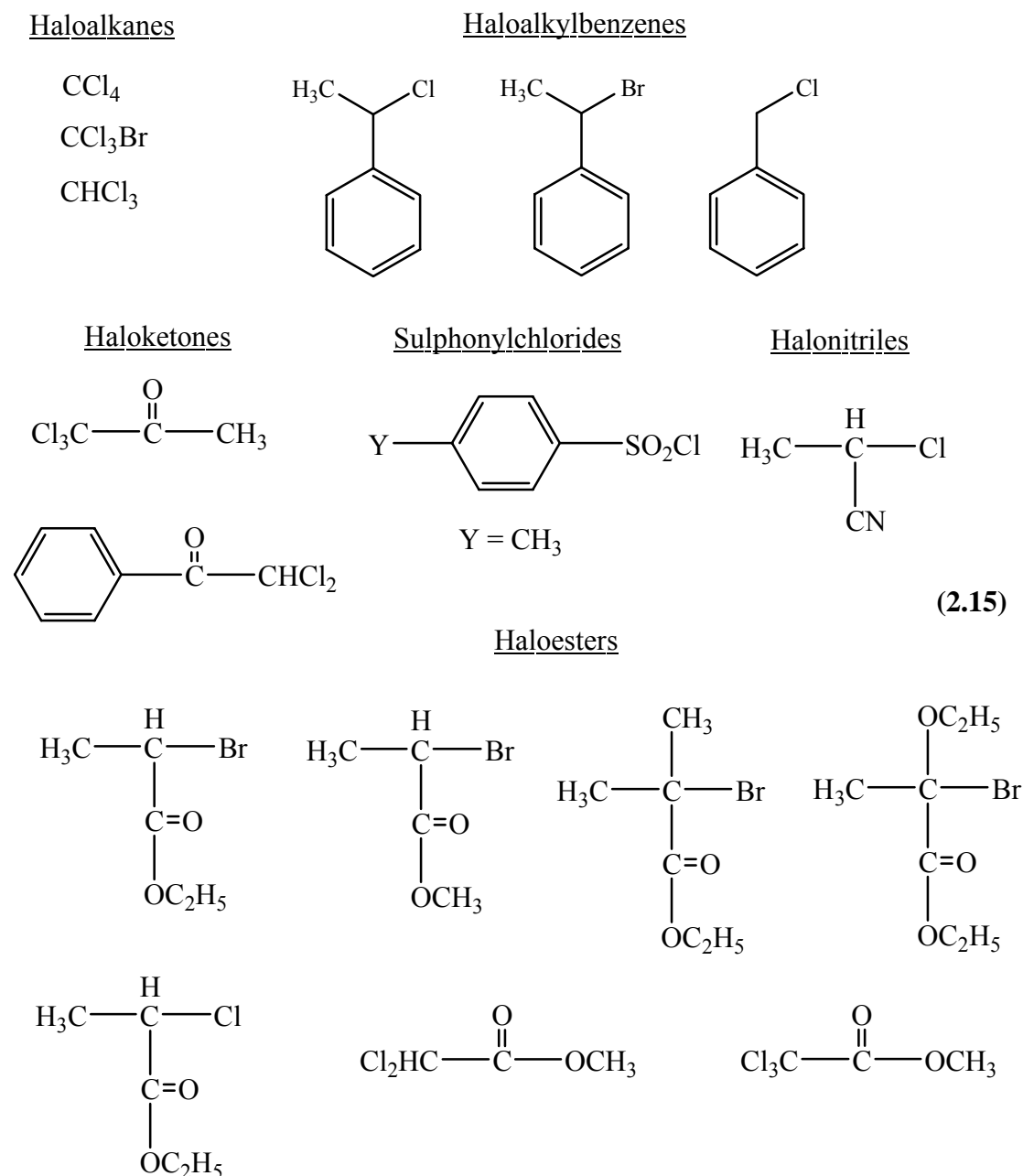
Well-defined poly(methyl methacrylate) can be prepared within the molecular weight range of 1000 to 180 000, and in analogy to acrylate esters, potentially a wide variety of

methacrylate esters can be polymerized using ATRP. The ranges within which the resulting polymer retains a narrow molecular weight distribution ($M_w/M_n < 1.5$) varies between catalyst systems.

2.3.1.2 Initiator

Another useful tool is the initiator, which, depending upon the propagation rate constant for a particular monomer and the equilibrium constant for the end group/catalyst pair, can be varied to assure that the apparent rate of initiation is faster than the apparent rate of propagation. In ATRP, alkyl halides (RX) are typically used as the initiator (2.15) and the rate of polymerization is first order with respect to the

concentration of RX. To obtain well-defined polymers with narrow molecular weight distribution, the halide group, X, must rapidly and selectively migrate between the growing chain and the transition-metal complex. Thus far, when X is either bromine or chlorine, the molecular weight control is the best. Iodine works well for acrylate polymerizations in copper-mediated ATRP [68]. Some pseudohalogens, specifically thiocyanates and thiocarbamates have been successfully used in the polymerization of acrylates and styrenes [68-70].



Generally, alkylhalides RX with either inductive or resonance stabilizing substituents are efficient initiators for ATRP. Often, the structure of the initiator is analogous to

the structure of the polymer end group. Polyhalogenated compounds (e.g., CCl_4 and CHCl_3) and compound with weak R-X bond, such as N-X, S-X, and O-X, can also be used as ATRP initiators. When the initiator moiety is attached to macromolecular species, macroinitiators are formed and can be used to synthesize block/graft copolymers [71].

2.3.1.3 Transition Metals and Ligands

Perhaps the most important component of ATRP is the catalyst. The catalyst typically consists of a transition metal center accompanied by a complexing ligand and counter-ion which can form a covalent or ionic bond with the metal center. In general, the rate of polymerization is first order with respect to the concentration of ATRP catalyst, and the molecular weights do not depend upon its concentration.

There are several requirements for an effective ATRP catalyst.

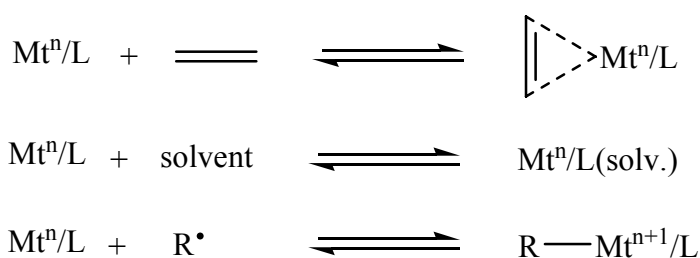
- i. The metal complex must have an accessible one-electron redox couple to promote atom transfer, but this requirement alone is not sufficient, because as its name indicates ATRP is an atom transfer not an electron transfer process.
- ii. Upon one electron oxidation, the coordination number of the metal center must increase by one in order to accommodate a new ligand, X. A brief review of known copper-based ATRP catalysts shows that in most systems the lower oxidation state of the metal is presumed to be tetracoordinate and the higher oxidation state is presumed to be pentacoordinate.
- iii. The catalyst must show selectivity for atom transfer and therefore possess a low affinity for alkyl radicals and the hydrogen atoms on alkyl groups. If not, then transfer reactions, such as β -H elimination and the formation of organometallic derivatives, may be observed. These reactions would reduce the selectivity of the propagation step and the control, or rather the “livingness”, of the polymerization.
- iv. The metal center must not be a strong Lewis acid, otherwise the ionization of certain initiators/end groups to carbocations may occur [58].

Additionally, the catalyst should not participate in any side reactions which would lower its activity or change the radical nature of the ATRA/ATRP process. The concurrent reactions which can occur during the catalytic process include: (a)

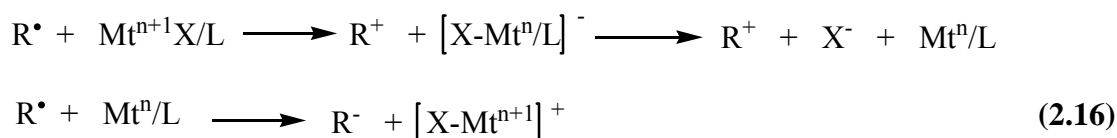
monomer, solvent or radical coordination, (b) oxidation/reduction of radicals to radical cations/anions, respectively, (c) β -hydrogen abstraction, (d) disproportionation, etc. (2.16).

So far, in ATRP, a variety of transition metal complexes have been successfully used for the polymerization of styrenes [60, 62, 72], (meth)acrylates [63, 64, 73-83], acrylonitriles [84-86], and acrylamides [87-89]. They include compounds from Groups 4 (Ti [90]), 6 (Mo [91, 92]), 7 (Re [93]), 8 (Fe [56, 57, 94-97], Ru [2]), 9 (Rh [98]), 10 (Ni [53], Pd [99]) and 11 (Cu [49, 52, 100-106]). However copper catalysts are superior in ATRP in terms of versatility and cost. Styrenes, (meth)acrylate esters and amides, and acrylonitrile have been successfully polymerized using copper-mediated ATRP [38, 58, 107].

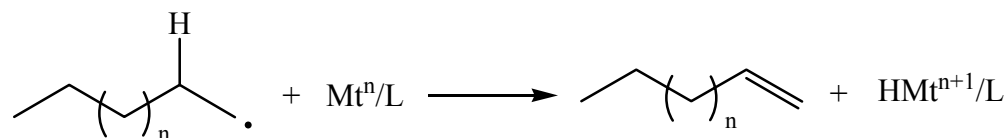
(a) Monomer, Solvent, and/or Radical Coordination



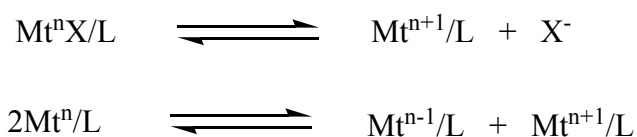
(b) Outer Sphere Electron Transfer



(c) β -Hydride Abstraction

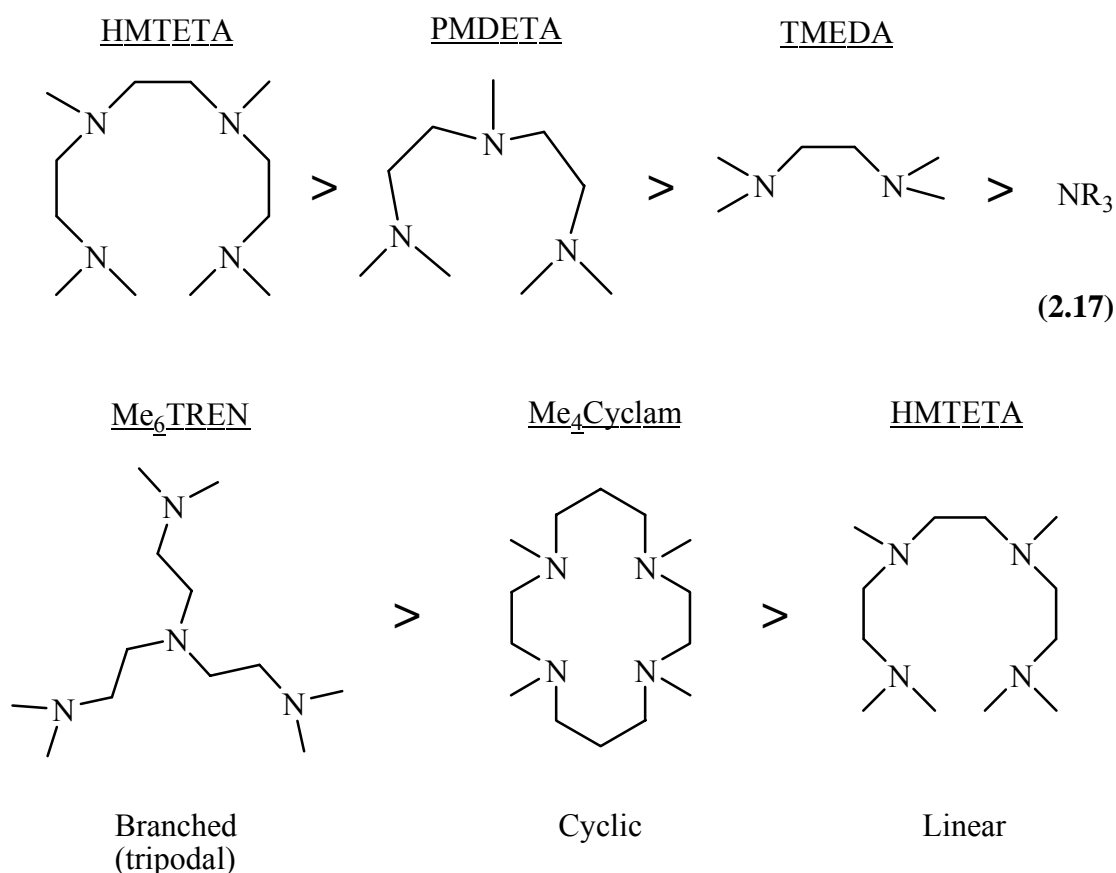


(d) Disproportionation and/or Halide Dissociation



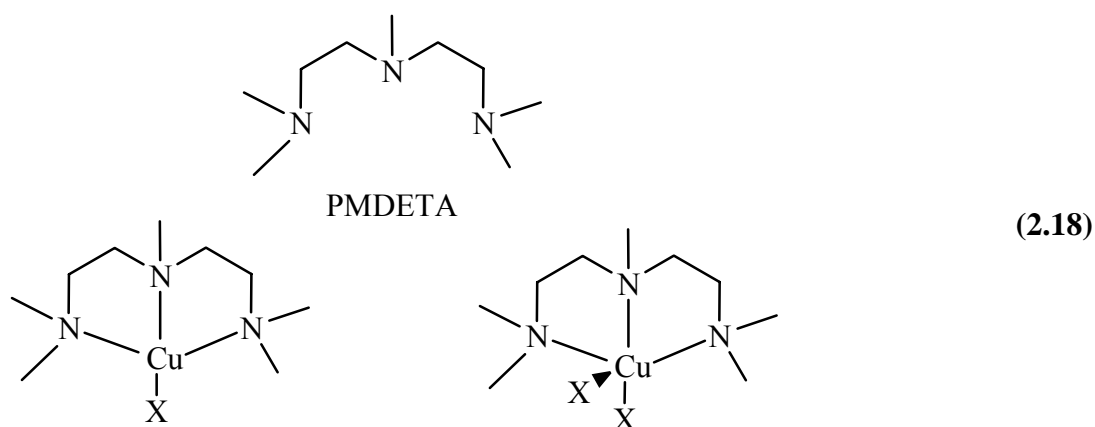
As a component of catalyst system the main roles of the ligand in ATRP is to solubilize the transition metal salt in the organic media and to adjust the redox

potential and halogenophilicity of the metal center forming a complex with an appropriate reactivity and dynamics for the atom transfer. The ligand should complex strongly with the transition metal. It should also allow expansion of the coordination sphere and should allow selective atom transfer without promoting other reactions. For copper mediated ATRP nitrogen-based ligands work particularly well. These are 2,2'-bipyridine (bpy) [3], 4,4'-di(5-nonyl)-2,2'- bipyridine (dNbpy) [39, 60], 1,10-phenanthroline (phen) [108], *N,N,N',N'*-tetramethylethylenediamine (TMEDA) [109, 110], *N*-propyl-(2-pyridyl)methanimine (NPrPMI), 2,2':6',2''-terpyridine (tpy) [111], 4,4',4''-tris(5-nonyl)-2,2':6',2''-terpyridine (tNtpy) [111], *N,N,N',N'',N''*-pentamethyldiethylenetriamine (PMDETA) [112], *N,N*-bis(2-pyridylmethyl)octylamine (BPMOA) [105], 1,1,4,7,10,10-hexamethyltriethylenetetramine (HMTETA) [105,109], tris[2-(dimethylamino)ethyl]amine (Me₆TREN) [113], tris[(2-pyridyl)methyl]amine (TPMA) [106] and 1,4,8,11-tetraaza-1,4,8,11-tetramethylcyclotetradecane (Me₄CYCLAM) [89]. The range of activity of catalyst complexes with different ligands exceeds one million (2.17).



The general order of activities of Cu complexes is related to their structure and follows the following order: tetradentate (cyclic-bridged) > tetradentate (branched) > tetradentate (cyclic) > tridentate > tetradentate (linear) > bidentate ligands. The nature of the N atom is also important and follows the order: pyridine > aliphatic amine > imine. The order of activity is shown above for a selection of N-based ligands (2.17).

Among the ligands used in copper catalyzed ATRP, PMDETA is an inexpensive ligand, forms nearly colorless complexes with Cu (I), and also provides fast and efficient polymerization of styrene, acrylates, and methacrylates. PMDETA and its complexes with copper (I) or (II) was depicted in (2.18).



2.3.1.4 Deactivator

The deactivator in ATRP is the higher oxidation state metal complex formed after atom transfer, and it plays a vital role in ATRP in reducing the polymerization rate and the MWD of the final polymer. In ATRP the concentration of deactivator continuously, but slowly, increases in concentration with conversion due to the persistent radical effect. While the final molecular weights do not depend upon the concentration of deactivator, the rate of polymerization will decrease with its increasing concentration. In the case of copper-mediated ATRP, it is possible to increase the observed polymerization rate by adding a small amount of metallic copper(0), which conproportionates with copper(II) to regenerate copper(I). This approach also allows for a significant reduction in the amount of catalyst required for polymerization [114].

2.3.1.5 Solvents

Typically, ATRP is conducted in bulk, but solvents may be used and are sometimes necessary when the polymer is insoluble in its monomer. Various solvents, benzene, toluene, anisole, diphenyl ether, ethyl acetate, acetone dimethyl formamide (DMF), ethylene carbonate, alcohol, water, carbondioxide, and many others used for different monomers. Solvent choice should be dictated by several factors. First, with some solvents there is the potential for chain transfer, depending upon the corresponding transfer constant, C_s . Second, solvent interactions with the catalyst system should be considered. Specific interactions with the catalyst, such as solvolysis of the halogen ligand or displacement of spectator ligands, should be avoided. Third, certain polymer end groups, such as polystyryl halides, can undergo solvolysis or elimination of HX at 110 to 130 °C in many polar solvents.

2.3.1.6 Temperature and Reaction Time

In ATRP, the observed rate of polymerization is enhanced by increasing temperature due to increases in both the rate constant for radical propagation and the atom transfer equilibrium constant. The energy of activation for radical propagation is appreciably higher than that for termination by radical combination and disproportionation. Consequently, the ratio k_p/k_t is higher and therefore better polymerization control (livingness) is observed at higher temperatures. If only the ratio of termination to propagation is considered, the best control will be observed for slower reactions at higher temperatures, but at elevated temperatures the rate of chain transfer and other side reactions will become faster. Therefore, an optimum temperature should be found for each type of ATRP system depending on monomer, and catalyst system.

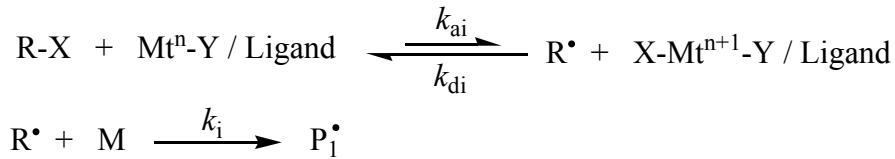
The effect of reaction temperature is also important. At high polymerization conversions the rate of propagation is very slow, because of the dependence upon monomer concentration. The rate of most side reactions does not depend upon monomer concentration, so such processes may still proceed at their observed rate. Even though the rate of such side reactions may be perceived as slow, they can have a significant effect upon the structure of final polymer. In such situations significant loss of endgroup functionality can occur. The fact that final MWD may be very narrow and the polymer may appear to be well-defined could be misleading.

Therefore, when conducting ATRP in which maintaining the endgroup functionality is a concern (i.e., in the preparation of block copolymers), the polymerization conversion should not exceed 95% in order to avoid potential endgroup loss.

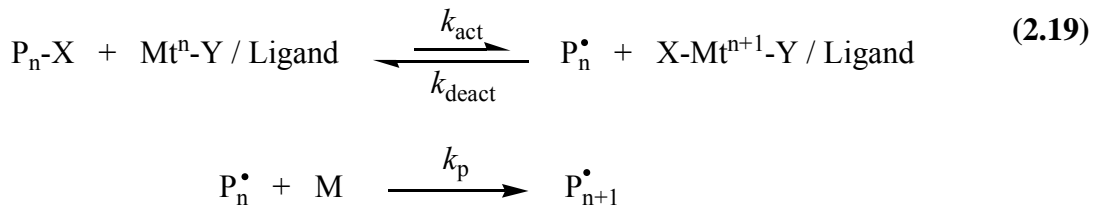
2.3.2 Kinetics and Mechanism of ATRP

The rate law for ATRP can be derived from (2.19) by neglecting contribution of termination, assuming that initiation is complete and using the fast equilibrium approximation [60]. Under these conditions the concentration of propagating radicals $[P^\bullet]$ and the rate of polymerization are given in equation (2.20) and (2.21) respectively. In equation (2.20), $[RX]_0$ refers to the initial concentration of the initiator which corresponds to the concentration of dormant chains ($[R-M_n-X]$). Results from kinetic studies of the polymerizations using soluble catalyst systems indicate that the rate of polymerization is first order with respect to monomer, alkyl halide (initiator), and copper (I) complex concentrations [60]. These observations are all consistent with eq. (2.21).

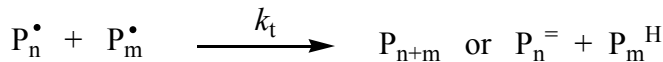
Initiation



Propagation



Termination



$$[P^\bullet] = (k_{act}/k_{deact})[R-M_n-X] ([Cu^I]/[XCu^{II}]) : \quad (2.20)$$

$$R_p = k_p^{app}[M] = k_p[P^\bullet][M] = k_p(k_{act}/k_{deact})[M][RX]_0([Cu^I]/[XCu^{II}]) \quad (2.21)$$

It is recognized that in ATRP and in all other LRP systems termination is not entirely eliminated. Therefore, chains will continuously terminate resulting in the increase of the persistent radical concentration and the progressive decrease of the growing radical concentration which may lead to some deviation from the first order kinetics in respect to monomer. However, contribution of the termination process under appropriate conditions is small and the concentrations of the radicals is reduced less than 10% during consumption of nearly all monomer and, therefore, deviation from the first order kinetics may not be detectable.

The polymerization rate is usually inverse first order with respect to the copper (II) complex concentration; however, determining the precise kinetic order with respect to the deactivator concentration is rather complex due to the generation of copper (II) via the persistent radical effect. In the atom transfer step, a reactive organic radical is generated along with a stable copper (II) species regarded as a persistent metallo-radical. If the initial concentration of copper (II) in the polymerization is not sufficiently large to ensure that the rate of deactivation is fast, then coupling of the organic radicals will occur leading to an increase in the deactivating copper (II) concentration. More radicals and deactivator will be formed and more radical combination will occur until the radical concentration decreases approximately to 10^{-3} M. At these concentrations the rate at which radicals combine ($k_{\text{term}} [\text{R}\cdot]^2$) will be significantly slower than the rate at which radicals will react with the copper (II) complex ($k_{\text{deact}} [\text{R}\cdot][\text{Cu(II)}]$) in a deactivation process, and a controlled/"living" radical polymerization will ensue. Under the aforementioned conditions, less than 10% of the polymer chains are terminated during this initial, short nonstationary process, but the majority of the chains (>90%) continue the polymerization successfully. If a small amount of a deactivator ($\approx 10\%$) is added initially to the polymerization, then the proportion of terminated chains is greatly reduced [60].

2.3.2.1 Molecular Weight Distribution ($\text{MWD} = M_w/M_n$)

In a polymerization based upon the ATRP catalytic cycle, the control of the polymerization and of the resulting polymers will depend upon the stationary concentration of the growing radicals and the relative of propagation and deactivation. Equation (2.22) explains how the MWD in polymerization systems with relatively fast exchange decrease with conversion, where p is the

polymerization conversion, $[RX]_0$ corresponds to the concentration of dormant polymer chains, and $[XCu^{II}]$ is the concentration of deactivator [115, 116].

$$M_w/M_n = 1 + \left(\frac{k_p[RX]_0}{k_{deact}[XCu^{II}]} \right) \left(\frac{2}{p} - 1 \right) \quad (2.22)$$

MWD is broader for shorter chains (higher $[RX]_0$) due to the fact that, relative to longer chains, the growth of smaller chains involves fewer activation-deactivation steps and therefore fewer opportunities for exchange and controlled growth. Second, the final MWD should be broader for higher values of the ratio, k_p/k_{deact} .

At the limit in which the deactivation process is very slow or does not occur ($k_p \gg k_{deact}$), ATRP simply becomes a conventional redox-initiated radical polymerization, [117] and broad MWD is observed. At the limit in which an average of one or a few monomer molecules are added per activation step, the polymerization is well-controlled and the MWD can approach a Poisson distribution [39].

Substantial studies [118-120] indicate that in order to obtain a polymer with a narrow molecular weight distribution, each of the following five requirements should be fulfilled.

- i. The rate of initiation is competitive with the rate of propagation. This condition allows the simultaneous growth of all the polymer chain.
- ii. The exchange between species of different reactivity is faster than propagation. This condition ensures that all the active chain termini are equally susceptible to reaction with monomer for a uniform growth.
- iii. There must be negligible chain transfer or termination.
- iv. The rate of depropagation is substantially lower than propagation. This guarantees that the polymerization is irreversible.
- v. The system is homogenous and mixing is sufficiently fast. Therefore all active centers are introduced at the onset of the polymerization.

2.3.2.2 Molecular Weight

ATRP is a catalytic process in which rates depend on concentrations of Cu(I) and Cu(II) species but molecular weights do not. Polymerization degree is exclusively

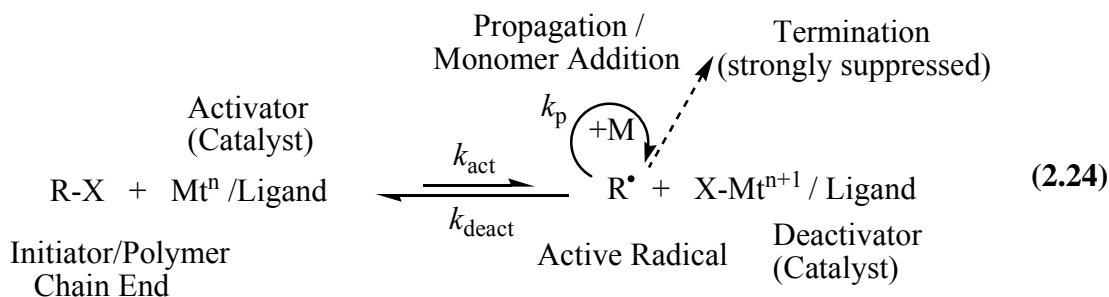
defined by the ratio of concentrations of the reacted monomer to the introduced initiator (provided that initiation is complete) as shown in eq. (2.23).

$$DP_n = \Delta[M]_0 / [RX]_0 \neq f([Cu^{I/II}]_0) \quad (2.23)$$

2.3.3 Procedures for Initiation of an ATRP Reaction

2.3.3.1 Normal Initiation

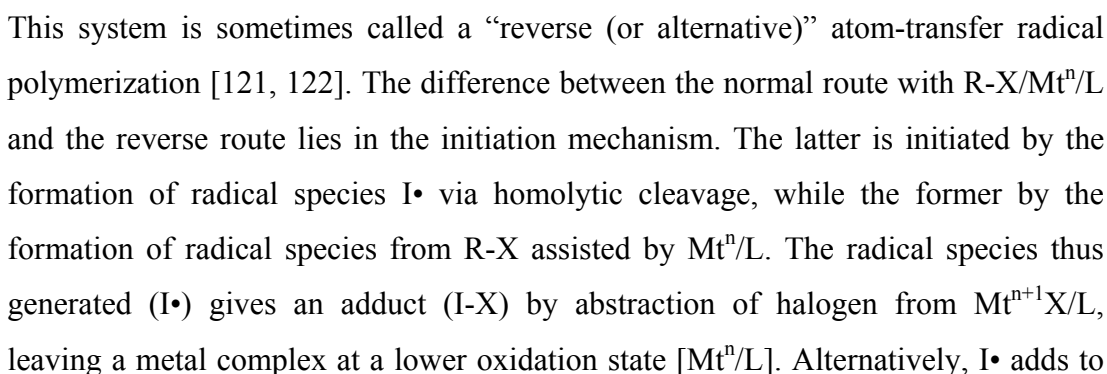
The procedure for “normal” initiation of an ATRP reaction, which was depicted in (2.24), employs a molecule, either a small molecule, macromolecule, or a functionalized surface, with one or more transferable atoms or groups, most often a (pseudo)halide, that undergoes a one electron redox reaction with a transition metal catalyst forming the reactive species [2, 3, 50, 53, 58]



The added initiator R-X can be a mono functional initiator, a multifunctional initiator, a macroinitiator, or an initiator attached to a surface; either a particle, flat surface or fiber.

The transition metal catalyst (M_t^n/L), where M_t^n is the transition metal in the lower oxidation state n complexed with appropriate ligand(s) L, reacts reversibly with the added initiator molecule and generates an oxidized transition metal halide complex ($X-M_t^{n+1}/L$) and a radical (R^\bullet). This radical propagates, adding monomer (M), and is rapidly deactivated by reaction with the oxidized transition metal halide complex to reform the lower oxidation state transition metal catalyst and an oligomeric X-terminated chain (P_1-X). This sequence can repeat itself, until the desired level of consumption of the monomer is reached, resulting in the synthesis of polymers with predetermined molecular weights ($DP_n = \Delta[M]/[RX]_0$) and narrow MWD ($M_w/M_n < 1.5$).

2.3.3.2 Reverse ATRP

$$\text{Free radical initiation} \quad \text{I-I} \xrightarrow{\Delta} 2 \text{I}^\bullet$$


the monomer to form an initiating radical species $[I-CH_2-C(R_1)-(R_2)\bullet]$ or a propagating species, which is also converted into a similar covalent species with a C-X bond accompanying reduction of $Mt^{n+1}X/L$. After formation of the dormant C-X species and the metal catalyst at a lower oxidation state, the polymerization proceeds similarly to the normal-type metal-catalyzed processes already discussed. The advantages of reverse ATRP include starting with the more stable transition metal complex, (which is particularly useful when one wants to use more active catalyst complexes, that are easily oxidized, and in miniemulsion systems) for the preparation of a range of linear copolymers with good chain end functionality.

The disadvantages of reverse ATRP are that it limits the terminal functionality remaining on the initiator residue (alpha-functionality) to that present as an additional functional group on the “I” residue and limits the topology of the polymers that can be prepared. One can only easily prepare linear (co)polymers. Furthermore the molecular weight of the final copolymer cannot be independently adjusted irrespective of the activity transition metal complex, since the transferable atom or group on the growing polymer chain end is introduced as a ligand on the added catalyst ((2.26) and (2.27)).

$$[M]_0 / [Cu^{II}X_2\text{-ligand}]_0 / [I\bullet]_0 = DP_{\text{target}} / 1 / 1 \quad (2.26)$$

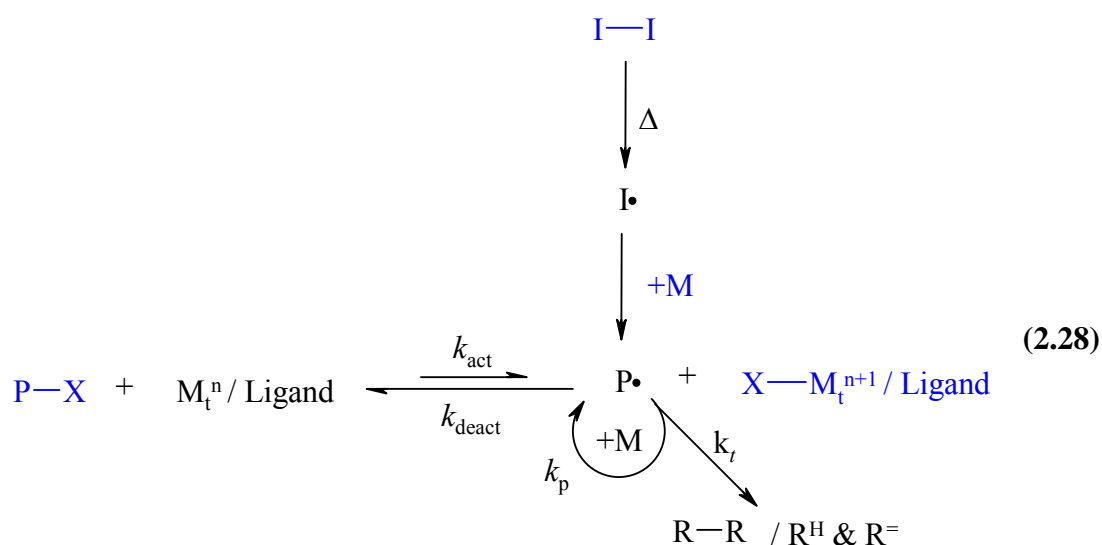
A high amount of catalyst (Cu^{II} -ligand) is required: $[Cu^{II}\text{-ligand}]_0 / [I - I]_0 = 1 - 1.5$

$$DP_{\text{target}} = \frac{\Delta [M]_0}{[I\bullet]_0} = \frac{\Delta [M]_0}{2 \times f_{I-I} \times [I-I]_0} \quad \text{and} \quad [I-I]_0 \sim [Cu^{II} / L]_0 \quad (2.27)$$

2.3.3.3 Simultaneous Reverse & Normal Initiation ATRP (SR&NI)

SR&NI was developed to overcome the problems “reverse” ATRP has with alpha-functionality, targeted MW and polymer architecture. In SR&NI a small amount of an active activating catalyst complex is generated by decomposition of a standard free radical initiator, such as AIBN, while the majority of the polymer chains are initiated by an alkyl halide via a normal ATRP process. This allows very active catalysts to be added to the reaction in their stable form and the bulk of the polymer to be formed from the added alkyl halide initiator.

The following equation (2.28) is a summary of the normal ATRP and reverse ATRP initiation mechanisms shown above showing how both initiation procedures are used in SR&NI. The reagents shown in blue are the reagents that are added to the SR&NI reaction. The first formed radicals undergo the reverse ATRP initiation reaction shown above but the bulk of the chains are initiated by a normal ATRP initiation mechanism. The degree of polymerization is predominately controlled by the concentration of alkyl halide, as expressed in the following equation (2.29), where f is the initiation efficiency of the added free radical initiator.



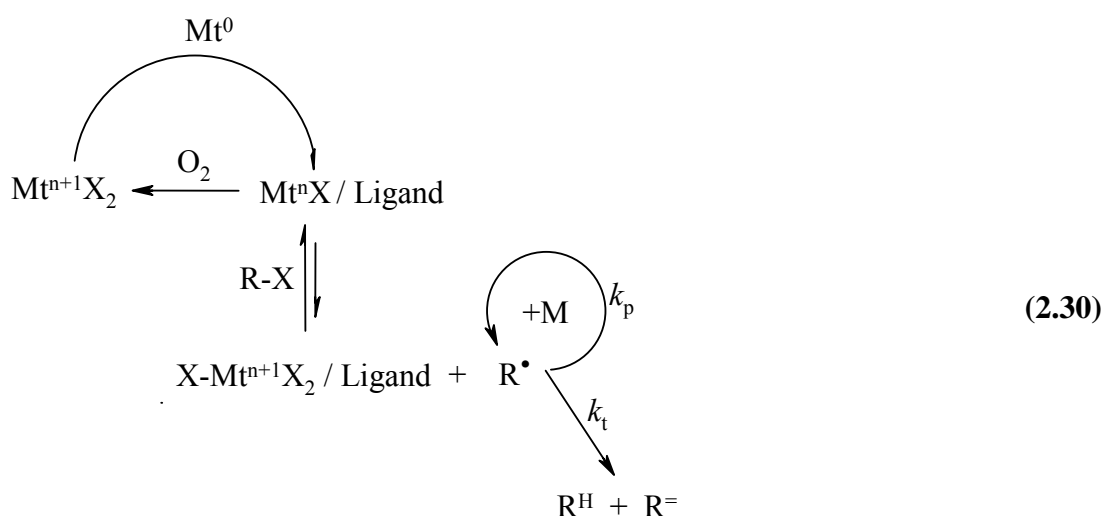
$$\text{DP} = \frac{\Delta[\text{M}]}{[\text{RX}]_0 + (2 \times f \times [\text{I—I}]_0)} \quad (2.29)$$

SR&NI was initially developed for bulk polymerization [123] where macroinitiators were used to prepare block copolymers. However SR&NI was quickly adapted to miniemulsion systems where addition of the catalyst precursor as an oxidatively stable salt prior to sonication simplifies the laboratory procedure [124-127] but major drawback is unavoidable homopolymer formation.

2.3.3.4 ATRP via *In Situ* Copper (I) Formation or Activator Generated via Electron Transfer ATRP (AGET)

The radical nature of the propagating species in ATRP is supported by the fact that addition of free-radical scavengers such as galvinoxyl or diphenylpicrylhydrazyl (DPPH) inhibits the ATRP [2, 49, 55]. However, Haddleton et. al. observed that a

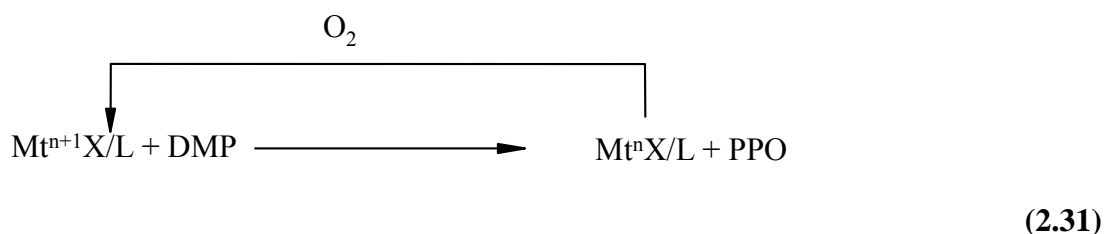
large excess of certain phenolic compounds increased the apparent rate of MMA polymerization in ATRP system, contradictory to their well-known inhibition role in radical polymerization [128-130]. The similar acceleration effect was reported by Heuts et al. for ATRP of MMA where octanethiol was used as a chain-transfer agent [131]. They claim that an acceleration effect is caused by a redox reaction between thiol and Cu (II), leading to the lowering of the concentration of both compounds. Moreover, the sulfonyl chlorides possessing phenol groups in the para position were used as initiators in ATRP without affecting the controlled polymerization condition [132, 133]. Furthermore, Matyjaszewski et al. reported that ATRP can be conducted in the presence of limited amount of oxygen and with unpurified monomers containing phenolic inhibitors [134]. In this case, the mixture of metal salts with their higher oxidation state and excess zero valent metals were employed. Because the Mt^nX is continuously produced by the redox reaction between zero valent metal and $Mt^{n+1}X_2$ in (2.30), after an induction period that can be attributed to the consumption of the oxygen by in situ formed Mt^nX , controlled polymerization conditions were achieved.



Inspired by this seminal works first ATRP system based on *in situ* copper (I) formation method was reported by Hızal et. al [135]. In this work, it was demonstrated that phenols in conjunction with Cu (II) / *N*, *N*, *N'*, *N''*, *N'''*-pentamethyldiethylenetriamine (PMDETA) complex can be successfully used to perform copper catalyzed ATRP of MMA, St, and methyl acrylate (MA) in the presence of limited amount of air. It was assumed that the electron transfer from phenol to Cu (II) would be the first step in this reaction. The Cu (I) so formed react

with either organic halide to form propagating radical or with oxygen to form copper salt in its higher oxidation state, which is then reduced to Cu(I) by excess phenol. Such regeneration of Cu(I) would be expected to lead to polymerization as a result of the consumption of oxygen and phenol as well.

Such a system, based on the redox couple of the metal complexes, is not specific to the ATRP but is applied to the other polymerization systems such as the oxidative coupling polymerization of 2,6-disubstituted alkyl phenols, where a wide variety of the Cu(I) and Cu(II)-amine complexes were used as catalyst [136] after its discovery in 1959 by Hay [137]. The chemistry of oxidative coupling polymerization of phenols involves the catalytic cycle of copper–amine complexes (2.31). Details of oxidative polymerization mechanism will be presented in section 2.4.



DMP = 2,6- dimethylphenol
PPO = Poly(phenylene oxide)
L = ligand (Amine)

ATRP via *in situ* copper (I) formation system is similar to a SR&NI ATRP in that it starts with alkyl halides as initiators and transition metal complexes in their oxidatively stable state (e.g., Cu^{II}Br₂/ligand) as catalyst precursors and therefore the most active catalyst complexes can be added to the reaction in their stable state. However, instead of employing a conventional radical initiator to activate the catalyst complex as in “reverse” ATRP and SR&NI, a non-radical forming reducing agent is employed to generate the activator.

However, this approach is different than the lower oxidation state metal initiated LRP in two respects:

- (i) In this system, reactive Cu(I) species are formed *in situ* via redox process between Cu(II) and phenols. Therefore, the small concentration of Cu(I) promotes the low concentration of transient radicals, in addition, the initial presence of Cu(II) (persistent radical) facilitates the deactivation process and thus suppresses undesirable radical-radical coupling reaction.

- (ii) The unavoidable oxidation of catalyst or the oxygen induced polymerization by the diffused oxygen as it was reported in lower oxidation state metal catalyzed LRP [138, 139] does not play detrimental role in this system.

Moreover, Matyjaszewski and coworkers demonstrated that this technique can be successfully applied to miniemulsion ATRP to prepare linear and star-shaped block copolymers. In this work, they used ascorbic acid as a reducing agent for copper (II) species. Since the copper (I) species, which is called activator as well, is formed via electron transfer from reducing agent, they named the process as activator generated via electron transfer (AGET) ATRP [140].

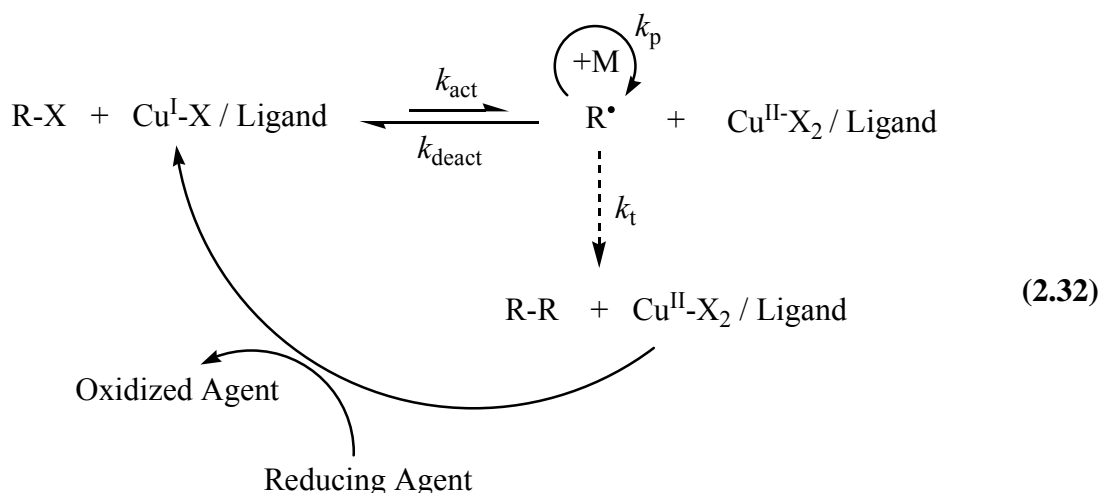
Same group reported that, tin(II) 2-ethylhexanoate ($\text{Sn}(\text{EH})_2$) can be used as a reducing agent for the catalyst precursor in an ATRP reaction. They further expanded the utility of the concept and conduct a simultaneous copolymerization of octadecyl methacrylate and ϵ -caprolactone. $\text{Sn}(\text{EH})_2$ was used simultaneously as the reductive agent for Cu(II) ATRP and as a catalyst for ring-opening polymerization (ROP) of ϵ -caprolactone, allowing formation of block copolymer in a one step by a dual mechanism [141].

Using the same approach, Hızal et. al. [142] reported the preparation of an oxidatively stable heterogeneous catalyst and its application for the benefits of the catalyst separation and recycling process in copper catalyzed ATRP. The details of this work will be given in the results and discussions part of this thesis.

Recently, Mert et. al. [143] performed the ATRP of St the presence of thiophenol derivatives such as sodium thiophenolate (PhSNa) or *p*-methoxythiophenol as a reducing agent for Cu(II) by using either 1-chloro-1-phenyl ethane (1-PECl) or ethyl-2-bromoisobutyrate (EiBr) as an initiator and *N,N,N',N'',N''*-pentamethyldiethylenetriamine (PMDETA) as ligand at 110 °C. The details of this work will be given in the results and discussions part of this thesis.

Moreover Matyjaszewski and coworkers, reported that the amount of copper catalyst in ATRP can be reduced to ppm levels if sufficient amount of reducing agent in conjunction with highly active catalyst such as tris(2-(dimethylamino)ethyl)amine (Me_6TREN) or tris(2-pyridylmethyl)amine (TPMA) was added. In this system, reducing agents constantly regenerate ATRP activator, the Cu (I) species, from the

Cu (II) species, formed during termination process, without directly or indirectly producing initiating species that generate new chains. a new system called activators regenerated by electron transfer (ARGET) ATRP [144, 145]. Reaction scheme was summarized in (2.32).



More recently, a highly active and versatile $\text{CuBr}_2/\text{N,N,N',N'}$ -tetra[(2-pyridyl)methyl]ethylenediamine ($\text{CuBr}_2/\text{TPEN}$)-tertiary amine catalyst system has been developed for atom transfer radical polymerization via activator-generated-by-electron transfer (ARGET ATRP or *in situ* copper (I) formation in ATRP) [146]. The catalyst mediates good control of the AGET ATRPs of methyl acrylate, methylmethacrylate, and styrene at 1 mol-% catalyst relative to initiator. A mechanism study shows that tertiary amines such as triethylamine reduces the $\text{CuBr}_2/\text{TPEN}$ complex to CuBr/TPEN . The $[\text{CuBr}_2(\text{TPEN})]/\text{tertiary amine}$ catalyst is highly active and versatile for AGET ATRP. By using TEA or TBA as the reducing agent and $[\text{CuBr}_2(\text{TPEN})]$ as the catalyst, well-controlled AGET ATRPs of MA, St, and MMA are obtained with 1 mol-% of catalyst relative to initiator, to produce PMA, PSt, and PMMA with molecular weights close to theoretical values and with narrow MWD. The volatile tertiary amines do not leave any residue in the resulting polymers.

In situ copper (I) formation method has attracted great attention in a short period of time since it has a significant advantage over “reverse” ATRP and SR&NI ATRP described above because it provides a route for synthesizing pure tele-functional polymeric materials of any desired architecture. [140-143, 147] The reagents directly

$$\begin{array}{c}
 \text{Cu(II)X}_2/\text{PMDETA} \\
 \downarrow \text{Reducing agent} \\
 \text{Oxidized product}
 \end{array}$$

$$R-X + \text{Cu(I)X/PMDETA} \xrightleftharpoons[k_{\text{deact}}]{k_{\text{act}}} R\cdot + \text{Cu(II)X}_2/\text{PMDETA} \quad (2.33)$$

$$R\cdot \xrightarrow[k_p]{+M} R^H + R^-$$

2.3.3.5 Macroinitiator Technique and Halogen Exchange

- i. The trivial one is that a maximum degree of livingness should be obtained for the first block. In general this requires some limitations to the maximum conversion in the synthesis of the first block. The probability of bimolecular

termination significantly increases if the polymerization would be carried out to (almost) complete monomer conversion.

- ii. The other important precaution concerns the sequence of block copolymer synthesis. Whether A–B or B–A is the preferred sequence mainly depends on the rate of initiation of the second monomer by the first block macroinitiator.

As an example, when PS-*b*-PMMA is the target structure, it is either the initiation of St polymerization by the poly(MMA) macroinitiator or the initiation of MMA polymerization by the PS macroinitiator. In the case of ATRP as the LRP technique of choice, and without the use of any advanced techniques initiation versus propagation needs to be studied. For the proper synthesis of a block copolymer a clean transition is required. Hence, initiation should be fast compared to propagation. When PS is used to initiate MMA this requirement is not met. Initiation is relatively slow, since for PS the activation–deactivation equilibrium lies strongly to the dormant side. To some extent this means that each chain that has undergone the transition to block copolymer is more reactive than the PS macroinitiator. The former chains will start to grow with a relatively high rate whereas the remaining macroinitiators still wait to be activated. The result is a broad molar mass distribution, or in the case of a low molar mass PMMA block, a large fraction of unreacted PS macroinitiator.

Conversely, when PMMA is used as a macroinitiator, initiation is relatively fast since the equilibrium between active and dormant chains lies more to the active side. The chains that get converted into block copolymer are less reactive in this case. In the limit it can be explained as a situation in which all the macroinitiators get converted into block copolymer before the chain growth of the second block [PS] commences.

As indicated above, this scenario holds for ATRP when no special techniques are invoked. There is one relatively straightforward technique to circumvent this forced order of block copolymer synthesis. This technique is called halogenexchange [148]. It relies on the difference in bond strength between an alkyl chloride and an alkyl bromide. The carbon–bromine bond is weaker than the carbon–chlorine bond. The result of this in a so-called mixed halogen system is that carbon–chlorine bonds are preferentially formed. In halogen exchange experiments, this phenomenon is used to slow down propagation relative to initiation.

In practice this would mean that PS-Br is synthesized from a bromine functional initiator using copper (I) bromide as the catalyst. In the second step, where MMA is polymerized, PS-Br macroinitiator is used in conjunction with copper(I) chloride. The macroinitiator chain gets activated and adds an MMA unit. Subsequently, it is deactivated by CuCl_2 (or CuClBr), which results in the formation of a carbon - chlorine bond, and thus a chlorine functional dormant block copolymer chain. Because of the difference in bond strength, the PS-Br is now more reactive than the $\text{P(St-}i\text{-b-MMA)-Cl}$. Hence, all the macroinitiator gets converted into dormant block copolymer chains, followed by propagation of the MMA block. Initially, the work by Matyjaszewski and co-workers on halogen exchange strongly emphasized the negative effect on propagation rate. This obviously leads to an increased ratio of initiation rate to propagation rate. At a later stage it was shown by Klumperman and co-workers that, apart from the effect on propagation rate, the use of copper chloride also leads to an increased rate of initiation (larger value of the activation rate constant of a bromine functional macroinitiator).

In summary, the need for halogen exchange arises due to a mismatch in reactivity when crossing over from terminal polymeric secondary alkyl halides to add monomers that form tertiary alkyl halides and is therefore recommended for the preparation of block copolymers when one is moving from a macroinitiator of lower activity, such as a styrene or an acrylate, to continue the polymerization with a more reactive monomer, such as a methacrylate or acrylonitrile [60, 86, 143, 149-155].

2.3.4 Controlled Composition, and Topology via ATRP

The spectrum of polymers that can be prepared by a well controlled ATRP presently includes polymers with any desired distribution in monomer units along the backbone and within any specific segment in a copolymer. This includes homopolymers, random copolymers, gradient copolymers, block, graft and star copolymers. Among them homopolymers, block copolymers, and star polymers will be outlined.

2.3.4.1 Homopolymers

Various monomers have been successfully polymerized using ATRP: styrenes, (meth)acrylates, (meth)acrylamides, dienes, acrylonitrile, and other monomers which contain substituents that can stabilize the propagating radicals. However, there are

still some limitations to the range of monomers that can be homopolymerized in an ATRP. The limitation is related to the requirement for repeated reactivation of the dormant species by the transition metal complex. With the current spectrum of catalysts there has to be a donor substituent adjacent to the transferable atom or group in order that the dormant chain end can be reactivated. The initial range of monomers that could be polymerized by ATRP included styrenes, (meth)acrylates, meth(acrylamides), and acrylonitrile which has recently been expanded to include 4-vinyl pyridine, and monomers containing an -OH group, such as 2-hydroxyethylacrylate (HEA) and 2-hydroxyethyl methacrylate (HEMA), glycidyl acrylate and ionic monomers. The major differences between the polymers prepared by ATRP and prior art radically polymerized polymers are the additional degree of structural control over molecular weight, PDI and telechelic functionality provided by LRP.

2.3.4.2 Block Copolymers

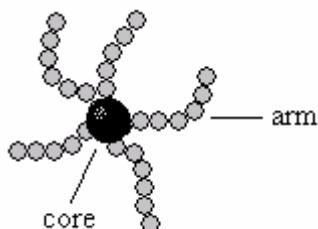
Linear diblock copolymers have long been studied for their microphase separation behavior and their ability in polymer blends to disperse incompatible phases and to increase interfacial adhesion. Diblock copolymers have been prepared using ATRP via two routes:

- i. by sequential addition of two monomers to the polymerization medium, or
- ii. by using isolated, purified ATRP homopolymers as macroinitiators [49, 53, 156].

When bifunctional initiators are used, ABA triblock copolymers can be prepared using these methods, including thermoplastic elastomers in which the central “A” segments are soft blocks such as *n*-butyl acrylate, methyl acrylate, and 2-ethylhexyl acrylate, and the outer “B” segments are hard blocks such as styrene, methyl methacrylate, and acrylonitrile [157] These types of block copolymers can also be synthesized by preparing segments using other polymerization techniques and then crossing over to ATRP. Crossover has been achieved from cationic polymerizations (Scheme 4) [158, 159], certain step-growth polymerizations [160], inorganic polymers, dendrimers [161, 162], and ring-opening metathesis polymerization (ROMP) [163].

2.3.4.3 Star Polymers

Star polymers constitute the simplest form of branched macromolecules where all the chains as arm segments of one molecule are linked to a center, which is called the core (2.34).

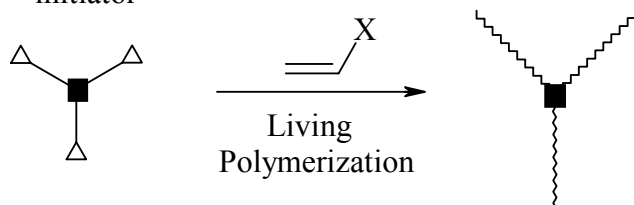


(2.34)

The core of the star polymer can be composed of a multifunctional low molar mass compound [164-167], a dendrimer [168], a hyperbranched polymer [169, 170], an arborescent structure [171] and a crosslinked microgel [172, 173]. Star polymers can be divided into two structural categories: homo- and mikto-arm star polymers. In the former case, the stars have arms with identical chemical composition, while in the latter case two or more than two different types of arms build the star molecule. Star polymers can be synthesized by one of three methods:

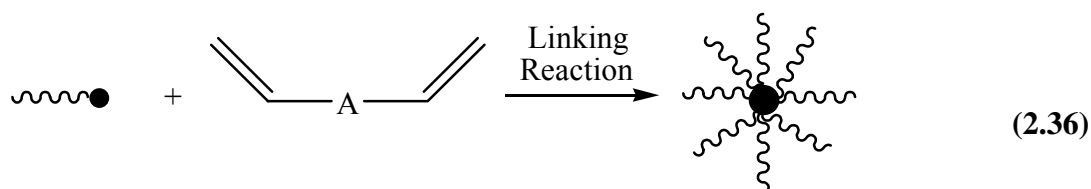
- i. “core-first” (2.35), where the controlled polymerization is conducted from well defined initiators with a known number of initiating groups [174-179] and less well defined multifunctional macromolecules [180-183];

Multifunctional
initiator



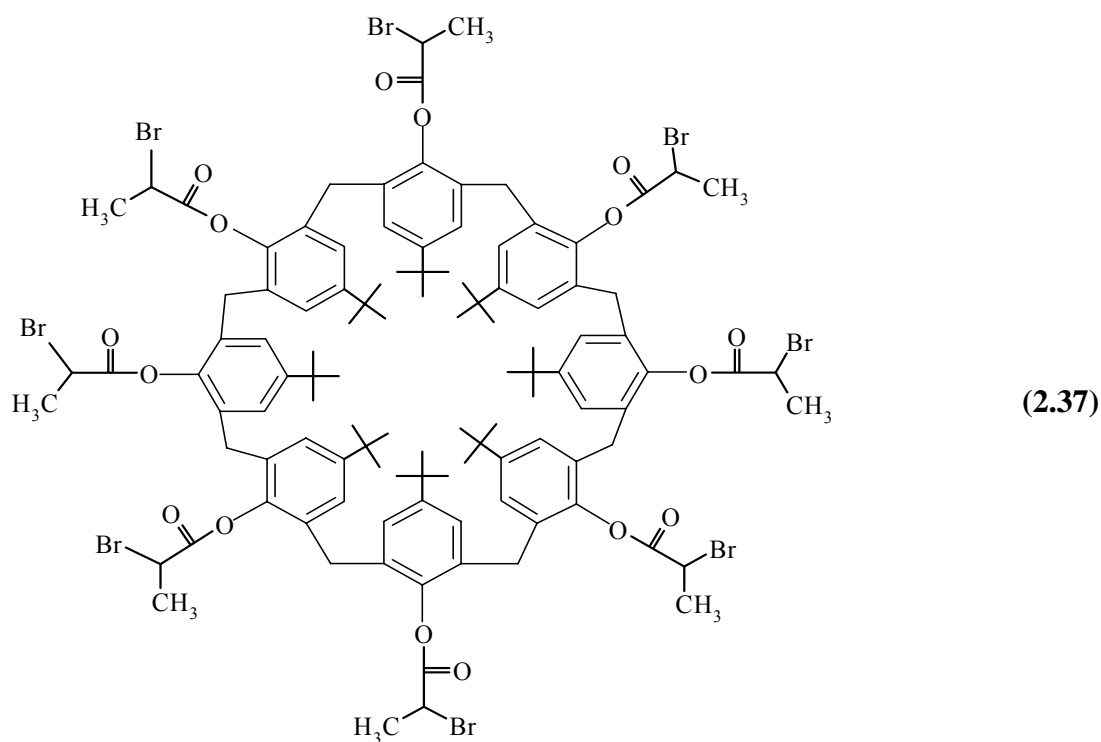
(2.35)

- ii. “arm-first” (2.36) [184-187] where a linear “living” copolymer chain is linked by continuing the copolymerization of a mono-functional monomer with a difunctional monomer forming a crosslinked core;



- iii. or their combination. [188-191] This synthetic strategy is a combination of “arm-first” and “core-first” methods and is particularly useful in the synthesis of miktoarm star copolymers. The retained initiating functionality in the arm first core is used in a grafting out copolymerization [190-192].

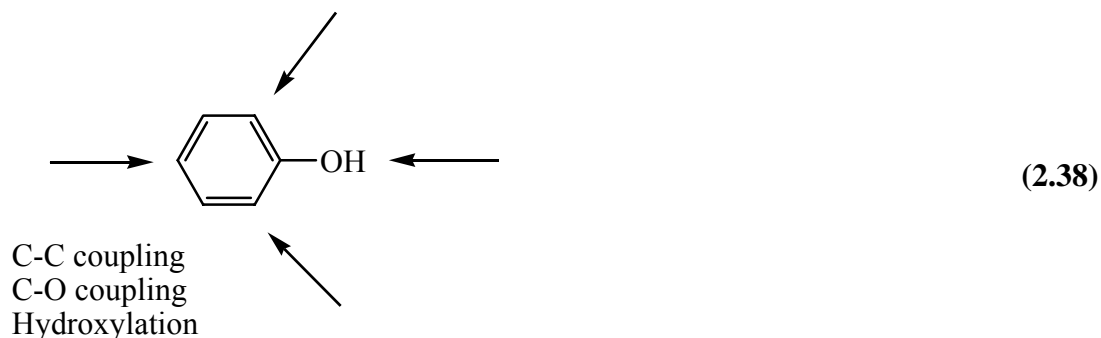
In this thesis, we synthesized 5,11,17,23,29,35,41,47-Octa-tert-butyl-49,50,51,52,53,54,55,56-Octakis-(2-bromopropionyloxy)calix[8]arene (2.37) according to a procedure reported by Angot et. al. [178] and used it as initiator for the ATRP of styrene to show the utility and convenience of the ATRP via *in situ* copper (I) formation method.



2.4 Oxidative Polymerization of Phenols

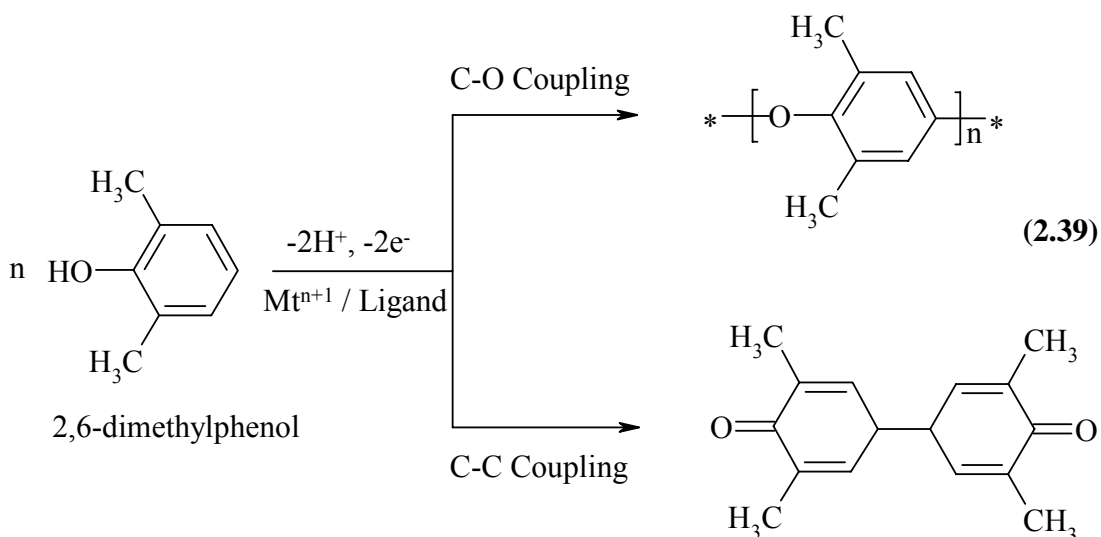
Oxidative polymerization of phenols catalyzed by a metal complex or an enzyme [137, 193-198] is one of the “green chemistry” processes where reaction conditions are mild and the only byproduct is water. Many phenols can be used in oxidative coupling polymerization reactions. These phenols usually have substituents in the

two *ortho* positions. Potential reaction sites in oxidation of phenol are shown in (2.38).



Most phenols with *ortho* alkyl, aryl, chloro or bromo substituents produce poly(phenylene oxide) in high yield. When the groups are bulky (e.g. *t*-butyl or isopropyl), the diphenoquinone becomes the main product and the yield of polymer is low. The diphenoquinone is also formed in significant quantities from 2,6-dimethoxyphenol. Phenols with only one *ortho* substituent and an open *para* position can be oxidatively coupled but the polymer is usually highly branched and colored. Presumably, oxidative coupling at the open *ortho* position leads to branching while other types of oxidation produce quinones and other colored moieties. Less branching is achieved by using a bulky amine as part of the catalyst to block the *ortho* position.

In particular, synthesis and properties of poly(2,6-dimethyl- 1,4-phenylene oxide) have been investigated in detail, because this polymer is widely used as an engineering plastics in industrial fields [199]. The copper catalyzed oxidation of 2,6-dimethyl phenol to PPO was first reported by Hay in 1959 (2.39) [137]. He found that the polymer (1) forms in high yield along with a small amount of a by-product, 3,3',5,5'-tetramethyl-4,4'-diphenoquinone (DPQ).

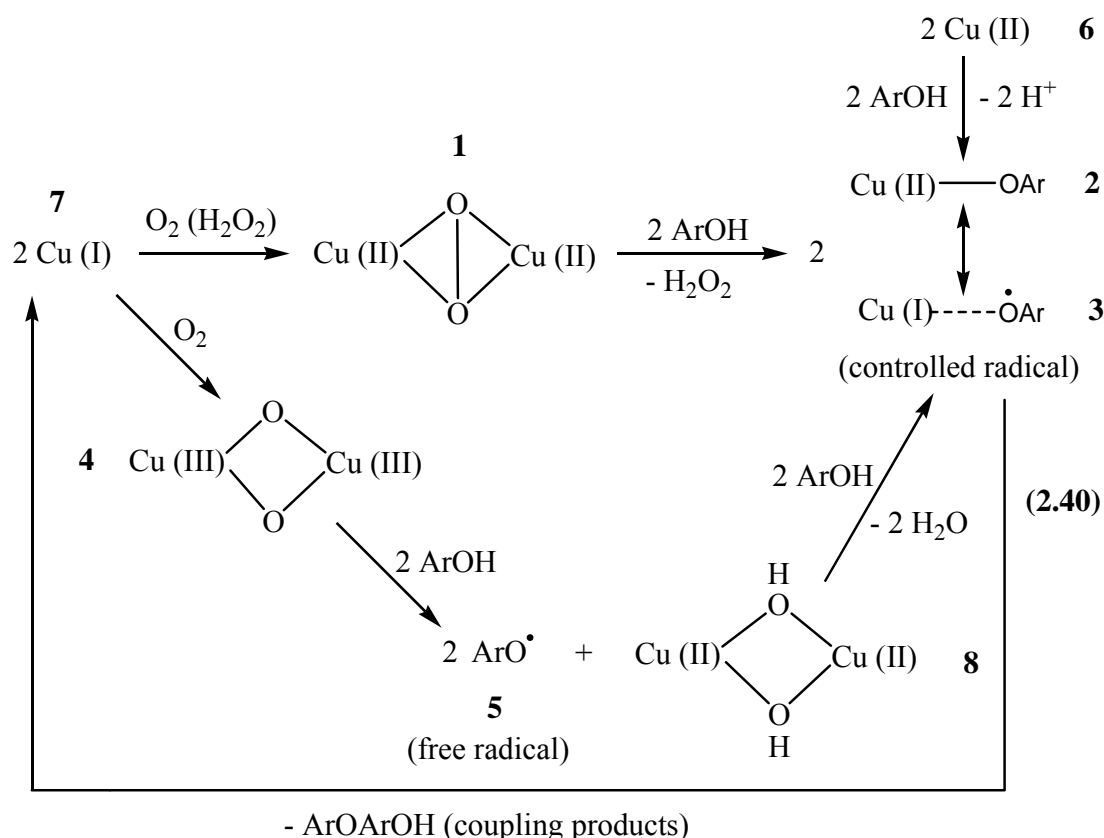


2.4.1 Mechanism

Direct synthesis of poly(1,4-phenyleneoxide) starting from phenol has been an attractive target for a long time [193, 197, 200]. Despite numerous efforts, no reports on successful regioselective oxidative polymerization of 2,6-unsubstituted phenols has been published until recently when Higashimura et al. reported very elegant “radical controlled” oxidative polymerization of *p*-phenoxyphenol by tyrosinase model complex catalyst to give poly(1,4-phenyleneoxide) [201, 202].

The working hypothesis explaining the regioselectivity of “radical controlled” oxidative polymerization is based on the formation of “controlled” radicals (2.40). μ - η^2 : η^2 -Peroxodicopper(II) complex 1 abstracts proton from phenol to give phenoxocopper(II) complex 2 which is equivalent to phenoxy radical-copper(I) complex 3. On the other hand electrophilic bis(μ -oxo)dicopper(III) complex 4 abstracts a hydrogen atom from phenol, generating free phenoxy radicals which are much more active compared to “controlled” radical 3 and, therefore, less selective.

Thus, high regioselectivity of tyrosinase model complexes is explained by the generation of mostly μ - η^2 : η^2 -peroxodicopper(II) complex 1 which is capable of “controlled” radicals 3 formation while electrophilic (μ -oxo)dicopper(III) complex 4 gives “free” phenoxy radicals having low regioselectivity [202]. On the other hand, experimental observations [203] and theoretical calculations [204] show fast and reversible isomerization between μ - η^2 : η^2 -peroxodicopper(II) and (μ -oxo)dicopper(III) complexes.



Moreover, they are almost isoenergetics which means perceptible concentration of (μ -oxo)dicopper(III) complexes in the reaction mixture generating free phenoxy radicals thus interfering “controlled” polymerization of phenols.

2.4.2 Metal Catalyst Systems for Oxidative Coupling Polymerization

Catalysts for oxidative coupling polymerizations are usually composed of a transition metal salt and a base. Molecular oxygen is normally the oxidizing agent. Most liquids that dissolve the polymer, such as benzene or toluene, can be used as solvents for the reaction. A desiccant or a polar liquid is often added to prevent water, a by-product of polymerization, from forming a separate phase which may interact with the catalyst. The transition metal is usually copper or manganese, although other metals, such as cobalt, are also active.

Copper catalyst systems often contain a copper halide and either an aliphatic or heterocyclic amine [137, 205]. *N, N'*-di-*t*-butylethylenediamine forms a very active catalyst that is not easily hydrolyzed during polymerization [205]. Di-*n*-butylamine also forms a catalyst with copper that is not sufficiently affected by water to require addition of a drying agent [206]. The types of heterocyclic amines that are used

include pyridine [137], morpholine and diazabicyclononene. Many polymeric amines are also reported to function as ligands, including poly(vinylpyridine) [207], imidazole polymers [208]. Copper catalysts using insoluble copper species [209], copper (II) chloride with potassium hydroxide, and mixtures of copper (I) and copper (II) ions [210] are also known.

2.5 Sulfur Chemistry

Sulfur (S) is a member of the oxygen family (the halcogenides) and in many respects it resembles oxygen, and also the heavier elements selenium (Se), and tellurium (Te). Alcohols, ethers, carbonyl compounds, and peroxides have their sulfur containing analogues; thiols (RSH), sulfides (thioethers), thiocarbonyl compounds, and disulfides (RSSR). There are, however, several distinct features of the sulfur atom in comparison with oxygen. Firstly, sulfur can form long stable polysulfide chains ($\text{R-S}_n\text{-R}'$, where $n \geq 2$) while oxygen can only form peroxides ($\text{R-O}_2\text{-R}'$). The O-O bonds (typical bond length 1.47 Å) are less stable than S-S bonds (ca. 2.04 Å) by around 20-40 kcal/mol due to stronger repulsion of the adjacent lone electron pairs and the lack of Π -bonding interactions in the former case. Secondly, sulfur can form compounds in which it exhibits a valence higher than two.

The lengths of the C-S and S-H bonds in alkyl thiols are about 1.77-1.82 and 1.34-1.40 Å respectively [211]. The bond dissociation energies (BDE) of S-H and C-S bonds in thiols and thioethers are markedly lower (typically, by 10-30 kcal/mol) than those of alcohols and ethers. The stability of C-S and C-O bonds are nearly equal only when the substituent at the halcogenide atom is capable of stabilizing (by resonance) the radicals formed by homolytic dissociation; examples of such substituents are the allyl and benzyl groups [212]. The average BDE of S-H bonds in alkyl thiols is 87 kcal/mol (compare to the values of 104 and 103 kcal/mol for the bonds O-H and N-H in alkyl alcohols and amines respectively). Similarly, the stability of the C-S bond in alkyl thiols (average BDE = 69 kcal/mol) is lower than that of the C-O (91 kcal/mol) or C-N (87 kcal/mol) bonds in alkyl alcohols and amines [213]. Thiols structurally resemble alcohols but the hydrogen bonds they form are significantly weaker, which is the reason for their high volatility. Thiols are stronger acids than the corresponding alcohols, with pK_a values for alkyl thiols of the order of 10-11. At the same time, sulfur is more polarizable than oxygen and thiols

and thiolates (RS^-) are significantly more nucleophilic, albeit less basic, than the similar oxygen compounds [214]. This is easily understood from the point of view of the theory of hard and soft acids and bases [215].

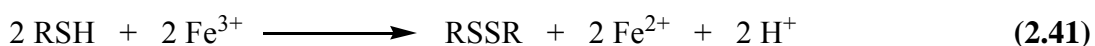
In contrast to the E-H and C-E bonds ($\text{E} = \text{O}$ or S), where the oxygen-containing compounds are more stable, as mentioned, the BDE of the S-S linkages are about 20-40 kcal/mol higher than that of O-O. The stability of the S-S bond depends strongly upon the nature of the substituents on the sulfur atoms and can drop significantly in the case of diaryl disulfides, due to the stability of the arylthiyl radical ($\text{ArS}\cdot$). For instance, the BDE of the disulfide bridge in Ph_2S_2 is only 20-26 kcal/mol, whereas in Et_2S_2 it is as high as 70 kcal/mol [212, 216]. The thermal stability of polysulfides decreases as the number of sulfur atom in the chain increases.

The photochemical degradation of disulfides [217] can lead to scission of either the S-S alone or both the S-S and C-S bonds, depending on light wavelength and disulfide structure. Thus, with 248 nm excitation the predominant dissociation pathway in dialkyl disulfides is S-S bond scission, whereas with excitation at 193 nm both mentioned bonds are cleaved [218, 219].

2.5.1 Oxidation of Thiols

Aliphatic and aromatic thiols are oxidized by a variety of reagents to disulfides and to higher oxidation products depending on the specific reaction conditions. In this chapter we shall mainly deal with the oxidation of thiols to disulfides by metal ions and salts.

Ions and oxides of transition metals which may exist in different valence states have been shown to oxidize thiols. Most of the studies so far available on this topic deal with the oxidation by ferric ions; careful investigations with many other metals have been carried out as well. Complexes of Fe^{III} as $\text{Fe}(\text{CN})_6^{3-}$ and ferric octanoate $[\text{Fe}(\text{Oct})_3]$ quantitatively oxidize thiols to disulfides in the absence of oxygen (2.41). This reaction has been largely employed in the synthesis of synthetic rubber [220].



Oxidation of thiols by $\text{Fe}(\text{Oct})_3$ has been carried out in acetone and xylene [221]. Kinetic studies indicate that the reaction follows a second order rate law. It is

suggested that disulfide arises from dimerization of thiyl radicals which are formed in the rate-determining reaction of thiol with $\text{Fe}(\text{Oct})_3$ (2.42), (2.43).



Like ferric ions, other heavy metal ions in their higher oxidation states reacts with thiols to give corresponding disulfides. Quite frequently complexation of thiols with the metal occurs followed by a one-electron transfer to give thiyl radicals which dimerize to disulfide. This is the case, for example with Ce^{IV} , Co^{III} , and V^{V} ions in acid solution [222-14].

2.5.2 Sulfur Containing Polymers

Due to the variety of structures and properties of sulfur-containing functional groups (enriched by the existence of several oxidation states of sulfur and the ability of sulfur atoms to form homopolyatomic chains), polymers with such groups have attracted great attention. Sulfur atoms can be either a part of the polymer backbone (e.g., in sulfide, polysulfide, sulfoxide, sulfone, thiocarbonate, and sulfonamide polymers), or substituents on the main chain [225-227]. Applications of polymers with sulfur based functionalities are diverse and include, among others, chemical and light resistant rubbers, [228, 229] ion exchange and chelating resins, [230] redox ('electron-exchange') polymers, [231, 232] membrane materials, [233] and conductive polymers. [234, 235] Sulfur containing polymers with di- and polysulfide groups have been the subject of many studies due to their resistance towards aggressive chemical agents (ozone, chlorine, etc.) and UV light.

Low molecular weight, oligomeric and polymeric di- and polythiols have been extensively studied in relation to their ability to form linear or crosslinked polymers with internal disulfide linkages upon mild oxidation [225, 236, 237]. The preparation of thiol containing polymers is therefore of significant interest. In principle, the thiol functionality can be introduced into a polymer using an appropriate sulfur-containing initiator. However, the direct application of thiol containing radical sources as initiators for the radical polymerization of vinyl monomers, which would lead to thiol-terminated polymers, is limited because of the large transfer constants of thiols

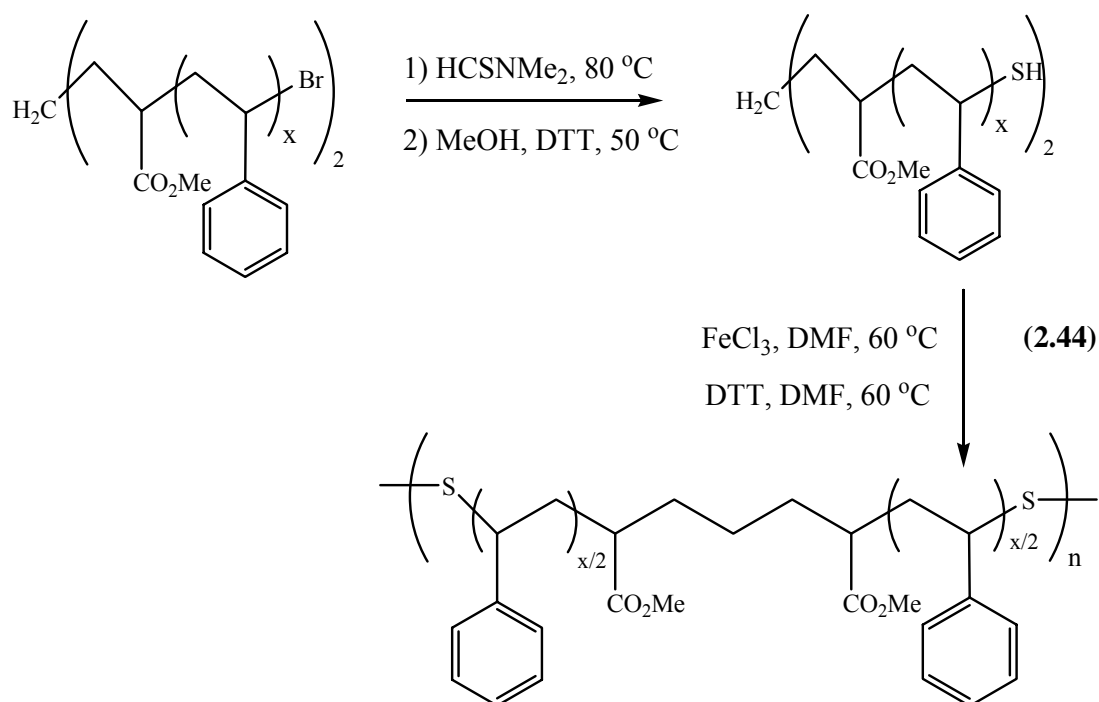
[238]. The use of protected thiols, with protective groups that can be removed after the polymerization, as radical initiators is therefore necessary. Thioether- or disulfide-based initiators can be used as precursors of thiols, because their transfer constants are significantly lower than those of thiols (For example, the transfer constant for dibutylsulfide in the polymerization of styrene at 60 °C is 0.0022; for dibutyldisulfide it is equal to 0.0024, and for butanethiol it is 22) [218, 238].

2.5.3 Application of Thiol-Disulfide Interchange in ATRP

Thiol-containing polymers can be prepared in two ways using ATRP. The halogen end-groups of the polymers obtained by ATRP [239] can be reacted with a sulfur-containing nucleophilic precursor of the thiol (e.g., (hydrogen)sulfide salts, thiourea, [240-242] thiodimethylformamide, etc. [243]), to form thiol end-functionalized polymers. On the other hand, the concept of using mono- or polyfunctional halide initiators with incorporated protected thiol groups can also be applied. For example, a 2, 4-dinitrophenyl-protected thiol-containing initiator has already been used for the ATRP of methyl methacrylate [244]. The success of ATRP in the presence of such thiol precursor relies on the significantly lower transfer constants of thioethers compared to thiols. As already mentioned, disulfides are another class of thiol precursors with relatively low transfer constants. Halide initiators with disulfide bond attached to a gold surface have already been employed for the ATRP of few vinyl monomers [218, 245, 246].

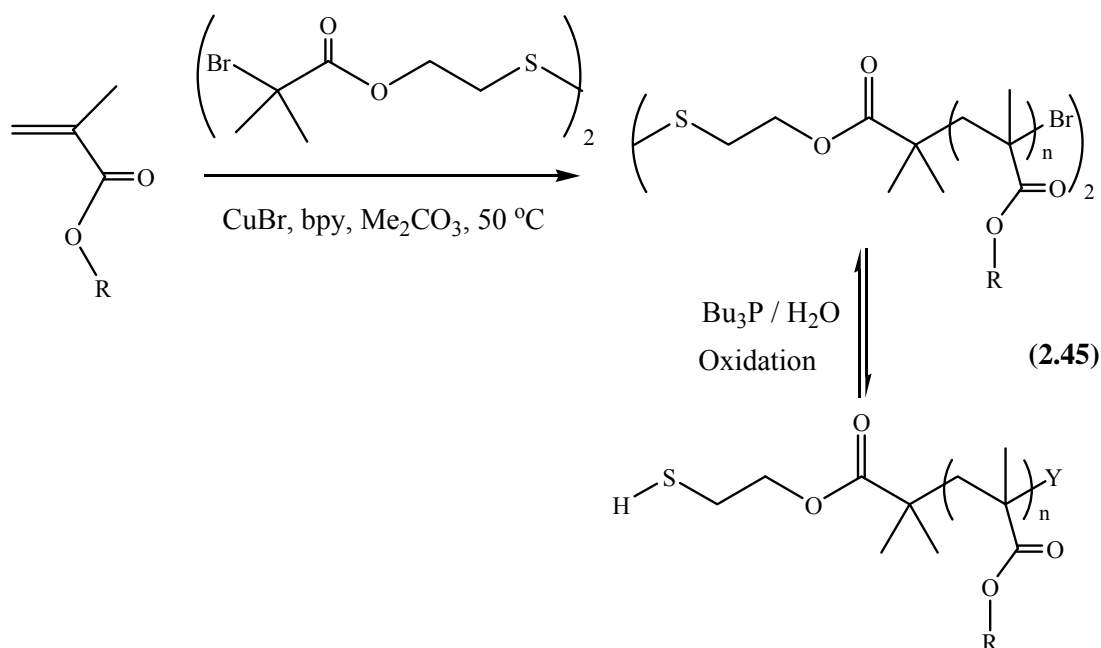
Moreover, Tsarevsky et al. [247] reported the use of diester of bis(2-hydroxyethyl) disulfide with 2-bromopropionic acid as initiator for the ATRP of styrene, leading to well-defined polymers with an internal disulfide bond. The catalyst employed was the CuBr complex of *N,N,N',N'',N'''*-pentamethyldiethylenetriamine. Radical coupling reactions were insignificant, especially when low catalyst concentration was used (0.2:1 vs the initiator). The reversible reductive cleavage of the disulfide bond in the presence of dithiothreitol (DTT) lead to polymers with a thiol end group. When the latter polymers were reacted with FeCl₃, oxidative coupling of the thiol groups occurred, regenerating the original polymer with an internal disulfide bridge. Both the reduction and oxidation reactions were efficient, and practically no unreacted starting polymer remained in the reaction mixtures.

Also a dibromo-terminated polystyrene was prepared by ATRP using the same catalytic system with dimethyl 2,6-dibromoheptanedioate as a difunctional initiator (2.44). The bromine end groups were successfully converted to thiol functionalities by a reaction with thiodimethylformamide, and the synthesized dimercapto-terminated polymer was oxidatively coupled to a high-molecularweight polymer with internal disulfide bonds using FeCl₃ as the oxidant.

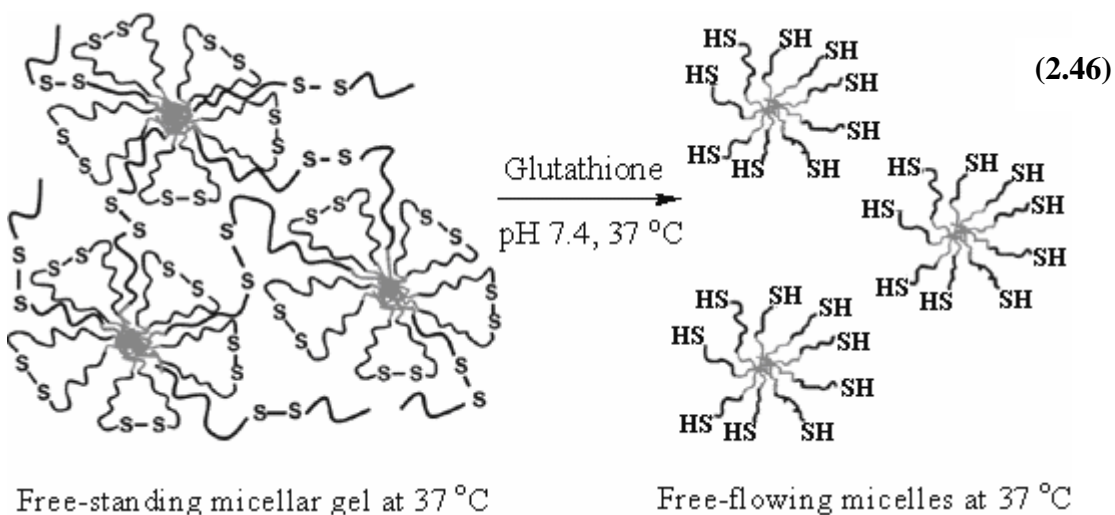


Same group reported the use of bis[2-(2-bromoisobutyryloxy)ethyl] disulfide as initiator for the ATRP of methyl, *tert*-butyl, and benzyl methacrylate, catalyzed by CuBr/2,2'-bipyridine, to yield well-defined linear polymers with internal disulfide bond [248]. The reductive cleavage of the latter with tributylphosphine was fast and efficient and produced polymers of lower molecular weight than the starting materials (2.45). Mixtures of methyl methacrylate (MMA) and a difunctional methacrylate monomer with internal disulfide bond were copolymerized by ATRP using disulfide containing initiator and the formed gels were successfully degraded upon reduction to form soluble, low molecular weight linear polyMMA fragments containing thiol groups at the chain ends and along the backbone (originating from the disulfide difunctional initiator and monomer, respectively). The disulfide-cross-linked gels contained alkyl bromide end groups and were used as “supermacroinitiators” in chain extension reactions with styrene, producing

degradable gels with pendant polystyrene chains that had higher swelling ratios in THF and toluene than the original polyMMA-based “supermacroinitiators”.



Furthermore, Li et. al. [249] have synthesized disulfide-based thermoresponsive triblock copolymer (PNIPAM-PMPC-S-S-PMPC-PNIPAM) via ATRP. Above LCST of NIPAAm they have obtained a free standing gel, by the cleavage of the central disulfide bond, micellar gel was dissolved irreversibly with no by-product (2.46). They have used Glutathione which is an important tripeptide antioxidant that is commonly found in cells to show that the cleavage can be achieved under physiologically relevant conditions. So these gelators are both biochemically responsive and thermoresponsive.



Distinctly, based on *in situ* generation of Cu (I) species strategy, we investigated the effectiveness of thiophenol derivatives bearing $-\text{NO}_2$, $-\text{OCH}_3$, etc. groups at *para* position in reducing copper (II) to copper (I) [250]. We observed that thiophenol derivatives with electron releasing groups tended to increase the rate of polymerization. Thus, sodium thiophenolate (PhSNa) was the most effective additive whereas *p*-nitrothiophenol was the least one. Based on these preliminary results and the literature given above, *in this thesis* among the thiophenol derivatives, we concentrated on PhSNa, and *p*-methoxythiophenol as reducing agent for copper (II) species.

2.6 Catalyst Residue in Products Prepared via ATRP

ATRP is very useful for synthesizing functional polymers of low molecular weight. For example, polymers with allyl [251, 252], vinyl [253], and hydroxyl groups [254-256] were readily prepared with molecular weights less than 10^5 . However, one of the major challenges facing ATRP is its low catalyst efficiency and thus the high catalyst concentration used. In a typical ATRP recipe, the initiator-to-catalyst ratio is usually 1:1, which is one catalyst molecule mediating one polymer chain. The metal halide usually is about 0.1-1% (molar) of the monomer. Residual catalyst in the polymer mixture deeply colors the product. Therefore, additional purification is required to remove the catalyst.

2.6.1 Postpolymerization Methods

In laboratory scale metal catalyst removal has been generally achieved by using alumina columns, precipitation of polymer to a nonsolvent, or precipitation of the Cu complex with sodium hydroxide (NaOH) or sodium sulfide (Na_2S). Although these methods are efficient, passing the viscous polymer mixture through a column of alumina is difficult on relatively large-scale reactions (>10 g). Additionally, repeated precipitations cause consuming of time and significant amounts of solvent. Furthermore ion-exchange resin treatment was reported by Matyjaszewski et. al. as a postpolymerization purification method, however it is not suitable for industry due to high cost [257].

2.6.2 Solid Supported ATRP

Heterogenization of homogeneous catalysts or products (solid phase synthesis [258]) for easy catalyst/ product separation and recovery has been widely used in industry for organic synthesis of small molecules or biopolymers such as peptides and oligonucleotides. Although solid phase chemistry is now considered almost routine for the synthesis of certain biological polymers (or synthetic polymers with biological activity), the use of insoluble supports has not been extensively developed for synthetic block copolymers. Solid-supporting technique (both solid phase ATRP and supporting the catalyst on a solid) has thus been explored for ATRP by immobilizing one of the separation components, the polymer or the catalyst, on a solid support [5].

2.6.2.1 Solid Phase ATRP

The use of insoluble supports to mediate organic transformations has been developed extensively over recent years. This chemistry has grown from the pioneering work of Merrifield [259] with “Merrifield” chloromethyl functionalized poly(styrene-*co*-divinylbenzene) beads being utilized for more than 20 years for the synthesis of medium-sized peptide using the *tert*-butoxycarbonyl (Boc) strategy. The use of a polymeric solid support (resin beads) for organic synthesis relies on three major requirements: (i) a crosslinked insoluble but solvent swellable polymeric material that is inert to the synthesis conditions, (ii) some means of linking the substrate to the solid phase that permit selective cleavage to give the final product, and (iii) a successful synthetic procedure compatible with the linker and the solid phase (Fig. 2.3).

One of the most commonly available resins used is Wang resin, which is based on cross-linked polystyrene onto which a 4-hydroxybenzyl alcohol moiety has been attached [260]. Angot et al. [261] immobilized the ATRP initiator group on Wang resins (2.47) and harvested the polymer chains by hydrolysis of the polymer-resin linkage through postpolymerization treatment.

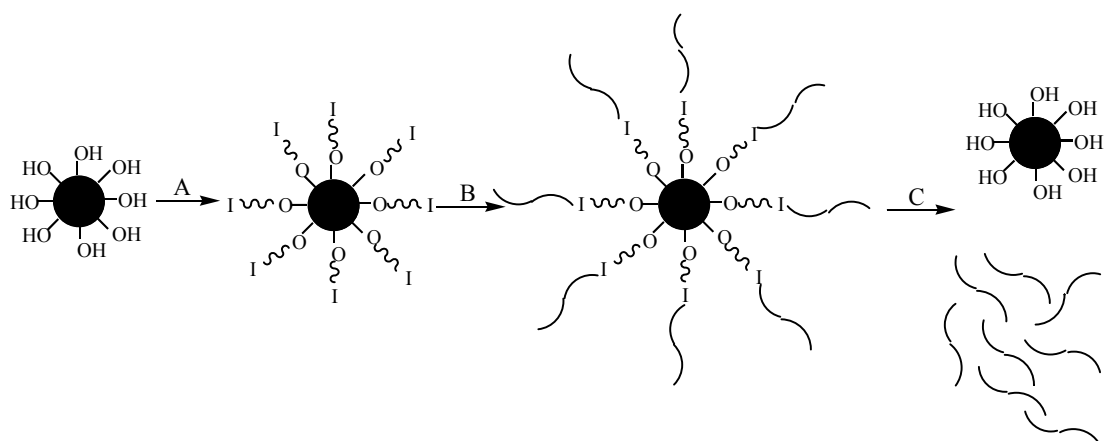
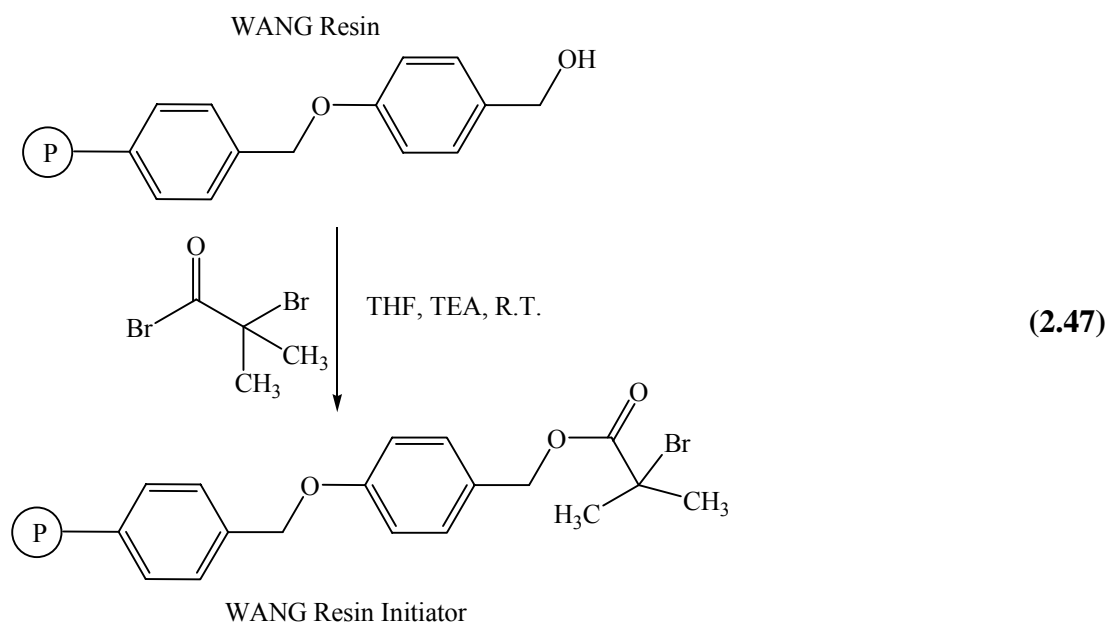


Figure 2.3: Solid-Phase ATRP. (A) Introducing Initiator Moieties; (B) 1, Solid Phase ATRP and 2, Separation and Purification; (C) Cleaving the Linkers and Polymer Harvesting.



Von Werne et al., Matyjaszewski and coworkers, have immobilized ATRP initiators on silica nanoparticles [262], polysilsesquioxane nanoparticles [10], or flat silicon surfaces [263]. In this system growing polymer chains on the solid surface is the key step. Excess of initiator (to produce Cu(II)) or Cu(II) must be added to suppress radical termination; otherwise, the Cu(II) concentration near the surface would be too low for an efficient deactivation. Polymerizations must be stopped at monomer conversions under 15%, as higher conversions resulted in interparticle coupling or gelation [264]. The MWD of the polymers was in the range of 1.2–1.4. This approach, however, requires extra catalysts or initiator and low monomer conversion, and thus is not expensive and not efficient. There is also a scale-up limitation [5].

2.6.2.2 Solid Supported Catalyst via Physical Adsorption

A possible solution to residual catalyst in the polymer mixture that colors the product is to support catalyst onto a solid that can be easily removed from the final product and ideally be recycled. Recently, ruthenium(II) catalyst supported onto amine-functionalized silica gel was successfully used for the heterogeneous ATRP of methyl methacrylate (MMA), which displayed typical living polymerization characteristics [265]. However, supporting CuBr for heterogeneous ATRP is not very successful. The copper bromide-hexamethyltriethylenetetramine (HMTETA) complex is an excellent catalyst for the ATRP of MMA, 2-(dimethylamino)ethyl methacrylate (DMAEMA), styrene (St), and methyl acrylate (MA) [252, 109]. It was demonstrated that CuBr/hexamethyltriethylenetetramine (HMTETA) could be adsorbed onto hydrophilic silica gel surface very effectively probably via hydrogen bonding of the silanol groups on the silica gel surface with the complex [266]. CuBr/HMTETA complex physically supported on the silica gel surface was successfully applied as catalyst for ATRP of MMA and macromonomer synthesis [267, 268]. The polymers resulting from these physically supported catalysts had well-controlled molecular weight and narrow MWD. The supported catalysts were recycled two to three times with good retention of the catalyst activities [267].

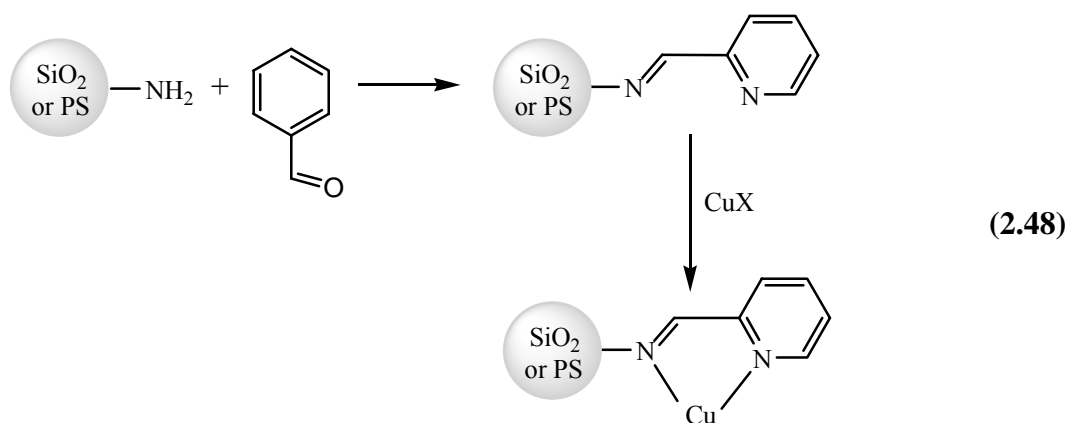
Additionally, a continuous polymerization process, which could *in situ* separate and reuse the catalyst, was also developed for the living homo- and block copolymerization of MMA using the silica gel supported CuBr/HMTETA [269, 270]. Homopolymerization of MMA was carried out by packing the supported catalyst in a tubular reactor, and the reactor was immersed in a water-bath. By continuously pumping the monomer and initiator solution through the reactor, the polymer was produced continuously. The reactor was stable in terms of activity and the molecular weight of the polymer produced for a period time depending on the flow rate and the silica gel/CuBr ratio. Compared to grafting methods [8, 271], this adsorption approach is much simpler and does not require special chemicals or tedious procedures. The controllability of the catalyst systems over the polymer molecular weight was even improved after recycling.

There are, however, several problems associated with these aforementioned techniques, the most important of which is that the catalyst has to be protected by inert atmosphere on separation process. Since these catalysts frequently lose their

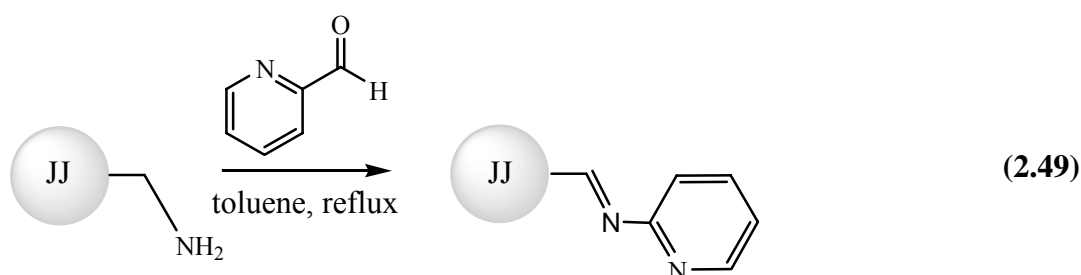
activity as a result of inevitable accumulation of Cu(II) (persistent radical effect) [15] during the first polymerization, a regeneration process of the catalyst, using a zero-valent metal was needed [4]. All these make the recycle procedure tedious, time-demanding, and expensive. Thus, Hizal et. al. [142] reported that the air-stable silica gel-CuCl₂/PMDETA catalyst complex can be successfully used for the ATRP via *in situ* copper (I) formation method. The details of this work will be given in the results and discussions part of this thesis.

2.6.2.3 Solid Supported Catalyst via Covalent Bonding

Continuous ATRP is an industrially important process that it continuously produces polymers, it offers a convenient control over the molecular weight of the product through adjustments in the flow rate, it reuses the catalyst, and it reduces the catalyst residue in the product. In continuous ATRP it was shown that the activity of the reactor packed with silica-gel-supported CuBr/HMTETA was stable over 100 h, but the activity declined afterward [269, 270]. The decrease in activity was ascribed to the catalyst loss from continuous washing out of the reactor because the catalyst was physically adsorbed on the silica gel. It is presumed that a reactor packed with the catalyst covalently bound on particles may have a better stability. Therefore, a covalently supported system for ATRP is desired for developing a stable continuous ATRP reactor. Silica-gel particles grafted with tetraethyldiethylenetriamine were synthesized as support for CuBr for the heterogeneous atom transfer radical polymerization of methyl methacrylate (MMA). The immobilized CuBr mediated a living polymerization of MMA, demonstrated by an increase in molecular weight with conversion and narrow MWD. An excessive amount of catalyst (typically, CuBr/initiator 5/1.5) was required to achieve a living process because of the limited mobility of the supported catalyst. The silica-gel concentration had a strong effect on the polymerization. The recycled catalyst still mediated a living process but showed a reduced catalytic activity due to the presence of Cu (II). After being regenerated by a reaction with Cu(0), the catalyst regained its activity [272]. Additionally Haddleton et. al. has shown that copper halide supported on silica gel/crosslinked polystyrene particles via alkylpyridylmethanimine can be used as catalyst in ATRP of methyl methacrylate (2.48). But polymerization did not show the characteristics of living polymerization [8].



Futhermore ATRP ligands were supported onto JandaJel resins (2.49) to allow for easy removal of the catalyst complex from the reaction mixture. Compared to divinylbenzene cross-linked resins, JandaJels have increased organic solvent compatibility and site accessibility due to the flexible cross-linker.

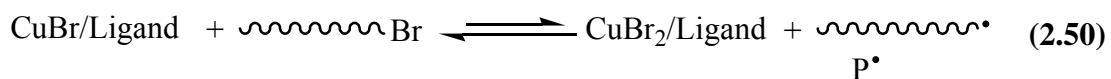


The JandaJel ligands were used in ATRP of methyl methacrylate (MMA), styrene, and 2-(dimethylamino)ethyl methacrylate (DMAEMA) [273]. Recyclability of the catalyst was demonstrated by reusing the catalyst for a second ATRP reaction. A PMMA-*b*-PDMAEMA copolymer was also synthesized using JandaJel ligands. After polymerization was complete, the catalyst/ligand complex was easily removed by filtration. Elemental analysis indicated 0.05-0.07% residual copper in the unpurified polymers.

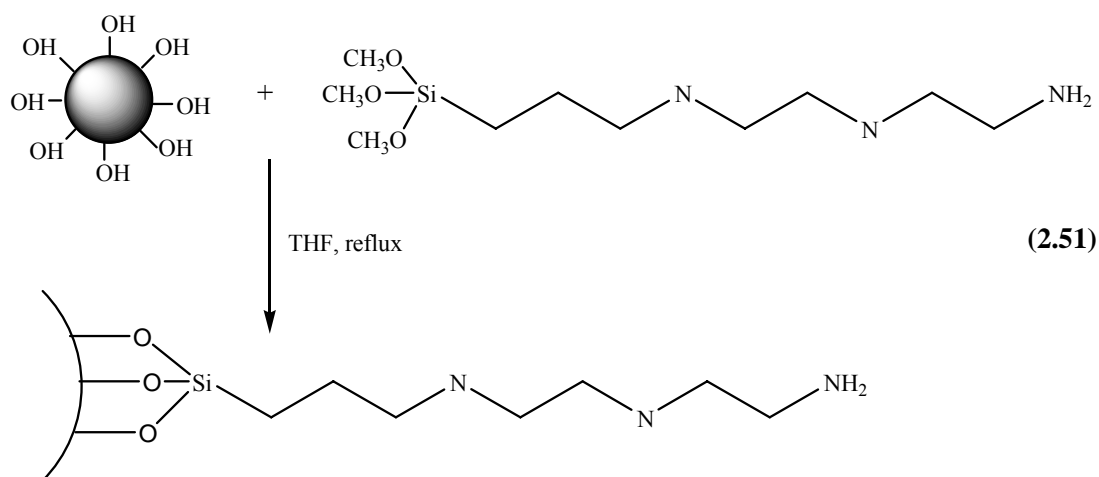
The JandaJel system does not remove copper as effectively as other copper removal systems such as the polyethylene supported ligand [274] or the hybrid system developed by Matyjaszewski and co-workers [4]. However, compared to the polyethylene system, the JandaJel ligands have shorter reaction times and the system seems better suited for a larger variety of monomers.

ATRP catalysts covalently supported on solids had much less control over polymerizations than unsupported catalysts, producing polymers with less controlled molecular weights and broad MWD [8, 271, 272, 275]. This lack of controllability of

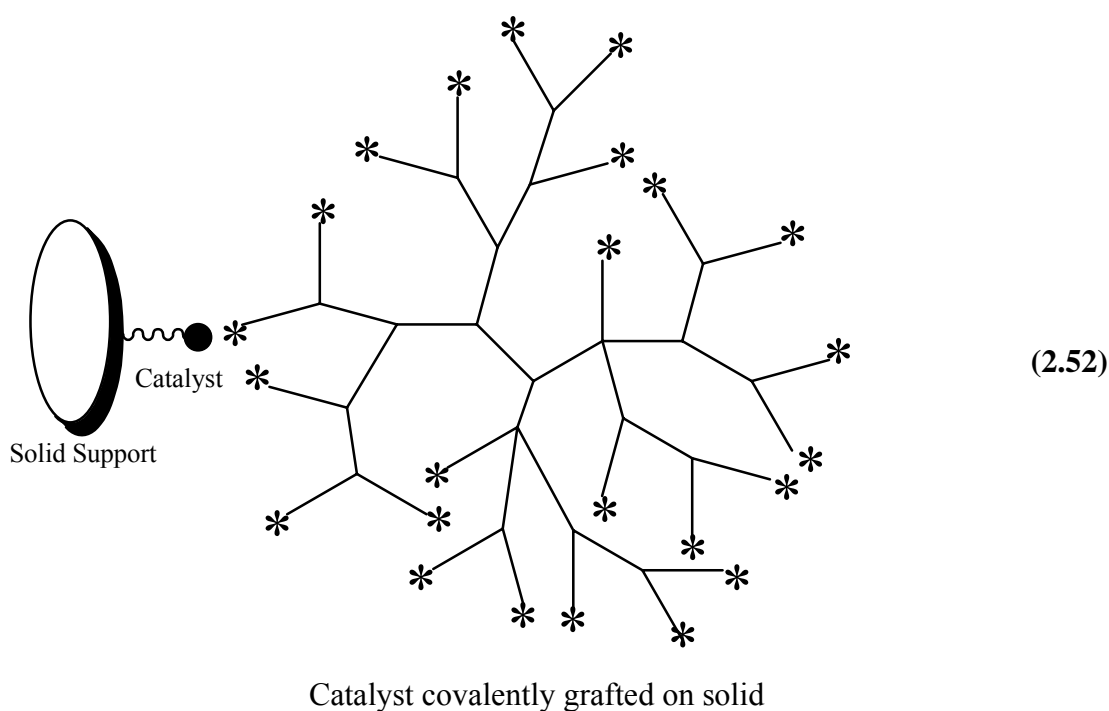
immobilized catalysts in ATRP might be caused by the diffusion limitation of the catalysts [4]. Since ATRP is based on a reversible activation/fast-deactivation process of radicals (2.50). It is critical for a good ATRP that the generated radicals be deactivated quickly to prevent side reactions; otherwise, the ATRP will behave like a conventional free radical polymerization.



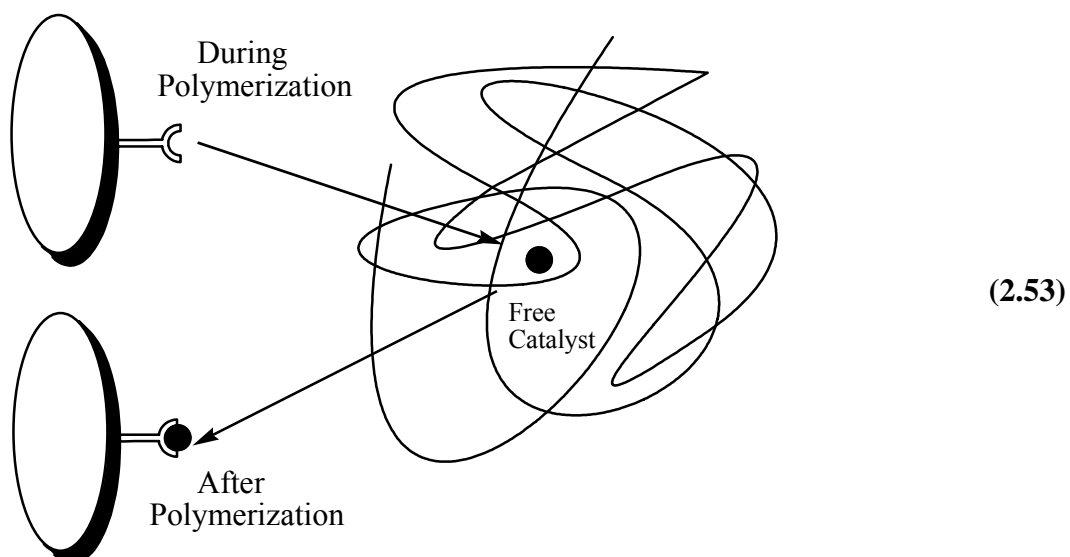
In a homogeneous catalyst system, the small molecules of catalyst can diffuse freely in solution and thus effectively regulate the polymer chain growth. However in an immobilized-catalyst system, the diffusion of polymer chains to the catalytic complexes anchored on a solid becomes rate determining step. The deactivation rate constant by the immobilized catalysts is thus reduced to the diffusion limit, ca. $10^5 \text{ L mol}^{-1} \text{ s}^{-1}$, compared with $10^9 \text{ L mol}^{-1} \text{ s}^{-1}$ of the diffusion limit for homogenous unsupported catalysts [4]. Thus the deactivation reaction (reverse reaction in (2.47)) may become slower, resulting in a less controlled ATRP. As a consequence, the overall effect of catalyst immobilization on solids is slowing the deactivation of the generated radicals, resulting in a high radical concentration (thus radical termination) and uncontrolled propagation of monomers. Thus it was proposed that the supporting spacer, through which the catalyst is attached to the particle, might affect the mobility of the catalyst (2.51). A short spacer provides the catalyst very limited mobility, while a long and flexible spacer renders the catalyst more freedom. However, a too long spacer may form coils surrounding the catalytic site and thus impede the access of the catalyst to the polymer ends for reaction (steric effect). The spacer effect was investigated by Shen et.al. by using silica gels grafted with tetraethyldiethylenetriamine (TEDETA) or di(2-picolyl)amine (DiPA) via poly(ethylene glycol) (PEG) spacers of different lengths for MMA polymerizations and it was found that the optimum spacer length was about three units of ethylene glycol since the supported catalyst had the highest reaction rate and the best control over the molecular weight of PMMA [275].



Another disadvantage of the catalyst immobilization on solids is the versatility of ATRP catalyst in synthesis of polymer structures. For example, solid-supported catalysts may not be useful in synthesis of hyperbranched polymers because they cannot reach inside the structure for catalysis (2.52).

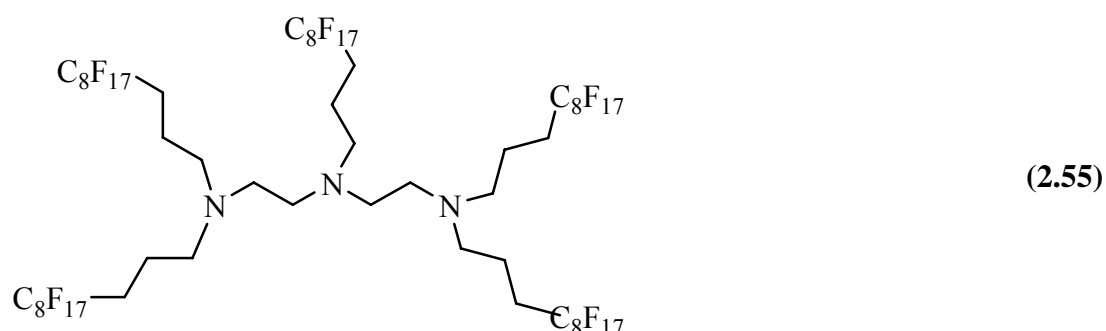


Therefore, a free catalyst is preferable for ATRP. Taking catalyst separation and recycling into consideration, an ideal catalyst immobilization for ATRP would be reversible, that is, the catalyst is in a free small molecule state under reaction conditions to effectively catalyze the polymerization, but associates on the solid support after the reaction for catalyst recycling (2.53).



It was demonstrated that the reversibly supported CuBr on polystyrene gel via triple hydrogen bonding of maleimide with diaminopyridine effectively mediated the polymerization of MMA, producing polymers with MWD as narrow as those by unsupported catalysts. In another work, the reversible catalyst supporting on silica gel using thymine-diaminopyridine triple hydrogen bonding pair was reported (2.55). The catalyst was attached on the diaminopyridine moiety via the ligand (TEDETA), and the silica gel was modified with thymine moieties. At room temperature, diaminopyridine and thymine subunits form ADA:DAD (A : acceptor, D : donor) type triple hydrogen bonding array, and thus the catalyst is bound to the silica gel, whereas at elevated polymerization temperature, the hydrogen bonding array breaks to release the catalyst for an effective catalysis (2.54) [276].

cyclization of unsaturated esters [284], reactions closely related to transition metal-mediated living radical polymerization. Liquid liquid biphasic systems based on the thermomorphic behavior of a fluorous biphasic system was first applied as ATRP medium by Haddleton et. al. [285]. ATRP of MMA performed in perfluoromethyl cyclohexane and equivolume of toluene was catalyzed by pentakis-N-(4,4,5,5,6,6,7,7,8,8,9,9,10,10,11,11,11-heptafluoroundecyl)-1,4,7 triazaheptane/Cu(I)Br (2.55). After polymerization, the reaction was cooled to ambient temperature and the two phases re-formed, a dark green lower layer and a colorless upper layer. After separation of the upper hydrocarbon layer, washing of the fluorous layer with toluene, and subsequent removal of volatiles, PMMA was obtained as a colorless glassy solid. Inductively Coupled Plasma (ICP) analysis of the product showed a copper level of 0.088% as opposed to 1.5%, which would be expected if all of the catalyst remained in the polymer.



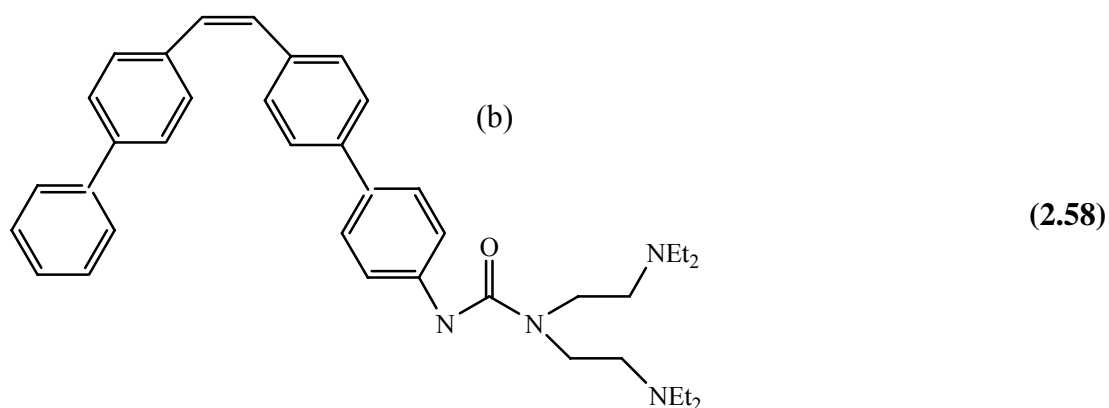
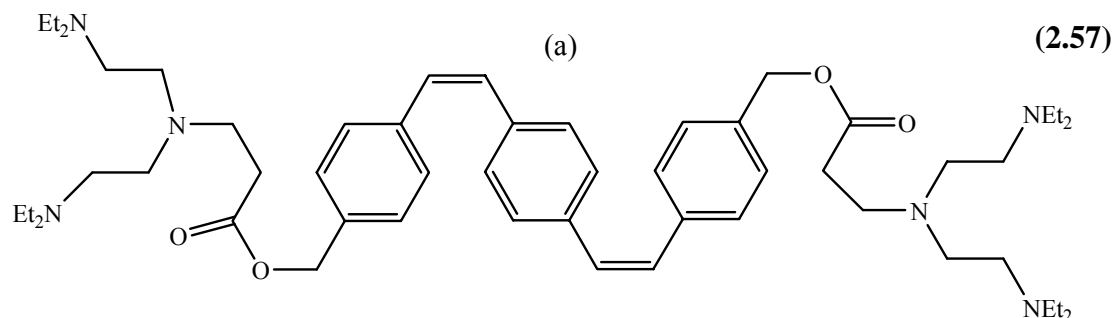
But its prohibitive cost and low efficiency in controlling the molar masses of the polymers renders it nonapplicable in industrial processes. Furthermore simple, molecular thermoresponsive CuBr/ hexasubstituted tetramine ligand-dioxane catalytic system for ATRP exhibiting both the advantages of simple recovery by filtration and optimal reactivity due to its homogeneous character at high temperature was reported [4] (2.56). In this work ATRP of methyl methacrylate (MMA) was carried out in 1,4-dioxane at 70 °C using CuBr/1 as catalyst.



2.6.3.2 Use of Precipitons

58

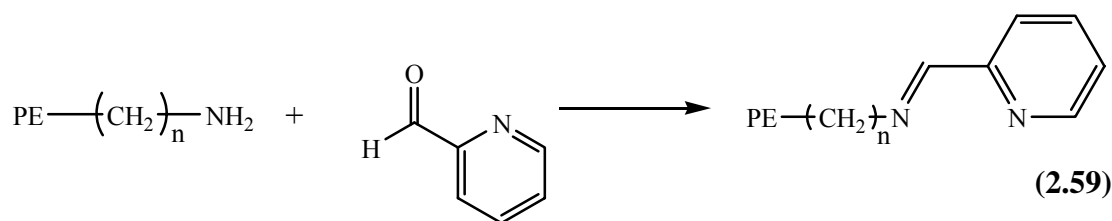
solution was cooled and exposed to UV radiation for 2 h. However, in this case the recovered catalyst complex loses its catalytic activity



The precipiton ligand precipitated and remained complexed with the Cu catalyst. The precipitated product can be isolated by decantation, filtration, or centrifugation. Copper content of the polymer solution was determined by UV spectroscopy and indicated no detectable copper based on the lack of absorbance at 680 nm. ICP analysis for copper content indicates <1% of original copper in the PMMA obtained using both ligands a and b. The PMMA from this reaction required no purification other than simple decantation.

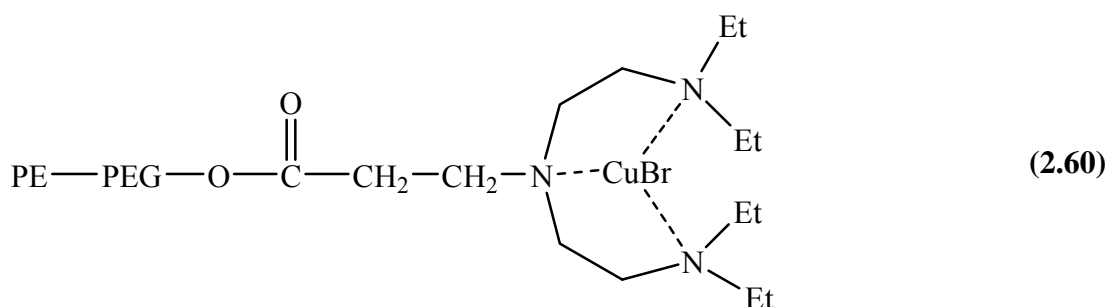
2.6.3.3 Soluble Linear or Hyperbranched Polymer Supported Catalyst

Poly(ethylene) (PE) is soluble under reaction conditions but precipitates from solution at room temperature due to the crystallization of PE, a property that has been exploited by Bergbreiter and co-workers in the design of catalyst systems [290]. Low molecular weight PE end-capped with appropriate ATRP ligands was used to mediate ATRP by Brittain and co-workers [274]. The synthesis of the PE ligand is shown in (2.59).



Compared with immobilized silica gel ligand, this polymeric PE-ligand offered somewhat better control of molecular weight and MWD with improved percent conversion. The molecular weight of produced PMMA was controllable, but the MWD was in the range of 1.4-1.5. PE-supported copper bromide was found to have very low activities even at 100 °C. Thus the ways to decrease the reaction time (26 h for 92.5 conversion) in order to decrease termination reactions need to be investigated.

Furthermore copper bromide supported on poly-(ethylene) via a poly(ethylene glycol) (PEG) spacer (2.60) was reported by Shen et. al. [278, 291]. Because PEG is soluble in common solvents, and its flexibility renders the catalyst more mobile at low temperature, which favors complexation of copper bromide with the ligand at ambient temperature and catalyst diffusion at higher reaction temperatures.

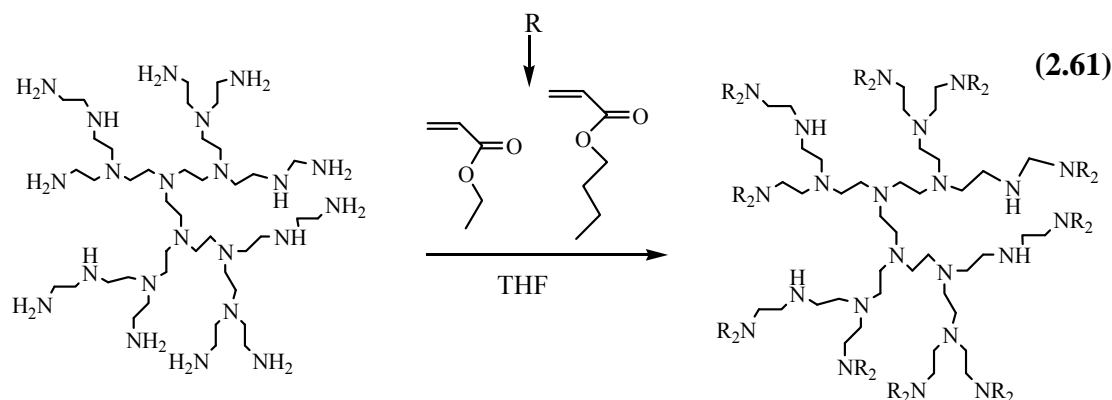


It was found that copper bromide supported to PE through a poly(ethylene glycol) (PEG) spacer gave high activities for the polymerization of methacrylates and styrene, producing polymers with well-controlled molecular weight and narrow MWD.

Additionally, ATRP using multidentate amine ligands supported on soluble hyperbranched polyglycidol was reported by Kumar et. al. [292]. The advantage of using hyperbranched polyglycidol lies in the availability of a large number of reactive end groups, which equals the degree of polymerization. Moreover, these hyperbranched polymers contribute little to the viscosity of the polymerization

medium owing to their low intrinsic viscosity. Use of a hyperbranched catalyst provides a system with high local concentrations of CuI and CuII complex moieties. Moreover most of the copper attached to this macroligand can be removed from the polymer by precipitation in methanol.

Moreover Shen et al. modified hyperbranched polyethylenimine (HPEI) by ethyl acrylate or butyl acrylate via the Michael addition reaction (2.61) [277].



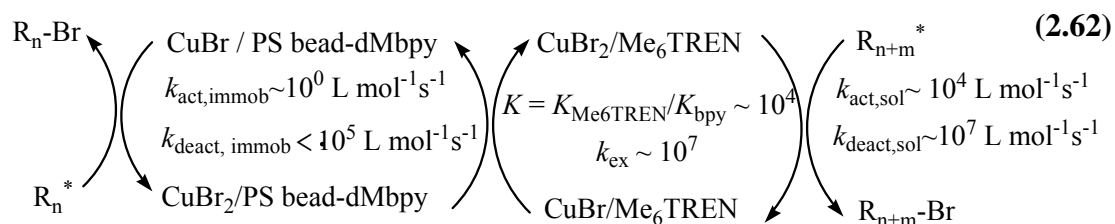
The resulting hyperbranched materials were utilized as macroligands for the copper-mediated ATRP of methyl methacrylate (MMA), representing an efficient catalyst system. Molecular weight distributions are narrow ($M_w/M_n < 1.4$), even at high conversion (96%), confirming that the ATRP of MMA with the hyperbranched macroligand/Cu(I) catalyst system represents a controlled process.

The use of HPEI possesses the following advantages: (i) Simple one-step-modified HPEI can be used directly as macroligand to form a complex with the Cu(I) catalyst for ATRP; however, as for other hyperbranched polymers, low-molecular-weight ligands have to be attached by multistep reactions. (ii) HPEIs possess low toxicity and are used widely in gene transfection [293-295], while low-molecular-weight ligands for ATRP, such as 2,2-bipyridines and their derivatives as well as multidentate amines, are toxic for humans as described by Aldrich. (iii) In addition, various molecular weight HPEIs are commercially available and considerably cheaper than other hyperbranched polymer supports.

2.6.3.4 Hybrid Catalyst Systems

The major factor controlling polymerization when using an immobilized catalyst system is the deactivation step, which is affected by both the mobility of the particles carrying the immobilized catalyst and the diffusion of the polymer chains in the

reaction mixture. While a homogeneous catalyst does not suffer from any diffusion barrier between higher oxidation state catalyst complex and growing radical, an immobilized catalyst attached to a bulky carrier hinders diffusion of the growing chain end to the catalytic site. Diffusion to a surface therefore may become the rate-determining step (2.62). This would result in a low apparent deactivation rate constant for an immobilized catalyst. A hybrid catalyst system for ATRP, composed of an immobilized catalyst and a small amount of soluble catalyst, was investigated for ATRP.



The level of control over the polymerization of vinyl monomers was significantly improved by the addition of part per million quantities of a secondary soluble catalyst to a solid supported immobilized catalyst. The role of the soluble catalyst component is to facilitate an effective deactivation process by delivering the halogen from the solid immobilized catalyst to growing polymeric radicals, thus overcoming diffusion barriers. The use of a hybrid catalyst system afforded a high conversion of monomers to polymers displaying a predetermined molecular weight and narrow molecular weight distribution. It was shown that $\text{CuBr}_2/\text{Me}_6\text{TREN}$, which is a more reducing soluble catalyst, was advantageous as the soluble catalyst component, since this characteristic accelerated the halogen exchange reaction. A range of suitable immobilized catalysts can be constructed from different supports, different attached ligands, and encompassing particles of different sizes and pore structures. The successful controlled polymerization of vinyl monomers such as MMA, MA, and styrene, providing polymers with various degrees of polymerization and different architectures (such as block copolymers), proves the versatility and living character of the system [296, 297]. In a batch polymerization system, the immobilized catalyst can be removed from the polymerization media by simple filtration or sedimentation, affording a colorless transparent polymer solution with a salient reduction of the residual transition metal in the final polymer products.

3. EXPERIMENTAL WORK

3.1 Materials and Chemicals

3.1.1 Monomers

Methyl methacrylate (MMA, 99%, Acros), styrene (St, 99%, Acros), *n*-butyl acrylate (*n*BA, 99%, Aldrich) were passed through a basic alumina column to remove inhibitor and distilled over calcium hydride (CaH_2) *in vacuo* prior to use if otherwise indicated.

3.1.2 Solvents

Toluene (98 %, J.T. Baker)

It was distilled over metallic sodium and stored under nitrogen.

Tetrahydrofuran (THF, 99.5%, J.T. Baker, HPLC grade)

It was dried and distilled over benzophenone-sodium.

***N*, *N*-dimethylformamide (DMF, 99%, Fluka, HPLC grade)**

It was used as received.

Methanol (Technical Grade)

It was used as received.

Acetonitrile (99.8%, J.T. Baker, HPLC grade)

It was used as received.

Ethylene carbonate (EC, 98%, Aldrich)

It was used as received.

Water (J.T. Baker, HPLC grade)

It was used as received.

Anisole (99%, Acros)

It was used as received.

3.1.3 Other Chemicals

***N,N,N',N'',N'''*-pentamethyldiethylenetriamine (PMDETA, 99%, Acros)**

It was used as a ligand for ATRP after distillation over NaOH.

1-chloro-1-phenyl ethane (1-PECl, Acros)

It was used as received.

4-*tert*-butylcalix[8]arene (97%, Acros)

It was used as received.

Ethyl-2-bromo*isobutyrate* (EiBr, 98%, Aldrich)

It was used as received.

Methyl-2-bromopropionate (MBP, 98 %, Aldrich)

It was used as received.

CuCl₂ (99.9 %, Aldrich)

It was used as received.

CuBr₂ (99.9 %, Aldrich)

It was used as received.

CuBr (99.9%, Aldrich)

It was used as received.

Triethylamine (99%, Merck)

It was used as received.

2-bromopropionylbromide (97%, Aldrich)

It was used as received.

D-fructose (98.5%, Merck)

It was used as received.

L-ascorbic acid (99%, Merck)

It was used as received.

***p*-methoxyphenol (99%, Aldrich)**

It was used as received.

***p-tert*-butylphenol (99%, Aldrich)**

It was used as received.

Dihydroquinone (99%, Aldrich)

It was used as received.

Sodium hydride (NaH, dry, 95%, Aldrich)

It was used as received.

Silica gel (Merck, particle size of 0.063–0.2mm and average pore diameter of 60 Å°)

It was boiled in deionized water for 5 h, filtered, and then vacuum dried.

Sodium Phenoxide (PhONa)

It was prepared by the reaction of phenol and sodium hydride (NaH) in tetrahydrofuran (THF). NaH (0.264g, 0.011 mol) was added to a solution of phenol (0.941g, 0.01 mol) in dry THF (50 mL). The reaction mixture was stirred for 3 h. at room temperature. After filtrating the reaction mixture, crude product was washed with dry THF. Product was isolated by vacuum filtration and then, dried at room temperature *in vacuo* for 1 day.

Thiophenol (PhSH, 99%, Acros)

It was used as received.

***p*-methoxythiophenol (99%, Aldrich)**

It was used as received.

Sodium Thiophenolate (PhSNa)

It was prepared by the reaction of thiophenol (PhSH) and sodium hydride (NaH) (dry, 95%, Aldrich) in dry THF. NaH (0.264g, 0.011 mol) was added to a solution of thiophenol (1.1g, 0.01 mol) in dry THF (50 mL). The reaction mixture was stirred for 3h. at room temperature. The purification procedure was done in the similar manner with the PhONa preparation procedure.

3.2 Equipment

3.2.1 Gel Permeation Chromatography (GPC)

The number-average molecular weight (M_n) and molecular weight distribution ($MWD = M_w/M_n$) of polymers were determined by Agilent Model 1100 gel permeation chromatography (GPC) consisting of a pump, refractive index, and four Waters styragel columns (HR5E, HR4E, HR3, and HR2). Measurements were conducted using THF as eluent at 30 °C and at a flow rate of 0.3 mL/min. Data analyses were performed with PL Caliber software. The system was calibrated with narrow PS standards (Polymer Laboratories).

3.2.2 Gas Chromatography (GC)

Monomer conversion was determined using a Unicam 610 Series gas chromatograph equipped with an FID detector using a J and W Scientific 15-m DBWAX wide-bore capillary column. Injector and detector were kept constant at 280 and 285 °C, respectively. Analysis was carried out isothermally at 40°C for 2 min followed by an increase of temperature to 160 °C at a heating rate of 20 °C/min and holding at 160 °C for 2 min. Conversion was calculated by detecting the decrease of the monomer peak area relative to the peak areas of the internal standard anisole.

3.2.3 UV-Visible (UV-VIS) Spectrophotometer

UV visible spectra were recorded on a Perkin-Elmer Lambda-2 spectrophotometer.

3.2.4 Nuclear Magnetic Resonance Spectroscopy (NMR)

The ^1H spectra were recorded on a Bruker NMR spectrometer (250 MHz for ^1H NMR) using CDCl_3 as solvent and tetramethylsilane as an internal standard.

3.2.5 Matrix Assisted Laser Desorption/Ionization Time-of-Flight (MALDI-TOF) Mass Spectrometer

Matrixassisted laser desorption/ionization time-of-flight (MALDI-TOF) spectra were recorded on an Applied Biosystems Voyager DE STR MALDI-TOF spectrometer equipped with 2-m linear and 3-m reflector flight tubes and a 337-nm nitrogen laser (3 ns pulse). All mass spectra were obtained with an accelerating potential of 20 kV in positive ion mode and in reflector mode. Dithranol (10 mg/mL in THF) was used as a matrix, silver trifluoroacetate (AgTFA) (1 mg/mL in THF) was used as a cationating agent, and PS samples were dissolved in THF (10 mg/mL). Poly(ethylene oxide) standard ($M_n = 2000$ g/mol) was used for calibration. All data were processed using the Data Explorer (Applied Biosystems) software, while the Polymerix (Sierra Analytics) software package was used to determine M_n .

3.2.6 Atomic Absorption Spectrometer

(PerkinElmer 3030 Ziman AA) was used to determine the amount of residual copper in the polymer.

3.3 Synthetic Procedures

3.3.1 UV–VIS Monitoring of *In Situ* Copper (I) Formation via Electron Transfer from Fructose

The preparation of a stock solution was done as follows: into a 10 mL of volumetric flask, PMDETA (455 μ L, 2.18 mmol), CuCl₂ (29.3 mg, 0.218 mmol), fructose (19.6 mg, 0.109 mmol) and water were added. From this homogeneous mixture, 0.5 mL of aliquot was diluted to 5 mL and the spectrum was immediately measured. A stock solution is then transferred to a 25 mL of flask equipped with rubber septum. The flask was subjected to nitrogen-vacuum cycles three times after which the reaction mixture was placed in a thermostated oil bath at 85 °C. 0.5 mL of aliquots were taken at given time intervals and diluted to 5 mL for UV–VIS measurements.

3.3.2 General Procedure for the Kinetic Studies of ATRP of St (or *n*BA) Catalyzed by Cu(II)/PMDETA/Reducing Agent (RA)

Monomer, PMDETA and CuX₂ (X: Cl or Br) were added into a Schlenk flask (25 mL) equipped with a magnetic stirring bar, and stirred for 10 minutes. Then RA, anisole (internal standard for GC), and initiator were added in that order. The first kinetic sample was taken from the reaction mixture for GC measurement, before it was degassed by using three freeze-pump-thaw (FPT) cycles. The reaction flask was back-filled with argon and immersed into an oil bath preheated to the appropriate temperature. Kinetic samples were taken from the polymerization mixture with argon purged-syringe at a given time interval under positive argon atmosphere and transferred into the sample vials. The post polymerization was inhibited by immediate immersion of the sample vials in liquid nitrogen. The kinetic samples were diluted with THF and purified by passing through short neutral alumina column to remove the copper salt and then filtered through poly(tetrafluoro ethylene) (PTFE) filter (0.2 μ m pore size) prior to GC and GPC analyses. When the conversion was in the range of 75-85 %, polymerization was stopped by exposing it to air. The remaining polymer was precipitated into excess of methanol and then isolated by vacuum filtration.

3.3.3 General Procedure for the Kinetic Studies of ATRP of St Catalyzed by Cu(II)/PMDETA/PhSNa in the Presence of Definite Amount of Air

St (10 mL, 87.2 mmol), PMDETA (911 μ L, 4.36 mmol) as ligand, and CuCl₂ (58.6 mg, 0.436 mmol) were added in a given order to a round-bottomed flask equipped with a magnetic stirring bar and stirred for 5 min. Then required amount of PhSNa, 1-PECl (115 μ L, 0.872 mmol) as initiator, and anisole (1 mL) as internal standard for GC measurements were added. The flask was sealed with a rubber septum. After evacuation of the flask by vacuum, air (8 mL, [O₂] = 1.3×10^{-2} mol/L) was introduced by a syringe and then the flask was immersed into an oil bath at 110 °C. Kinetic samples were taken with a nitrogen-flashed syringe at given time intervals under the positive nitrogen atmosphere to avoid further diffusion of air into the polymerization flask. Samples were diluted with THF and filtered through poly(tetrafluoroethylene) (PTFE) filter (0.2 μ m pore size) prior to GC and GPC analyses.

3.3.4 UV–VIS Monitoring of *In Situ* Cu (I) Formation via Electron Transfer from PhSNa

The preparation of the stock solution was given as follows: into a 10 mL of volumetric flask, PMDETA (450 μ L, 2.16 mmol), CuCl₂ (29 mg, 0.216 mmol), PhSNa (43 mg, 0.32 mmol), and DMF were added. The stock solution is then transferred to a 25 mL of flask equipped with rubber septum. The flask was subjected to nitrogen vacuum cycles three times and then 8 mL of air was injected to the system. The first sample was taken before the reaction mixture was placed in a thermostated oil bath at 110 °C. Aliquots (0.5 mL) were then taken and diluted to 10 mL for UV-VIS measurements at given time intervals.

3.3.5 General Procedure for the Kinetic Studies of ATRP of MMA Catalyzed by Cu(II)/PMDETA/PhSNa (or *p*-methoxythiophenol) in the Presence of Definite Amount of Air

MMA (10 mL, 93.3 mmol), PMDETA (0.974 mL, 4.66 mmol) as ligand, and CuCl₂ (0.0626 g, 0.466 mmol) were added in a given order to a round-bottomed flask equipped with a magnetic stirring bar and stirred for 5 min. Then PhSNa (0.0924 g, 0.699 mmol) or *p*-methoxythiophenol (0.086 mL, 0.699 mmol), EiBr (0.136 mL, 0.933 mmol) as initiator, toluene (8 mL) as solvent, and anisole (2 mL) as internal

standard for GC measurements were added. The flask was sealed with a rubber septum. After evacuation of the flask by vacuum, air (8 mL, $[O_2] = 1.3 \times 10^{-2}$ mol/L) was introduced by a syringe and then the flask was immersed into an oil bath at 90 °C. Kinetic samples were taken with a nitrogen-flashed syringe at given time intervals under the positive nitrogen atmosphere to avoid further diffusion of air into the polymerization flask. Samples were diluted with THF and filtered through poly(tetrafluoroethylene) (PTFE) filter (0.2 μ m pore size) prior to GC and GPC analyses.

3.3.6 Block Copolymerization and Chain Extension Polymerizations

3.3.6.1 Preparation of Linear Homo- and Block Co-Polymers via ATRP

Preparation of linear PS macroinitiator (PS-Br) (**H1**) :

St (5 mL, 43.6 mmol), PMDETA (182 μ L, 0.872 mmol), and CuBr₂ (97.4 mg, 0.436 mmol) were charged into a 25 mL Schlenk tube equipped with a magnetic stirring bar and stirred for 10 minutes. Fructose (6.9 mg, 0.043 mmol), and EiBr (128 μ L, 0.872 mmol) were then added, in that order. The reaction mixture was subjected to three FPT cycles and left under vacuum. The tube was then placed in an oil bath set at 110 °C for 50 minutes. The reaction mixture was cooled to room temperature and the contents were diluted with THF and passed through a column of neutral alumina. The excess of THF was evaporated under reduced pressure. The polymer was precipitated in methanol. The solid product was dried under vacuum, yielding the desired polymer. ($M_{n,theo} = 1750$, $M_n = 1800$, $M_n, NMR = f = 0.97$, $M_w/M_n = 1.10$ at 30% conversion). The conversion was determined gravimetrically.

Preparation of linear PS macroinitiator (PS-Br) (**H2**) :

St (5 mL, 43.6 mmol), PMDETA (303 μ L, 1.45 mmol), and CuBr₂ (0.162 g, 0.727 mmol) were charged into a 25 mL Schlenk tube equipped with a magnetic stirring bar and stirred for 10 minutes. Fructose (13 mg, 0.073 mmol), 5 mL of toluene and EiBr (213 μ L, 1.45 mmol) were then added, in that order. The reaction mixture was subjected to three FPT cycles and left under vacuum. The tube was then placed in an oil bath set at 110 °C for 100 minutes. The purification procedure was done in the similar manner as for the PS macroinitiator. Homopolymer was finally obtained as a white powder ($M_{n,theo} = 1650$, $M_n = 1650$, $f = 1$, $M_w/M_n = 1.11$ at 46% conversion).

Preparation of linear PS-*b*-PMMA copolymer (**H3**) :

St (3.2 mL, 29.8 mmol), PMDETA (12 μ L, 0.06 mmol), and CuCl₂ (4 mg, 0.03 mmol) were added in given order to a Schlenk tube equipped with a magnetic stirring bar and stirred for 10 min. Fructose (0.3 mg, 0.0015 mmol), and a solution of PS-Br (**H2**) (98 mg, 0.06 mmol; $M_n = 1650$) in 3.2 mL of toluene were then added respectively. Three FPT cycles were performed and the tube was sealed under vacuum. The polymerization was conducted for 48 h at 90 °C. The purification procedure was done in the similar manner as for the PS macroinitiator. The block copolymer was finally obtained as a white powder ($M_{n,theo} = 13150$, $M_n = 26850$, $f = 0.49$, $M_w/M_n = 1.10$ at 23 % conversion).

Preparation of linear PS-*b*-PMMA copolymer (**H4**) :

MMA (3.2 mL, 29.8 mmol), PMDETA (12 μ L, 0.06 mmol), and CuCl₂ (4 mg, 0.03 mmol) were added in given order to a Schlenk tube equipped with a magnetic stirring bar and stirred for 10 min. Fructose (3 mg, 0.015 mmol), and a solution of PS-Br (**H2**) (98 mg, 0.06 mmol; $M_n = 1650$) in 3.2 ml of toluene were then added respectively. Three FPT cycles were performed and the tube was sealed under vacuum. The polymerization was conducted for 22 h at 90 °C. The purification procedure was done in the similar manner as for the PS macroinitiator. The block copolymer was finally obtained as a white powder. ($M_{n,theo} = 38200$, $M_n = 54950$, $f = 0.7$, $M_w/M_n = 1.26$ at 73 % conversion).

Preparation of linear PS-*b*-PMMA copolymer (**H5**) :

MMA (3.2 mL, 29.8 mmol), PMDETA (31 μ L, 0.15 mmol), and CuCl₂ (4 mg, 0.03 mmol) were added in given order to a Schlenk tube equipped with a magnetic stirring bar and stirred for 10 min. Fructose (3 mg, 0.015 mmol), and a solution of PS-Br (**H2**) (98 mg, 0.06 mmol; $M_n = 1650$) in 3.2 ml of toluene were then added respectively. Three FPT cycles were performed and the tube was sealed under vacuum. The polymerization was conducted for 20 h at 90 °C. The purification procedure was done in the similar manner as for the PS macroinitiator. The block copolymer was finally obtained as a white powder. ($M_{n,theo} = 50200$, $M_n = 102900$, $f = 0.49$, $M_w/M_n = 1.31$ at 97 % conversion).

Preparation of linear PS macroinitiator (PS-Br) (**H6**) :

St (32 mL, 280 mmol), PMDETA (292 μ L, 1.4 mmol), and CuBr₂ (156 mg, 0.7 mmol) were added in given order to a reaction flask equipped with a magnetic stirring bar and stirred for 10 min. Then, ascorbic acid (31 mg, 0.18 mmol) and EiBr (204 μ L, 1.4 mmol) were added. The mixture was degassed by conducting three FPT cycles and the flask was immersed into an oil bath at 110 °C. After polymerization for 80 min., the reaction mixture was cooled to room temperature and the contents were diluted with THF and passed through a column of neutral alumina. The excess of THF was evaporated under reduced pressure. The polymer was precipitated in methanol. The solid product was dried under vacuum, yielding the desired polymer. ($M_{n,theo}$ = 3150, M_n = 3350, f = 0.94, M_w/M_n = 1.13 at 15% conversion). The conversion was determined gravimetrically.

Preparation of linear PS-*b*-PMMA copolymer (**H7**) :

MMA (4.79 mL, 45 mmol), PMDETA (19 μ L, 0.09 mmol), CuCl₂ (6 mg, 0.045 mmol) were added in given order to a reaction flask equipped with a magnetic stirring bar and stirred for 10 min. Then, ascorbic acid (4 mg, 0.02 mmol), toluene (4.79 mL), and prepared linear macroinitiator PS-Br (**H6**) (0.3 g, 44.8 mmol; M_n = 3350) were added and the mixture was degassed by conducting three FPT cycles. The polymerization was conducted for 20 h at 90 °C. The polymer was recovered as described above. The block copolymer was finally obtained as a white powder. ($M_{n,theo}$ = 31400, M_n = 39300, f = 0.8 M_w/M_n = 1.43 at 56% conversion).

Preparation of linear PS-*b*-PMMA copolymer (**H8**) :

MMA (4.8 mL, 45 mmol), PMDETA (48 μ L, 0.23 mmol), CuCl₂ (6 mg, 0.045 mmol) were added in given order to a reaction flask equipped with a magnetic stirring bar and stirred for 10 min. Then, ascorbic acid (4 mg 0.023 mmol), toluene (4.8 mL), and prepared linear macroinitiator PS-Br (**H6**) (0.3 g, 0.09 mmol; M_n = 3350) were added and the mixture was degassed by conducting three FPT cycles. The polymerization was conducted for 20 h at 90 °C. The purification procedure was done in the similar manner as for the PS macroinitiator. The block copolymer was finally obtained as a white powder. ($M_{n,theo}$ = 45400, M_n = 64400, f = 0.71, M_w/M_n = 1.16 at 84% conversion).

Preparation of linear PS macroinitiator (PS-Br) (**H9**) :

St (5 mL, 43.6 mmol), PMDETA (1.518 mL, 7.27 mmol), and CuBr₂ (162 mg, 0.72 mmol) were added in given order to a reaction flask equipped with a magnetic stirring bar and stirred for 10 min. Then, *p*-methoxyphenol (270 mg, 2.18 mmol), EtBr (213 μ L, 1.45 mmol), toluene (5 mL) were added. The mixture was degassed by conducting three FPT cycles and the flask was immersed into an oil bath at 110 °C. After polymerization for 75 min., the reaction mixture was cooled to room temperature and the contents were diluted with THF and passed through a column of neutral alumina. The excess of THF was evaporated under reduced pressure. The polymer was precipitated in methanol. The solid product was dried under vacuum, yielding the desired polymer. ($M_{n,theo} = 500$, $M_n = 1200$, $f = 0.94$, $M_w/M_n = 1.17$ at 11% conversion). The conversion was determined gravimetrically.

Preparation of linear PS-*b*-PMMA copolymer (**H10**) :

MMA (2.26 mL, 21.2 mmol), PMDETA (44.2 μ L, 0.21 mmol), CuCl₂ (2.84 mg, 0.021 mmol) were added in given order to a reaction flask equipped with a magnetic stirring bar and stirred for 10 min. Then, *p*-methoxyphenol (7.8 mg 0.063 mmol), toluene (2.26 mL), and prepared linear macroinitiator PS-Br (**H9**) (50 mg, 0.042 mmol; $M_n = 1200$) were added and the mixture was degassed by conducting three FPT cycles. The polymerization was conducted for 20 h at 90 °C. The purification procedure was done in the similar manner as for the PS macroinitiator. The block copolymer was finally obtained as a white powder. ($M_{n,theo} = 15700$, $M_n = 28900$, $f = 0.54$, $M_w/M_n = 1.07$ at 29% conversion).

Preparation of linear PS-*b*-PMMA copolymer (**H11**) :

MMA (4.53 mL, 42.3 mmol), PMDETA (88 μ L, 0.42 mmol), CuCl₂ (5.6 mg, 0.042 mmol) were added in given order to a reaction flask equipped with a magnetic stirring bar and stirred for 10 min. Then, *p*-methoxyphenol (21 mg, 0.169 mmol), toluene (4.53 mL), and prepared linear macroinitiator PS-Br (**H9**) (0.1 g, 0.08 mmol; $M_{n, GPC} = 1200$) were added and the mixture was degassed by conducting three FPT cycles. The polymerization was conducted for 20 h at 90 °C. The purification procedure was done in the similar manner as for the PS macroinitiator. The block copolymer was finally obtained as a white powder. ($M_{n,theo} = 29750$, $M_n = 45000$, $f = 0.65$, $M_w/M_n = 1.16$ at 57% conversion).

3.3.6.2 Preparation of Star Homo- and Block Co-Polymers via ATRP

Synthesis of octafunctional initiator, 5, 11, 17, 23, 29, 35, 41, 47-octa-tert-butyl-49, 50, 51, 52, 53, 54, 55, 56-octakis- (2-bromopropionyloxy) calix[8]arene, **1** :

The octafunctional initiator, **1** was synthesized according to a procedure reported by Angot et al. [178]. In a 250 ml two-neck flask, equipped with a magnetic stirrer, 2 g (1.53×10^{-3} mol) of TBC-8 was suspended in 20 mL of dry THF. Then 5.1 mL of triethylamine (3.67×10^{-2} mol) was added and the mixture became homogenous upon stirring. The solution was cooled to 0°C and 3.84 mL (3.67×10^{-2} mol) of 2-bromopropionyl bromide dissolved in 20 ml of THF were added dropwise over a period of 1h. And then the reaction mixture was stirred at room temperature for 24 h. The solution was concentrated and precipitated in ice cold water. The crude solid compound thus obtained was dissolved in diethylether and washed successively with dilute K_2CO_3 water solution and dried over anhydrous Na_2SO_4 . Ether was removed and the concentrate precipitated from a mixture of methanol/water (90/10 v/v). The precipitation was repeated two more times to obtain a white powder of **1** in 82 % yield. 1H NMR ($CDCl_3$), δ (ppm): 7.01 (s, 2H, aromatic protons), 4.34 (s, 1H, CHBr), 3.69 (s, 2H, CH_2), 1.54 (s, 3H, CH_3), 1.16 (s, 9H, tert-butyl).

Preparation of octa-arm star PS-Br macroinitiator (**H12**) :

St (14.458 mL, 126 mmol), PMDETA (70 μ L, 0.336 mmol) and $CuBr_2$ (37 mg, 0.168 mmol) were added into a 25 mL Schlenk flask equipped with magnetic stirring bar and stirred for 10 min. After adding fructose (8 mg, 0.042 mmol) and octa-functional initiator, **1** (0.1 g, 0.042 mmol) into the reaction mixture, the flask was degassed by FPT cycles. Then the reaction mixture was placed in an oil bath heated at 110 °C. After polymerization for 40 minutes, the reaction mixture was cooled to room temperature and the contents were diluted with THF and passed through a column of neutral alumina. The excess of THF was evaporated under reduced pressure. The polymer was precipitated in methanol. The solid product was dried under vacuum, yielding the desired polymer. ($M_{n, \text{theo}} = 14900$, $M_n = 17300$, $f = 0.86$, $M_{n, \text{NMR}} = 23850$, $M_w/M_n = 1.17$ at 4% conversion). The conversion was determined gravimetrically.

Hydrolysis of octa-arm star PS macroinitiator :

0.15 g of octa-arm star PS-Br macroinitiator was dissolved in 15 mL of THF in a 100 mL round-bottomed flask fitted with a condenser and nitrogen inlet. 10 mL of KOH (1 M solution in ethanol) was then added and refluxed for 96 h. The solution was evaporated, dissolved in THF, and finally precipitated into methanol and filtered. The polymer (**H7**) was dried under vacuum ($M_n = 3300$, $M_w/M_n = 1.43$) (**H13**).

Preparation of octa-arm star PS-*b*-PMMA copolymer (**H14**) :

MMA (11.9 mL, 111 mmol), PMDETA (8 μ L, 0.04 mmol), and CuCl₂ (3 mg, 0.02 mmol) were added in given order to a Schlenk flask equipped with a magnetic stirring bar and stirred for 10 min. To this mixture, fructose (1 mg, 0.005 mmol) and a solution of previously obtained octa-arm star PS-Br macroinitiator (120 mg, 0.005 mmol) in 11.9 mL of toluene were added. The mixture was degassed by conducting three FPT cycles. The flask was immersed into an oil bath at 90 °C. After polymerization for 4 h, the mixture was diluted with THF and catalyst was removed by passing the polymer solution through a short neutral alumina column. The resulting polymer was precipitated into excess methanol ($M_{n,theo} = 200100$, $M_{n,GPC} = 155000$, $M_{n,NMR} = 237400$, $f = 0.84$, $M_w/M_n = 1.16$ at 8% conversion).

3.3.6.3 Preparation of Linear Homo- and Block Co-Polymers via ATRP in the Presence of Definite Amount of Air

General procedure for the synthesis of PS-Cl macroinitiator (**H15**) :

St (3 mL, 26 mmol), PMDETA (271 μ L, 1.31 mmol), and CuCl₂ (17 mg, 0.13 mmol) were added in given order to a reaction flask equipped with a magnetic stirring bar and stirred for 5 min. Then, PhSNa (17 mg, 0.13 mmol) and 1-PECl (34 μ L, 0.26 mmol) were added. The flask was closed with rubber septum and evacuated by vacuum. After introducing 28 mL of air ($[O_2] \sim 4.55 \times 10^{-2}$ mol/ L) by a syringe, the flask was immersed into an oil bath at 110 °C. After polymerization for 6 h, the reaction mixture was cooled to room temperature and the contents were diluted with THF and passed through a column of neutral alumina. The excess of THF was evaporated under reduced pressure. The polymer was precipitated in methanol. The solid product was dried under vacuum, yielding the desired polymer. ($M_{n,theo} = 6900$, $M_n = 7200$, $f = 0.96$, $M_w/M_n = 1.27$ at 65% conversion). The conversion was determined gravimetrically.

Chain extension polymerization using PS-Cl as macroinitiator (**H16**) :

PS macroinitiator (1 g, 0.138 mmol, $M_n = 7200$) was dissolved in St (7.95 mL, 69.4 mmol), and CuCl_2 (9 mg, 0.069 mmol), PMDETA (145 μL , 0.69 mmol), and PhSNa (9 mg, 0.069 mmol) were added. The flask was evacuated and 23 mL of air ($[\text{O}_2] \sim 3.7 \times 10^{-2} \text{ mol/L}$) was introduced by a syringe. The polymerization was carried out at 110 °C for 20 h. The purification procedure was done in the similar manner as for the PS macroinitiator. The chain extended polymer was finally obtained as a white powder. ($M_{n,\text{GPC}} = 41600$, $M_w/M_n = 1.48$ at 67% conversion).

General procedure for the synthesis of PS-Br macroinitiator (**H17**) :

St (11 mL, 96 mmol), PMDETA (1.002 mL, 4.8 mmol), and CuBr_2 (107 mg, 0.48 mmol) were added in given order to a reaction flask equipped with a magnetic stirring bar and stirred for 5 min. Then, *p*-methoxy thiophenol (177 μL , 1.44 mmol) and EtBr (140 μL , 0.96 mmol) were added. The flask was closed with rubber septum and evacuated by vacuum. After introducing 19 mL of air ($[\text{O}_2] = 3.1 \times 10^{-2} \text{ mol/L}$) by a syringe, the flask was immersed into an oil bath at 110 °C. After polymerization for 30 min, the reaction mixture was cooled to room temperature and the contents were diluted with THF and passed through a column of neutral alumina. The excess of THF was evaporated under reduced pressure. The polymer was precipitated in methanol. The solid product was dried under vacuum, yielding the desired polymer. ($M_{n,\text{theo}} = 2600$, $M_n = 2800$, $f = 0.93$, $M_w/M_n = 1.17$ at 24% conversion).

Preparation of linear PS-*b*-PMMA copolymer (**H18**) :

The PS macroinitiator (0.3 g, 0.107 mmol, $M_n = 2800$) was dissolved in toluene (5.73 mL) and MMA (5.73 mL, 53.5 mmol), and CuCl (10.6 mg, 0.107 mmol), and PMDETA (22 μL , 0.107 mmol) were added. The mixture was degassed by conducting three FPT cycles. The flask was immersed into an oil bath at 90 °C. After polymerization for 24 h. the polymer was recovered as described above ($M_{n,\text{theo}} = 40800$, $M_n = 72500$, $f = 0.56$, $M_w/M_n = 1.29$ at 76% conversion).

Preparation of linear PS-*b*-PMMA copolymer (**H19-22**) :

The PS macroinitiator (0.3 g, 0.107 mmol, $M_n = 2800$) was dissolved in toluene (5.73 mL) and MMA (5.73 mL, 53.5 mmol), and CuCl_2 (7 mg, 0.053 mmol), PMDETA (111 μL , 0.53 mmol), and required amount of *p*-methoxy thiophenol were added.

The flask was evacuated and 11 mL of air was introduced by a syringe. The polymerization was carried out at 90 °C for 48 h, and then the polymer was recovered as described above.

General procedure for the synthesis of PS-Br macroinitiator (**H23**) :

St (10 mL, 87 mmol), PMDETA (364 μ L, 1.74 mmol) and CuBr (250 mg, 1.74 mmol) were added into a 25 mL Schlenk flask equipped with magnetic stirring bar and stirred for 10 min. After adding EiBr (256 μ L, 1.74 mmol) into the reaction mixture, the flask was degassed by FPT cycles. Then the reaction mixture was placed in an oil bath heated at 90 °C for 20 minutes. The reaction mixture was cooled to room temperature and the contents were diluted with THF and passed through a column of neutral alumina. The excess of THF was evaporated under reduced pressure. The polymer was precipitated in methanol. The solid product was dried under vacuum, yielding the desired polymer ($M_{n, \text{theo}} = 2100$, $M_n = 2100$, $f = 1$, $M_w/M_n = 1.12$ at 40% conversion). The conversion was determined gravimetrically.

Preparation of linear PS-*b*-PMMA copolymer (**H24-27**) :

The PS macroinitiator (0.3 g, 0.142 mmol, $M_n = 2100$) was dissolved in toluene (5.73 mL) and MMA (7.64 mL, 71.4 mmol), and CuCl₂ (96 mg, 0.071 mmol), PMDETA (149 μ L, 0.71 mmol), and required amount of PhSNa were added. The flask was evacuated and 11 mL of air was introduced by a syringe. The polymerization was carried out at 90 °C for 24 h., and then the polymers were recovered as described above.

3.3.6.4 Preparation of Linear Homo- and Block Co-Polymers via ATRP Using PhONa as Reducing Agent

Preparation of the macroinitiator PS-Cl (**H28**) :

PS macroinitiator was prepared in a separate experiment. St (6 mL, 52mmol), silica gel (0.352 g), PMDETA (546 μ L, 2.62 mmol), and CuCl₂ (35 mg, 0.26 mmol) were added in given order to a reaction flask equipped with a magnetic stirring bar and stirred for 5 min. Then, *p*-methoxyphenol (98 mg, 0.78 mmol) and 1-PECl (69 μ L, 0.52 mmol) were added. The flask was closed with rubber septum and evacuated by vacuum. After introducing 8 mL of air by a syringe, the flask was immersed into an oil bath at 110 °C. After polymerization for 3 h, the mixture was diluted with toluene

and catalyst was removed by filtration. The resulting polymer was precipitated into excess methanol ($M_n = 2000$, $M_w/M_n = 1.27$ at 19% conversion). The conversion was determined gravimetrically.

Chain extension polymerization (**H29**) :

The PS macroinitiator (**H28**) (0.175 g, 0.088 mmol; $M_n = 2000$) was dissolved in toluene (5 mL), and St (5 mL, 44 mmol), silica gel (0.06 g), CuCl₂ (0.006 g, 0.044 mmol), PMDETA (0.091 mL, 0.44 mmol), and *p*-methoxyphenol (0.006 g, 0.044 mmol) were added. The flask was evacuated and 8 mL of air was introduced by a syringe. The polymerization was carried out at 110 °C for 26 h. The same work-up procedure given for PS macroinitiator was followed to obtain the resulting polymer ($M_{n,theo}=13500$, $M_{n,GPC} = 15000$, $f = 0.9$, $M_w/M_n = 1.18$ at 22% conversion).

3.3.7 General Procedure for the Kinetic Studies of ATRP of St Catalyzed by Silica Gel Supported CuCl₂/PMDETA

St (4.5 mL, 39.3 mmol), silica gel (0.264 g), PMDETA (819 µL, 3.93 mmol) as ligand, and CuCl₂ (26.4 mg, 0.196 mmol) were added in a given order to a round-bottomed flask equipped with a magnetic stirring bar and stirred for 5 min. The silica gel to CuCl₂ (w/w) ratio of 10 was employed for the all polymerizations. Then PhONa (33 mg, 0.295 mmol), 1-PECl (52 µL, 0.393 mmol) as initiator, and anisole (0.4 mL), which is used as internal standard for GC measurements, were added. The flask was sealed with a rubber septum. After evacuation of the flask by vacuum, air (8 mL, [O₂] ~ 1.3 x 10⁻² mol/L) was introduced by a syringe and then the flask was immersed into an oil bath at 110 °C. Kinetic samples were taken with a nitrogen-flashed syringe at given time intervals under the positive nitrogen atmosphere to avoid further diffusion of air into the polymerization flask. Samples were diluted with THF and filtered through polytetrafluoroethylene (PTFE) filter (0.2 µm pore size) prior to GC and GPC analyses. Upon completion of the polymerization, the flask was cooled and the content was diluted with toluene. The mixture was filtered through a Sartorius PTFE filter (0.45 µm pore size) and the remaining light blue-colored solid on the filter was washed twice with toluene, which afforded a light yellow-colored clear polymer solution. The polymer solution was precipitated by the addition to methanol. The polymer was obtained as a white powder. The catalyst recovered by filtration was air dried and then vacuum-dried at 35 °C for 24 h.

3.3.8 General Procedure for the Catalyst Reuse

The vacuum-dried SG-CuCl₂/PMDETA catalyst recovered from previous polymerization was transferred into a round-bottomed flask. Again, St (4.5 mL, 39.3 mmol), anisole (1 mL), PMDETA (205 μ L, 0.98 mmol), and PhONa (33 mg, 0.295 mmol) were added and the mixture stirred for 5 min. Then, 1-PECl (52 μ L, 0.393 mmol) was added to the reaction mixture. A similar experimental procedure as the first run was employed.

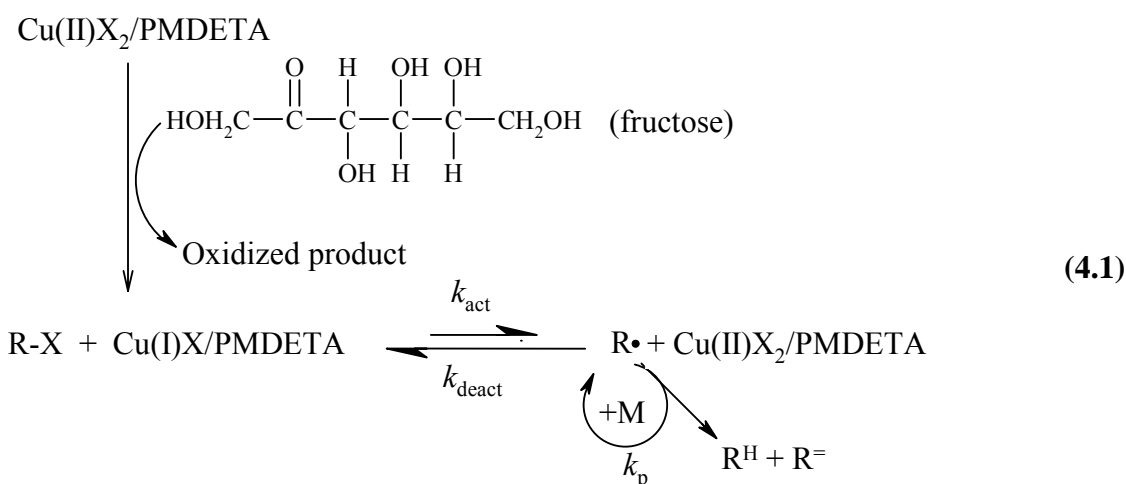
3.3.9 UV–VIS Monitoring of *In Situ* Copper (I) Formation via Electron Transfer from Sodium Phenoxide

The preparation of a stock solution was given as follows: into a 10mL of volumetric flask, PMDETA (450 μ L, 2.16mmol), CuCl₂ (29.3 mg, 0.218 mmol), PhONa (75.8 mg, 0.65 mmol) and acetonitrile were added. From this homogenous mixture, 0.5 mL of aliquot was diluted to 10 mL and spectrum was immediately measured. A stock solution is then transferred to a 25 mL of flask equipped with rubber septum. The flask was subjected to nitrogenvacuum cycles three times and then 8 mL of air was injected to the system. The reaction mixture was placed in a thermostated oil bath at 80 °C. 0.5mL of aliquots were taken and diluted to 10 mL for UV–VIS measurements at given time intervals.

4. RESULTS and DISCUSSION

4.1 Fructose as a Reducing Agent for *In Situ* Generation of Copper(I) Species via Electron Transfer Reaction in ATRP of Styrene (St)

For many years, oxidation of α -hydroxyl ketones, such as fructose, by higher oxidation state metal (Cu(II)) complexes such as Benedict's reagent has been a well known procedure [298]. During *in situ* generation of the lower oxidation state of the metal (Cu(I)), a more stable transition metal complex abstracts an electron from α -hydroxyl ketones, thus converting it into a diketone form. The use of various reducing monosaccharides as an additive in conventional ATRP of butyl methacrylate (BMA) was reported previously [299]. When fructose was employed together with the catalyst Cu(I)Br, the initiator toluene-4-sulfonyl chloride and the ligand PMDETA in the ATRP of BMA, rate enhancement at the expense of control was observed up to 50% conversion. Based on *in situ* generation of Cu(I) species strategy, we investigated the use of fructose as a reducing agent (RA) in Cu(II)-catalyzed ATRP for the design of homopolymers (both linear and star) and their corresponding block copolymers (4.1).



4.1.1 UV-VIS Monitoring of Copper (II) Complex Consumption and Copper (I) Complex Formation

In order to demonstrate the *in situ* generation of Cu (I), UV-VIS measurements were performed. The UV-VIS spectrum of Cu(II)Cl₂/PMDETA/fructose mixture in water showed a characteristic absorbance in the region of 450-900 nm (Fig. 4.1).

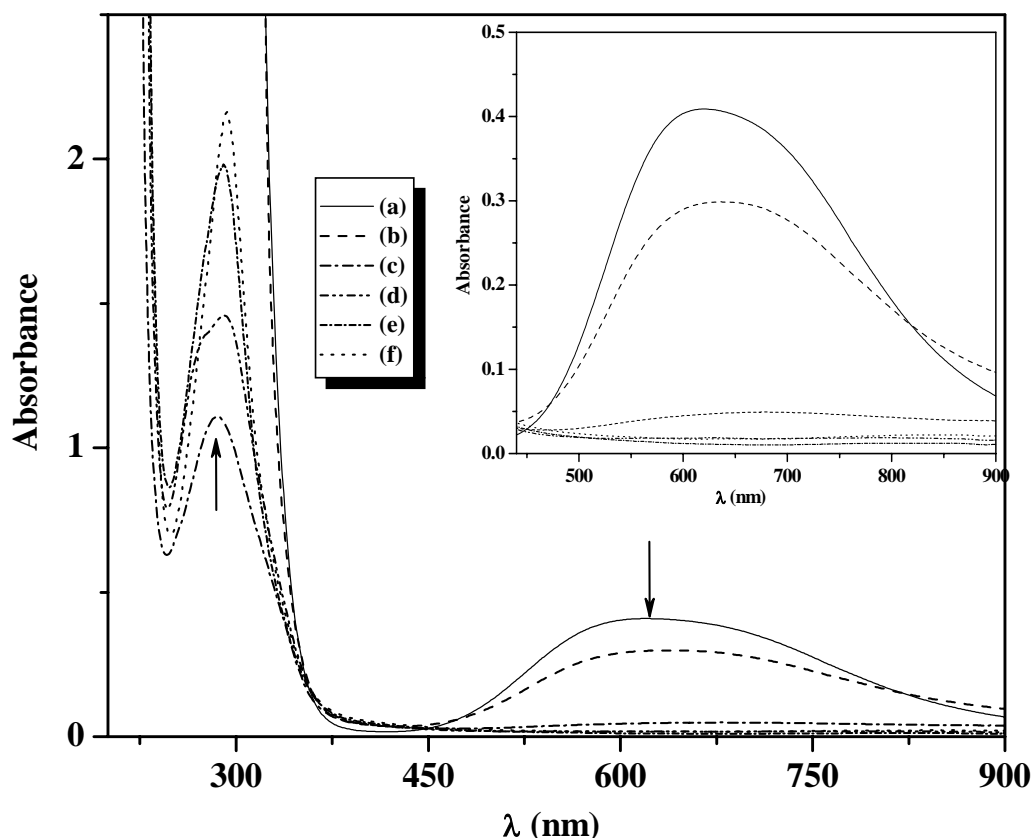


Figure 4.1: UV–VIS spectra of CuCl₂/PMDETA/fructose mixture in water at different reaction times; [CuCl₂]₀ = 2.18 × 10^{−4} M; [CuCl₂]₀/[PMDETA]₀/[fructose]₀ = 1/10/0.5. (a) room temperature; t = 0 min; (b) t = 5 min. at 85 °C; (c) t = 15 min. at 85 °C; (d) t = 30 min. at 85 °C; (e) t = 80 min. at 85 °C; (f) t = 140 min at 85 °C.

The absorption at 620 nm might be attributed to d-d band transition of Cu (II) halide [300, 301]. Upon heating the mixture, this absorption gradually decreases. When the consumption of Cu (II) attains 90% in the course of 15 min, a new absorption band appears at 290 nm related to Cu (I)/PMDETA complex, which gradually increases as the reaction proceeds. Thus UV measurements clearly indicate that Cu (II) halide converts to Cu (I) in the presence of fructose as a RA.

4.1.2 Effect of Fructose Concentration on ATRP of St

Fructose concentration plays an important role in the reduction of Cu (II) species to Cu(I), which is the key step of ATRP. In order to investigate this parameter, two series of kinetic experiments were carried out using either 1-PECl/CuCl₂ or EiBr/CuBr₂ initiator/catalyst system in bulk at 110 °C.

The first kinetic experiment was conducted at molar ratios of [St]₀ : [1-PECl]₀ : [CuCl₂]₀ : [PMDETA]₀ : [Fructose]₀ = 100 : 1 : 0.5 : 1 : 0.125 (or 0.250). As shown in Figure 4.2, ln([M]₀/[M]) versus time plot displayed a linear behavior indicating that the polymerization rate was first order with respect to St concentration and the active chain concentration was constant throughout the polymerization.

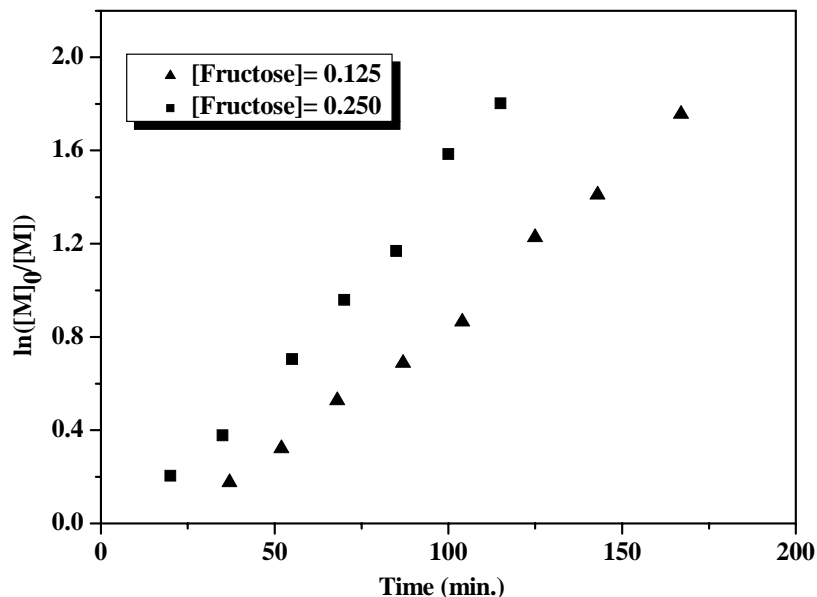


Figure 4.2: The first-order kinetic plot for ATRP of St in bulk at 110 °C using fructose as a RA. [St]₀= 7.73M; [St]₀ : [1-PECl]₀ : [CuCl₂]₀ : [PMDETA]₀ : [Fructose]₀= 100 : 1 : 0.5 : 1 : 0.125 (or 0.250).

Furthermore, it was observed that an increase in fructose concentration led to a smaller induction period, which is attributed to a higher disappearing rate of the Cu(II) at early stage of ATRP. The number average molecular weight (M_n) values determined by GPC increased linearly with conversion and molecular weight distribution ($MWD = M_w/M_n$) tends to decrease with respect to conversion.

Nevertheless, the molecular weights of the obtained polymers are higher than the theoretical ones (Fig. 4.3).

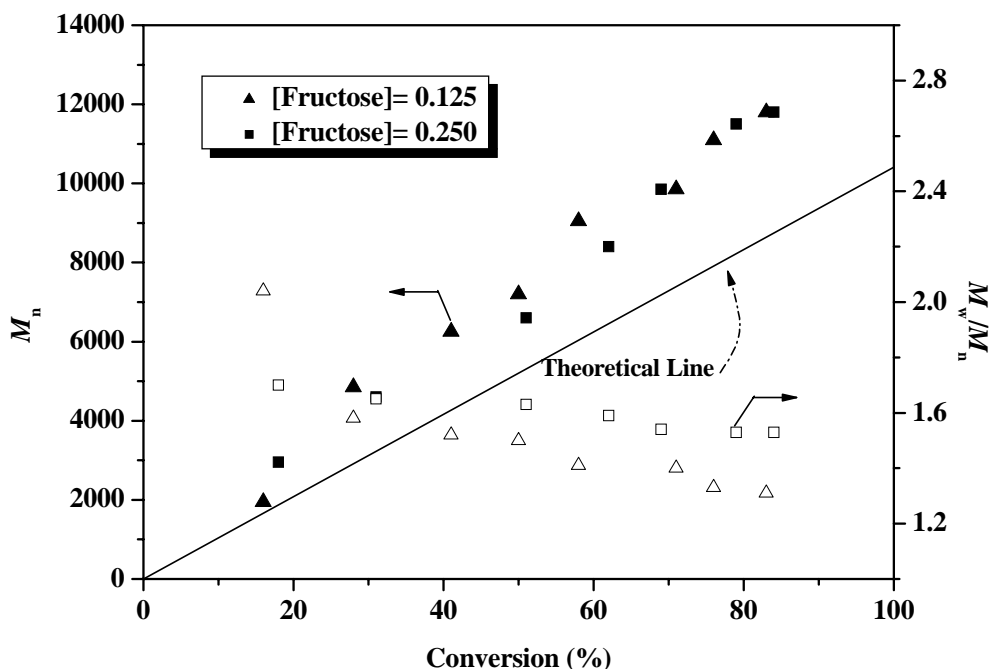


Figure 4.3: The dependence of M_n , and M_w/M_n , upon monomer conversion for ATRP of St in bulk at 110 °C (Experimental conditions as in Fig. 4.2).

4.1.3 ATRP of St Applying Different Initiator/Catalyst Systems

The effect of fructose as a RA in ATRP of St was also studied for different initiator/catalyst (EiBr/CuBr₂ and MBP/CuBr₂) systems using molar ratios of $[St]_0/[Initiator]_0/[CuBr_2]_0/[PMDETA]_0/[Fructose]_0 = 30/1/0.5/1/0.05$. All polymerizations were conducted in toluene (1/1, v/v) at 110 °C. Both $\ln([M]_0/[M])$ versus time and M_n versus conversion (and M_w/M_n vs. conversion) plots were obtained. For both systems, the plot of $\ln([M]_0/[M])$ vs. time is linear, confirming that first order kinetics are obtained with respect to monomer concentration (Fig. 4.4).

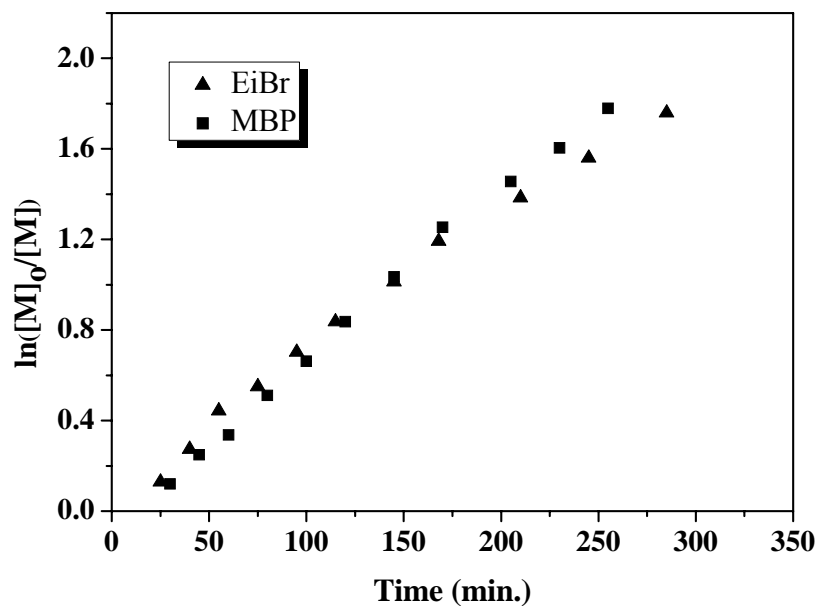


Figure 4.4: The first-order kinetic plot for ATRP of St in toluene (50/50, v/v) at 110 °C using fructose as a RA. Initiator: EiBr (▲) or MBP (■); [St]₀ = 3.96 M; [St]₀ : [Initiator]₀ : [CuCl₂]₀ : [PMDETA]₀ : [Fructose]₀ = 30 : 1 : 0.5 : 1 : 0.05.

M_n values obtained by GPC are higher than those of $M_{n, \text{theo}}$ (4.2) and a linear increase in M_n vs. conversion % plot can be observed up to 60 % conversion in both cases (Fig. 4.5).

$$M_{n, \text{theo}} = [M]_0 / [I]_0 \times \text{Conversion \%} \times 104 \quad (4.2)$$

Notably, M_w/M_n values are in the range of 1.1-1.2 throughout both polymerization systems. All results given clearly confirmed the controlled/living radical polymerization of St using fructose as a RA in both initiator/catalyst systems (1-PECl/CuCl₂ and EiBr/CuBr₂) at 110 °C.

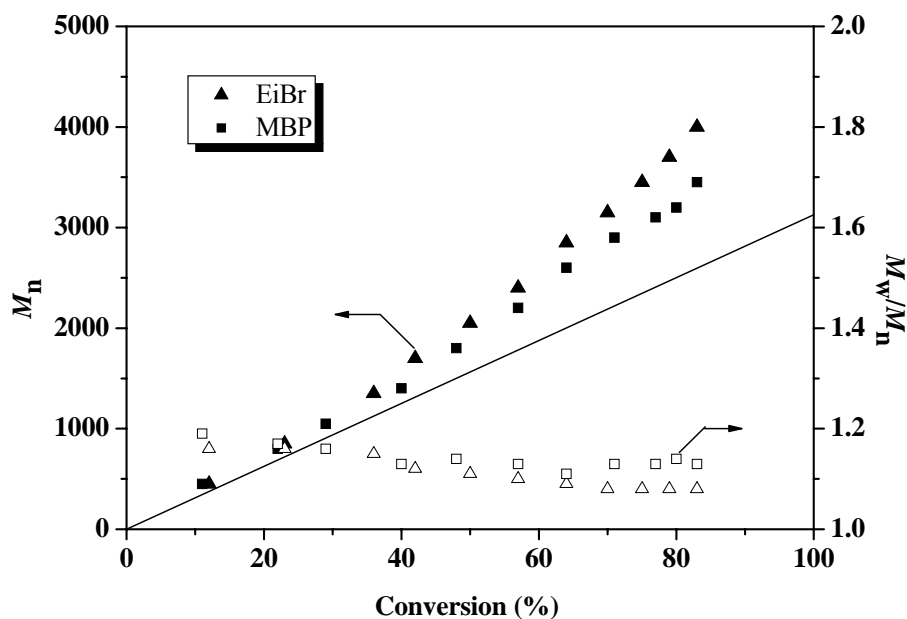


Figure 4.5: The dependence of M_n , and M_w/M_n , upon monomer conversion for ATRP of St in solution at 110 °C (Experimental conditions as in Fig. 4.4).

4.1.4 ATRP of *n*-Butyl Acrylate

We demonstrated the use of fructose as a RA in ATRP of *n*-BA for different catalyst ($\text{CuBr}_2/\text{PMDETA}$ and $\text{CuCl}_2/\text{PMDETA}$) systems using molar ratios of $[\textit{n}\text{-BA}]_0/[\text{EiBr}]_0/[\text{CuX}_2]_0/[\text{PMDETA}]_0/[\text{Fructose}]_0=100/1/0.25/0.5/0.5$. All polymerizations were conducted in ethylene carbonate (EC) (10/1, v/v) at 70 °C. Linear semilogarithmic plot was observed for the system using CuCl_2 as copper salt, however a deviation in semilogarithmic plot was observed at later stages of polymerization for the other system, this might be due to some negligible elimination or termination reactions [62, 302]. Apparent rate constants calculated from the initial slopes of semilogarithmic plots are $k_p^{\text{app}} = 1.01 \times 10^{-4}$, 5.06×10^{-5} for the systems using CuBr_2 , CuCl_2 as copper salt respectively (Fig. 4.6). Higher polymerization for the system applying CuBr_2 can be attributed to easier breakage of C-Br bond compared to C-Cl bond. M_n values showed a linear dependence on monomer conversion and M_w/M_n remained low ($M_w/M_n < 1.2$) throughout the polymerization. (Fig. 4.7).

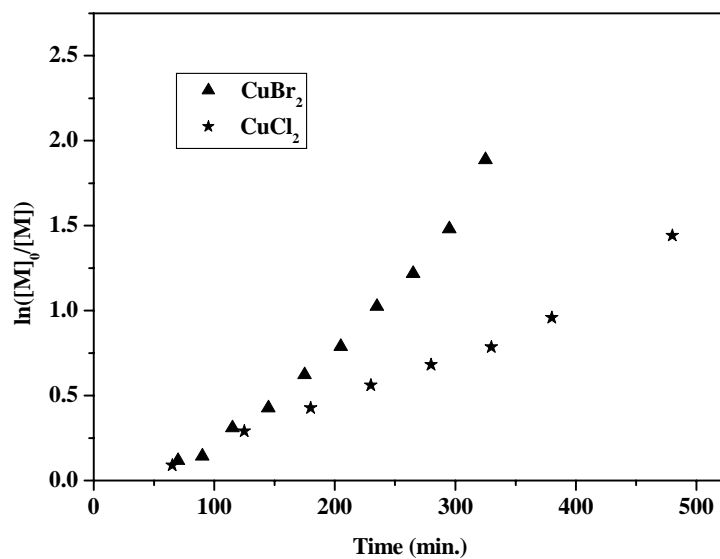


Figure 4.6: The first-order kinetic plot for ATRP of *n*BA in EC (10/1, v/v) at 70 °C using fructose as a RA. Copper salt: CuBr₂ (▲) or CuCl₂ (★) ; [BA]₀ = 5.73M; [*n*-BA]₀ : [Initiator]₀ : [CuBr₂]₀ : [PMDETA]₀ : [Fructose]₀ = 100 : 1 : 0.25 : 0.5 : 0.5.

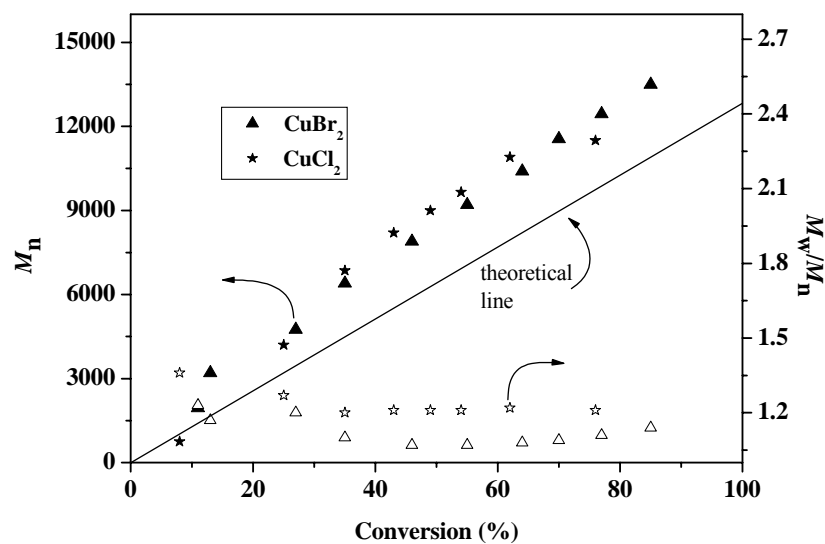


Figure 4.7: The dependence of M_n , and M_w/M_n , upon monomer conversion for ATRP of *n*BA at 70 °C in solution (Experimental conditions as in Fig. 4.6).

4.2 Ascorbic Acid as a RA for *In Situ* Generation of Cu (I) Species in ATRP of St

In this part the results regarding ATRP of St which employs ascorbic acid as RA were summarized. Ascorbic acid known as Vitamin C is oxidized to dehydroascorbic acid via two electron oxidation step in its redox reaction [303]. The use of ascorbic acid as electron transfer compound in miniemulsion ATRP was reported [140]. Figure 4.8 shows the results of experiments where two different ascorbic acid concentration were used to provide fine kinetics. Two kinetic experiments at molar ratios of $[St]_0 : [1-PECl]_0 : [CuCl_2]_0 : [PMDTA]_0 : [Ascorbic\ acid]_0 = 100 : 1 : 0.5 : 1 : X$ were conducted. The experimental conditions and the results of these studies were shown in Fig. 4.8 and Fig. 4.9. Linear semilogarithmic plots were observed for both concentration levels of ascorbic acid.

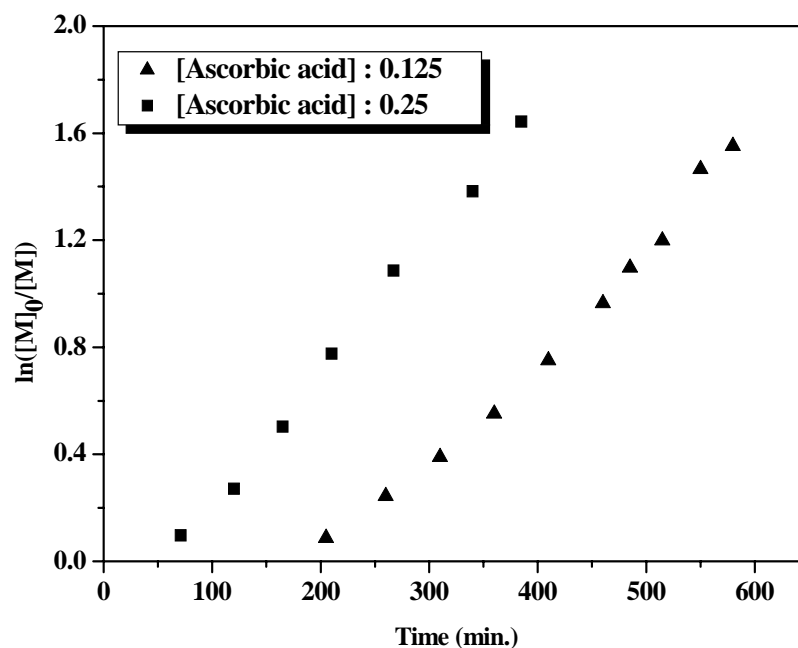


Figure 4.8: The first-order kinetic plot ATRP of St in bulk at 110 °C using ascorbic acid as a RA. $[St]_0 = 7.73M$; $[St]_0 : [1-PECl]_0 : [CuCl_2]_0 : [PMDTA]_0 : [Ascorbic\ acid]_0 = 100 : 1 : 0.5 : 1 : 0.125$ (or 0.250).

Furthermore M_n values showed a linear dependence on monomer conversion. MWD became narrower with increasing monomer conversion and finally reached to 1.2. These results confirmed that polymerization was well controlled under these

conditions. Moreover according to $\ln([M]_0/[M])$ -time plot one can easily say that increase in ascorbic acid concentration provided not only an increase in polymerization rate but also a decrease in induction period. Apparent rate constants (k_p^{app}) for St propagation were found $5.9 \times 10^{-5} \text{ s}^{-1}$ and $8.25 \times 10^{-5} \text{ s}^{-1}$ for $[1\text{-PECl}]_0 : [\text{Ascorbic acid}]_0 = 1 : 0.125$ and $1 : 0.25$ respectively. Additionally, MWD became narrower when ascorbic acid concentration was decreased, as presented in Figure 4.9.

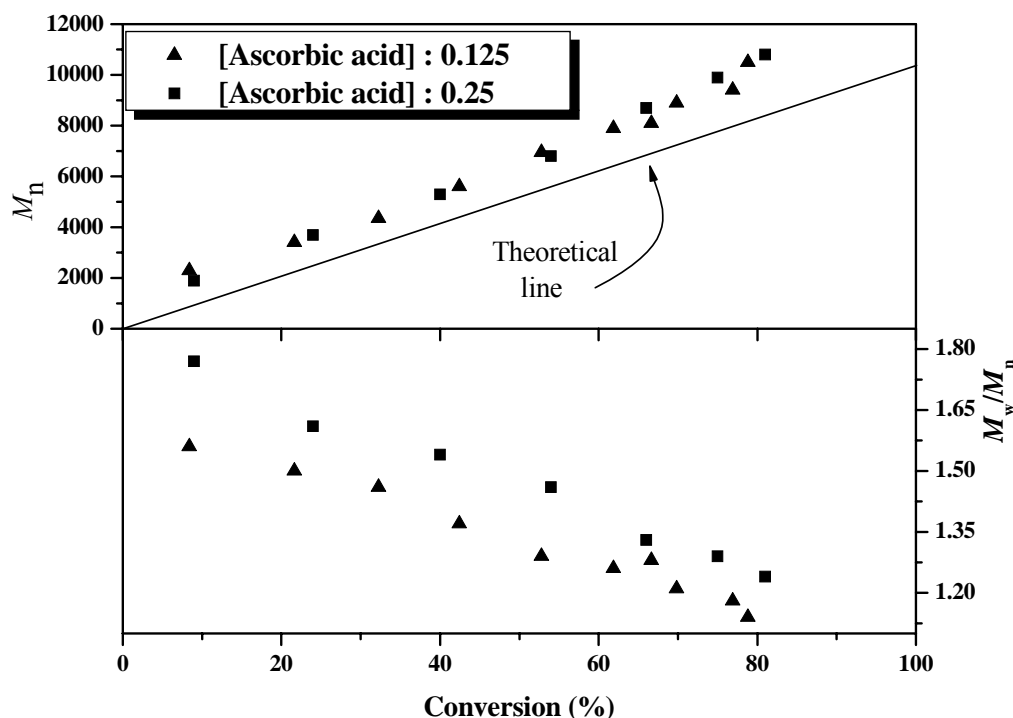


Figure 4.9: The dependence of M_n , and M_w/M_n , upon monomer conversion for ATRP of St at 110 °C in bulk (Experimental conditions as in Fig. 4.8).

4.2.1 The Effect of PMDETA Concentration on ATRP of St

We expanded our studies with the investigation of the dependence of polymerization rates and induction period on PMDETA concentration. PMDETA concentration was varied from 0.362 M to 0.0724 M ($[PMDETA]_0/[CuCl_2]_0 = 5/0.5$ and $1/0.5$) and the other polymerization parameters were kept constant with molar ratios of $[St]_0/[1\text{-PECl}]_0/[CuCl_2]_0/[Ascorbic acid]_0 = 100/ 1/ 0.5/0.125$. Fig. 4.10 presents the dependence of $\ln([M]_0/[M])$ on reaction time for the 1-PECl/ $CuCl_2$ /ascorbic acid/St system. The apparent rate constants (k_p^{app}), estimated from the maximum slopes of

the first-order kinetic curves, are $5.9 \times 10^{-5} \text{ s}^{-1}$ and $1.2 \times 10^{-4} \text{ s}^{-1}$ for the systems with 10:1 and 2:1 stoichiometry of ligand-to-copper(II) chloride respectively.

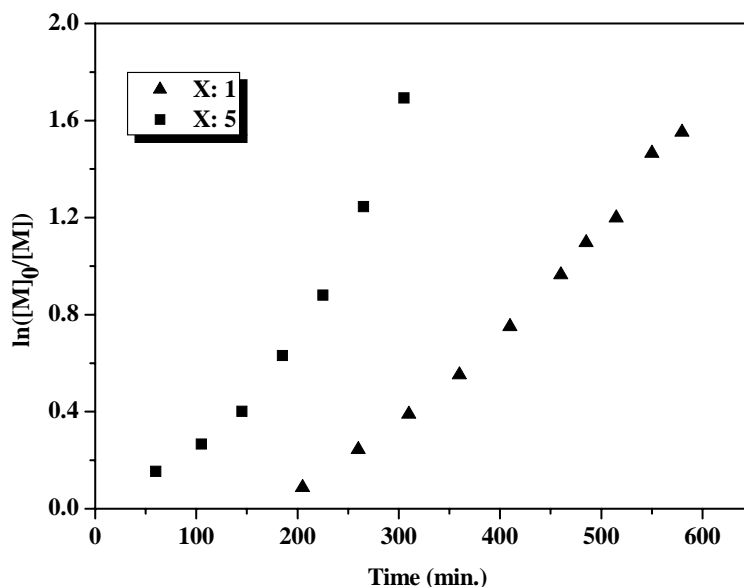


Figure 4.10: The first-order kinetic plot ATRP of St in bulk at 110 °C using ascorbic acid as a RA. $[\text{St}]_0 : [1\text{-PECl}]_0 : [\text{CuCl}_2]_0 : [\text{PMDETA}]_0 : [\text{Ascorbic acid}]_0 = 100 : 1 : 0.5 : X : 0.125$. (▲): $[\text{St}]_0 = 7.73 \text{ M}$; (■): $[\text{St}]_0 = 7.26 \text{ M}$.

Not only fast polymerization but also disappearance of induction period were observed when five fold excess PMDETA used. These might be attributed to increasing solubility of copper (II) complex and in the following faster formation copper (I) species which is activator in ATRP equilibrium. The molecular weight and MWD of the produced polystyrenes (PS) under various concentrations of PMDETA were further examined, as shown in Fig. 4.11. In all cases M_n increases and MWD becomes narrower with the increase of monomer conversion. As expected experimental molecular weights were found closer to theoretical values in the case lower PMDETA concentration since this polymerization is slower and more controlled compared to other kinetic study.

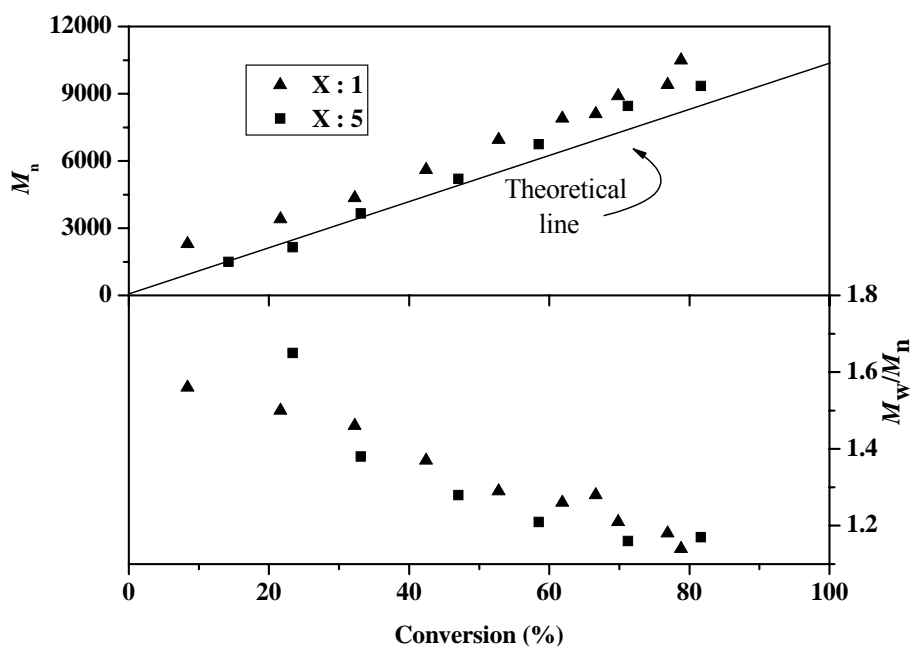
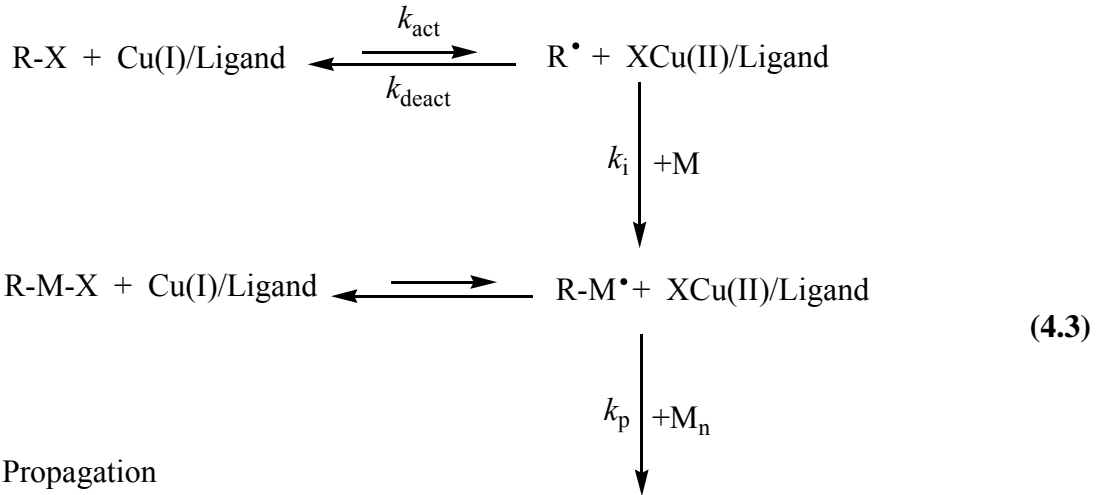


Figure 4.11: The dependence of M_n , and M_w/M_n , upon monomer conversion for ATRP of St at 110 °C in bulk (Experimental conditions as in Fig. 4.10).

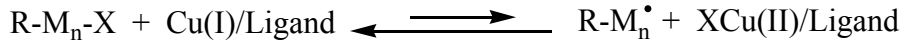
4.3 Fructose versus Ascorbic Acid as a RA in ATRP of St

Figure 4.12 presents the results of the kinetic studies where ascorbic acid or fructose was used as RA in bulk ATRP of St employing molar ratios of $[St]_0/[1-PECl]_0/[CuCl_2]_0/[PMDETA]_0/[Ascorbic\ acid\ or\ fructose]_0 = 100/1/0.5/1/0.25$. As shown, plots of $\ln([M]_0/[M])$ versus time were linear, which confirmed that the polymerization rate was first-order with respect to monomer concentration and the concentration of radicals was constant throughout the polymerization. Based on the slope of $\ln([M]_0/[M])$ vs. time plot k_p^{app} s were determined as $2.76 \times 10^{-4} \text{ s}^{-1}$ and $8.25 \times 10^{-5} \text{ s}^{-1}$ for the system using fructose and ascorbic acid as RA respectively. From the initiation and propagation steps in ATRP (4.3) the following rate laws were derived assuming a fast preequilibrium, a necessary condition to observe low M_w/M_n values in controlled/ "living" free-radical polymerizations (eqs 4.4 and 4.5) [304].

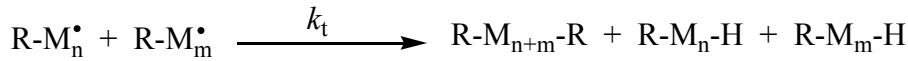
Initiation



Propagation



Termination



$$K_{\text{eq}} = \frac{k_{\text{act}}}{k_{\text{deact}}} = \frac{[\text{P}^\bullet] [\text{Cu(II)X}]}{[\text{Cu(I)X}] [\text{PX}]} \tag{4.4}$$

$$R_p = k_p^{\text{app}} [\text{M}] = k_p [\text{P}^\bullet] [\text{M}] = k_p K_{\text{eq}} [\text{In}] \frac{[\text{Cu(I)}]}{[\text{Cu(II)X}]} [\text{M}] \tag{4.5}$$

Equation (4.5) in combination with the values of k_p^{app} from Figure 4.12 (fructose: $2.76 \times 10^{-4} \text{ s}^{-1}$; ascorbic acid: $8.25 \times 10^{-5} \text{ s}^{-1}$) and the known rate constant of radical propagation for St ($k_p = 1.6 \times 10^3 \text{ M}^{-1} \text{ s}^{-1}$ at 110°C [67]) can be used to estimate the steady-state concentration of radicals in the polymerization. In this case, the calculated concentrations of radicals are 1.7×10^{-7} and $5.1 \times 10^{-8} \text{ M}$, for the polymerizations applying fructose and ascorbic acid as RA, respectively, which are sufficiently low for a minimal number of chains to undergo termination during the timespan in which the polymerization can go to high conversion. The bulk polymerization value (10^{-7} M at 110°C) can be compared to that found for the corresponding TEMPO-mediated St polymerizations at 130°C ($< 10^{-8} \text{ M}$) [304, 305]. Molecular weights evolved linearly with conversion in both systems (Figure 4.13). When ascorbic acid was used as RA, MWD values were narrow finally reached 1.2 towards the end of the polymerization.

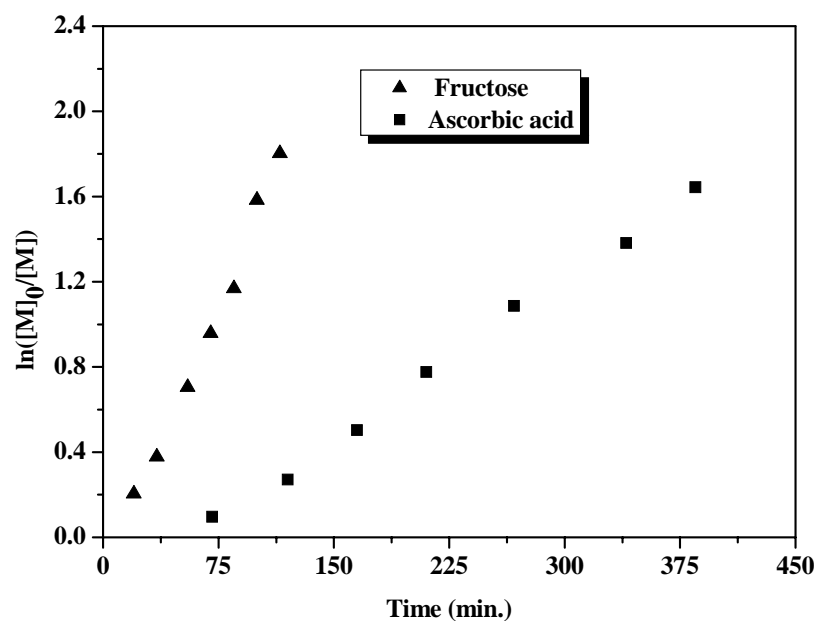


Figure 4.12: The first-order kinetic plot ATRP of St in bulk at 110 °C using ascorbic acid as a RA. $[St]_0 = 7.73M$; $[St]_0 : [1-PECl]_0 : [CuCl_2]_0 : [PMDETA]_0 : [Fructose \text{ or } Ascorbic \text{ acid}]_0 = 100 : 1 : 0.5 : 1 : 0.25$.

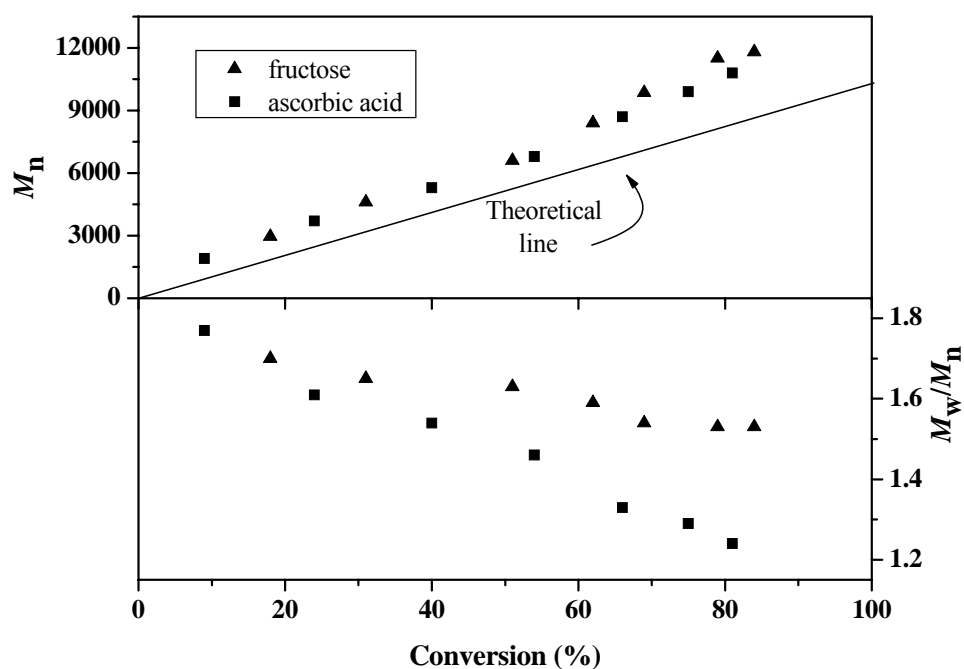


Figure 4.13: The dependence of M_n , and M_w/M_n , upon monomer conversion for ATRP of St at 110 °C in bulk (Experimental conditions as in Fig. 4.12).

Depending on these results one can easily say ascorbic acid is a milder RA compared to fructose. Thus higher polymerization rate and poor control over polymerization were obtained when fructose was used as RA.

4.4 Phenol Derivatives as a RA for *In Situ* Generation of Copper (I) Species in ATRP of St

Successful use of phenol and derivatives as RA in ATRP of methyl methacrylate (MMA), St, and methyl acrylate in the presence of limited amount of air was demonstrated by Hızal et. al. [135]. In here we presented the use of *p*-methoxyphenol, *p*-*tert*-butylphenol, and dihydroquinone as RA in ATRP of St under anaerobic conditions. Figure 4.14 presents the semilogarithmic kinetic plot for the polymerization of St catalyzed by CuCl₂/PMDETA in the presence of *p*-methoxyphenol. Kinetic study at molar ratios of [St]₀/[1-PECl]₀/[CuCl₂]₀/[PMDETA]/[*p*-methoxyphenol] = 100/ 1/ 0,5/ 5/ 3 was not fast enough and there was an induction period of ~ 100 min. Thus we used two fold excess PMDETA ([PMDETA]₀/[CuCl₂]₀ = 10/0.5). In this case the rate of polymerization increased but induction period did not disappear.

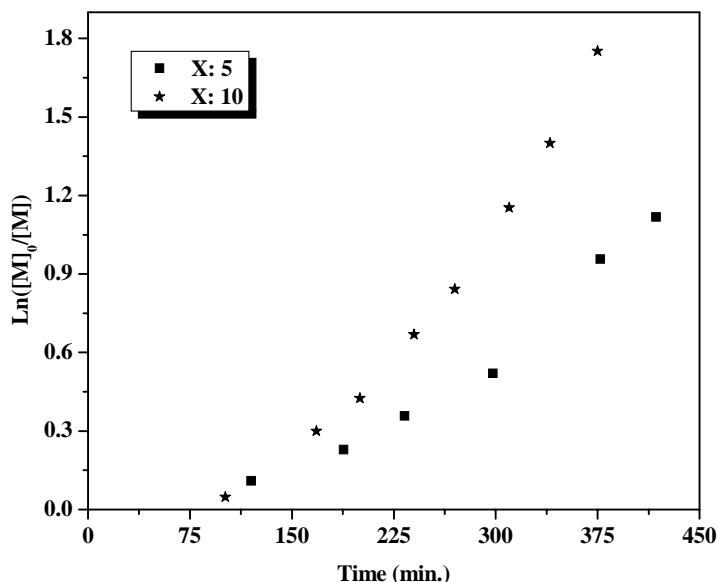


Figure 4.14: Time dependence of $\ln([M]_0/[M])$ for the bulk polymerization of St at 110 °C using *p*-methoxyphenol as a RA. [St]₀ : [1-PECl]₀ : [CuCl₂]₀ : [PMDETA] : [*p*-methoxyphenol] = 100 : 1 : 0,5 : X : 3. (■) : [St]₀ = 7.26 M; (★): [St]₀ = 7.13 M.

Figure 4.15 presents the evolution of molecular weight and molecular weight distribution with conversion. Linear plots were observed. The experimental molecular weight obtained from GPC analyses using linear polystyrene standards were close to theoretical values. Narrow MWD values were obtained (<1.4) indicating good control over polymerization.

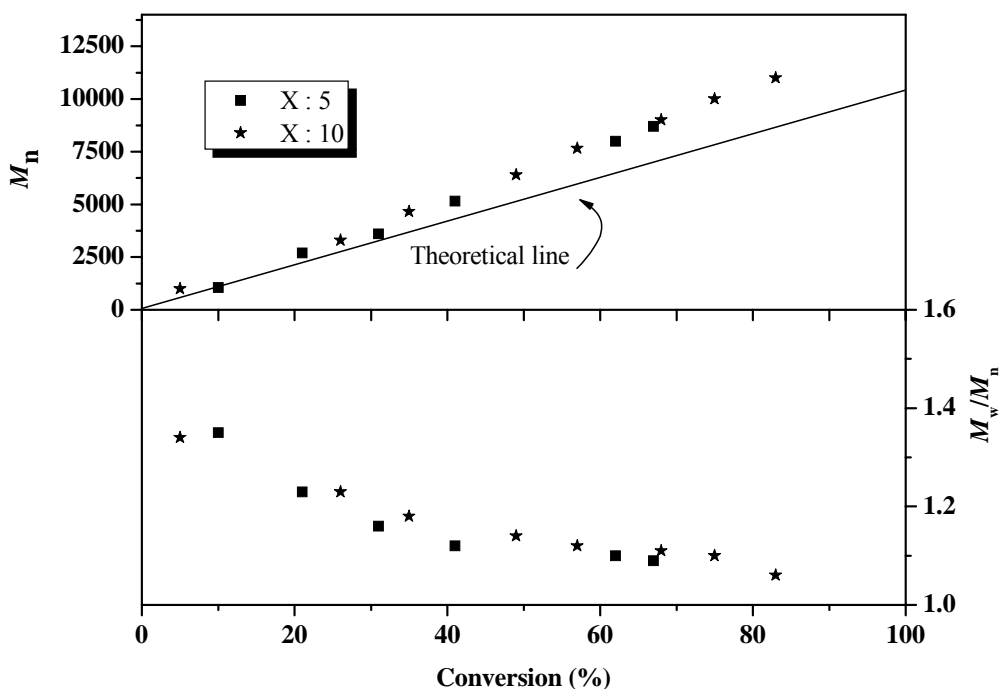


Figure 4.15: The dependence of M_n , and M_w/M_n , upon monomer conversion for ATRP of St at 110 °C in bulk (Experimental conditions as in Fig. 4.14).

Figure 4.16 presents the semilogarithmic kinetic plots of ATRP of St catalyzed by $\text{CuCl}_2/\text{PMDETA}$ in the presence of *p*-*tert*-butyl phenol as RA. A curvature of the semilogarithmic kinetic plots was observed, experimental molecular weights were found to those theoretically predicted (Fig. 4.17). MWD values became narrower with increasing monomer conversion.

We also tried dihydroquinone as RA in ATRP of St catalyzed by $\text{CuCl}_2/\text{PMDETA}$. Although linear plot was observed in semilogarithmic coordinates (Fig. 4.18) molecular weights were found higher than calculated values indicating low initiation efficiency (Fig. 4.19). Depending on these results dihydroquinone can not be regarded as an efficient RA.

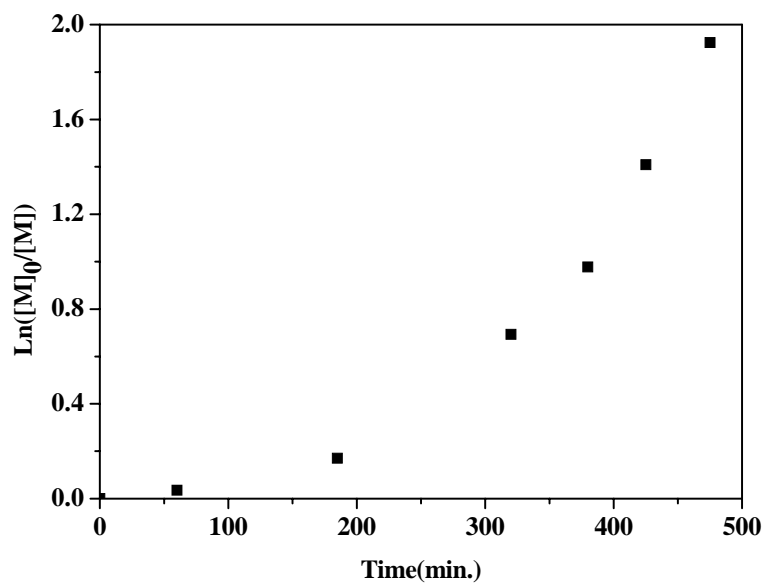


Figure 4.16: Time dependence of $\ln([M]_0/[M])$ for the bulk polymerization of St at 110°C; $[St]_0 = 6 \text{ mol. L}^{-1}$
 $[St]_0 : [1\text{-PECl}]_0 : [PMDETA]_0 : [CuCl_2]_0 : [p\text{-tert-butylphenol}]_0 = 100: 1 : 5: 0,5: 0,25$

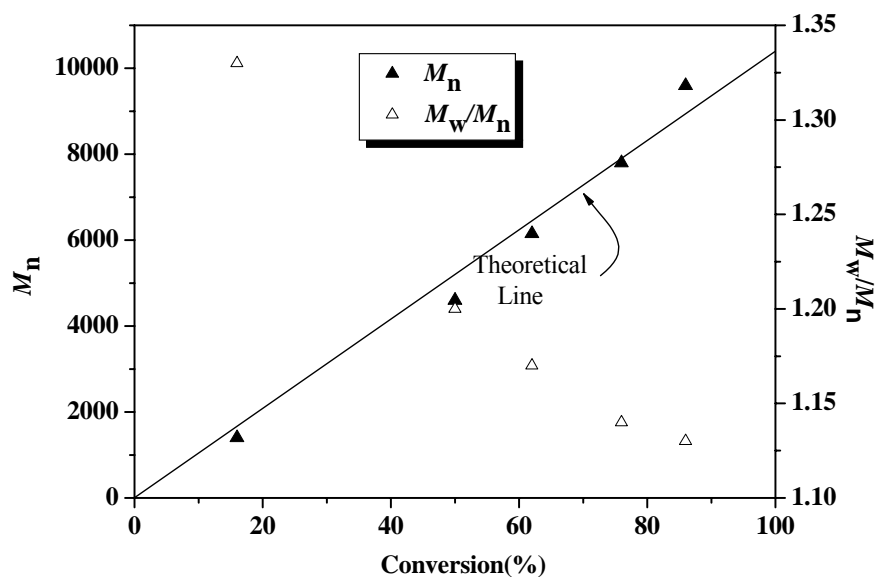


Figure 4.17: Dependence of M_n and MWD versus percent conversion for the bulk polymerization of St at 110°C (Experimental conditions as in Fig. 4.16).

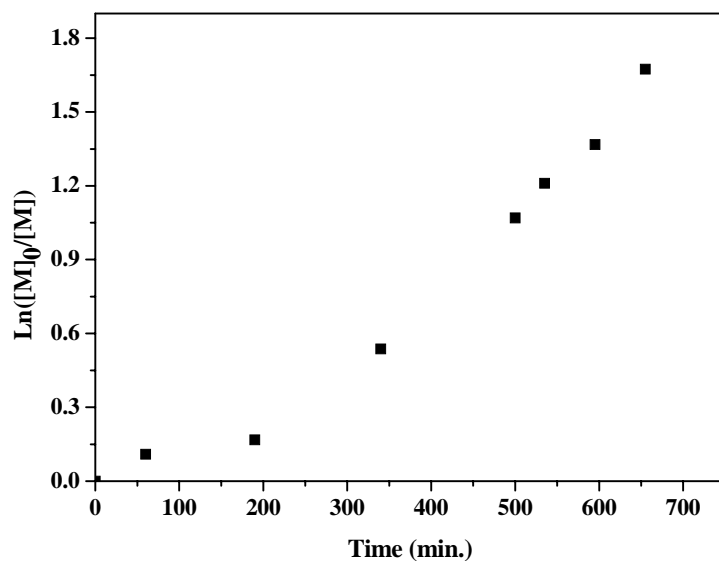


Figure 4.18: Time dependence of $\ln([M]_0/[M])$ for the bulk polymerization of St at 110°C; $[M]_0 = 6 \text{ mol. L}^{-1}$ $[St]_0 : [1\text{-PECl}]_0 : [PMDETA]_0 : [CuCl_2]_0 : [Dihydroquinone]_0 = 100: 1 : 5: 0,5: 0,75$.

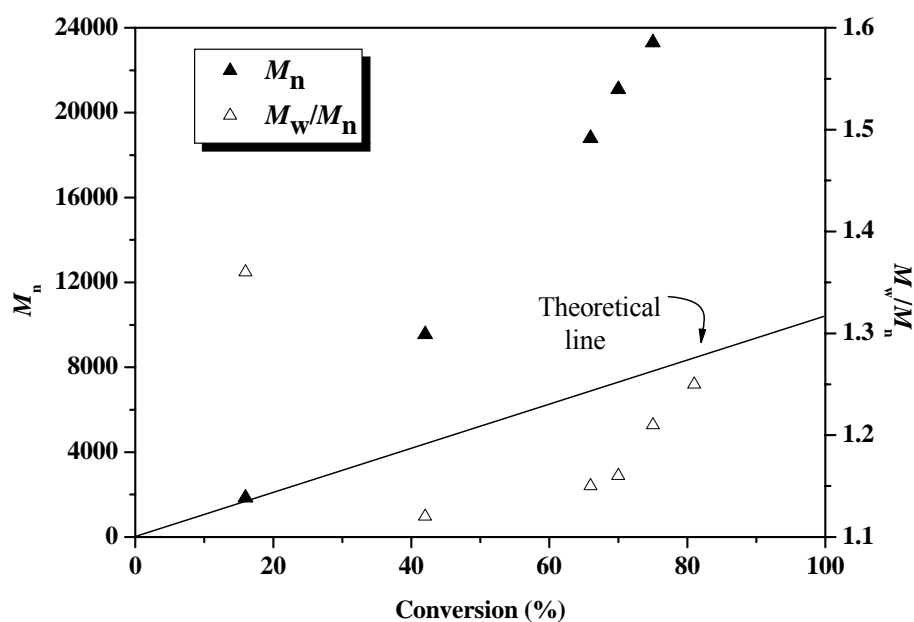
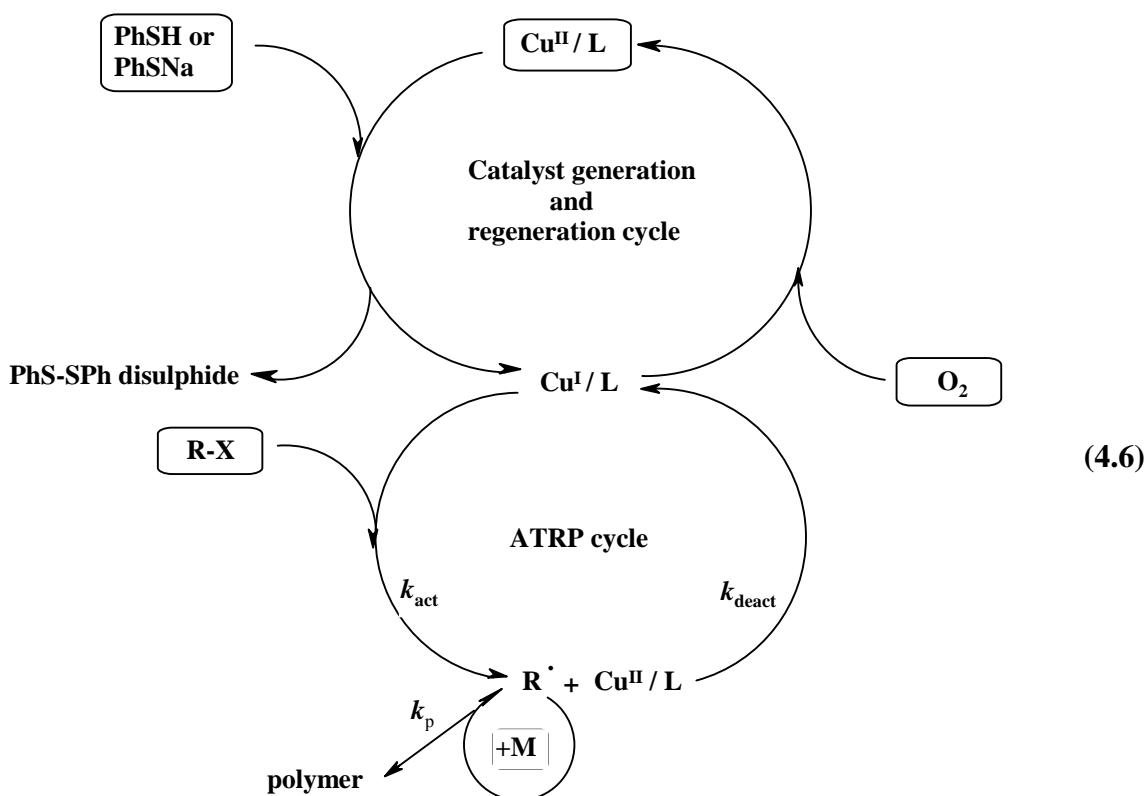


Figure 4.19: Dependence of M_n and M_w/M_n versus percent conversion for the bulk polymerization of St at 110°C. (Experimental conditions as in Fig. 4.18).

4.5 Thiophenol Derivatives as a RA for *In Situ* Generation of Cu(I) Species via Electron Transfer Reaction in ATRP of St in the Presence of Definite Amount of Air

ATRP of St was carried out in the presence of $\text{CuX}_2/\text{PMDETA}$ complexes and thiophenol derivatives such as *p*-methoxythiophenol or sodium thiophenolate (PhSNa) at 110 °C. A plausible mechanism of Cu (I) generation in the $\text{CuCl}_2/\text{PMDETA}$ mediated ATRP using thiophenol derivative is given in equation (4.6).



4.5.1 Effect of PhSNa Concentration on ATRP of St

In order to investigate the effect of PhSNa concentration on polymerization, several kinetic experiments were achieved using $[\text{St}]_0 : [1\text{-PECl}]_0 : [\text{CuCl}_2]_0 : [\text{PMDETA}]_0 : [\text{PhSNa}]_0 = 100 : 1 : 0.5 : 5 : 0.25\text{-}3$. As shown in Figure 4.20, linear semilogarithmic plots were obtained for all cases, except at $[\text{CuCl}_2]_0 : [\text{PhSNa}]_0 = 0.5 : 0.25$, a deviation was observed throughout the polymerization. In this case, an induction period was also detected.

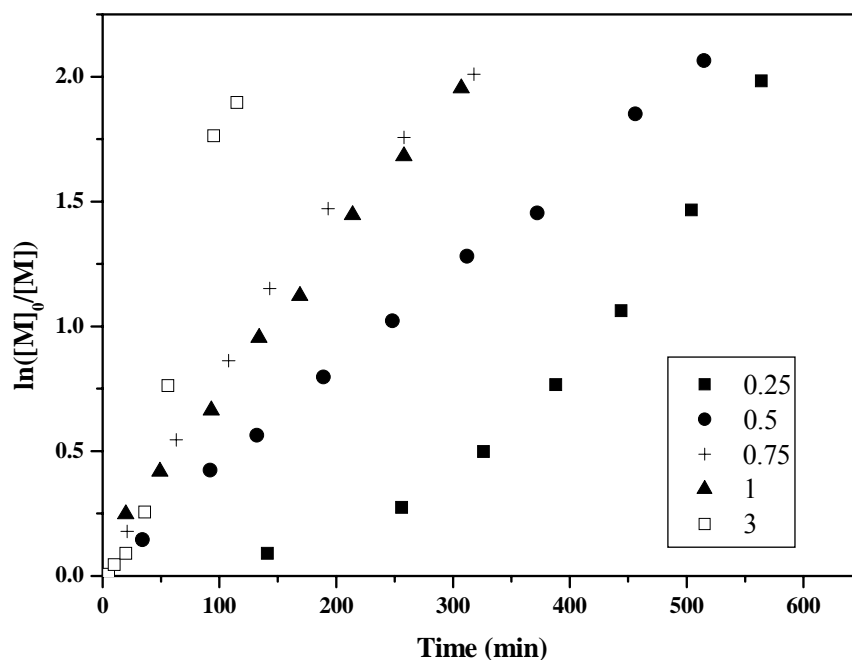


Figure 4.20: Time dependence of $\ln([M]_0/[M])$ for the polymerization of St at 110 °C in the presence of various amounts of PhSNa. $[St]_0 = 7.26 \text{ mol.L}^{-1}$
 $[St]_0 : [1\text{-PECl}]_0 : [CuCl_2]_0 : [PMDETA]_0 : [PhSNa]_0 = 100 : 1 : 0.5 : 5 : X$.
(X = ■ : 0.25; ● : 0.5; ★ : 0.75; ▲ : 1; □ : 3).

This would be explained by the prolonged time required for the formation of lower oxidation state metal salt, which is necessary for the generation of initiating radicals. This result is consistent with those obtained for the system using phenols in LRP of St [135]. Figure 4.21 showed dependence of M_n and M_w/M_n vs. conversion % plot. Theoretical molecular weights fit very well with experimental values. It should also be noted that experimental M_n values are not dependent on variation of PhSNa concentration. This is a strong evidence that PhSNa does not act as a chain transfer agent in ATRP of St in the range of 0.5: 0.25-1 (a molar ratio of Cu(II) to PhSNa). However, we have found that uncontrolled polymerization is observed at $[CuCl_2]_0 : [PhSNa]_0 = 0.5 : 3$ ratio and might be explained by the process in which the Cu(II) was almost consumed as a result of the reduction by excess amount of PhSNa.

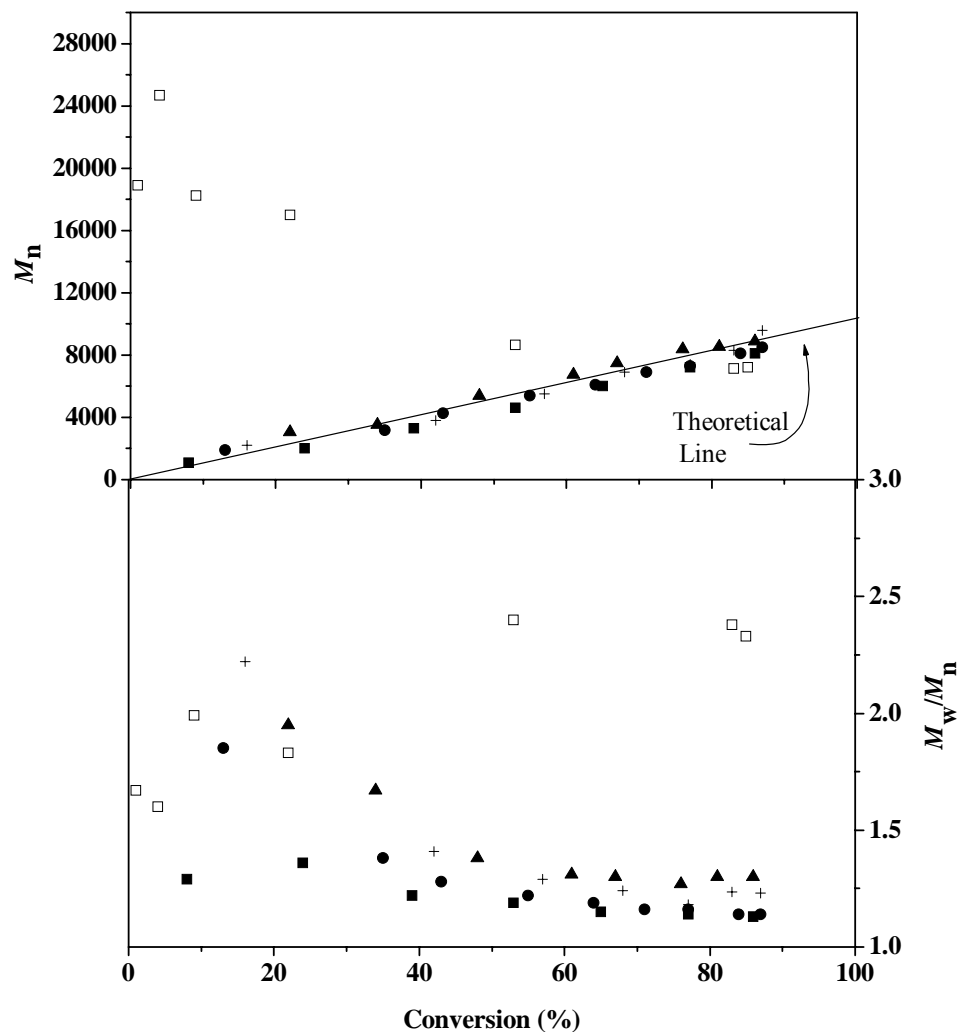


Figure 4.21: Dependence of M_n and M_w/M_n vs. percent conversion for the bulk polymerization of St at 110°C. $M_{n,theo}$ (—). (Experimental conditions as in Figure 4.20).

4.5.2 *p*-Methoxythiophenol versus PhSNa as a RA

The bulk polymerization of St catalyzed by 1-PECI/PMDETA/CuCl₂/*p*-methoxythiophenol or PhSNa was investigated (Fig. 4.22).

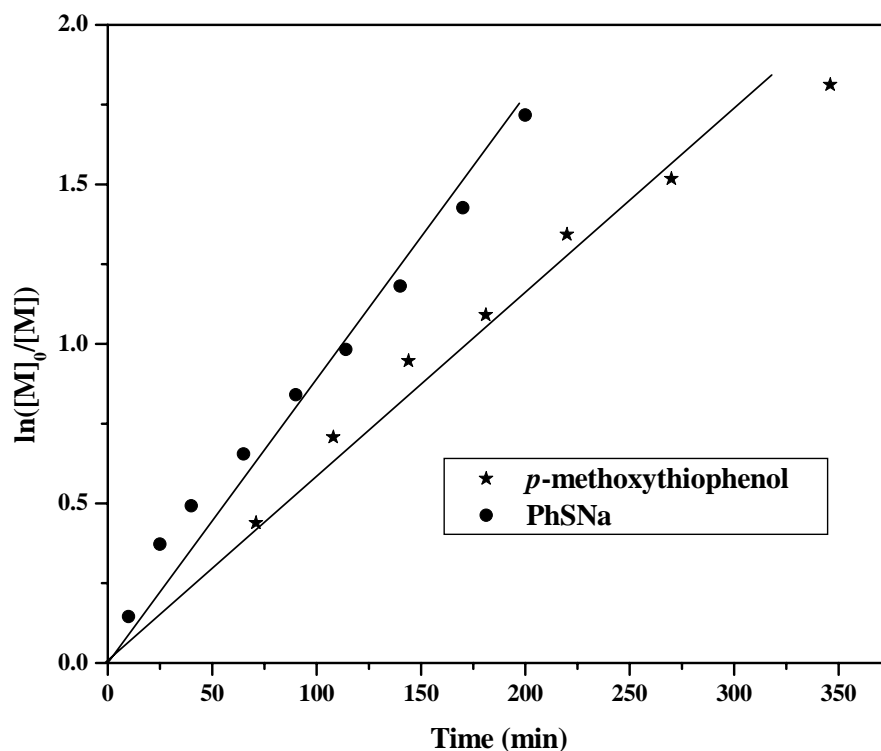


Figure 4.22: Time dependence of $\ln([M]_0/[M])$ for the polymerization of St at 110°C. $[St]_0 : [1-PECl]_0 : [CuCl_2]_0 : [PMDETA]_0 : [PhSNa \text{ or } p\text{-methoxythiophenol}]_0 = 100 : 1 : 0.5 : 5 : 1.5$; $[St]_0 = 7.26 \text{ mol.L}^{-1}$.

An increase in the apparent rate of polymerization was observed in the system using PhSNa as a RA. This can be attributed to a more electron donation ability of thiophenolate anion than *p*-methoxythiophenol. M_n and M_w/M_n vs. conversion % plot clearly showed that the controlled polymerization conditions were achieved in both cases (Fig. 4.23). Theoretical molecular weights well agreed with those of experimental values.

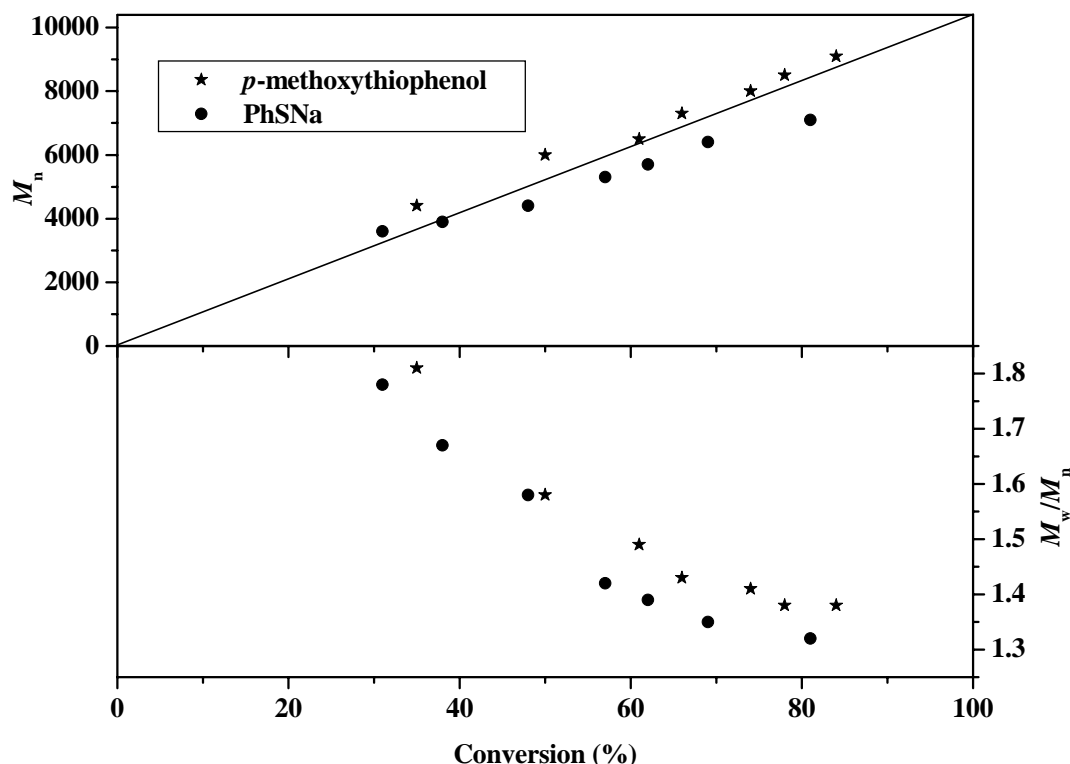


Figure 4.23: Dependence of M_n and M_w/M_n vs. conversion % for the bulk polymerization of St at 110°C. $M_{n,theo}$ (—). (Experimental conditions as in Figure 4.22).

4.5.3 Comparison of Different Initiator/Catalyst Systems

Figure 4.24 presents the results for bulk ATRP of St using different initiator/catalyst (EiBr/CuBr₂ and 1-PECl/CuCl₂) systems using molar ratios of $[St]_0/[Initiator]_0/[CuX_2]_0/[PMDETA]_0/[PhSNa]_0 = 100/1/0.5/5/0.75$. Within an experimental error, the apparent rate constants (k_p^{app}), estimated from the maximum slopes of the first-order kinetic curves (Fig. 4.24), are nearly identical for both systems. They are $k_p^{app} = 2.038 \times 10^{-4}$; and 1.36×10^{-4} for EiBr/CuBr₂ and 1-PECl/CuCl₂ systems respectively which indicates comparable polymerization rates. A deviation was observed in $\ln([M]_0/[M])$ -time graphs approximately after 80% which might be reasonable in bulk systems due to increasing viscosity at higher conversion (80%<). Furthermore M_n versus conversion (and M_w/M_n vs. conversion) plots were obtained (Fig. 4.25). Theoretical molecular weights were found closer to experimental ones for 1-PECl/CuCl₂ system. Narrow MWD values were obtained for both systems.

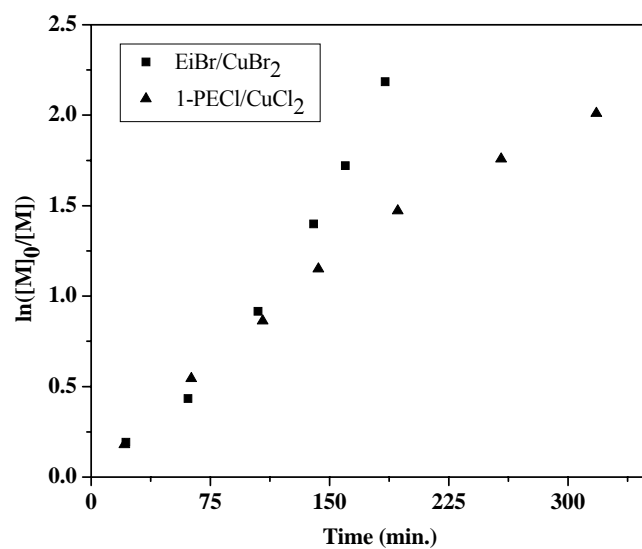


Figure 4.24: Time dependence of $\ln([M]_0/[M])$ for the ATRP of St at 110°C. $[St]_0 : [In]_0 : [CuX_2]_0 : [PMDETA]_0 : [PhSNa]_0 = 100 : 1 : 0.5 : 5 : 0.75$. $[St]_0 = 7.26 \text{ mol.L}^{-1}$.

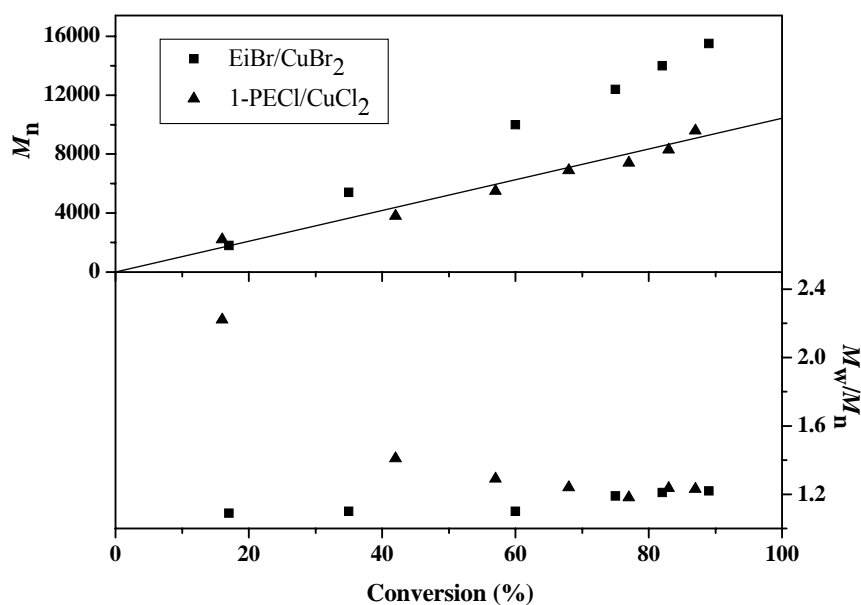


Figure 4.25: Dependence M_n and M_w/M_n versus percent conversion for the bulk polymerization of St at 110°C. $M_{n,theo}$ (—) (Experimental conditions as in Figure 4.24).

4.5.4 Dependence of Propagation Rate on Temperature

The effect of temperature on the rate of polymerization was studied at three different temperatures (90, 110 and 130 °C) using PhSNa as a RA. Fig. 4.26 shows the first order kinetics plots. The linearity between $\ln([M]_0/[M])$ and time in all cases indicates that the concentration of growing species remains constant and k_p^{app} increases with increasing the temperature of the polymerization. The apparent rate constant of propagation was calculated from the slopes derived from $\ln([M]_0/[M])$ -time graphs ($k_p^{\text{app}} = 3.9 \times 10^{-5}$ at 90 °C, 1.05×10^{-4} at 110 °C and $4.26 \times 10^{-4} \text{ s}^{-1}$ at 130 °C). The apparent activation energy (E_a^{app}) was found to be 73.6 kJ/mol from Arrhenius plot (Fig. 4.27), via equation (4.7), was slightly higher than that found for chloride mediated conventional ATRP of St ($E_a^{\text{app}} = 64.3 \text{ kJ/mol}$) [60].

$$k = A \times e^{-E_a/RT} \quad (4.7)$$

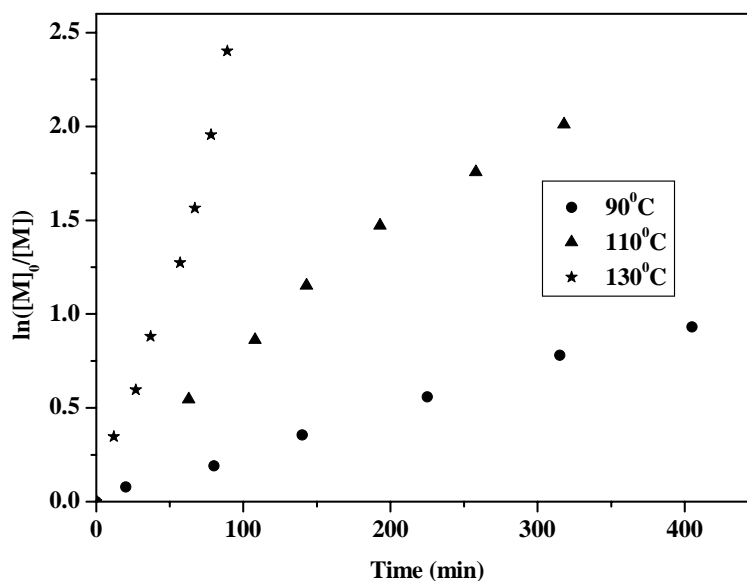


Figure 4.26: Time dependence of $\ln([M]_0/[M])$ for the ATRP of St at different temperatures. $[St]_0 = 7.26 \text{ mol.L}^{-1}$
 $[St]_0 : [1\text{-PECl}]_0 : [CuCl_2]_0 : [PMDETA]_0 : [PhSNa]_0 = 100 : 1 : 0.5 : 5 : 0.75$.

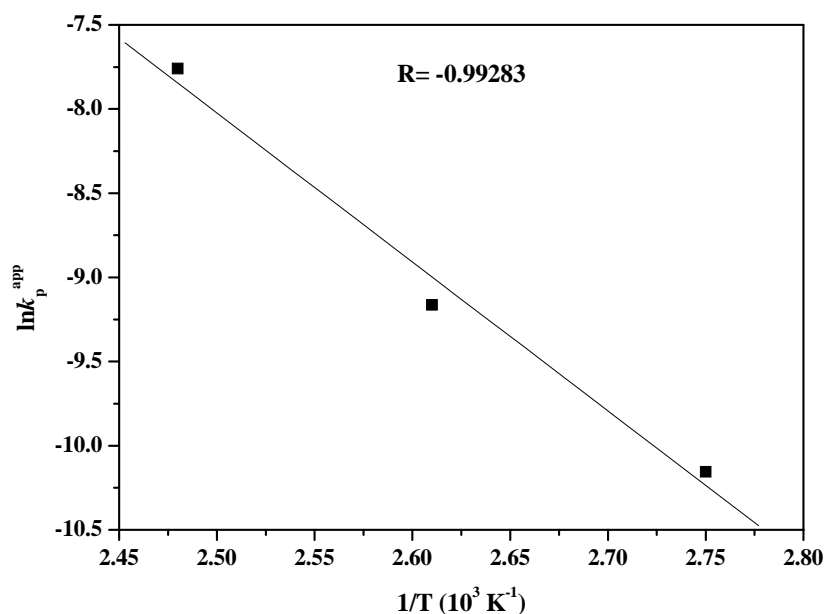


Figure 4.27: Arrhenius plot for the polymerization of St. $[\text{St}]_0 = 7.26 \text{ mol.L}^{-1}$; $[\text{St}]_0 : [1\text{-PECl}]_0 : [\text{CuCl}_2]_0 : [\text{PMDETA}]_0 : [\text{PhSNa}] = 100: 1 : 0.5 : 5: 0.75$.

4.5.5 UV-VIS Monitoring of Cu(II) Complex Consumption

In order to see Cu(II)/PMDETA complex consumption in the presence of PhSNa, UV-VIS measurements were studied. In UV-VIS spectra, the absorption at 720 nm attributed to d-d band of Cu(II)X_2 gradually decreased as the reaction proceeded in DMF at 110 °C (Fig. 4.28). However, because of an overlapping, formation of Cu (I) cannot be monitored as a characteristic peak of Cu (I)/ PMDETA at 290 nm.

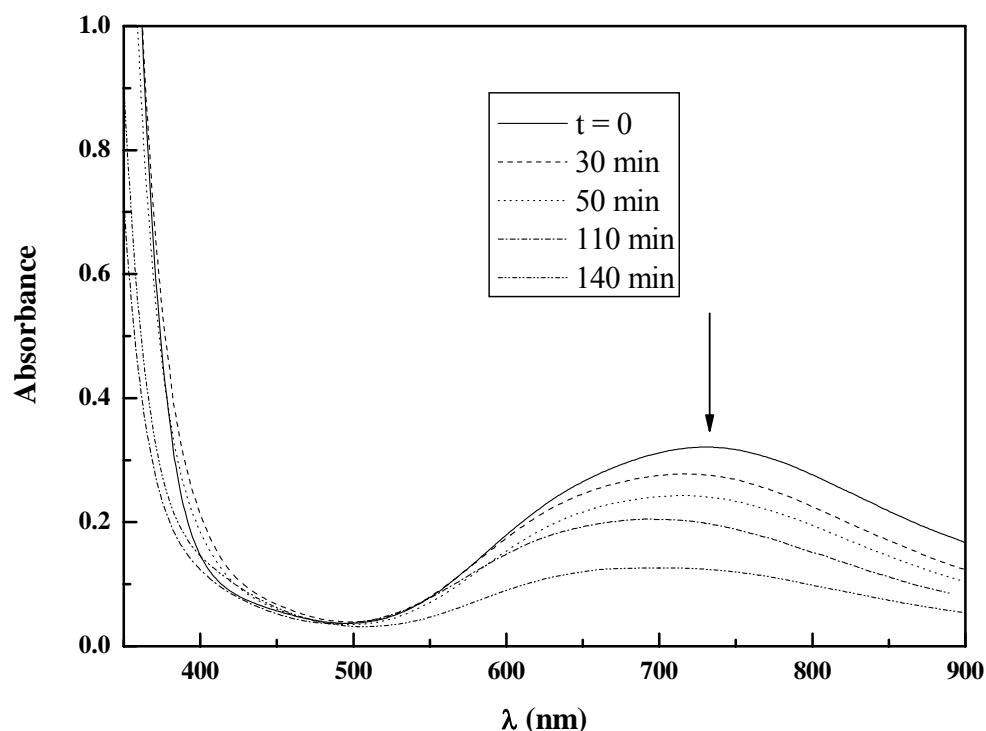
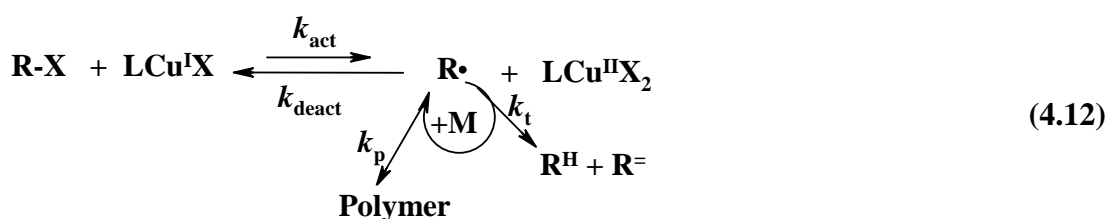


Figure 4.28: UV–vis spectra of $\text{CuCl}_2/\text{PMDETA}/\text{PhSNa}$ system in DMF; $[\text{CuCl}_2] = 2.18 \times 10^{-4} \text{ M}$; $[\text{CuCl}_2] : [\text{PMDETA}] : [\text{PhSNa}] = 1 : 10 : 1.5$.

It is well known that oxidation of thiophenols give disulfides in the presence of higher oxidation state metal complexes [306]. The oxidizing strength of the Cu(II) center permits the formation of metal-stabilized thiyl radical. Second-order reactivity ($k \cong 10^9 \text{ M}^{-1}\text{s}^{-1}$) with respect to inner-sphere, S-bonded intermediates, leading to concerted two-electron transfer and S-S bond formation is more common [307-310]. Holwerda and coworkers reported that the oxidation of cysteine (cys-SH) was carried out using [2,2',2''-tris(dimethylamino) triethylamine]copper(II) ($\text{Cu}(\text{Me}_6\text{tren})^{2+}$) and [tris(2-pyridylmethyl)amine]copper(II) ($\text{Cu}(\text{tmpa})^{2+}$) complexes resulted in S-S bond formation [311]. We can therefore assume that the reaction of Cu(II) complex with thiophenol derivative in Eq. (4.8) is feasible. Under the condition of the present study, the detailed reaction pathway for the generation of Cu(I) in the presence of thiophenol is given as follows.



where, L= PMDETA (in excess); X=Cl or Br; Y=H or Na



Notably, conversion of thiophenol into phenyl disulphide in the presence of Cu(II)/PMDETA in CDCl₃ was proved by ¹H NMR measurement at room temperature. A signal assigned to $-SH$ proton of thiophenol at 4.46 ppm disappeared and new signals at 7.5-7.4 ppm appeared corresponding to *ortho* protons of disulphide. Thus forming Cu(I) can undergo two competitive reactions as illustrated in Eqs (4.9) and (4.11). However, the oxidation Cu (I) has predominantly occurred ($k_{ox} \gg k_{act}$) under this condition. The bis(μ oxo) dicopper or $\mu\eta^2: \eta^2$ -peroxodicopper (II) complex [312], which is readily formed by oxidation process further reacts with remaining thiophenol derivative in order to give Cu (I). Such generation of Cu (I) would be expected to initiate the polymerization as a result of the consumption of oxygen and thiophenol as well. Phenyl disulfide formed by the oxidation process of thiophenol may act as an initiator and/or a chain transfer agent (CTA) in polymerization of St. However, an addition of arylthyl radical (ArS \cdot) to olefins shows greater reversibility than that of alkylthiyl radical [313]. Therefore, its contribution to initiation process can be considered as negligible. The chain transfer constant (C_{tr}) of phenyl disulfide was found to be as 0.15 in St polymerization at 60 °C [314].

In addition, low reactivity of ArS^\cdot to molecular oxygen and in H atom abstraction has been known [315, 316]. Overall, the mechanism for *in situ* generation of Cu (I) in the presence of Cu(II)/PMDETA/PhSY presented in Equations (4.8)-(4.13) seems to be reasonable.

4.5.6 ATRP of Methyl Methacrylate (MMA)

The solution ATRP of MMA catalyzed by $\text{EtBr/PMDETA/CuCl}_2/p$ -methoxythiophenol or PhSNa was investigated (Fig. 4.29). The apparent rate constants determined from the slopes of semilogarithmic plots are $k_p^{\text{app}}=9.65 \times 10^{-5}$ and 1.59×10^{-4} for the system using *p*-methoxythiophenol or PhSNa as RA respectively. Although there is no such big difference in the rate of polymerizations, the system applying PhSNa was found to be faster compared to other one. Thus PhSNa can be regarded as more effective RA than *p*-methoxythiophenol. This result agrees with the one obtained in ATRP of St applying *p*-methoxythiophenol or PhSNa as RA (Part 4.2.2).

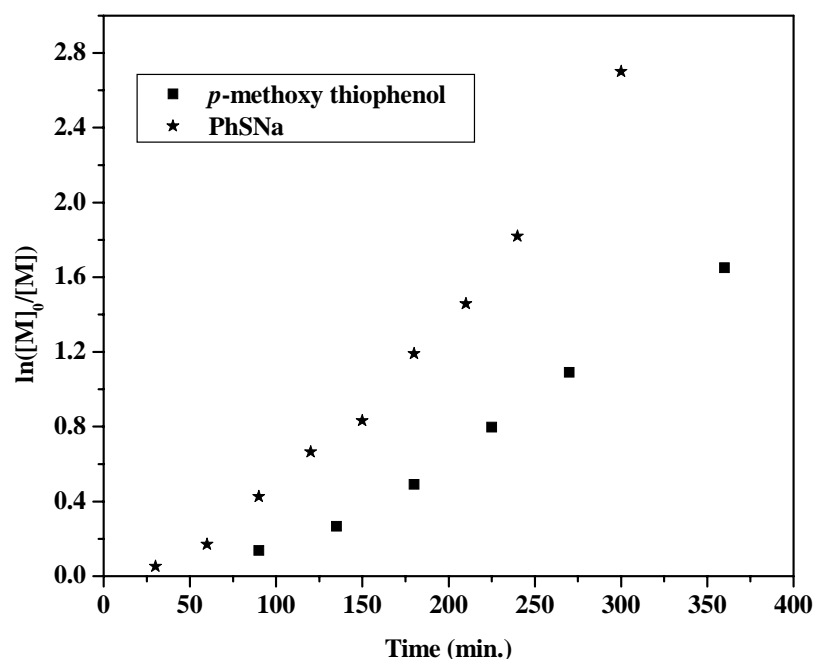


Figure 4.29: The first-order kinetic plots for ATRP of MMA in toluene (1/1, v/v) at 90 °C. $[\text{MMA}]_0 : [\text{EtBr}]_0 : [\text{CuCl}_2]_0 : [\text{PMDETA}]_0 : [\text{PhSNa or } p\text{-methoxythiophenol}]_0 = 100 : 1 : 0.5 : 5 : 0.75$; $[\text{MMA}]_0 = 4.58 \text{ mol.L}^{-1}$.

As shown in Figure 4.30 molecular weights evolved linearly with monomer conversion and fit well with theoretical molecular weights. Besides MWD values remained very narrow throughout polymerization. All these results indicate excellent control over polymerization for both cases.

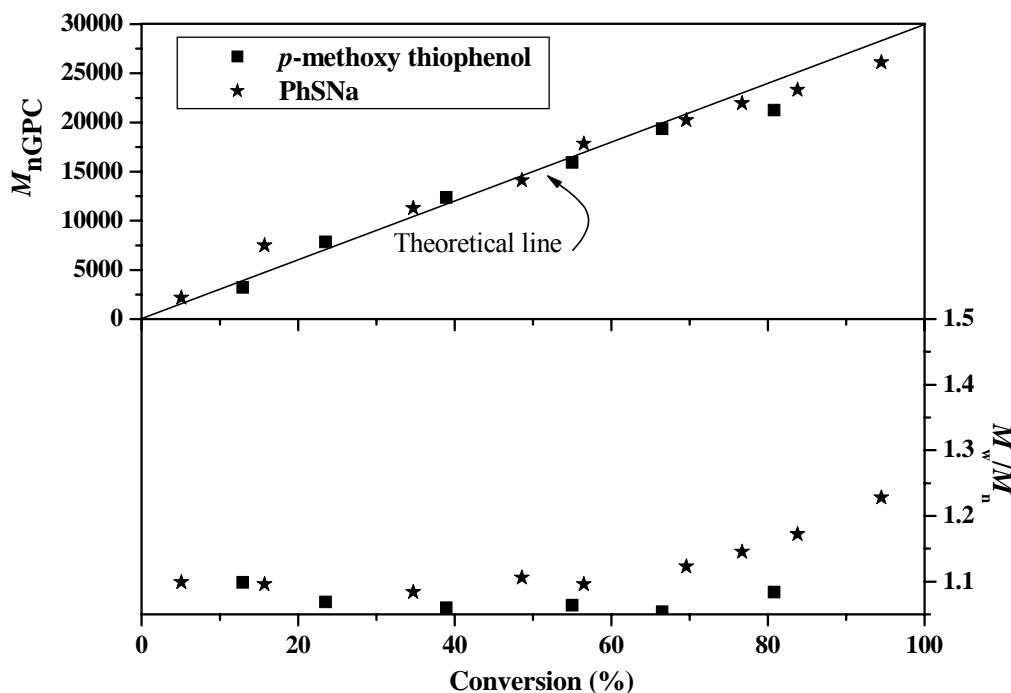


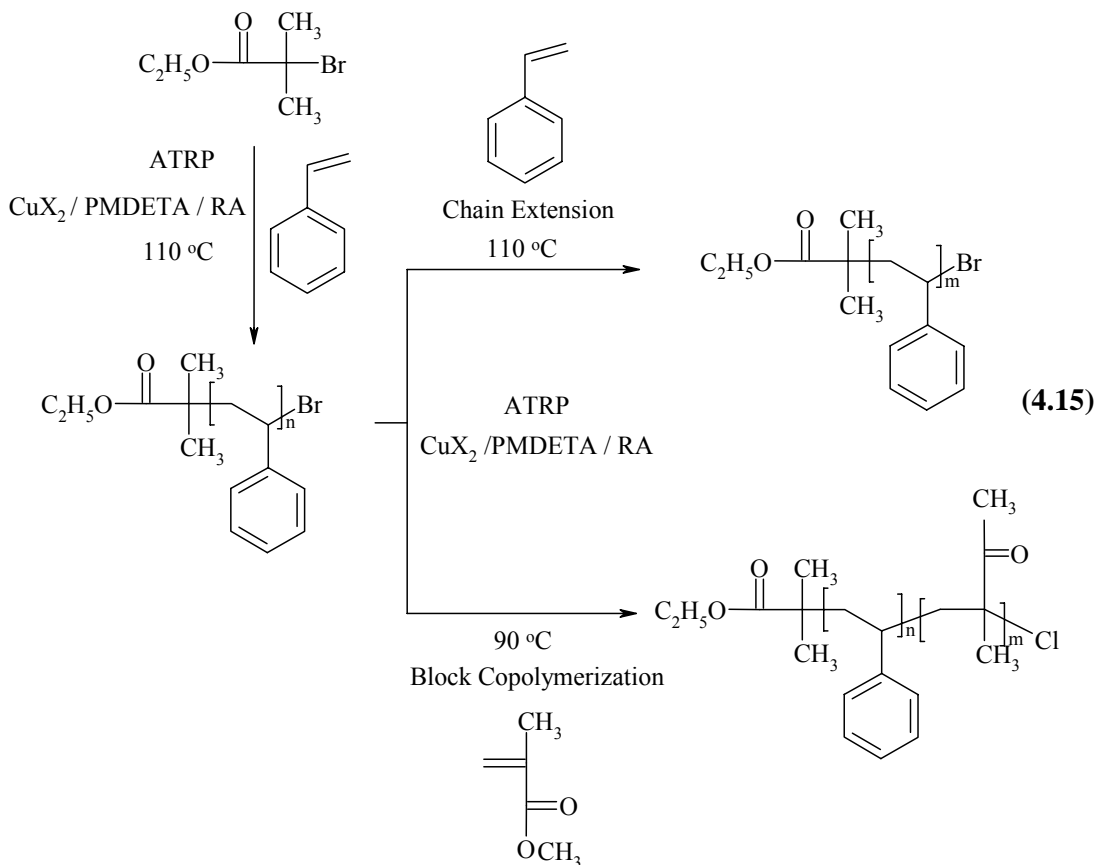
Figure 4.30: Dependence of M_n and M_w/M_n vs. conversion % for the bulk polymerization of MMA at 110°C (Experimental conditions as in Figure 4.29).

4.6 Chain Extension and Block (Co)Polymerization

PS macroinitiators were synthesized via bulk (if otherwise indicated) ATRP at 110 °C using $\text{EtBr/CuBr}_2/\text{PMDETA}$ or $1\text{-PECl/CuCl}_2/\text{PMDETA}$ initiator/catalyst complex system in the presence of RA (4.15). The experimental number average molecular weights were determined by GPC based on linear PS standards. The theoretical M_n values were calculated by using the following equation:

$$M_{n,\text{theo}} = ([M]_0/[I]_0) \times \text{Conversion \%} \times 104 + (\text{MW}_{\text{initiator}}) \quad (4.14)$$

where $MW_{\text{initiator}}$ is the molecular weight of the initiator (EiBr or 1-PECl) and $[M]_0$ and $[I]_0$ are the initial concentrations of the monomer and initiator, respectively. GPC traces of the obtained polymers displayed narrow and monomodal MWD.



4.6.1 Characterization of Linear PS Macroinitiator Synthesized via ATRP under Inert Atmosphere using Fructose as a RA

The structure of PS-Br ($M_n = 1800$, $M_w/M_n = 1.11$) (**H1**, Table 4.1) was confirmed by ^1H NMR. Two signals assignable to $\text{CH}_3\text{CH}_2\text{OC}=\text{O}$ as α - and $\text{PhCH}-\text{Br}$ as ω -end group of PS-Br were observed at 3.7 and 4.5 ppm, respectively. No peak was detected corresponding to PS with alkene end group, which would occur from HBr elimination during the polymerization process. In addition, a matrix-assisted laser desorption/ionization time-of-flight (MALDI-TOF) mass spectrometry study on linear PS-Br obtained from the aforementioned strategy ($[\text{St}]_0/[\text{EiBr}]_0/[\text{CuBr}_2]_0/[\text{PMDTA}]_0/[\text{Fructose}]_0 = 50/1/0.5/1/0.05$; bulk; $M_{n,\text{theo}} = 1750$; $M_{n,\text{NMR}} = 1900$; $M_n = 1800$; $M_w/M_n = 1.10$) was performed for structural identification, especially α - and ω - end group determination.

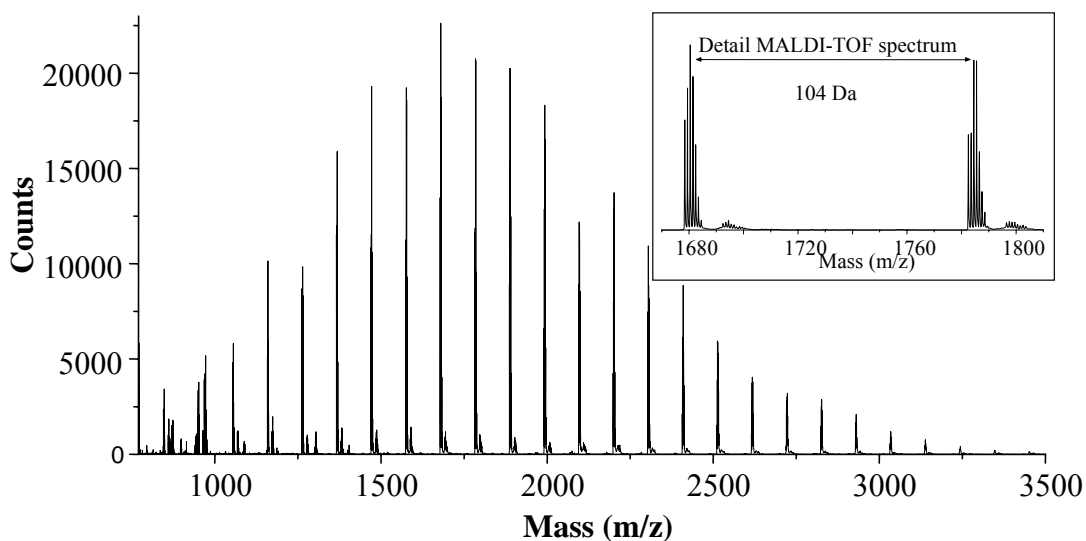


Figure 4.31: MALDI-TOF mass spectrum of linear PS-Br macroinitiator; $[St]_0 = 8.6$ M; $[St]_0/[EtBr]_0/[CuBr_2]_0/[PMDTA]_0/[Fructose]_0 = 50/1/0.5/1/0.05$; at 110 °C. In the inset, a detail of the MALDI-TOF mass spectrum is given. Matrix, dithranol; cationating agent, AgTFA.

The MALDI-TOF spectrum of linear PS-Br is depicted in Figure 4.31 ($M_{n,MALDI} = 1860$, $M_w/M_n = 1.09$). Up to 3 different series of peaks, each separated by 104 Da (molar mass of St repeating unit), can be observed (Fig. 4.32). From the comparison between the measured and the theoretical isotope distribution, the major series (1) can be attributed to the silver adduct of PS that is initiated by EtBr and has an alkene end group. The elimination of HBr is a consequence of the fragmentation of the carbon-to-bromine bond in the MALDI process [317]. The small series (2) corresponds to silver cationized PS with a methylene exo double bond at the ω -end. This can be ascribed to MALDI-induced PS scission. It has been reported by Zammit et al [318] that part of the PS-chains can fragment during a MALDI analysis, leaving a vinyl group on the chain end. The latter series overlaps with series (3), which is 18 Da higher than the main series. Until now, the origin of series (3) remains unknown. It can not be ascribed to PS of which the Br end group has been replaced by a hydroxyl group as a result of the precipitation method in methanol, since precipitation of the same polymer in hexane gives the same MALDI-TOF spectrum. Both the signals attributed to recombined polymer chains with an initiator fragment at each chain end (calculated $m/z = 1669.8$ Da) and the signals as a result of thermal initiation (calculated $m/z = 1691.9$ Da) could not be detected. All these data confirm

the controlled character of the polymerizations in the presence of fructose as RA. The polymerization conditions and the results of GPC analysis were summarized in Table 4.1.

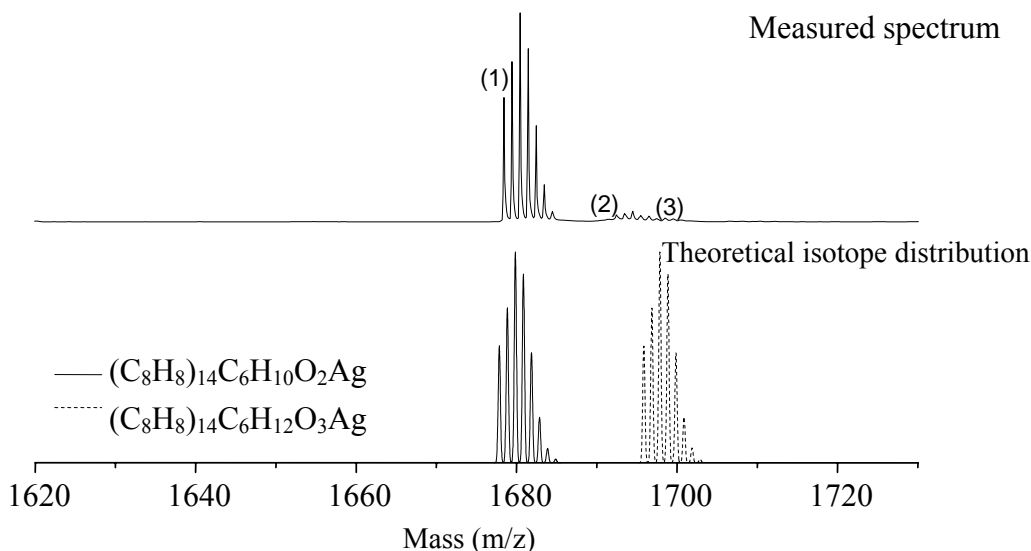


Figure 4.32: Comparison of experimental and theoretical isotope distribution of ions formed in the MALDI process.

4.6.2 Preparation of Linear PS-*b*-PMMA Copolymer

The synthesis of linear PS-*b*-PMMA block copolymers was achieved by ATRP of MMA using previously obtained PS-Br as macroinitiator fructose as a RA and Cu(II)Cl₂/PMDETA as catalyst system (Table 4.1). Block copolymerizations were performed in toluene (1/1; v/v) at 90 °C to give linear PS-*b*-PMMA (**H3-5**). Figure 4.33 displays the overlay of PS macroinitiator (**H2**) and corresponding PS-*b*-PMMA copolymer (**H3**). A clear shift in GPC chromatogram demonstrates that the chain ends of the homopolymer mostly possess halide end group. From the GPC trace, the amount of the dead chains (PS macroinitiator) was calculated to be 3.6 % of the resulting chain extended polymer using deconvolution method (by Peak Fit program, Seasolve).

Table 4.1: Characteristics of Linear Homo- and Block Co-Polymers Prepared via ATRP Using Fructose as a RA.

Run	Monomer	Initiator	$[M]_0$ (mol/L)	$[M]_0:[I]_0:[CuX_2]_0:[PMDTA]_0:[RA]^a_0$	Temp. (°C)	Time (h.)	Conv. ^b (%)	$M_{n, \text{theo}}^c$	M_n	M_w/M_n	f^d
H1^e	St	EiBr	8.6	50 : 1 : 0.5 : 1 : 0.05	110	0.83	30	1750	1800	1.10	0.97
H2	St	EiBr	4.15	30 : 1 : 0.5 : 1 : 0.05	110	1.67	46	1650	1650	1.11	1
H3	MMA	H2	4.67	500 : 1 : 0.5 : 1 : 0.025	90	48	23	13150	26850	1.10	0.49
H4	MMA	H2	4.67	500 : 1 : 0.5 : 1 : 0.25	90	22	73	38200	54950	1.26	0.70
H5	MMA	H2	4.65	500 : 1 : 0.5 : 2.5 : 0.25	90	20	97	50200	102900	1.31	0.49

Polymerizations were performed in toluene (monomer / toluene = 1 (v/v)). CuBr₂ and CuCl₂ were used as transition metal catalyst for homo- and block co-polymerization respectively.

^a Fructose was used as RA.

^b Conversions were determined gravimetrically.

^b Theoretical molecular weights were determined as follows: $M_{n, \text{theo}} : ([M]_0/[I]_0 \times \text{conversion \%} \times \text{MW(MMA)}) + M_n(\text{PS macroinitiator})$ for block copolymers.

^d $f = M_{n, \text{theo}} / M_n$

^e Polymerization was performed in bulk.

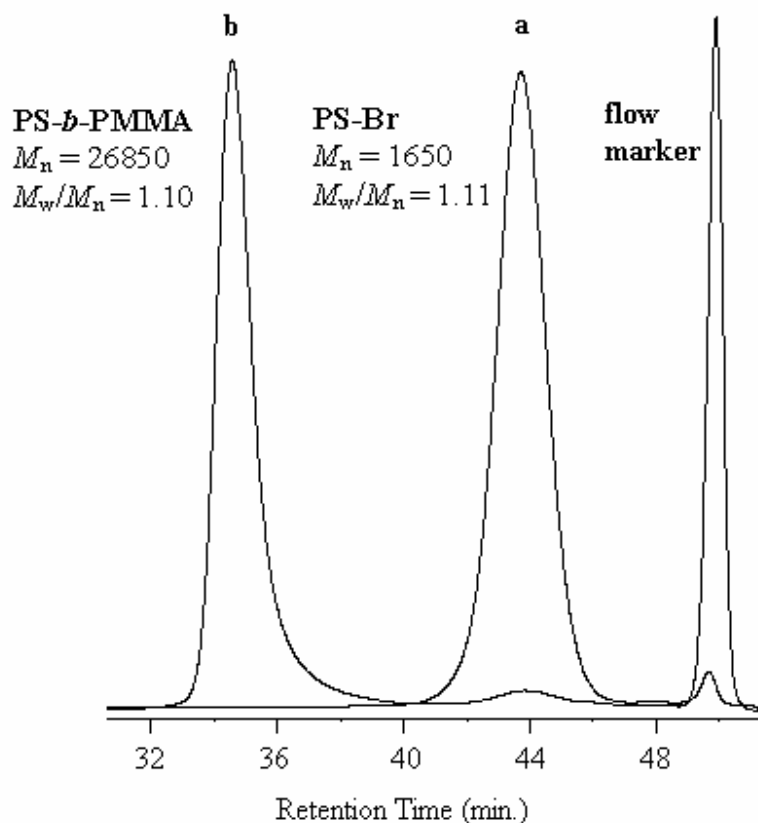


Figure 4.33: GPC traces of (a) linear PS-Br macroinitiator (**H2**) and (b) linear PS-*b*-PMMA (**H3**).

When fructose concentration was increased ten fold while keeping all the other parameters constant, not only an increase in rate of polymerization but also an improvement in initiation efficiency was observed. GPC traces of PS macroinitiator (**H2**) and PS-PMMA block copolymer (**H4**) are shown in Figure 4.34. The complete disappearance of the peak due to macroinitiator suggests that high initiation efficiency ($f = M_{n,theo} / M_n = 0.7$) was attained. Then we increased the PMDETA concentration 2.5 fold to improve the solubility of $CuBr_2$ /PMDETA catalyst complex. Increasing PMDETA concentration led to an increase in rate of polymerization but no improvement was observed in initiation efficiency. A clear shift to higher molecular weight region was observed in GPC chromatogram (Fig. 4.35) of PS homopolymer (**H2**) and corresponding PS-PMMA block copolymer (**H5**) indicating efficient block copolymerization. Based on these results optimum molar ratios for block

copolymerization using fructose as RA was found to be $[MMA]_0:[H2]_0:[CuBr_2]_0:[PMDTA]_0:[Fructose]_0 = 500 : 1 : 0.5 : 1 : 0.25$.

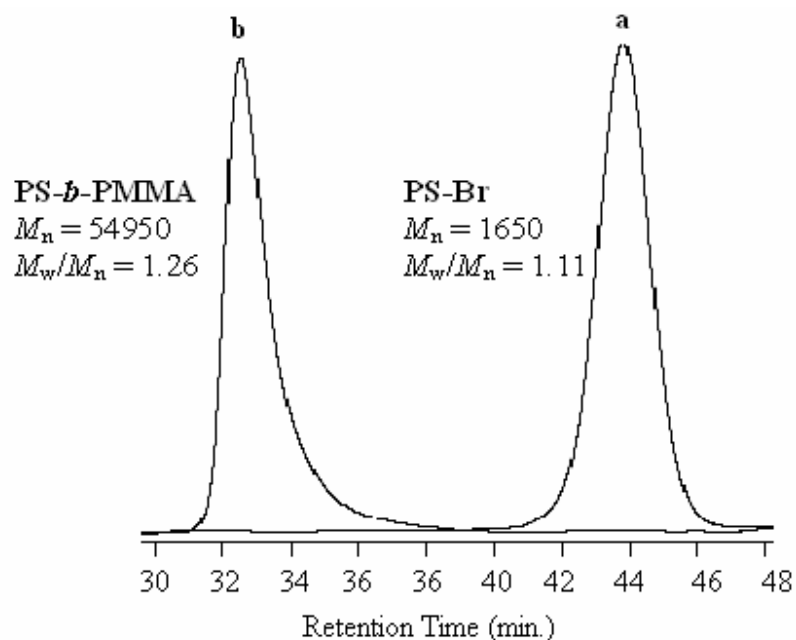


Figure 4.34: GPC traces of (a) linear PS-Br macroinitiator (**H2**) and (b) linear PS-*b*-PMMA (**H4**).

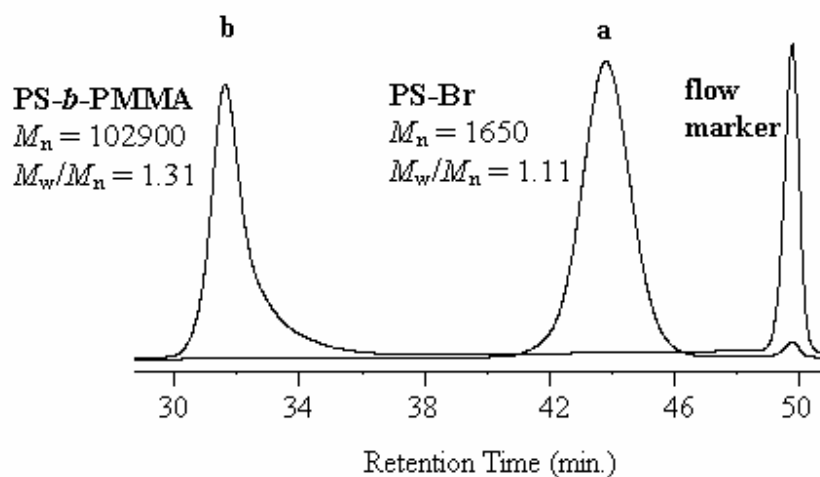


Figure 4.35: GPC traces of (a) linear PS-Br macroinitiator (**H2**) and (b) linear PS-*b*-PMMA (**H5**).

Also PS homopolymer (**H6**) prepared via ATRP using $CuBr_2$ /PMDTA/ascorbic acid catalyst system was used as macroinitiator in block copolymerization with MMA. Table 4.2 shows the polymerization conditions and characteristics of homo- and block co-

polymers. Also the GPC traces of PS macroinitiator (**H6**) and PS-PMMA block copolymer (**H7**) are shown in Figure 4.36. Not very efficient block copolymerization was observed when $[\text{CuCl}_2]_0 / [\text{PMDETA}]_0 = 1/2$ molar ratio was applied. A shoulder in low molecular weight region was detected in GPC chromatogram. From the GPC trace, the amount of the dead chains (PS macroinitiator) was calculated to be 6 % of the resulting chain extended polymer using deconvolution method (by Peak Fit program, Seasolve).

When 2.5 fold excess PMDETA ($[\text{CuCl}_2]_0 / [\text{PMDETA}]_0 = 1/5$) was used more efficient block copolymerization was observed. Figure 4.37 shows the GPC traces of PS-PMMA block copolymer (**H8**) and its precursor (**H6**). This GPC chromatogram shows the formation of the PMMA block. After polymerization of MMA, the GPC trace shifts to the higher molecular weights region along with complete disappearance of the peak of the precursor indicating that efficient block copolymerization has occurred. Moreover, narrow MWD (1.16) indicated a controlled growth of the PMMA block. Increasing PMDETA concentration provided more controlled polymerization yielding block copolymer with low M_w/M_n (1.16).

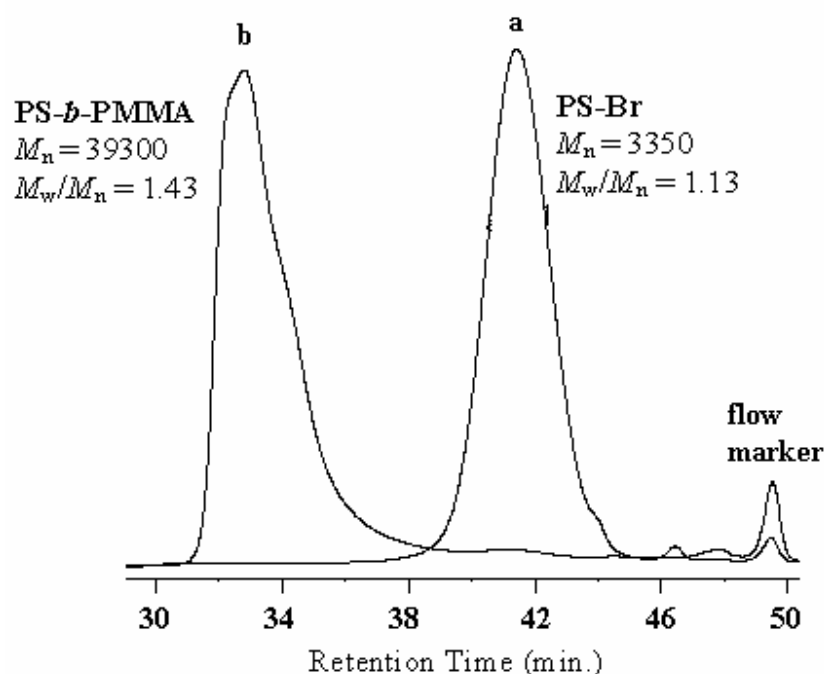


Figure 4.36: GPC traces of (a) linear PS-Br macroinitiator (**H6**) and (b) linear PS-*b*-PMMA (**H7**).

Table 4.2: Characteristics of Linear Homo- and Block Co-Polymers Prepared via ATRP Using Ascorbic Acid as a RA.

Run	Monomer	Initiator	$[M]_0$ (mol/L)	$[M]_0:[I]_0:[CuX_2]_0:[PMDTA]_0:[RA]^a_0$	Time (h.)	Conv. ^b (%)	$M_{n,theo}^c$	M_n	M_w/M_n	f^d
H6	St	EiBr	8.6	200 : 1 : 0.5 : 1 : 0.125	1.33	15	3150	3350	1.13	0.94
H7	MMA	H6	4.67	500 : 1 : 0.5 : 1 : 0.25	20	56	31400	39300	1.43	0.80
H8	MMA	H6	4.65	500 : 1 : 0.5 : 2.5 : 0.25	20	84	45400	64400	1.16	0.70

CuBr₂ and CuCl₂ was used as transition metal catalyst for homo- and block co-polymerization respectively. Bulk polymerization of St was carried out at 110 °C, whereas block copolymerizations were performed at 90 °C in toluene (monomer / toluene =1 (v/v)).

^a Ascorbic acid was used as RA.

^b Conversions were determined gravimetrically.

^c Theoretical molecular weights were determined as follows: $M_{n,theo} : ([M]_0/[I]_0 \times \text{conversion \%} \times \text{MW(MMA)}) + M_n(\text{PS macroinitiator})$ for block copolymers.

^d $f = M_{n,theo} / M_n$

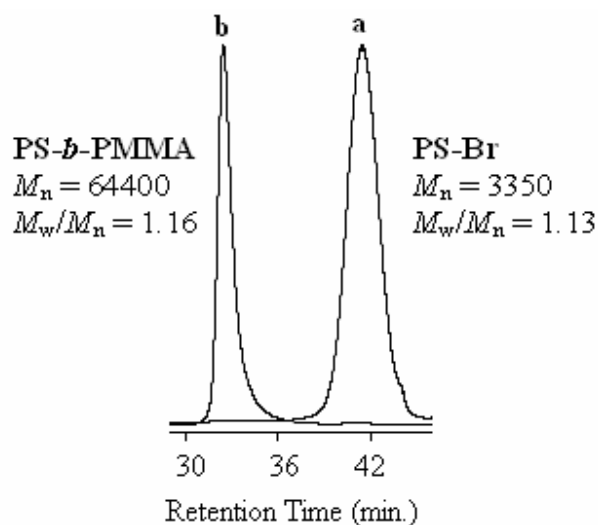


Figure 4.37: GPC traces of (a) linear PS-Br macroinitiator (**H6**), and (b) PS-*b*-PMMA (**H8**).

Based on these results one can easily say for the MMA/PMDETA/CuCl₂/ascorbic acid system the molar ratios of [MMA]₀/[PS-Br]₀/[CuCl₂]₀/[PMDETA]₀/[ascorbic acid]₀ = 500/ 1/ 0.5/ 2.5/ 0.25 is more efficient.

4.6.3 Characterization of Linear PS-Br Macroinitiator and PS-*b*-PMMA Copolymer Synthesized via ATRP Using *p*-Methoxyphenol as a RA

PS homopolymer (**H9**) was prepared via ATRP in toluene at 110 °C using CuBr₂/PMDETA/*p*-methoxyphenol catalyst system. Then this PS homopolymer was employed as a macroinitiator for the ATRP of MMA in the presence of CuCl₂/PMDETA/*p*-methoxyphenol complex system as the catalyst in bulk at 90 °C (Table 4.3). The GPC traces of macroinitiator and PS-PMMA block copolymers are shown in Figure 4.38 and 4.39. These chromatograms show the formation of the PMMA blocks. After polymerization of MMA, the GPC traces shift to the higher molecular weights region. When [PS]₀/[*p*-methoxyphenol]₀ = 1/1.5 molar ratio was employed for block copolymerization with MMA, a peak related to PS dead chains was detected. The amount of these dead chains (PS macroinitiator) was calculated to be 4 % of the resulting chain extended polymer using deconvolution method. By using more *p*-methoxyphenol ([PS]₀/[*p*-methoxyphenol]₀ = 1/2) the percent of these dead chains was

decreased to 1. Moreover increasing RA concentration improved the rate of polymerization as expected.

Table 4.3: Characteristics of Linear Homo- and Block Co-Polymers Prepared via ATRP Using *p*-Methoxyphenol as a RA.

Run	Monomer	$[M]_0/[I]_0$	$[I]_0/[RA]_0^a$	In	Time (h)	Conv (%)	M_n	$M_{n,theo}$	M_w/M_n
H9^b	St	30	1.5	EiBr	1.25	11	1200	500	1.17
H10^c	MMA	500	1.5	H9	19.5	29	28900	15700	1.07
H11^c	MMA	500	2	H9	19.5	57	45500	29750	1.16

All polymerizations were carried out in toluene (monomer / toluene =1 (v/v)), at molar ratios of $[I]_0 : [CuBr_2]_0 : [PMDTA]_0 = 1 : 0.5 : 5$

^a *p*-methoxyphenol was used as RA.

^b The solution polymerization was carried out at 110 °C.

^c The solution polymerization was carried out at 90 °C.

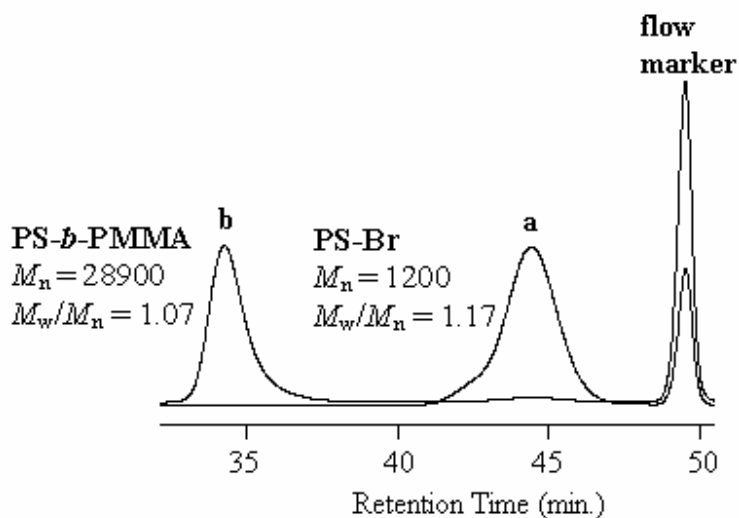


Figure 4.38: GPC traces of (a) linear PS-Br macroinitiator (**H9**), and (b) PS-*b*-PMMA (**H10**).

When we compare this CuX_2 /PMDTA/*p*-methoxyphenol catalyst system with the systems applying fructose or ascorbic acid as RA, we can easily say that more *p*-methoxyphenol and PMDTA were required to obtain efficient homo- and block co-polymerization indicating low efficiency of *p*-methoxyphenol in reducing copper (II) to

copper (I) species. As a conclusion molar ratios of $[MMA]_0/[PS-Br_2]_0/[CuCl_2]_0/[PMDTA]_0/[p\text{-methoxyphenol}]_0 = 500/1/0.5/5/2$ can be offered as an optimum condition for this system.

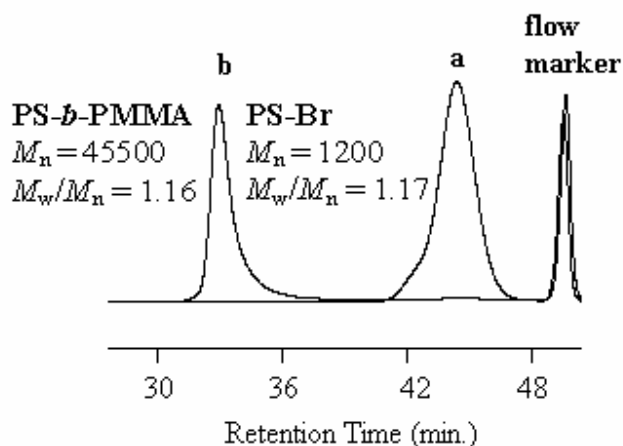


Figure 4.39: GPC traces of (a) linear PS-Br macroinitiator (**H9**), and (b) PS-*b*-PMMA (**H11**).

4.6.4 Star Block Copolymer Synthesis

4.6.4.1 Synthesis of Octafunctional Initiator 5,11,17,23,29,35,41,47-octa-*tert*-butyl-49,50,51,52,53,54,55,56-octakis(2-bromopropionyloxy)calix[8]arene (**1**)

It was synthesized by a procedure similar to this reported by Angot et. al. [178]. The octafunctional initiator, (**1**), was prepared from 4-*tert*-butylcalix[8]arene (TBC-8) and 2-bromopropionyl bromide in ca. 82% yield (Figure 4.40). The obtained initiator, (**1**), was then characterized by $^1\text{H-NMR}$. $^1\text{H-NMR}$ spectrum of the initiator showed no signal corresponding to residual phenolic protons of the starting TBC-8, indicating its quantitative esterification (Figure 4.41). $^1\text{H-NMR}$ (CDCl_3), δ : 7.01 (s, 2H, aromatic protons), 4.34 (s, 1H, $-\text{CHBr}-$), 3.69 (s, 2H, $-\text{CH}_2-$), 1.54 (s, 3H, CH_3-), 1.16 (s, 9H, *tert*-butyl).

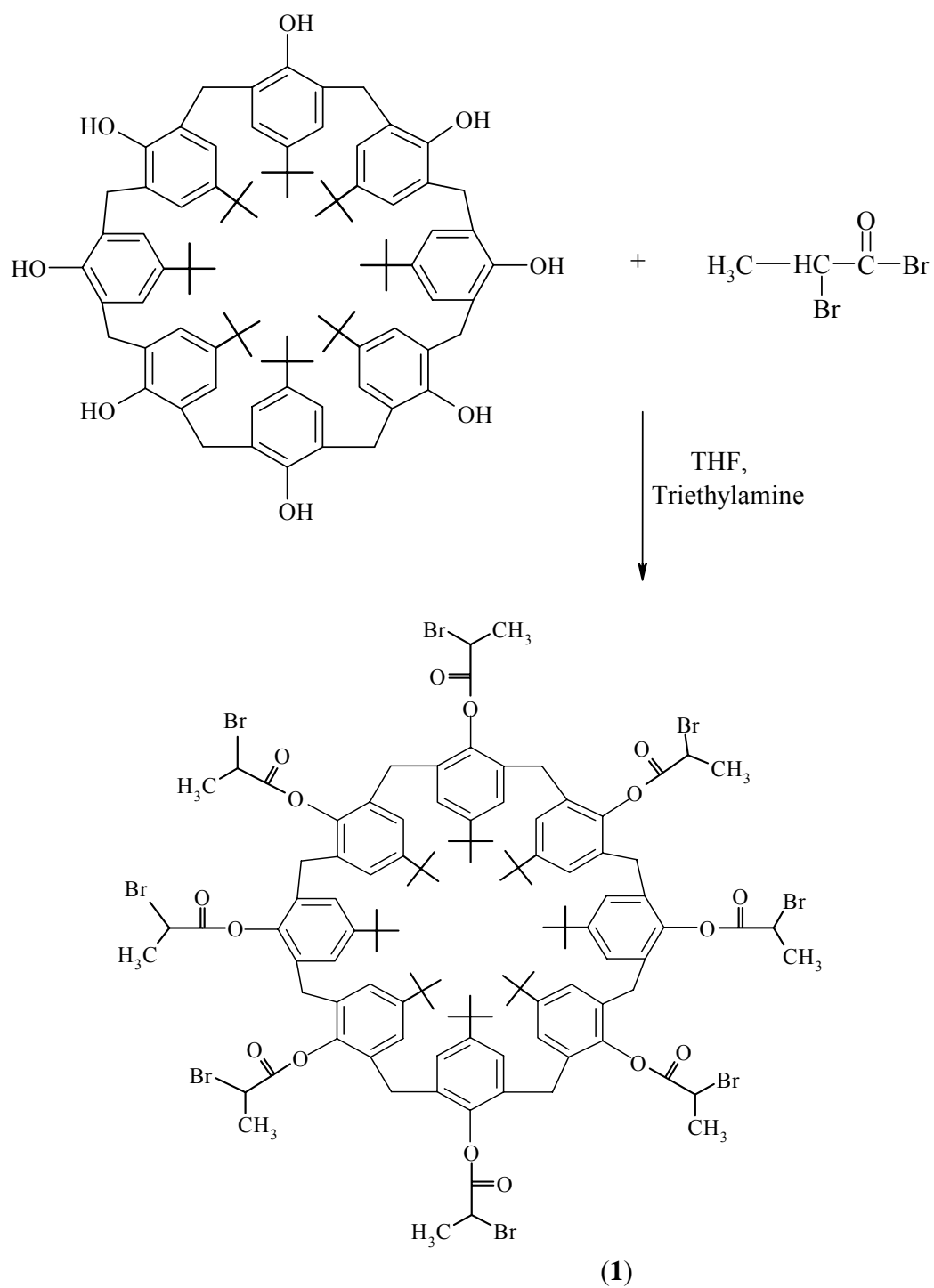


Figure 4.40: Synthesis of 5,11,17,23,29,35,41,47-Octa-*tert*-buty-49,50,51,52,53,54,55,56-Octakis-(2-bromopropionyloxy)calix[8]arene, (1).

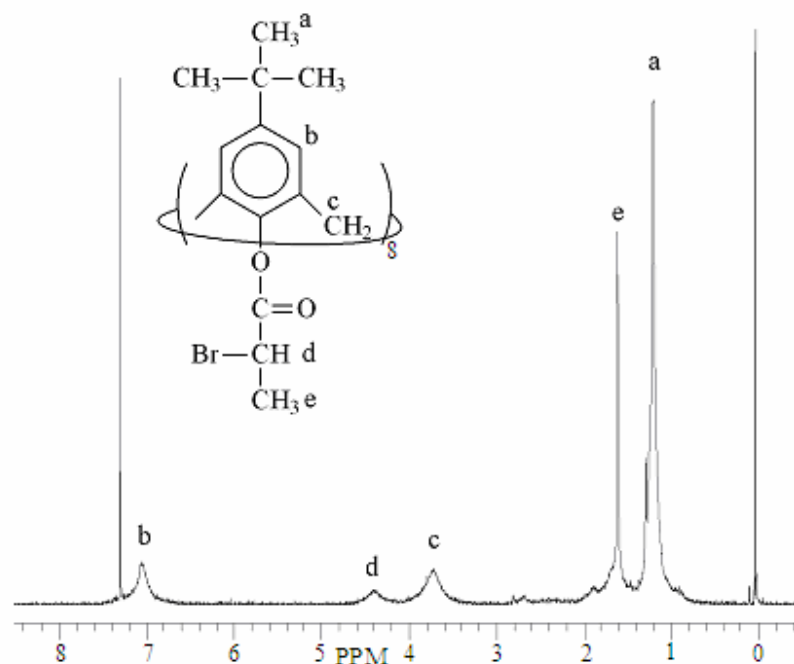


Figure 4.41: The ^1H -NMR spectrum of the initiator, (**1**), 5,11,17,23,29,35,41,47-Octa-*tert*-butyl-49,50,51,52,53,54,55,56- Octakis-(2-bromopropionyloxy)calix[8]arene in CDCl_3 .

4.6.4.2 Preparation of Octa-Arm PS Stars

A similar strategy was applied for the preparation of a star polymer based on St. Thus, octa-arm star PS-Br (**H12**) ($M_{n,\text{theo}} = 14900$ (Eq. 4.16), $M_n = 17300$, $M_{n,\text{NMR}} = 23850$, $f = M_{n,\text{theo}} / M_{n,\text{NMR}} = 0.62$, $M_w/M_n = 1.17$ at 4% conversion) was obtained by ATRP of St using fructose as a RA, $\text{CuBr}_2/\text{PMDETA}$ as a catalyst system, and an octa-functional initiator, **1** in bulk at 110°C (Eq. 4.17). Monomer conversion was kept below 15-20% due to a probability of irreversible coupling reactions of growing radicals. The theoretical number average molecular weights were calculated by the following formula:

$$M_{n,\text{theo}}: ([M]_0/[I]_0 \times \text{conversion}\% \times \text{MW}(\text{St})) + 2378.85 \text{ g/mol} \quad (4.16)$$

^1H NMR spectrum (Figure 4.42) of octa-arm star PS-Br (**H12**) exhibited a signal at 4.5 ppm, which might be assigned to PhCH-Br end group.

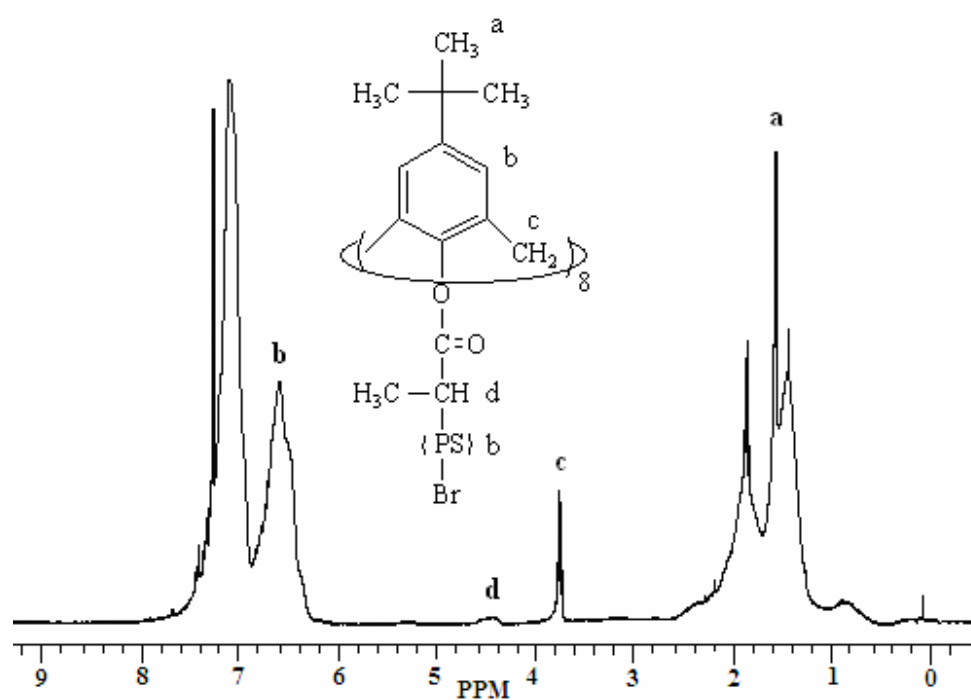
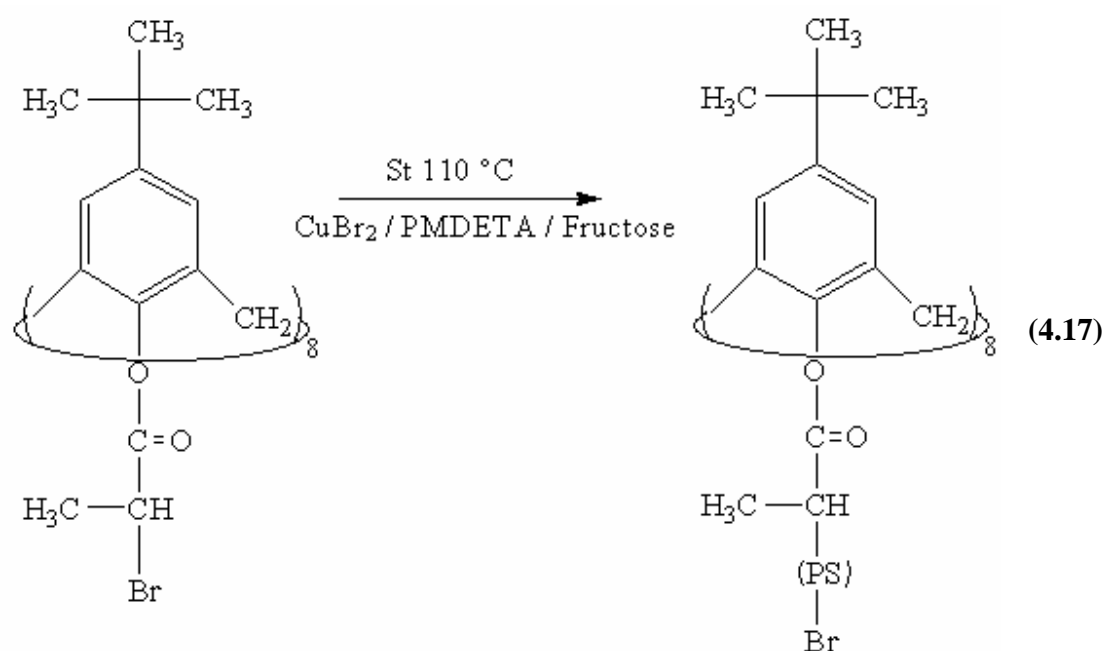


Figure 4.42: The ^1H -NMR spectrum of Octa-arm PS Macroinitiator (**H12**) in CDCl_3 , 110°C .

$M_{n,\text{NMR}}$ of octa-arm star PS-Br was calculated from the ratio of peak areas of CH_2 protons of the calixarene core around 3.7 ppm and aromatic protons of PS at 6.5-7.5

ppm. The molecular weight of **1** was added to this calculated value, resulting in $M_{n,NMR} = 23850$. Additionally, $M_n = 17300$ of octa-arm star PS-Br, which is lower than that obtained from NMR because of the calibration with linear PS-standards, reveals a star structure. However, to better characterize the starlike structure and to determine the number of arms, basic hydrolysis was performed yielding linear PS. After hydrolysis, M_n and M_w/M_n values of linear PS (**H13**) were found to be 3300 and 1.44, respectively. A ratio of $M_{n,NMR}$ of star PS-Br to M_n of linear PS was found to be close to 8 (Fig. 4.43).

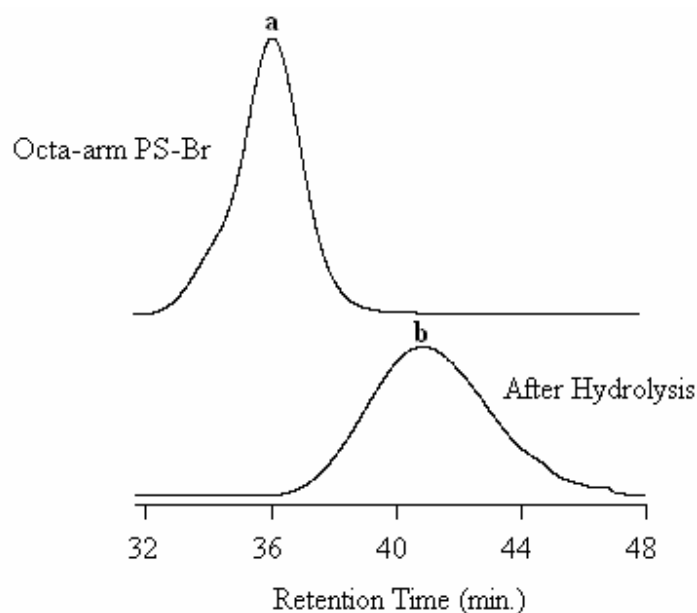
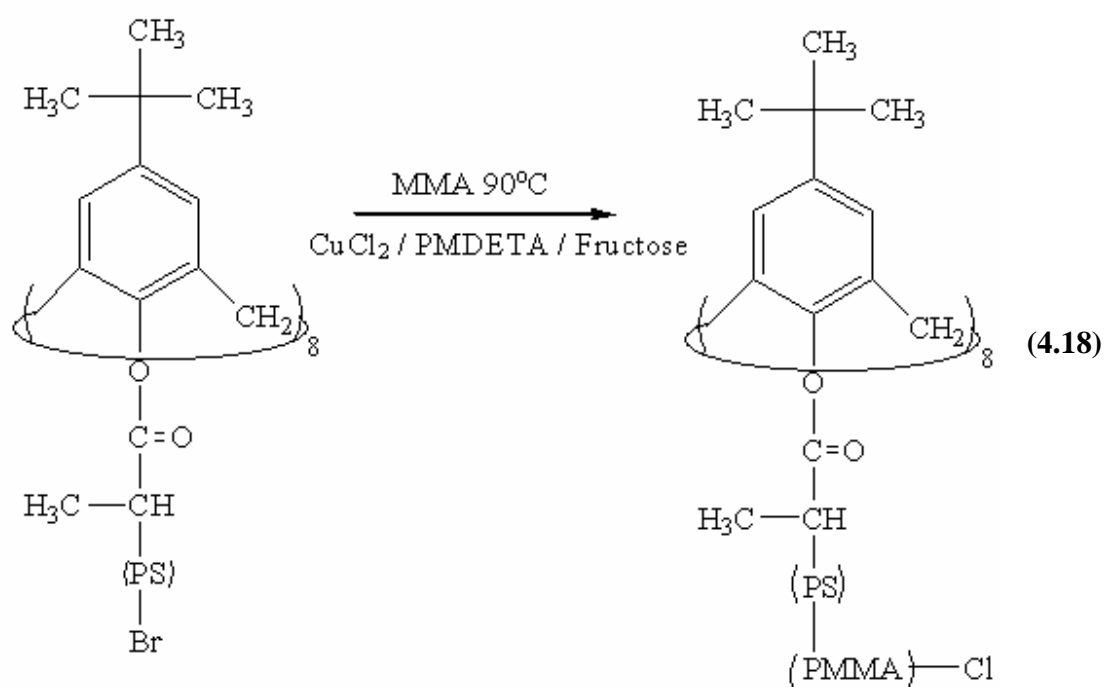


Figure 4.43: GPC traces of octa-arm star PS-Br ($M_{n, NMR} = 23850$) obtained using $[M]/[I]$ of 3000 (a) before (**H12**) and (b) after (**H13**) hydrolysis of the ester function.

4.6.4.3 Preparation of Octa-Arm PS-*b*-PMMA Stars

Also the octa-arm star PS-Br (**H12**) ($M_{n,NMR} = 23850$, $M_w/M_n = 1.17$) was employed as a macroinitiator together with MMA ($[M]_0/[I]_0 = 22000$), fructose and $CuCl_2/PMDETA$ in order to obtain well-defined octa-arm star PS-*b*-PMMA copolymer (Eq. 4.18).



Thus obtained octa-arm star PS-*b*-PMMA (**H14**) copolymer ($M_n = 155000$, $M_w/M_n = 1.16$) had narrow MWD and its GPC trace was monomodal. From Figure 4.44, a clear shift to higher molecular weight was also observed between GPC traces of star-shaped PS and the corresponding star-block copolymer.

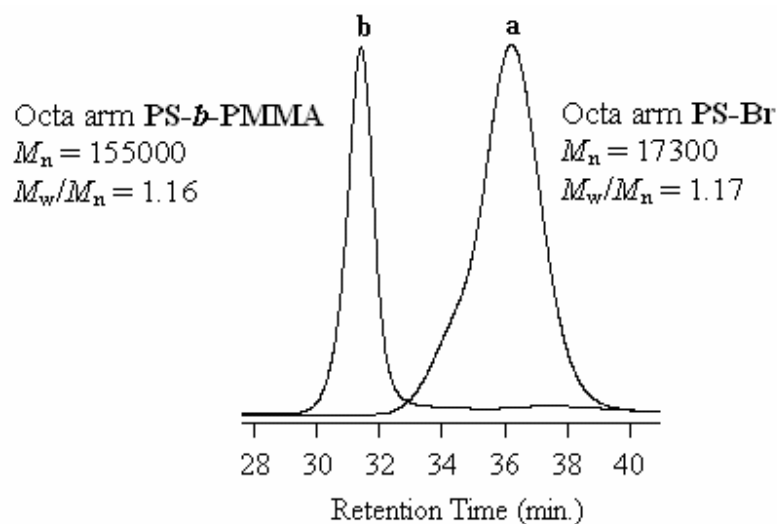


Figure 4.44: GPC traces of octa-arm PS-Br star macroinitiator (**H12**) (a), and octa-arm star PS-*b*-PMMA (**H14**) (b).

$M_{n,NMR}$ of octa-arm star PS-*b*-PMMA was calculated from an integration of signals at 6.5-7.5 ppm of St (ArH) and 3.58 ppm of MMA (OCH₃) segment and was found to be 237400 (Fig. 4.45).

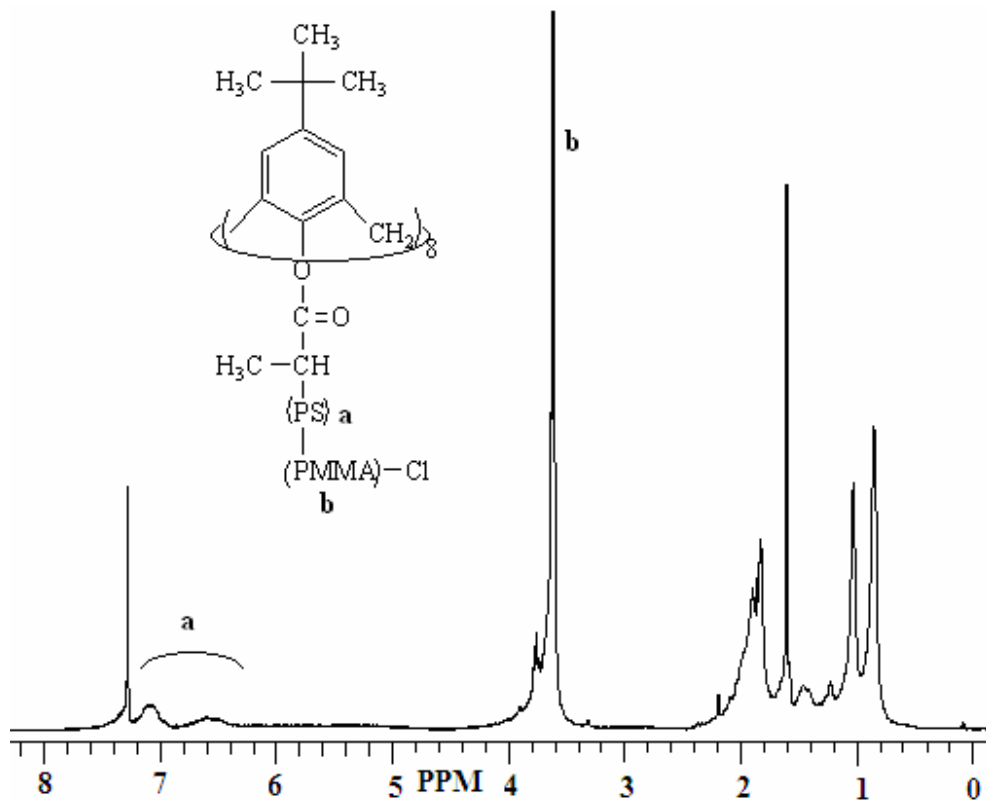


Figure 4.45: The ¹H-NMR spectrum of Octa-arm PS-*b*-PMMA (**H14**) in CDCl₃.

4.6.5 Characterization of PS Macroinitiator and PS-*b*-PMMA Copolymers Synthesized via ATRP in the Presence of Definite Amount of Air

4.6.5.1 Chain Extension Polymerization

PS-Cl (**H15**) ($M_n = 7200$, $M_w/M_n = 1.27$ at 65% conversion) was used as a macroinitiator in chain extension polymerization in order to show reliability of halogen end group. The chain extension polymerization was conducted with the reactants ratio of [St]/[**H15**]/[CuCl₂]/[PMDETA]/[*p*-methoxythiophenol] = 500 / 1 / 0.5 / 5 / 0.5 for 20h at 110 °C. GPC traces of PS macroinitiator (**H15**) and chain extended polymer (**H16**) ($M_n = 41600$, $M_w/M_n = 1.48$ at 67 % conversion). A clear shift in GPC chromatogram demonstrates that the chain ends of the homopolymer mostly possess halide end group

(Fig. 4.46). From the GPC trace, the amount of the dead chains (PS macroinitiator) was calculated to be 1 % of the resulting chain extended polymer using deconvolution method (by Peak Fit program, Seasolve).

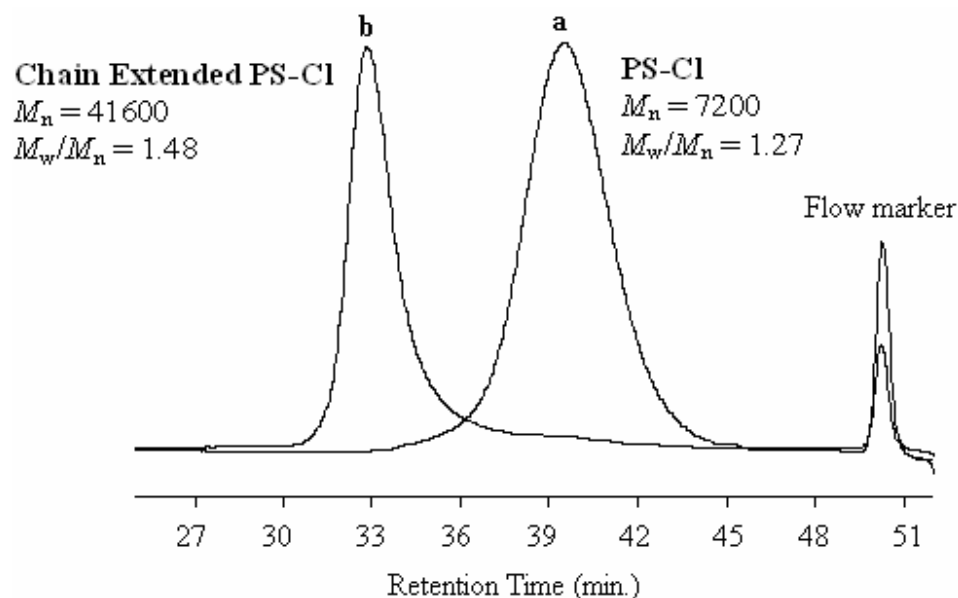
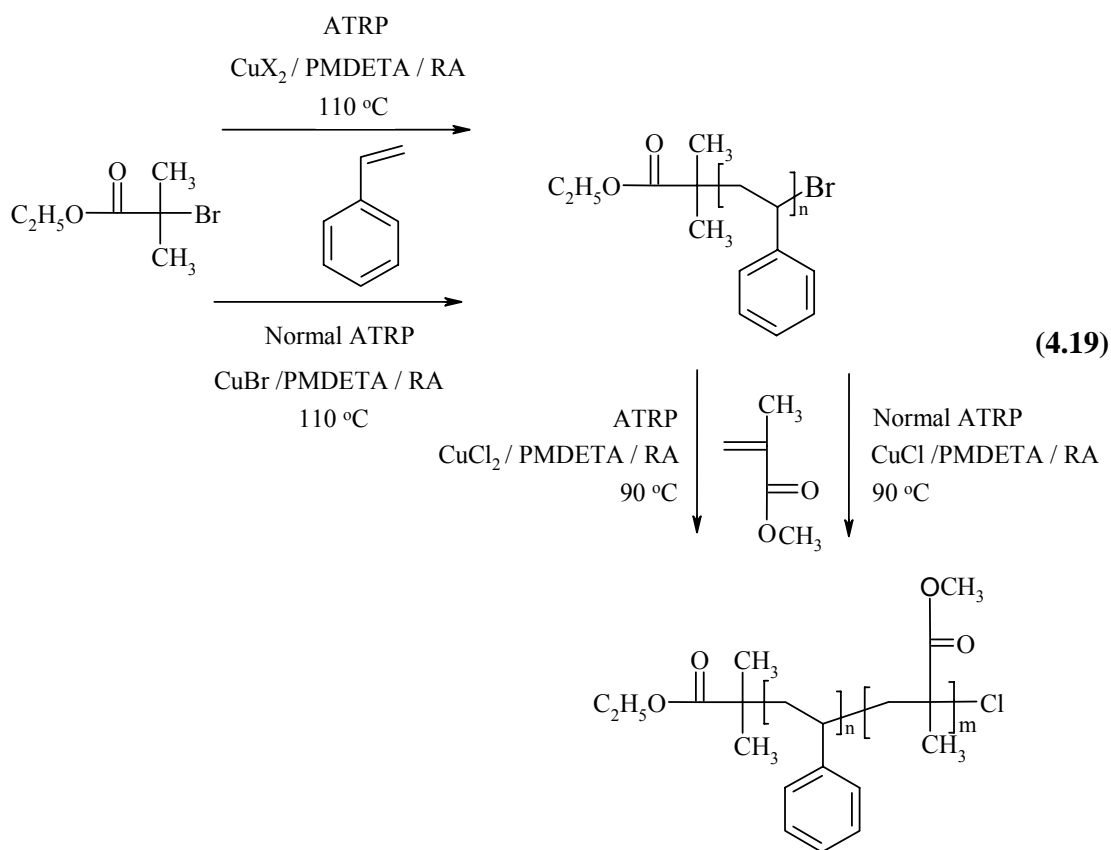


Figure 4.46: GPC traces of PS macroinitiator (**H15**), (a), and the chain-extended polymer (**H16**).

4.6.5.2 Block Copolymerization : Normal ATRP versus ATRP via *In Situ* Copper (I) Formation

In this part PS homopolymers (**H23**, **H17**) prepared by normal ATRP or ATRP via *in situ* copper (I) formation method respectively were used as macroinitiator for the block copolymerization with MMA using normal ATRP or ATRP via *in situ* copper (I) formation. Besides the comparison of the initiation efficiencies of the homopolymers prepared by different ATRP methods, the effect of RA concentration was also investigated. Reaction scheme was summarized in 4.19.



The structure of PS-Br (**H17**) ($M_n = 2800$, $M_w/M_n = 1.17$) was confirmed by ^1H NMR (Fig. 4.47). Two signals assignable to $\text{CH}_3\text{CH}_2\text{OC}=\text{O}$ as α - and $\text{PhCH}-\text{Br}$ as ω -end group of PS-Br were observed at 3.7 and 4.5 ppm, respectively. No peak was detected corresponding to PS with alkene end group, which was resulted from HBr elimination during the polymerization process.

In addition, MALDI-TOF mass spectrometry study on linear PS-Br ($M_n = 2800$) obtained from method B, was performed for structural identification, especially α - and ω - end group determination. The MALDI-TOF spectrum of linear PS-Br is depicted in Figure 4.48 ($M_{n,\text{MALDI}} = 2865$, $M_w/M_n = 1.13$). Two different series of peaks, each separated by 104 Dalton (molar mass of St repeating unit), can be observed. From the comparison between the measured and the theoretical isotope distribution (Theoretical mass (for $\text{DP}_n = 26$) = 2926.60; experimental = 2926.50), the major series (**1**) can be attributed to the silver adduct of PS, which is initiated by EtBr and has an alkene as end group (Fig. 4.48) The elimination of HBr is a consequence of the fragmentation of the carbon-to-bromine bond in the MALDI process [317]. The latter series overlaps with

series (2), which is 18 Da higher than the main series. This corresponds to a series in which PS chain is occurred by recombination (Theoretical mass (for DP_n = 25) = 2941.92; experimental = 2942.45). MALDI-TOF analysis confirms the controlled character of the polymerizations in the presence of *p*-methoxythiophenol. Overall, these findings clearly indicate that initiation or termination process by thiyl radicals is totally excluded, MALDI-TOF and ¹H NMR results confirmed the mechanism, since the obtained polymer mainly possessed initiator fragment at α- and halide atom at ω-position.

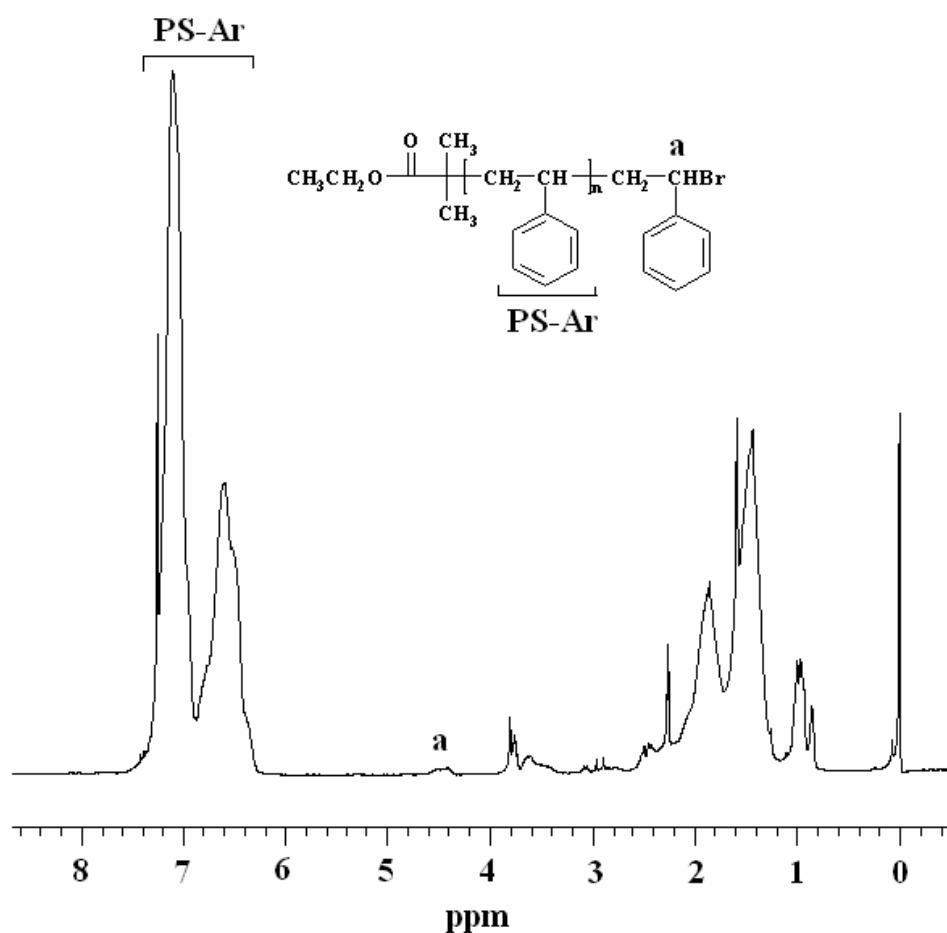


Figure 4.47: The ¹H-NMR spectrum of PS-Br (H17) macroinitiator in CDCl₃.

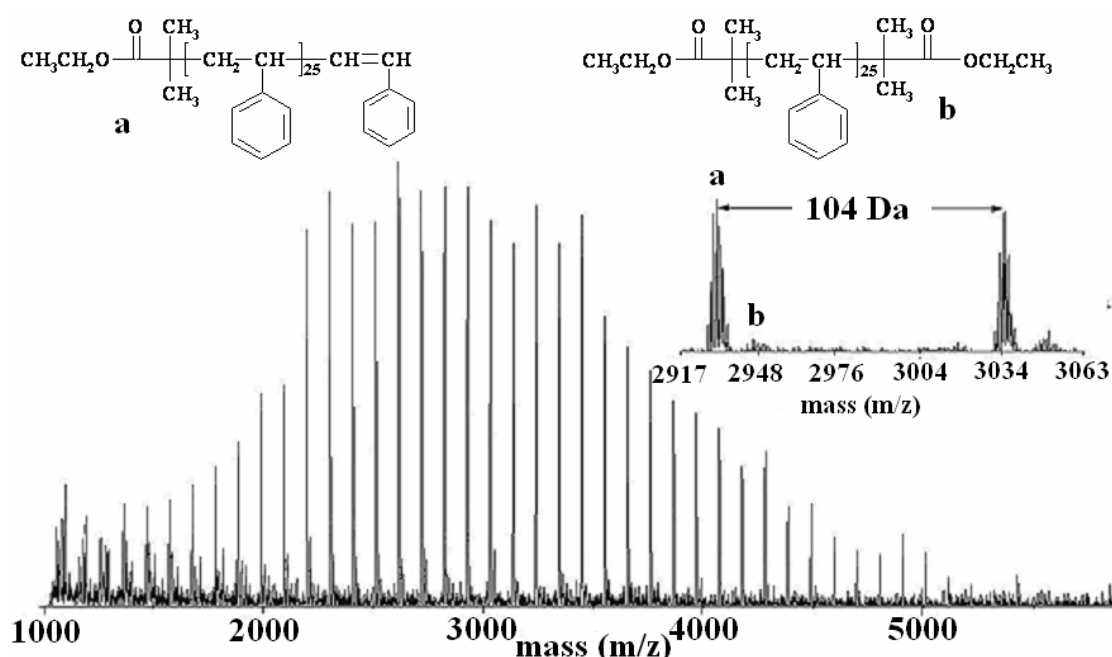


Figure 4.48: MALDI-TOF spectra of PS-Br (**H17**) ($M_n = 2800$, $M_w/M_n = 1.17$).

In addition, PS-*b*-PMMA (**H18-22**) copolymers were prepared via macroinitiator technique in ATRP using this PS-Br (**H17**) ($M_n = 2800$, $M_w/M_n = 1.17$) in order to show the utility and convenience of the $\text{CuCl}_2/\text{PMDETA}/p$ -methoxythiophenol catalyst system. The block copolymerizations were conducted with molar ratios of $[\text{MMA}]/[\text{H15}]/[\text{CuCl}_2]/[\text{PMDETA}]/[p\text{-methoxythiophenol}] = 500/1/0.5/5/X$ (0.5 to 2) for 48 h. at 90 °C using different amounts of *p*-methoxythiophenol (**H19-22**). Also a block copolymerization was conducted in normal ATRP conditions using molar ratios of $[\text{MMA}]_0/[\text{H17}]_0/[\text{CuCl}]/[\text{PMDETA}] = 500/1/1/1$ for 24 h at 90°C (**H18**). Polymerization conditions and characteristics of homo- and block co-polymers were summarized in Table 4.4. GPC traces of PS macroinitiator and block copolymers are shown in Figure 4.49. Most effective block copolymerization was obtained at molar ratios of $[\text{CuCl}_2]/[p\text{-methoxythiophenol}] = 1$ (**H19**). However, a little amount of dead end polymer (<1 %) was found by deconvolution of the corresponding GPC trace. With increasing *p*-methoxythiophenol concentration a deformation in GPC peaks occurred indicating termination reactions (**H20-22**).

Table 4.4: Characteristics of Linear Homo- and Block Co-Polymers Prepared via ATRP Using *p*-Methoxythiophenol as a RA.

Run	$[M]_0/[I]_0$	In.	$[SH]_0^a/[CuCl_2]_0$	Time (h)	Conv. ^b (%)	$M_{n,theo}^c$	$M_{n,HNMR}$	M_n	M_w/M_n	f	Composition ^d (%)	
											PS	PMMA
H17^e	100	EiBr	3	0.5	18	2800	-	2800	1.17	1	100	-
H18^f	500	H17	-	24	76	40800	51000	72500	1.29	0.56	6	94
H19	500	H17	1	48	98	51900	53000	87000	1.27	0.6	5	95
H20	500	H17	2	48	80	42900	43000	65000	1.27	0.66	7	93
H21	500	H17	3	48	36	20800	24250	38600	1.31	0.54	12	88
H22	500	H17	4	48	67	36350	37250	45000	2.05	0.8	8	92

Block copolymerizations were carried out at 90 °C in toluene (monomer / toluene=1 (v/v)).

^a *p*-methoxythiophenol was used as RA.

^b Conversions were calculated gravimetrically.

^c for homopolymer; $M_{n,theo} = ([M]_0/[I]_0) \times \text{Conversion \%} \times 104 + (MW_{\text{EiBr}})$, for block copolymers; $M_{n,theo} = ([M]_0/[I]_0) \times \text{Conversion \%} \times 100.12 + (MW_{\text{macroinitiator}})$.

^d Compositions were calculated using GPC and ¹H NMR results.

^e Homopolymerization was carried out at 110°C at molar ratios of $[St]_0/[EiBr]_0/[CuBr_2]/[PMDETA]/[p\text{-methoxythiophenol}] = 100/1/0.5/5/1.5$.

^f Normal ATRP at molar ratios of $[M]_0 : [I]_0 : [CuCl] : [PMDETA] = 500 : 1 : 1 : 1$ for 24 h at 90°C.

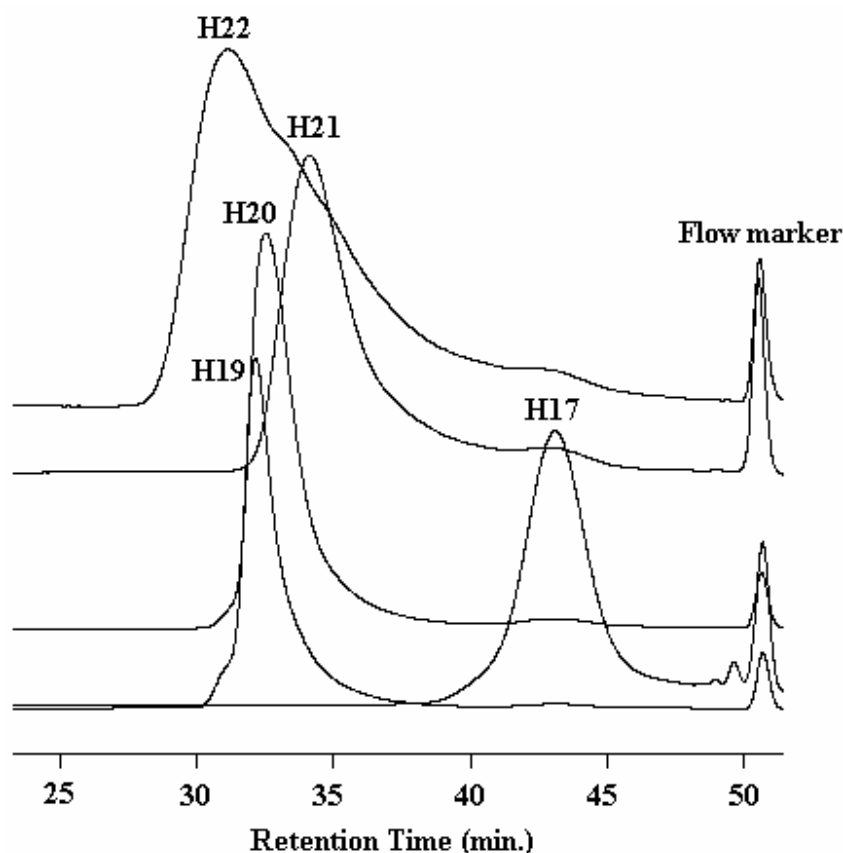


Figure 4.49: GPC traces of PS macroinitiator (**H17**) ($M_n = 2800$, $M_w/M_n = 1.17$ at 18 % conversion), (a), and the related PS-*b*-PMMA copolymers (**H19-22**).

Based on these results $[MMA]/[H17]/[CuCl_2]/[PMDETA]/[p\text{-methoxythiophenol}] = 500/1/0.5/5/0.5$ molar ratios can be offered as optimum conditions to attain efficient block copolymerization for the systems employing $CuCl_2/PMDETA/p\text{-methoxythiophenol}$ as catalyst complex (**H19**).

Besides block copolymerization was performed via normal ATRP using molar ratios of $[MMA]_0/[H17]_0/[CuCl]/[PMDETA] = 500/1/1/1$ at $90^\circ C$ to compare the efficiency of both systems. Normal ATRP system was found to be two times faster compared to system applying $CuCl_2/PMDETA/p\text{-methoxythiophenol}$ as catalyst. This is reasonable since time is required to reduce copper (II) to copper (I) species via electron transfer from *p*-methoxythiophenol. The GPC traces of PS-*b*-PMMA copolymer (**H18**) prepared via normal ATRP and its precursor (**H17**) are shown in Figure 4.50. The amount of dead end polymer (<2 %) was found by deconvolution of the corresponding GPC trace.

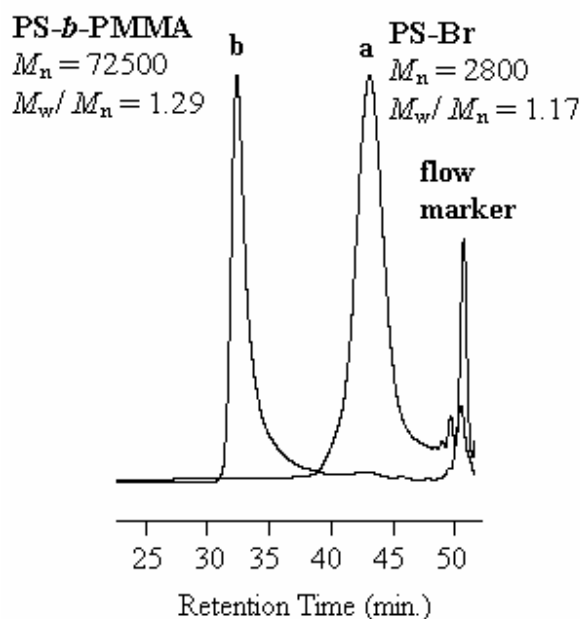


Figure 4.50: GPC traces of PS macroinitiator (**H17**) ($M_n = 2800$, $M_w/M_n = 1.17$ at 18 % conversion), (a), and the related PS-*b*-PMMA copolymer (**H18**).

Moreover, PS-Br (**H23**) ($M_n = 2100$, $M_w/M_n = 1.12$) macroinitiator prepared via normal ATRP using molar ratios of $[St]_0/[EtBr]_0/[CuBr]/[PMDETA]/[PhSNa] = 50/1/1/1$ at 110 °C was used as macroinitiator to synthesize PS-*b*-PMMA copolymers to compare the initiation efficiency of the macroinitiators prepared via normal ATRP (**H17**) and ATRP applying $CuCl_2/PMDETA/PhSNa$ as catalyst. The block polymerization was conducted with a ratio of $[MMA]/[H23]/[CuCl_2]/[PMDETA]/[PhSNa] = 500/1/0.5/5/X$ for 24 h. at 90 °C using different amount of PhSNa. GPC traces of PS macroinitiator and block copolymers are shown in Figure 4.51. Clear shifts in GPC chromatograms indicate efficient crossover-propagation during block copolymerization. For this system $[MMA]/[H23]/[CuCl_2]/[PMDETA]/[PhSNa] = 500/1/0.5/5/0.25$ molar ratios were found as optimum conditions. Initiation efficiencies of PS homopolymers prepared by ATRP via *in situ* copper (I) formation method (**H17**) and normal ATRP (**H23**) were found to be comparable.

Table 4.5: Characteristics of Linear Homo- and Block Co-Polymers prepared via ATRP using PhSNa as a RA.

Run	$[M]_0/[I]_0$	Initiator	$[SH]^a_0/[I]_0$	Time (h)	Conv. ^b (%)	$M_{n,theo}^c$	$M_{n,HNMR}$	M_n^d	M_w/M_n	Composition (%) ^e	
										PS	PMMA
H23^f	50	EiBr	-	0.33	40	2100	-	2100	1.12	100	-
H24	500	H23	0.25	24	40	22100	23000	37000	1.13	9	91
H25	500	H23	0.5	24	93	48700	59850	67000	1.4	4	96
H26	500	H23	1	24	26	15100	19500	26000	1.39	11	89
H27	500	H23	1.5	24	28	16100	32700	25000	1.39	6	94

All polymerizations were carried out at 90 °C in toluene (monomer / toluene=1 (v/v)), at molar ratios of $[M]_0 : [I]_0 : [CuCl_2] : [PMDTA] : [PhSNa] = 500 : 1 : 0,5 : 5 : X$

^a *p*-methoxy thiophenol was used as RA.

^b Conversions were calculated gravimetrically.

^c $M_{n,theo} = ([M]_0/[I]_0) \times \text{Conversion \%} \times 100.12 + (MW_{macroinitiator})$.

^d Calculated from GPC calibrated with linear polystyrene standards.

^e Compositions were calculated using GPC and ¹H NMR results.

^f Homopolymerization of St was carried out at 110°C using classic ATRP conditions $[M]_0 : [I]_0 : [CuBr] : [PMDTA] = 50 : 1 : 1 : 1$.

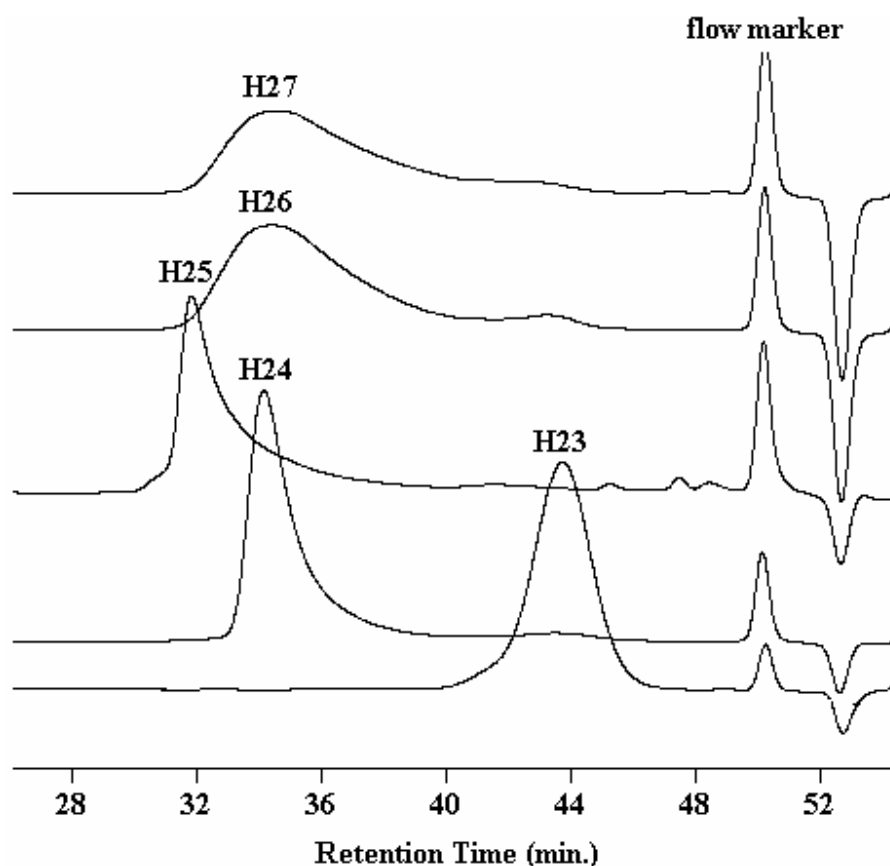


Figure 4.51: GPC traces of PS macroinitiator (**H23**) ($M_n = 2100$, $M_w/M_n = 1.12$ at 40 % conversion), (a), and the PS-*b*-PMMA block copolymers (**H24-27**).

4.7 Air- Stable and Recoverable Catalyst for ATRP of St

A schematic representation of generation and regeneration of the Cu(I) species in the CuCl₂/PMDETA mediated ATRP together with oxygen and phenol consumption processes is given in 4.20. The silica gel supported polymerization of St was carried out as follows: Upon addition of CuCl₂ to the stirring mixture of St-silica gel-PMDETA, an immediate formation of the blue colored CuCl₂/PMDETA complex was occurred. Once stirring is stopped, the blue particles settled to the bottom leaving the upper layer solution colorless. This indicates that the CuCl₂/PMDETA complex was adsorbed onto silica gel. After adding PhONa and 1-PECl, polymerization was conducted at 110 °C. Figure 4.52 shows the first order time-conversion plot for copper catalyzed LRP of St. A linear dependence of the monomer consumption with time indicates that the radical concentration remains constant throughout the polymerization.

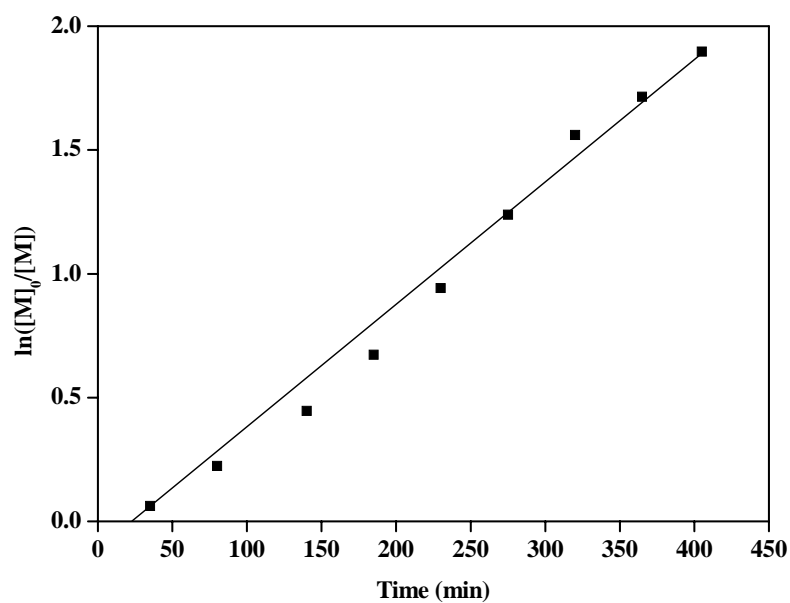
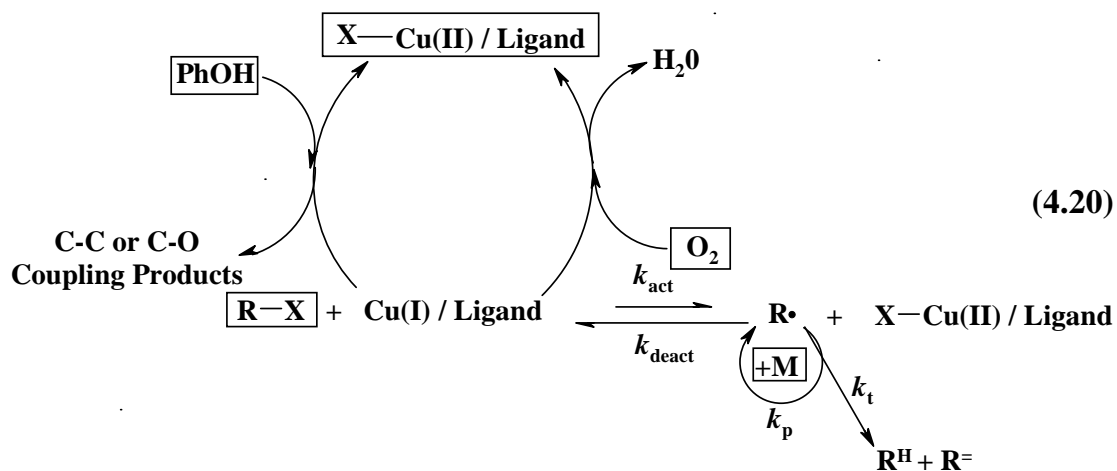


Figure 4.52: First-order kinetic plot for the polymerization of St catalyzed by SG-CuCl₂/PMDETA at 110 °C; [St]₀ = 6.8 M; [St]₀/[1-PECl]₀/[CuCl₂]/[PMDETA]/[PhONa] = 100/1/ 0.5/10/0.75; silica gel / CuCl₂ = 10 (w/w).

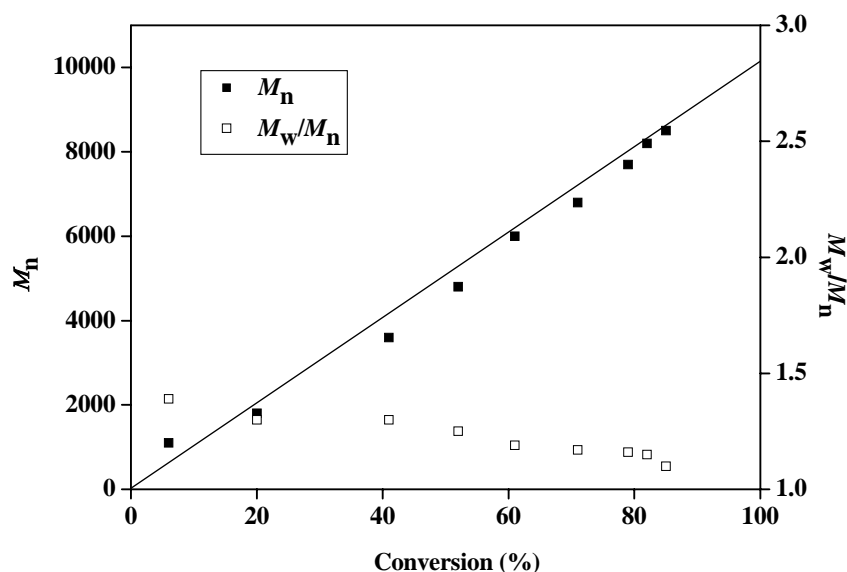
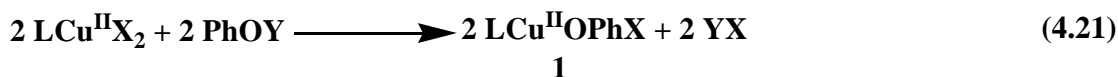
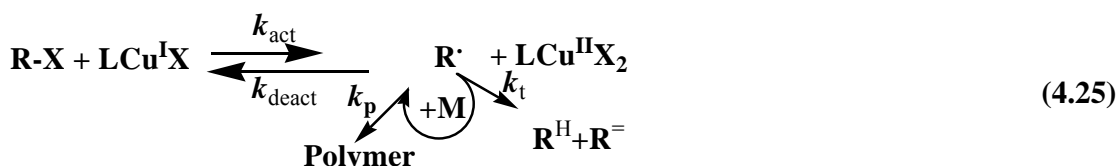
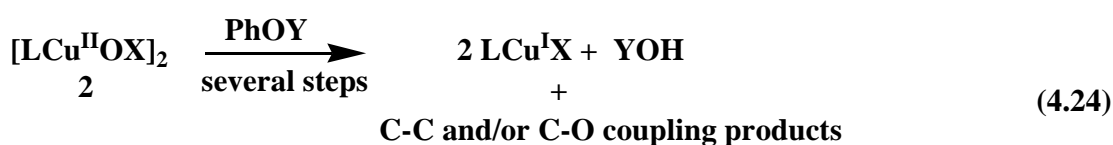
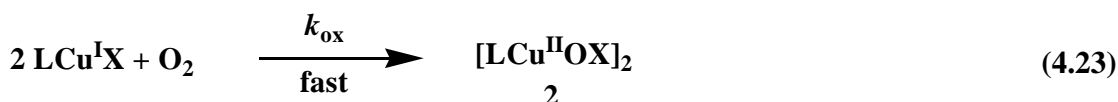
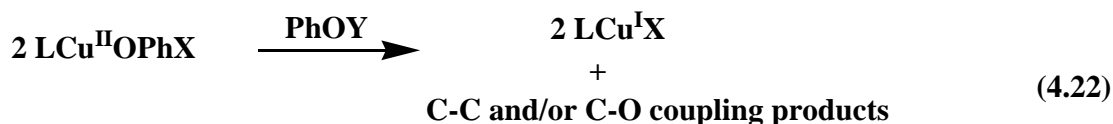


Figure 4.53: The dependences of M_n and M_w/M_n on monomer conversion in the polymerization of St catalyzed by SG-CuCl₂/PMDETA at 110 °C $M_{n,theo}$ (—). (Experimental conditions as in Fig. 4.52).

The apparent rate constant of propagation ($k_p^{app} = 9.5 \cdot 10^{-5} \text{ s}^{-1}$) was calculated from the slope. As reported previously, an induction period (approximately 25 min) for St was observed [135]. M_n and M_w/M_n of polymers as a function of monomer conversion are shown in Figure 4.53. The M_n increases linearly with monomer conversion and agreed well with the theoretical values up to 85 % conversion. At this point the polymerization was stopped because of the system viscosity was so great that the sampling was practically impossible. The M_w/M_n decreases as the conversion increases and reaches the values < 1.2 . These features are typical for the controlled radical polymerization. Under the condition of the present work, the reaction pathway for the generation of Cu(I) species is postulated on the basis of oxidative polymerization chemistry of the phenols [193] and is given in (4.20). It is known that, the PhOH or PhONa reacts with the labile halide anion of the $LCu(II)X_2$ complex to give the phenoxo-copper(II) complex **1**, and HX or NaX is produced as a byproduct (4.21) [319-322]. It should be noted that excess ligand used in this polymerization neutralizes any generated HX (eq 4.26).



where, L= PMDETA (in excess); X= Cl or Br; Y= H or Na



The dissociation of halide anion from CuBr₂/PMDETA complex was further supported by the results of the recent EXAFS (Extended X-ray Absorption Fine Structure) study on this complex in polar solvents [323]. The electron transfer (ET) from aromatic ring to two copper centers in the intermediate complex **1** generates LCu(I)X complexes and phenoxy radicals. Two molecules of phenoxy radical combine to give C-O coupling or C-C coupling product (4.22). In spite of this reaction (4.22) involves free radicals, which may also initiate the polymerization in the presence of monomer, our experimental data reveal their negligible contribution on the overall of the polymerization. The Cu(I) species formed from the phenoxo- copper (II) complex **1** can undergo two distinctly different type of competitive reactions as illustrated in (4.23) and (4.25). Active Cu(I) species reacts with O₂ to form bis (μ oxo) dicopper or μ^{η²:η²}-peroxodicopper (II) complex **2** depending on the nature of the used ligand [312], (4.23) or alternatively, is subjected to the reaction with alkyl halide to afford the initiating radicals for the polymerization (4.25). We assumed that the oxidation of the Cu(I) has a priority to the

reaction with alkyl halide (activation step in ATRP). There are several reasons for this expectation. The first reason is that the oxidation of Cu(I) with O₂ is a very fast reaction at ambient temperature ($k_{\text{ox}} \approx 10^7 \text{ M}^{-1} \text{ s}^{-1}$) [324]. Although, the exact value of k_{act} for the 1-PECL/CuCl/PMDETA system used in this work is not known, the available literature data of the rate constant of activation k_{act} in copper catalyzed LRP represent much lower values such as 1.5 and $5.6 \times 10^{-5} \text{ M}^{-1} \text{ s}^{-1}$ for the 1-PECL/CuCl/tris[(2-dimethylamino)ethyl]amine (Me₆TREN) and 1-PECL/CuCl/dinonylbipyridine (dNBpy) systems, respectively [46]. It appears reasonable that the k_{act} for PMDETA would be lower than that of the Me₆TREN and higher than that of the dNBpy ($k_{\text{act,dNBpy}} \ll k_{\text{act,PMDETA}} < k_{\text{act,Me}_6\text{TREN}}$) considering the intermediate behavior of PMDETA as a ligand in copper catalyzed ATRP. Consequently, we can conclude that oxidation of Cu(I) is predominantly occurred under these circumstances. The bis (μ oxo) dicopper or $\mu\eta^2:\eta^2$ -peroxodicopper (II) complex **2**, which is readily formed by oxidation process, is known as a highly reactive catalyst in oxidative polymerization of phenols and oxidation of catechols [319]. Equation 4.24 represents that the reaction of this complex with phenol leads to regeneration of the Cu(I) complex and formation of water as byproduct. Such generation of Cu(I) would be expected to initiate the polymerization as a result of the consumption of the oxygen and phenol as well. This interpretation is consistent with the observations from preliminary control experiments; the initiator, PhONa or phenol derivatives, and SG-CuCl₂/PMDETA catalyst were all required to achieve LRP of St. The absence of PhONa resulted in failure of the polymerization to yield a detectable amount of polymer at 110 °C for 9 h. It is also reported that auto-polymerization of St in presence CuCl₂/bipyridine at 110 °C yielded PS (conv. % <10 for > 30 h) [325].

4.7.1 UV-VIS Monitoring of Cu(II) Complex Consumption

UV-VIS spectrum of CuCl₂/PMDETA/PhONa mixture in acetonitrile shows two characteristic maxima in the region of 400-900 nm (curve 1) in Figure 4.54. The absorptions at 450 and 720 nm are attributed to phenolato-to-Cu(II) charge-transfer (CT) transition and d-d band of the Cu(II)-halide, respectively [300, 301, 326]. Upon heating the mixture, two maxima at 450 and 720 nm gradually decreased as the reaction proceeds (curves 2-4). This results pointed out a consumption of Cu(II).

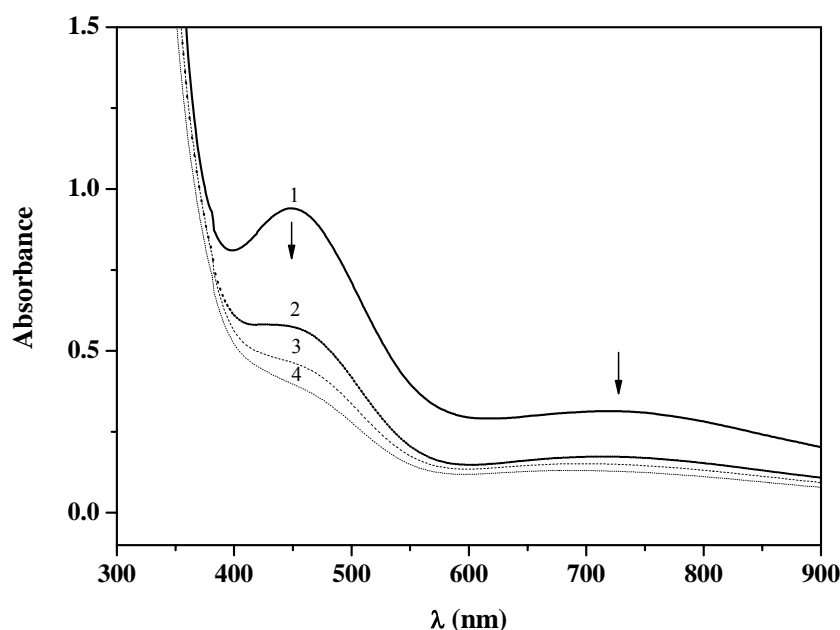


Figure 4.54: UV-VIS spectra of (1) $[\text{CuCl}_2] = 1.09 \times 10^{-3} \text{ M}$, $[\text{CuCl}_2]: [\text{PMDETA}]: [\text{PhONa}] = 1: 10: 3$ in acetonitrile, at room temperature, (1) $t = 0$; (2) $t = 30 \text{ min}$ at 80°C ; (3) $t = 50 \text{ min}$ at 80°C ; (4) $t = 80 \text{ min}$ at 80°C .

However, due to overlapping, formation of Cu(I) can not be monitored as a characteristic peak of Cu(I)/PMDETA at 290 nm.

4.7.2 Synthesis of PS Macroinitiator and Chain Extension Polymerization

In order to achieve further insight into the mechanism of silica gel supported copper catalyzed ATRP of St in the presence of air and phenol, chain extension polymerization was carried out. It was previously shown that phenols with electron releasing groups such as methoxy, alkyls etc. can be used to generate Cu(I) species from Cu(II) with an electron transfer reaction [135]. In comparison, these phenols work less efficiently than that of PhONa for the polymerization of St. On the other hand, this result can be used beneficially as a tool in a copper catalyzed ATRP process where the less activator concentration, consequently, less radical concentration is needed. Moreover, our previous attempt to synthesize a chain extended PS using PhONa as RA gave a mixture of both PS macroinitiator and chain extended polymer [135]. This result might be

explained that the high radical concentration caused some side reaction at the initiation step of the polymerization. Therefore, *p*-methoxyphenol was chosen as a mild RA for the preparation of PS macroinitiator and for the chain extension polymerization. In first step, chloro-terminated PS macroinitiator (**H28**) was synthesized using SG-CuCl₂/PMDETA catalyst as described in experimental part. The resulting polymer had $M_n = 2000$, $M_w/M_n = 1.27$ at 19% conversion. The PS macroinitiator with low molecular weight was purposely targeted to demonstrate a clear shift of the molecular weight of the chain extended polymer in the overlaid chromatogram. The polymerization was stopped at low conversion (19%) to have high chain end functionality. The chain extension polymerization was conducted for 26 h, under the similar reaction condition with the reactants ratio $[St]/[PS]/[CuCl_2]/[PMDETA]/[p\text{-methoxyphenol}] = 500 / 1 / 0.5 / 5/0.5$. GPC traces of PS macroinitiator and chain extended polymer (**H29**) ($M_n = 15000$, $M_w/M_n = 1.18$ at 22 % conversion, $M_{n,theo}=13500$) are shown in Figure 4.55. The complete disappearance of the peak due to macroinitiator suggests that high initiation efficiency ($f = M_{n,theo}/ M_n = 0.9$) is attained. It should be noticed that no other peak corresponding to the concurrent initiation by air (oxygen) [139] was observed in GPC. These results imply that a) all the chain ends of the PS macroinitiator possess the halide end group, it is also confirmed that the ¹H NMR spectrum of –PhCHCl end group of PS macroinitiator displayed a signal at 4.3 ppm, b) the initiation or/and termination processes with aryloxy radicals are negligible, and c) during the induction period of the polymerization, oxygen was consumed by the reactions were given in Eqs. 4.23 and 4.24. Therefore, the initiation by air (oxygen) is eliminated using the phenol or its derivatives.

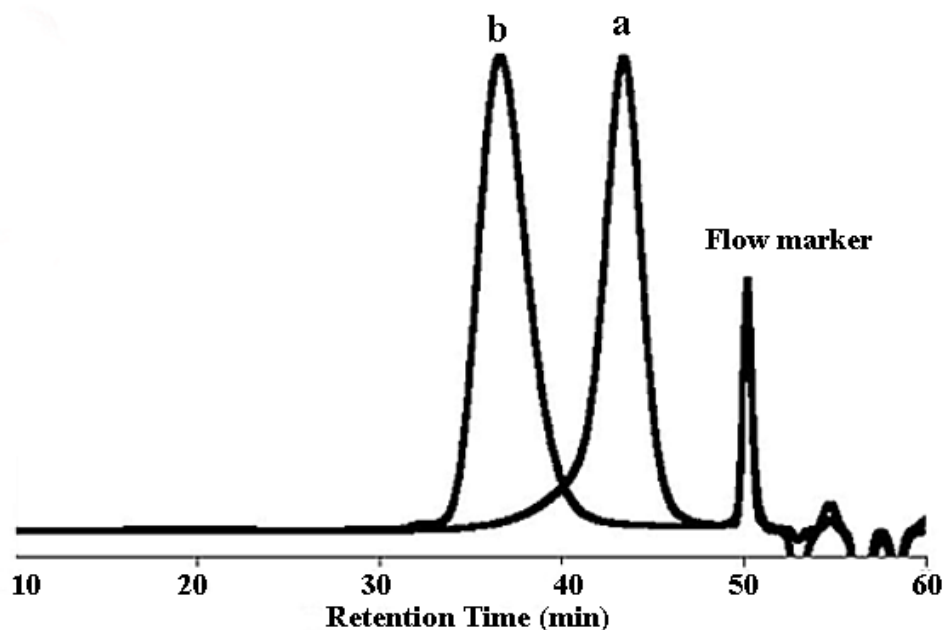


Figure 4.55: GPC traces of PS macroinitiator (**H28**) ($M_n = 2000$, $M_w/M_n = 1.27$ at 20 % conversion), (a), and the chain-extended polymer ($M_n = 15000$, $M_w/M_n = 1.18$ at 22 % conversion) (**H29**), (b).

4.7.3 Catalyst Reuse

After the first polymerization was complete, the catalyst was simply recovered by filtration and washed by toluene for several times. Finally, the recovered catalyst was air-dried and then vacuum dried at 35 °C for 24 h. Previous studies on the use of silica supported catalyst in LRP were concerned mainly, on the catalytic activity of the fresh and recycled catalysts and the amount of the residual copper in the obtained polymers [5]. In addition, the ligand loss is likely occurred after each reuse and it is one of the possible reasons of the reported decrease in catalytic activity of the reused catalysts [4, 5]. Furthermore, Zhu and coworkers [325] recently reported that the temperature dependent catalyst partitioning occurred during copper catalyzed LRP of methyl methacrylate catalyzed by silica gel supported CuBr/HMTETA [327]. The most of these polymerizations were carried out with molar equivalent amount of ligand and Cu(I). However, in our method, the catalyst was prepared by a high ligand-to- Cu(II) ratio (i.e., $[\text{amine}]/[\text{Cu(II)}] \geq 10$) in order to facilitate the reduction of Cu(II) and resulting in increasing of the polymerization rate as it was reported for the oxidative

polymerization of phenols [319]. Therefore, the amine content of the recovered catalyst was determined by elemental analysis. It was found that 25 % mol of the originally used amount of PMDETA was leached during the catalyst recovery process. The residual copper content of the resulting polymer was determined by atomic absorption spectrometer and was found to be 5.74 ppm, which indicated that the most of the copper was retained in silica gel. The catalyst recovered from the first polymerization was placed into a reaction flask and used for the subsequent run. The flask was charged with the same amount of St, 1-PECl, PhONa as in the first polymerization and 25 % of the originally used amount of PMDETA. St concentration (6.8 M) was kept constant by adding anisole to the polymerization. The polymerization was carried out as described in the experimental part. As seen in Figure 4.56, the first order kinetic was observed in monomer concentration for the recycled SG-CuCl₂/PMDETA catalyzed polymerization of St, after the consumption of oxygen within 25 min. The apparent rate constant of propagation ($k_p^{\text{app}} = 8.5 \cdot 10^{-5} \text{ s}^{-1}$) was calculated from the slope. This result implies that the recycled catalyst retained 90 % of its original activity (a ratio of the slopes, k_p^{app} , of the first-order kinetic plots) in second use. The M_n values increased with monomer conversion and the MWD became narrower as the polymerization proceeded and reached the value < 1.3 at 81 % conversion (Fig. 4.57). The M_n values were slightly higher than predicted ones. However, this result is not particular for our recycled catalyst and it has been observed in the other reported heterogeneous catalysts in copper catalyzed LRP [5].

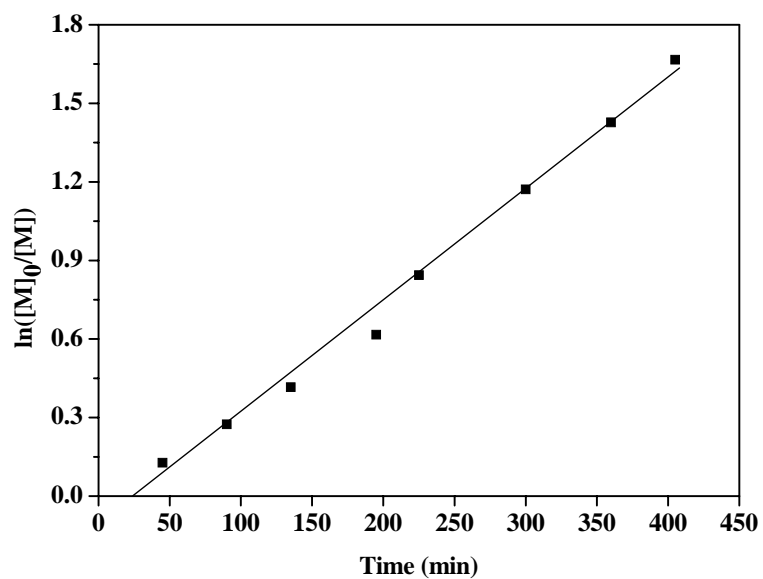


Figure 4.56: First-order kinetic plot for the polymerization of St catalyzed by recycled SG-CuCl₂/PMDETA at 110 °C; [St]₀ = 6.8 M; silica gel/CuCl₂ = 10 (w/w). [St]₀/[1-PECl]₀/[CuCl₂]/[PMDETA]/[PhONa] = 100 / 1 / 0.5 / 2.5 / 0.75.

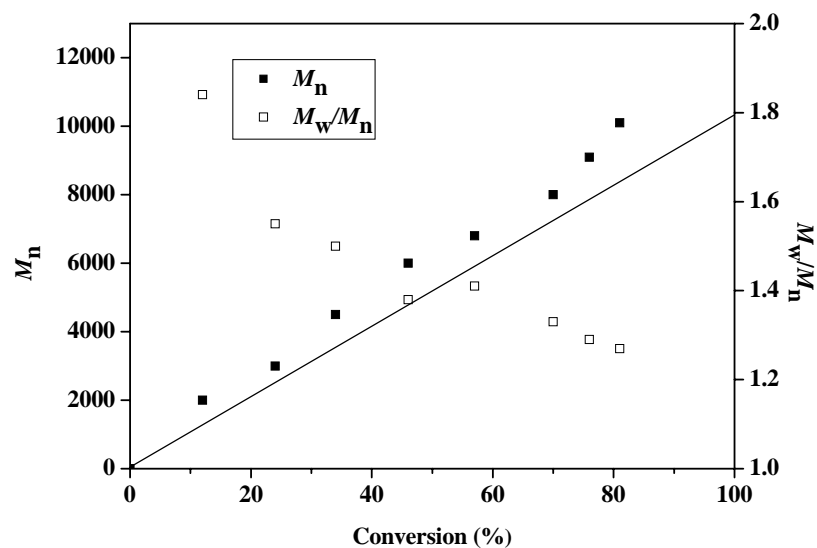


Figure 4.57: The dependences of M_n and M_w/M_n on monomer conversion in the polymerization of St catalyzed by recycled SG-CuCl₂/PMDETA at 110 °C $M_{n,theo}$ (—). (Experimental conditions as in Fig. 4.56).

5. CONCLUSION

In this PhD thesis, a new method for conducting ATRP was developed. The procedure used to generate copper (I) species relies on electron transfer from reducing agents to copper (II) species rather than reduction by organic radicals. This novel procedure has all the benefits of a normal ATRP process combined with the additional benefit of adding the catalyst complex to the reaction mixture in its more stable higher oxidation state. In contrary to reverse ATRP, concentration of active catalyst in ATRP via *in situ* copper (I) formation method can be changed independently of the initiator to improve control of reactions. Besides, this approach further improves the simultaneous reverse and normal initiation (SR&NI) by eliminating free radical initiators for the activation of the higher oxidation state catalyst complex. Thus it provides a simple route for synthesizing pure polymers with complex architectures such as star copolymers, block copolymers, etc.

In this regard we demonstrated the successful use of fructose as a reducing agent with RX/Cu(II)/PMDETA for ATRP of St in inert atmosphere. The polymerizations followed first-order kinetics and M_n values of the obtained linear PS increased linearly with conversion using either 1-PECl/CuCl₂, EiBr or MBP/CuBr₂ system. In addition, fructose as a reducing agent was also successfully utilized in ATRP for the preparation of either linear or octa-arm star PS-*b*-PMMA copolymer. Also, *p*-tert-butylphenol, dihydroquinone, and ascorbic acid were also used as reducing agent together with 1-PECl/Cu(II)/PMDETA catalyst system for ATRP of St in inert atmosphere.

Furthermore we demonstrated the effective use of RX/Cu(II)/PMDETA/thiophenol derivatives such as PhSNa or *p*-methoxythiophenol as catalyst system for ATRP of St in the presence of definite amount of air. The polymerizations followed first-order kinetics and the M_n values of the obtained polymers fit very well with those of $M_{n,theo}$. MALDI-TOF analysis of obtained PS clearly demonstrated that majority of PS chain possessed initiator fragment (C₆H₁₁O₂-) and alkene end group (HX elimination occurred during MALDI-TOF analysis). This result clearly reveals that

initiation or termination process by thiyl radicals is totally excluded. This method is also successfully employed both in chain extension and block copolymerization.

In the last part we demonstrated that the air-stable SG-CuCl₂/PMDETA catalyst complex can be successfully used for the ATRP of St. The polymerizations followed first-order kinetics and the M_n values of the obtained polymers were consistent with $M_{n,theo}$ ones. The results from the chain extension polymerization of St using the SG-CuCl₂/PMDETA catalyst complex clearly indicated that the obtained PS macroinitiator with this method possess halide end group and possible interactions of phenoxy radicals with propagating radicals and/or monomer are negligible. The chlorine end group of PS macroinitiator was further confirmed by ¹H NMR spectrum. More interestingly, the concurrent initiation by air (oxygen) was eliminated using phenols as a result of a regeneration process of Cu (I) from Cu (II) via electron transfer reaction during the observed induction period of the polymerization. The recycled catalyst retained 90 % of its original activity in the subsequent polymerization and thus, the controlled polymerization condition was achieved for St. However, M_n values were higher than those of $M_{n,theo}$. The use of SG-CuCl₂/PMDETA catalyst complex with phenol derivatives will have the greatest benefit for the catalyst separation and recycling process in ATRP, since all manipulations could be performed in an air atmosphere.

The *in situ* generation of Cu (I) species from its higher oxidation state analogues by reducing agents such as phenols would open a new way to the use of an air-stable heterogeneous or homogeneous catalyst. It is anticipated that *in situ* copper (I) formation method will facilitate the commercial application of ATRP and simplify the preparation of many new materials, including molecular hybrids, bioconjugates, and nanocomposites.

REFERENCES

- [1] **Moad, G. and Solomon, D.H.**, 1995. The Chemistry of Free Radical Polymerization, Oxford: Pergamon/Elsevier, UK.
- [2] **Kato, M., Kamigaito, M., Sawamoto, M., and Higashimura, T.**, 1995. Polymerization of Methyl Methacrylate with the Carbon Tetrachloride/Dichlorotris(triphenylphosphine) ruthenium(II)/Methylaluminum-bis-(2,6-di-*tert*-butylphenoxide) Initiating Systems Possibility of Living Radical Polymerization, *Macromolecules*, **28**(5), 1721-1723.
- [3] **Wang, J.S., and Matyjaszewski, K.**, 1995. Controlled Living Radical Polymerizations Atom Transfer Radical Polymerization in the Presence of Transition-Metal Complexes, *J. Am. Chem. Soc.*, **117**(20), 5614-5615.
- [4] **Hong, S.C., and Matyjaszewski, K.**, 2002. Fundamentals of Supported Catalysts for Atom Transfer Radical Polymerization (ATRP) and Application of an Immobilized/Soluble Hybrid Catalyst System to ATRP, *Macromolecules*, **35**(20), 7592-7605.
- [5] **Shen, Y., Tang, H., and Ding, S.**, 2004. Catalyst separation in Atom Transfer Radical Polymerization, *Prog. Polym. Sci.*, **29**(10), 1053-1078.
- [6] **Kubisa, P.**, 2004. Application of Ionic Liquids as Solvents for Polymerization Processes, *Prog. Polym. Sci.*, **29**(1), 3-12.
- [7] **Qiu, J., Charleux, B., and Matyjaszewski, K.**, 2001. Controlled/Living Radical Polymerization in Aqueous Media: Homogeneous and Heterogeneous Systems, *Prog. Polym. Sci.*, **26**(10), 2083-2134.
- [8] **Haddleton, D.M., Kukulj, D., and Radigue, A.P.**, 1999. Atom Transfer Polymerisation of Methyl Methacrylate Mediated by Solid Supported Copper Catalysts, *Chem. Commun.* (1), 99-100.
- [9] **Barre, G., Taton, D., Lastecoueres, D., and Vincent, J.-M.**, 2004. Closer to the "Ideal Recoverable Catalyst" for Atom Transfer Radical Polymerization Using a Molecular Non-Fluorous Thermomorphic System, *J. Am. Chem. Soc.*, **126**(25), 7764-7765.
- [10] **Pyun, J., Matyjaszewski, K., Kowalewski, T., Savin, D., Patterson, G., Kickelbick, G., and Huesing, N.**, 2001. Synthesis of Well-Defined Block Copolymers Tethered to Polysilsesquioxane Nanoparticles and Their Nanoscale Morphology on Surfaces, *J. Am. Chem. Soc.*, **123**(38), 9445-9446.

- [11] **Webster, O.W.**, 1991. Living Polymerization Methods, *Science*, **251(22)**, 887-893
- [12] **Yağcı, Y., Mishra, and M.K.**, 1994. Macroinitiators for Chain Polymerization, in *Advanced Polymers via Macromolecular Engineering (APME) Series, Macromolecular Design: Concept and Practice*, Polymer Frontiers International. Inc., New York.
- [13] **Otsu, T., Yoshida, M., and Tazaki, T.**, 1982. A Model for Living Radical Polymerization, *Makromol. Chem. Rapid Commun.*, **3(2)**, 133-140.
- [14] **Fischer, H.**, 1997. The Persistent Radical Effect In "Living" Radical Polymerization, *Macromolecules*, **30(19)**, 5666-5672.
- [15] **Fischer, H.**, 1999. The Persistent Radical Effect in Controlled Radical Polymerizations, *J. Polym. Sci. Part A: Polym. Chem.*, **37(13)**, 1885-1901.
- [16] **Georges, M.K., Veregin, R.P.N., Kazmaier, P.M., and Hamer, G.K.**, 1993. Narrow Molecular Weight Resins by a Free-Radical Polymerization Process, *Macromolecules*, **26(11)**, 2987-2988.
- [17] **Hawker, C.J., Bosman, A.W., and Harth, E.**, 2001. New Polymer Synthesis by Nitroxide Mediated Living Radical Polymerizations, *Chem. Rev.*, **101(12)**, 3661-3688.
- [18] **Wayland, B.B., Poszmik, G., Mukerjee, S.L., and Fryd, M.**, 1994. Living Radical Polymerization of Acrylates by Organocobalt Porphyrin Complexes, *J. Am. Chem. Soc.*, **116(17)**, 7943-7944.
- [19] **Matyjaszewski, K., Gaynor, S., and Wang, J.-S.**, 1995. Controlled Radical Polymerizations: The Use of Alkyl Iodides in Degenerative Transfer, *Macromolecules*, **28(6)**, 2093-2095.
- [20] **Moad, C.L., Moad, G., Rizzardo, E., and Thang, S.H.**, 1996. Chain Transfer Activity of α -Unsaturated Methyl Methacrylate Oligomers, *Macromolecules*, **29(24)**, 7717-7726.
- [21] **Chiefari, J., Chong, Y.K., Ercole, F., Krstina, J., Jeffery, J., Le, T.P.T., Mayadunne, R.T.A., Meijs, G.F., Moad, C.L., Moad, G., Rizzardo, E., and Thang, S.H.**, 1998. Living Free-Radical Polymerization by Reversible Addition-Fragmentation Chain Transfer: The RAFT Process, *Macromolecules*, **31(16)**, 5559-5562.
- [22] **Destarac, M., Charnot, D., Franck, X., and Zard, S.Z.**, 2000. Dithiocarbamates as Universal Reversible Addition-Fragmentation Chain Transfer Agents, *Macromol. Rapid Comm.*, **21(15)**, 1035-1039.
- [23] **Curran, D.P.**, 1988. The Design and Application of Free Radical Chain Reactions in Organic Synthesis, *Synthesis*, **7**, Part 2, pp. 489.

- [24] **Curran, D.P.**, 1988. The Design and Application of Free Radical Chain Reactions in Organic Synthesis, *Synthesis*, **6**, Part 1, pp 417-439; Part 2, pp. 489.
- [25] **Kharasch, M.S., Jensen, E.V., and Urry, W.H.**, 1945. Addition of Carbon Tetrachloride and Chloroform to Olefins, *Science*, **102(3)**, 128.
- [26] **Kharasch, M.S., Jensen, E.V., and Urry, W.H.**, 1945. Addition of derivatives of chlorinated acetic acids to olefins, *J. Am. Chem. Soc.*, **67(9)**, 1626.
- [27] **Hey, D.H., and Waters, W.A.**, 1937. Some Organic Reactions Involving the Occurrence of Free Radicals in Solution, *Chem. Rev.*, **21(1)**, 169-208.
- [28] **Kharasch, M.S., Engelmann, H., and Mayo, F.R.**, 1938. The Peroxide Effect in the Addition of Reagents to Unsaturated Compounds. XV. The Addition of Hydrogen Bromide to 1- and 2-Bromo- and Chloropropenes, *J. Org. Chem.*, **2(3)**, 288-302.
- [29] **Bellus, D.**, 1985. Copper-Catalyzed Additions of Organic Polyhalides to Olefins: A Versatile Synthetic Tool, *Pure Appl. Chem.*, **57(12)**, 1827-1839.
- [30] **Udding, J.H., Tuijp, K.J.M., van Zanden, M.N.A., Hiemstra, H., and Meyerstein, D.**, 1994. Transition Metal-Catalyzed, Chlorine-Transfer Radical Cyclizations of 2-(3-Alken-1-oxy)-2-Chloroacetates. Formal Total Synthesis of Avenaciolide and Isoavenaciolide, *J. Org. Chem.*, **59(8)**, 1993-2003.
- [31] **Nagashima, H., Ozaki, N., Ishii, M., Seki, K., Washiyama, M., and Itoh, K.**, 1993. Transition Metal-Catalyzed Radical Cyclizations: A Low-Temperature Process for the Cyclization of N-Protected N-Allyltrichloroacetamides to Trichlorinated γ -Lactams and Application to the Stereoselective Preparation of β,γ -Disubstituted γ -Lactams, *J. Org. Chem.*, **58(2)**, 464-470.
- [32] **Metzger, J.O., and Mahler, R.**, 1995. Radical Additions of Activated Haloalkanes to Alkenes Initiated by Electron Transfer from Copper in Solvent-Free Systems, *Angew. Chem. Int. Ed. Engl.*, **34(8)**, 902-904.
- [33] **Grove, D.M., van Koten, G.A., and Verschuuren, H.M.**, 1988. New Homogeneous Catalysts in the Addition of Polyhalogenoalkanes to Olefins; Organonickel(II) Complexes $[\text{Ni}\{\text{C}_6\text{H}_3(\text{CH}_2\text{NMe}_2)_2\text{-}o,o'\}\text{X}]$ (X = Cl, Br, I), *J. Mol. Catal.*, **45(2)**, 169-174.
- [34] **Tsuji, J., Sato, K., and Nagashima, H.**, 1981. Activation of Polyhaloalkanes by Palladium Catalyst. Facile Addition of Polyhaloalkanes to Olefins, *Chem. Lett.*, **10(8)**, 1169-1170.
- [35] **Nagashima, H., Wakamatsu, H., Ozaki, N., Ishii, T., Watanabe, M., Tajima, T., and Itoh, K.**, 1992. Transition Metal Catalyzed Radical Cyclization: New Preparative Route to Gamma -Lactams from Allylic Alcohols via the [3.3]-Sigmatropic Rearrangement of Allylic

Trichloroacetimidates and the Subsequent Ruthenium-Catalyzed Cyclization of N-allyltrichloroacetamides, *J. Org. Chem.*, **57**(6), 1682-1689.

- [36] **Minisci, F.**, 1975. Free-Radical Additions to Olefins in the Presence of Redox Systems, *Acc. Chem. Res.*, **8**(5), 165-171.
- [37] **Iqbal, J., Bhatia, B., and Nayyar, N.K.**, 1994. Transition Metal-Promoted Free-Radical Reactions in Organic Synthesis: The Formation of Carbon-Carbon Bonds, *Chem. Rev.*, **94**(2), 519-564.
- [38] **Matyjaszewski, K.**, 1999. Transition Metal Catalysis in Controlled Radical Polymerization: Atom Transfer Radical Polymerization, *Chem. Eur. J.*, **5**(11), 3095-3102.
- [39] **Patten, T.E., Xia, J., Abernathy, T., and Matyjaszewski, K.**, 1996. Polymers with Very Low Polydispersities from Atom Transfer Radical Polymerization, *Science*, **272**, 866-868.
- [40] **Goto, A., and Fukuda, T.**, 2004. Kinetics of Living Radical Polymerization, *Prog. Polym. Sci.*, **29**(4), 329-385.
- [41] **Matyjaszewski, K.**, 1998. Mechanistic Aspects of Atom Transfer Radical Polymerization, in *Controlled Radical Polymerization*, **685**, pp. 258-283, Ed., Matyjaszewski, K., American Chemical Society, Washington, DC.
- [42] **Matyjaszewski, K., and Woodworth, B.E.**, 1998. Interaction of Propagating Radicals with Copper(I) and Copper(II) Species, *Macromolecules*, **31**(15), 4718-4723.
- [43] **Matyjaszewski, K.**, 1999. Lifetimes of Polystyrene Chains in Atom Transfer Radical Polymerization, *Macromolecules*, **32**(26), 9051-9053.
- [44] **Matyjaszewski, K.**, 2002. Mechanistic Features and Radical Intermediates in Atom Transfer Radical Polymerization, *Macromol. Symp.*, **183**, 71-82.
- [45] **Matyjaszewski, K.**, 2002. Factors Affecting Rates of Comonomer Consumption in Copolymerization Processes with Intermittent Activation, *Macromolecules*, **35**(18), 6773-6781.
- [46] **Matyjaszewski, K.**, 2002. Structure-Reactivity Correlation in Atom Transfer Radical Polymerization, *Macromol. Symp.*, **182**, 209-225.
- [47] **Pintauer, T., McKenzie, B., and Matyjaszewski, K.**, 2003. Toward Structural and Mechanistic Understanding of Transition Metal-Catalyzed Atom Transfer Radical Processes; Advances in Controlled/Living Radical Polymerization, *ACS Symposium Series*, **854**, 130-147.
- [48] **Singleton, D.A., Nowlan III, D.T., Jahed, N., and Matyjaszewski, K.**, 2003. Isotope Effects and the Mechanism of Atom Transfer Radical Polymerization, *Macromolecules*, **36**(23), 8609-8616.

- [49] **Wang, J.S., and Matyjaszewski, K.,** 1995. Controlled/"Living" Radical Polymerization. Halogen Atom Transfer Radical Polymerization Promoted by a Cu(I)/Cu(II) Redox Process, *Macromolecules*, **28(23)**, 7901-7910.
- [50] **Percec, V., and Barboiu, B.,** 1995. "Living" Radical Polymerization of Styrene Initiated by Arenesulfonyl Chlorides and CuI(bpy)_nCl, *Macromolecules*, **28(23)**, 7970-7972.
- [51] **Percec, V., Barboiu, B., Neumann, A., Ronda, J.C., and Zhao, M.,** 1996. Metal-Catalyzed "Living" Radical Polymerization of Styrene Initiated with Arenesulfonyl Chlorides. From Heterogeneous to Homogeneous Catalysis, *Macromolecules*, **29(10)**, 3665-3668.
- [52] **Haddleton, D.M., Jasieczek, C.B., Hannon, M.J., and Shooter, A.J.,** 1997. Atom Transfer Radical Polymerization of Methyl Methacrylate Initiated by Alkyl Bromide and 2-Pyridinecarbaldehyde Imine Copper(I) Complexes, *Macromolecules*, **30(7)**, 2190-2193.
- [53] **Granel, C., Dubois, P., Jerome, R., and Teyssie, P.,** 1996. Controlled Radical Polymerization of Methacrylic Monomers in the Presence of a Bis(ortho-chelated) Arylnickel(II) Complex and Different Activated Alkyl Halides, *Macromolecules*, **29(27)**, 8576-8582.
- [54] **Uegaki, H., Kotani, Y., Kamigaito, M., and Sawamoto, M.,** 1997. Nickel-Mediated Living Radical Polymerization of Methyl Methacrylate¹, *Macromolecules*, **30(8)**, 2249-2253.
- [55] **Ando, T., Kato, M., Kamigaito, M., and Sawamoto, M.,** 1996. Living Radical Polymerization of Methyl Methacrylate with Ruthenium Complex: Formation of Polymers with Controlled Molecular Weights and Very Narrow Distributions¹, *Macromolecules*, **29(3)**, 1070-1072.
- [56] **Ando, T., Kamigaito, M., and Sawamoto, M.,** 1997. Iron(II) Chloride Complex for Living Radical Polymerization of Methyl Methacrylate¹, *Macromolecules*, **30(16)**, 4507-4510.
- [57] **Matyjaszewski, K., Wei, M., Xia, J., and McDermott, N.E.,** 1997. Controlled/"Living" Radical Polymerization of Styrene and Methyl Methacrylate Catalyzed by Iron Complexes¹, *Macromolecules*, **30(26)**, 8161-8164.
- [58] **Patten, T.E., and Matyjaszewski, K.,** 1998. Atom Transfer Radical Polymerization and the Synthesis of Polymeric Materials, *Adv. Mater.*, **10(12)**, 901-915.
- [59] **Percec, V., and Tirrel, D.A.,** 2000. Living or Controlled?, *J. Polym. Sci., Part A: Polym Chem.*, **38 (10)**, 1705-1752.
- [60] **Matyjaszewski, K., Patten, T.E., and Xia, J.,** 1997. Controlled/"Living" Radical Polymerization. Kinetics of the Homogeneous Atom Transfer

Radical Polymerization of Styrene, *J. Am. Chem. Soc.*, **119**(4), 674-680.

- [61] **Matyjaszewski, K., Davis, K., Patten, T.E., and Wei, M.L.**, 1997. Observation and Analysis of a Slow Termination Process in the Atom Transfer Radical Polymerization of Styrene, *Tetrahedron*, **53**(45), 15321-15329.
- [62] **Qiu, J., and Matyjaszewski, K.**, 1997. Polymerization of Substituted Styrenes by Atom Transfer Radical Polymerization, *Macromolecules*, **30**(19), 5643-5648.
- [63] **Grimaud, T., and Matyjaszewski, K.**, 1997. Controlled/"Living" Radical Polymerization of Methyl Methacrylate by Atom Transfer Radical Polymerization, *Macromolecules*, **30**(7), 2216-2218.
- [64] **Wang, J.L., Grimaud, T., and Matyjaszewski, K.**, 1997. Kinetic Study of the Homogeneous Atom Transfer Radical Polymerization of Methyl Methacrylate, *Macromolecules*, **30**(21), 6507-6512.
- [65] **Gilbert, R.G.**, 1996. Critically-Evaluated Propagation Rate Coefficients in Free Radical Polymerizations I. Styrene and Methyl Methacrylate, (Technical Report) Commission on Polymer Characterization and Properties, *Pure Appl. Chem.*, **68**(7), 1491-1494.
- [66] **Beuermann, S., Buback, M., Davis, T.P., Gilbert, R.G., Hutchinson, R.A., Olaj, O.F., Russell, G.T., Schweer, J., and van Herk, A.M.**, 1997. Critically Evaluated Rate Coefficients for Free-Radical Polymerization, 2.. Propagation Rate Coefficients for Methyl Methacrylate, *Macromol. Chem. Phys.*, **198**(5), 1545-1560.
- [67] **Buback, M., Gilbert, R.G., Hutchinson, R.A., Klumperman, B., Kuchta, F.-D., Manders, B.G., O'Driscoll, K.F., Russell, G.T., and Schweer, J.**, 1995. Critically Evaluated Rate Coefficients for Free-Radical Polymerization, 1. Propagation rate coefficient for styrene, *Macromol. Chem. Phys.*, **196**(10), 3267-3280.
- [68] **Davis, K., O'Malley, J., Paik, H.-J., Matyjaszewski, K.**, 1997. Effect of the Counteranion in Atom Transfer Radical Polymerization Using Alkyl (Pseudo)Halide Initiators, *Polym. Prepr. (Am. Chem. Soc., Div. Polym. Chem.)*, **38**(1), 687.
- [69] **Nishimura, M., Kamigaito, M., Sawamoto, M.**, 1999. Living Radical Polymerization of Styrene with Transition Metal Dithiocarbamate/AIBN Systems: Halogen-Free Living Processes, *Polym. Prepr. (Am. Chem. Soc., Div. Polym. Chem.)*, **40**(2), 470.
- [70] **Singha, N.K., and Klumperman, B.**, 2000. Atom-Transfer Radical Polymerization of Methyl Methacrylate (MMA) Using CuSCN as the Catalyst, *Macromol. Rapid Commun.*, **21**(16), 1116-1120.

- [71] **Matyjaszewski, K., Coca, S., Gaynor, S.G., Nakagawa, Y., Jo, S.M.**, 1989. Preparation of Novel Homo- and Copolymers Using Atom Transfer Radical Polymerization, *United States Patent*, No: 5789487 dated 04.08.1998.
- [72] **Xia, J., Zhang, X., and Matyjaszewski, K.**, 1999. Atom Transfer Radical Polymerization of 4-Vinylpyridine, *Macromolecules*, **32(10)**, 3531-3533.
- [73] **Davis, K.A., Paik, H.-J., and Matyjaszewski, K.**, 1999. Kinetic Investigation of the Atom Transfer Radical Polymerization of Methyl Acrylate, *Macromolecules*, **32(6)**, 1767-1776.
- [74] **Beers, K.L., Boo, S., Gaynor, S.G., and Matyjaszewski, K.**, 1999. Atom Transfer Radical Polymerization of 2-Hydroxyethyl Methacrylate, *Macromolecules*, **32(18)**, 5772-5776.
- [75] **Davis, K.A., and Matyjaszewski, K.**, 2000. Atom Transfer Radical Polymerization of *tert*-Butyl Acrylate and Preparation of Block Copolymers, *Macromolecules*, **33(11)**, 4039-4047.
- [76] **Davis, K.A., and Matyjaszewski, K.**, 2001. ABC Triblock Copolymers Prepared Using Atom Transfer Radical Polymerization Techniques, *Macromolecules*, **34(7)**, 2101-2107.
- [77] **Davis, K.A., and Matyjaszewski, K.**, 2004. Investigation of the ATRP of *n*-Butyl Methacrylate Using the Cu(I)/N,N,N',N'',N''-Pentamethyldiethylenetriamine Catalyst System, *Chin. J. Polym. Sci.*, **22(2)**, 195-204.,
- [78] **Huang, J., Pintauer, T., and Matyjaszewski, K.**, 2004. Effect of Variation of [PMDTA]₀/[Cu(I)Br]₀ ratio on Atom Transfer Radical Polymerization of *n*-Butyl Acrylate, *J. Polym. Sci., Part A: Polym. Chem.*, **42(13)**, 3285-3292.
- [79] **Matyjaszewski, K., Nakagawa, Y., and Jasieczek, C.B.**, 1998. Polymerization of *n*-Butyl Acrylate by Atom Transfer Radical Polymerization. Remarkable Effect of Ethylene Carbonate and Other Solvents, *Macromolecules*, **31(5)**, 1535-1541.
- [80] **Matyjaszewski, K., Coca, S., and Jasieczek, C.B.**, 1997. Polymerization of Acrylates by Atom Transfer Radical Polymerization. Homopolymerization of Glycidyl Acrylate, *Macromol. Chem. Phys.*, **198(12)**, 4011-4017.
- [81] **Zhang, X., and Matyjaszewski, K.**, 1999. Synthesis of Well-Defined Amphiphilic Block Copolymers with 2-(Dimethylamino)ethyl Methacrylate by Controlled Radical Polymerization, *Macromolecules*, **32(6)**, 1763-1766.

- [82] **Ziegler, M.J., and Matyjaszewski, K.,** 2001. Atom Transfer Radical Copolymerization of Methyl Methacrylate and *n*-Butyl Acrylate, *Macromolecules*, **34(3)**, 415-424.
- [83] **Shinoda, H., Matyjaszewski, K., Okrasa, L., Mierzwa, M., and Pakula, T.,** 2003. Structural Control of Poly(methyl methacrylate)-*g*-poly(dimethylsiloxane) Copolymers Using Controlled Radical Polymerization: Effect of the Molecular Structure on Morphology and Mechanical Properties, *Macromolecules*, **36(13)**, 4772-4778.
- [84] **Matyjaszewski, K., Jo, S.M., Paik, H.-J., and Gaynor, S.,** 1997. Synthesis of Well-Defined Polyacrylonitrile by Atom Transfer Radical Polymerization, *Macromolecules*, **30(20)**, 6398-6400.
- [85] **Matyjaszewski, K., Jo, S.M., Paik, H.-J., and Shipp, D.A.,** 1999. An Investigation into the CuX/2,2'-Bipyridine (X = Br or Cl) Mediated Atom Transfer Radical Polymerization of Acrylonitrile, *Macromolecules*, **32(20)**, 6431-6438.
- [86] **Tang, C., Kowalewski, T., and Matyjaszewski, K.,** 2003. Preparation of Polyacrylonitrile-block-poly(*n*-butyl acrylate) Copolymers Using Atom Transfer Radical Polymerization and Nitroxide Mediated Polymerization Processes, *Macromolecules*, **36(5)**, 1465-1473.
- [87] **Teodorescu, M., and Matyjaszewski, K.,** 1999. Atom Transfer Radical Polymerization of (Meth)acrylamides, *Macromolecules*, **32(15)**, 4826-4831.
- [88] **Neugebauer, D., and Matyjaszewski, K.,** 2003. Copolymerization of N,N-Dimethylacrylamide with *n*-Butyl Acrylate via Atom Transfer Radical Polymerization, *Macromolecules*, **36(8)**, 2598-2603.
- [89] **Konak, C., Ganchev, B., Teodorescu, M., Matyjaszewski, K., Kopeckova, P., and Kopecek, J.,** 2002. Poly[N-(2-hydroxypropyl)methacrylamide-block-*n*-butyl acrylate] Micelles in Water/DMF Mixed Solvents, *Polymer*, **43(13)**, 3735-3741.
- [90] **Kabachii, Y.A., Kochev, S.Y., Bronstein, L.M., Blagodatskikh, I.B., and Valetsky, P.M.,** 2003. Atom Transfer Radical Polymerization with Ti(III) Halides and Alkoxides, *Polym. Bull.*, **50(4)**, 271-278.
- [91] **Brandts, J.A.M., van de Geijn, P., van Faassen, E.E., Boersma, J., and van Kotten, G.,** 1999. Controlled Radical Polymerization of Styrene in the Presence of Lithium Molybdate(V) Complexes and Benzylic Halides, *J. Organomet. Chem.*, **584(2)**, 246-253.
- [92] **Le Grogne, E., Claverie, J., and Poli, R.,** 2001. Radical Polymerization of Styrene Controlled by Half-Sandwich Mo(III)/Mo(IV) Couples: All Basic Mechanisms Are Possible, *J. Am. Chem. Soc.*, **123(39)**, 9513-9524.

- [93] **Kotani, Y., Kamigaito, M., and Sawamoto, M.**, 1999. Re(V)-Mediated Living Radical Polymerization of Styrene:¹ ReO₂I(PPh₃)₂/R-I Initiating Systems, *Macromolecules*, **32**(8), 2420-2424.
- [94] **Teodorescu, M., Gaynor, S., and Matyjaszewski, K.**, 2000. Halide Anions as Ligands in Iron-Mediated Atom Transfer Radical Polymerization, *Macromolecules*, **33**(7), 2335-2339.
- [95] **Gibson, V.C., O'Reilly, R.K., Reed, W., Wass, D.F., White, A.J.P., and Williams, D.J.**, 2002. Four-coordinate Iron Complexes Bearing α -diimine Ligands: Efficient Catalysts for Atom Transfer Radical Polymerisation (ATRP), *Chem. Commun.*, **17**, 1850-1851.
- [96] **Gibson, V.C., O'Reilly, R.K., Wass, D.F., White, A.J.P., and Williams, D.J.**, 2003. Polymerization of Methyl Methacrylate Using Four-Coordinate (α -Diimine)iron Catalysts: Atom Transfer Radical Polymerization vs Catalytic Chain Transfer, *Macromolecules*, **36**(8), 2591-2593.
- [97] **Gibson, V.C., O'Reilly, R.K., Wass, D.F., White, A.J.P., and Williams, D.J.**, 2003. Iron Complexes Bearing Iminopyridine and Aminopyridine Ligands as Catalysts for Atom Transfer Radical Polymerisation, *Dalton Trans.*, **14**, 2824-2830.
- [98] **Moineau, G., Granel, C., Dubois, P., Jérôme, R., and Teyssié, P.**, 1998. Controlled Radical Polymerization of Methyl Methacrylate Initiated by an Alkyl Halide in the Presence of the Wilkinson Catalyst, *Macromolecules*, **31**(2), 542-544.
- [99] **Lecomte, P., Drapier, I., Dubois, P., Teyssie, P., and Jerome, R.**, 1997. Controlled Radical Polymerization of Methyl Methacrylate in the Presence of Palladium Acetate, Triphenylphosphine, and Carbon Tetrachloride, *Macromolecules*, **30**(24), 7631-7633.
- [100] **Davis, K.A., and Matyjaszewski, K.**, 2004. Effect of (Pseudo)halide Initiators and Copper Complexes with Non-halogen Anions on the ATRP, *Journal of Macromolecular Science, Pure and Applied Chemistry*, **41**, 449-465.
- [101] **Gobelt, B., and Matyjaszewski, K.**, 2000. Diimino- and Diaminopyridine Complexes of CuBr and FeBr₂ as Catalysts in Atom Transfer Radical Polymerization (ATRP), *Macromol. Chem. Phys.*, **201**(14), 1619-1624.
- [102] **Gromada, J., Spanswick, J., and Matyjaszewski, K.**, 2004. Synthesis and ATRP Activity of New TREN-Based Ligands, *Macromol. Chem. Phys.*, **205**(5), 551-566.
- [103] **Sarbu, T., and Matyjaszewski, K.**, 2001. ATRP of Methyl Methacrylate in the Presence of Ionic Liquids with Ferrous and Cuprous Anions, *Macromol. Chem. Phys.*, **202**(17), 3379-3391.

- [104] **Xia, J., Johnson T., Gaynor, S.G., Matyjaszewski, K., and DeSimone, J.,** 1999. Atom Transfer Radical Polymerization in Supercritical Carbon Dioxide, *Macromolecules*, **32(15)**, 4802-4805.
- [105] **Xia, J., and Matyjaszewski, K.,** 1999. Controlled/"Living" Radical Polymerization. Atom Transfer Radical Polymerization Catalyzed by Copper(I) and Picolylamine Complexes, *Macromolecules*, **32(8)**, 2434-2437.
- [106] **Xia, J.; Zhang, X.; and Matyjaszewski, K.,** 2000. The Effect of Ligands on Copper-Mediated Atom Transfer Radical Polymerization, *ACS Symp. Ser.*, **760**, 207-223.
- [107] **Patten, T.E., and Matyjaszewski, K.,** 1999. Copper(I)-Catalyzed Atom Transfer Radical Polymerization, *Acc. Chem. Res.*, **32(10)**, 895-903.
- [108] **Destarac, M., Bessiere, J.M., and Boutevin, B.,** 1997. Transition Metal Catalyzed Atom Transfer Radical Polymerization (ATRP): from Heterogeneous to Homogeneous Catalysis Using 1,10-phenanthroline and its Derivatives as New Copper(I) Ligands, *Macromol. Rapid Commun.*, **18(11)**, 967-974.
- [109] **Xia, J., and Matyjaszewski, K.,** 1997. Controlled/"Living" Radical Polymerization. Atom Transfer Radical Polymerization Using Multidentate Amine Ligands, *Macromolecules*, **30(25)**, 7697-7700.
- [110] **Zhang, X., Xia, J., and Matyjaszewski, K.,** 1998. Controlled/"Living" Radical Polymerization of 2-(Dimethylamino)ethyl Methacrylate, *Macromolecules*, **31(15)**, 5167-5169.
- [111] **Kickelbick, G., and Matyjaszewski, K.,** 1999. 4,4',4''-Tris(5-nonyl)-2,2' : 6',2''-terpyridine as Ligand in Atom Transfer Radical Polymerization (ATRP), *Macromol. Rapid Commun.*, **20(6)**, 341-346.
- [112] **Xia, J., Zhang, X., Matyjaszewski, K.,** 2000. Transition Metal Catalysis in Macromolecular Design, American Chemical Society, p. 207., Ed. Novak, B. M., Washington, DC.
- [113] **Xia, J., Gaynor, S.G., and Matyjaszewski, K.,** 1998. Controlled/"Living" Radical Polymerization. Atom Transfer Radical Polymerization of Acrylates at Ambient Temperature, *Macromolecules*, **31(17)**, 5958-5959.
- [114] **Matyjaszewski, K., Coca, S., Gaynor, S.G., Wei, M.L., and Woodworth, B.E.,** 1997. Zerovalent Metals in Controlled/"Living" Radical Polymerization, *Macromolecules*, **30(23)**, 7348-7350.
- [115] **Matyjaszewski, K., and Lin, C.H.,** 1991. Exchange Reactions in the Living Cationic Polymerization of Alkenes, *Makromol. Chemie, Macromol. Symp.*, **47**, 221-237.

- [116] **Litvinienko, G., and Müller, A.H.E.,** 1997. General Kinetic Analysis and Comparison of Molecular Weight Distributions for Various Mechanisms of Activity Exchange in Living Polymerizations, *Macromolecules*, **30(5)**, 1253-1266.
- [117] **Bamford, C.H.,** 1989. Comprehensive Polymer Science, **3**, pp. 123, Allen, G., Aggarwal, S. L. and Russo, S., Eds. Pergamon, Oxford,
- [118] **Matyjaszewski, K.,** 1996. The Importance of Exchange Reactions in Controlled/Living Radical Polymerization in the Presence of Alkoxyamines and Transition Metals, *Technical Report*, **A697903**, Carnegie Mellon University Department of Chemistry, PA.
- [119] **Coleman, B.D., and Fox, T.G.,** 1963. A multistate mechanism for homogeneous ionic polymerization. II. The molecular weight distribution, *J. Am. Chem. Soc.*, **85(9)**, 1241-1244.
- [120] **Matyjaszewski, K.,** 1996. Cationic Polymerizations: Mechanisms, Synthesis, and Applications, pp. 768 Eds. Dekker, New York.
- [121] **Moineau, G., Dubois, P., Jérôme, R., Senninger, T., and Teyssié, P.,** 1998. Alternative Atom Transfer Radical Polymerization for MMA Using FeCl₃ and AIBN in the Presence of Triphenylphosphine: An Easy Way to Well-Controlled PMMA, *Macromolecules*, **31(2)**, 545-547.
- [122] **Wang, J.S., and Matyjaszewski, K.,** 1995. "Living"/Controlled Radical Polymerization. Transition-Metal-Catalyzed Atom Transfer Radical Polymerization in the Presence of a Conventional Radical Initiator, *Macromolecules*, **28(22)**, 7572-7573.
- [123] **Gromada, J., and Matyjaszewski, K.,** 2001. Simultaneous Reverse and Normal Initiation in Atom Transfer Radical Polymerization, *Macromolecules*, **34(22)**, 7664-7671.
- [124] **Matyjaszewski, K.; Gromada, J.; Li, M.,** 2003. Simultaneous Reverse and Normal Initiation of ATRP, *United States Patent*, WO 03031481 dated 17.04.2003.
- [125] **Li, M., and Matyjaszewski, K.,** 2003. Further Progress in Atom Transfer Radical Polymerizations Conducted in a Waterborne System, *J. Polym. Sci., Part A: Polym. Chem.*, **41(22)**, 3606-3614.
- [126] **Li, M., Min, K., and Matyjaszewski, K.,** 2004. ATRP in Waterborne Miniemulsion via a Simultaneous Reverse and Normal Initiation Process, *Macromolecules*, **37(6)**, 2106-2112.
- [127] **Li, M., Jahed, N.M., Min, K., and Matyjaszewski, K.,** 2004. Preparation of Linear and Star-Shaped Block Copolymers by ATRP Using Simultaneous Reverse and Normal Initiation Process in Bulk and Miniemulsion, *Macromolecules*, **37(7)**, 2434-2441.

- [128] **Haddleton, D.M., Shooter, A.J., Heming, A.M., Crosmann, M.C., Duncalf, D.J., Morsley, S.R.**, 1997. Controlled Radical Polymerization; Matyjaszewski, K., Ed.; ACS Symp. Ser. Vol. 685; American Chemical Society: Washington, DC, 1997, p 284.
- [129] **Haddleton, D.M., Clark, A.J., Crosmann, M.C., Duncalf, D.J., Heming, A.M., Morsley, S.R., and Shooter, A.J.**, 1997. Atom Transfer Radical Polymerisation (ATRP) of Methyl Methacrylate in the Presence of Radical Inhibitors, *Chem. Commun.*, **(13)**, 1173-1174.
- [130] **Haddleton, D.M., Clark, A.J., Duncalf, D.J., Heming, A.M., Kukulj, D., and Shooter, A.J.**, 1998. Copper Diimine Complexes: The Synthesis and Crystal Structures of $[\text{Cu}(\text{C}_{10}\text{H}_{14}\text{N}_2)_2(\text{MeOH})][\text{BF}_4]$, $[\text{Cu}(\text{C}_{10}\text{H}_{20}\text{N}_2)_2]\text{Br}$, $[\{(\text{C}_{10}\text{H}_{14}\text{N}_2)\text{CuBr}(\mu\text{-OMe})\}_2(\text{MeOH})]$ and $[\{(\text{C}_{10}\text{H}_{20}\text{N}_2)\text{CuBr}(\mu\text{-OMe})\}_2]$, *J. Chem. Soc. Dalton Trans.*, **3**, 381-386.
- [131] **Heuts, J.P.A., Mallesch, R., and Davis, T.P.**, 1999. Atom Transfer Radical Polymerization in the Presence of a Thiol: More Evidence Supporting Radical Intermediates, *Makromol. Chem. Phys.*, **200(6)**, 1380-1385.
- [132] **Percec, V., Kim, J.H., and Barboiu, B.**, 1997. Scope and Limitations of Functional Sulfonyl Chlorides as Initiators for Metal-Catalyzed "Living" Radical Polymerization of Styrene and Methacrylates, *Macromolecules*, **30(26)**, 8526-8528.
- [133] **Percec, V., Barboiu, B., Bera, T.K., Van Der Sluis, M., Grubbs, R.B., and Frechet, J.M.J.**, 2000. Designing Functional Aromatic Multisulfonyl Chloride Initiators for Complex Organic Synthesis by Living Radical Polymerization, *J. Polym. Sci. Part A: Polym. Chem.*, **38(S1)**, 4776-4791.
- [134] **Matyjaszewski, K., Coca, S., Gaynor, S.G., Wei, M., and Woodworth, B.E.**, 1998. Controlled Radical Polymerization in the Presence of Oxygen, *Macromolecules*, **31(17)**, 5967-5969.
- [135] **Gnanou, Y., and Hizal, G.**, 2004. Effect of Phenol and Derivatives on Atom Transfer Radical Polymerization in the Presence of Air, *J. Polym. Sci. Part A: Polym. Chem.*, **42(2)**, 351-359,
- [136] **Kricheldorf, H.R.**, 1992. Handbook of Polymer Synthesis; Ed. Marcel Dekker, New York.
- [137] **Hay, A.S., Blanchard, H.S., Endres, G.F., and Eustance, J.W.**, 1959. Polymerization by Oxidative Coupling, *J. Am. Chem. Soc.*, **81(23)**, 6335-6336.
- [138] **Acar, A.E., Yagci, M.B., and Mathias, L.J.**, 2000. Adventitious Effect of Air in Atom Transfer Radical Polymerization: Air-Induced (Reverse) Atom Transfer Radical Polymerization of Methacrylates in the Absence of an Added Initiator, *Macromolecules*, **33(21)**, 7700-7706.

- [139] **Nanda, A.K., Hong, S.C., and Matyjaszewski, K.,** 2003. Concurrent Initiation by Air in the Atom Transfer Radical Polymerization of Methyl Methacrylate, *Macromol. Chem. Phys.*, **204(9)**, 1151-1159.
- [140] **Min, K., Gao, H., and Matyjaszewski, K.,** 2005. Preparation of Homopolymers and Block Copolymers in Miniemulsion by ATRP Using Activators Generated by Electron Transfer (AGET), *J. Am. Chem. Soc.*, **127(11)**, 3825-3830.
- [141] **Jakubowski, W. and Matyjaszewski, K.,** 2005. Activator Generated by Electron Transfer for Atom Transfer Radical Polymerization, *Macromolecules*, **38(10)**, 4139-4146
- [142] **Hızal, G., Tunca, U., Aras, S., and Mert H.,** 2006. Air-Stable and Recoverable Catalyst for Copper-Catalyzed Controlled/Living Radical Polymerization of Styrene; In Situ Generation of Cu(I) Species via Electron Transfer Reaction, *Journal of Polymer Science: Part A: Polymer Chemistry*, **44(1)**, 77-87.
- [143] **Mert, H., Tunca, U., and Hızal, G.,** 2006. Thiophenol Derivatives as a Reducing Agent for In Situ Generation of Cu(I) Species via Electron Transfer Reaction in Copper-Catalyzed Living/Controlled Radical Polymerization of Styrene, *Journal of Polymer Science: Part A: Polymer Chemistry*, **44(20)**, 5923-5932.
- [144] **Jakubowski, W., Min, K., Matyjaszewski, K.,** 2006. Activators Regenerated by Electron Transfer for Atom Transfer Radical Polymerization of Styrene, *Macromolecules*, **39(1)**, 39-45
- [145] **Jakubowski, W., Matyjaszewski, K.,** 2006. Activators Regenerated by Electron Transfer for Atom-Transfer Radical Polymerization of (Meth)acrylates and Related Block Copolymers, *Angew. Chem. Int. Ed.*, **45(27)**, 4482 –4486.
- [146] **Tang, H., Radosz, M., Shen, Y.,** 2006. CuBr₂/N,N,N',N'-Tetra[(2-pyridyl)methyl]ethylenediamine/Tertiary Amine as a Highly Active and Versatile Catalyst for Atom-Transfer Radical Polymerization via Activator Generated by Electron Transfer, *Macromol. Rapid Commun.*, **27(14)**, 1127–1131
- [147] **Matyjaszewski, K., Bombalski, L., Jakubowski, W., Min, K., Spanswick, J., Tsarevsky, N.,** 2004. Atom Transfer Radical Polymerization in the Presence of a Reducing Agent, *United States Patent*, No: WO 2005087819 dated 03. 2004.
- [148] **Matyjaszewski, K., Shipp, D.A., Wang, J.-L., Grimaud, T., Patten, T.E.,** 1998. Utilizing Halide Exchange To Improve Control of Atom Transfer Radical Polymerization, *Macromolecules*, **31(20)**, 6836-6840,

- [149] **Shipp, D.A.; Wang, J.-L.; Matyjaszewski, K.** 1998. Synthesis of Acrylate and Methacrylate Block Copolymers Using Atom Transfer Radical Polymerization, *Macromolecules*, **31(23)**, 8005-8008.
- [150] **Matyjaszewski, K., Shipp, D.A., McMurtry, G.P., Gaynor, S.G., Pakula, T.**, 2000. Simple and Effective One-Pot Synthesis of (Meth)Acrylic Block Copolymers Through Atom Transfer Radical Polymerization, *J. Polym. Sci., Part A: Polym. Chem.*, **38(11)**, 2023-2031.
- [151] **Hong, S.C., Pakula, T., Matyjaszewski, K.**, 2001. Preparation of Polyisobutene-graft-Poly(methyl methacrylate) and Polyisobutene-graft-Polystyrene with Different Compositions and Side Chain Architectures Through Atom Transfer Radical Polymerization (ATRP), *Macromolecular Chemistry and Physics*, **202(17)**, 3392-3402.
- [152] **Matyjaszewski, K., Gaynor, S.G., Paik, H.-J., Pintauer, T., Pyun, J., Qiu, J., Teodorescu, M., Xia, J., Zhang, X.**, 2000. Application of Atom Transfer Radical Polymerization to Water-Borne Polymerization Systems, United States Patent, No: WO6121371.
- [153] **Jousset, S., Qiu, J., Matyjaszewski, K., Granel, C.**, 2001. Atom Transfer Radical Polymerization of Methyl Methacrylate in Water-Borne System, *Macromolecules*, **34(19)**, 6641-6648.
- [154] **Tsarevsky, N.V., Sarbu, T., Goebelt, B., Matyjaszewski, K.**, 2002. Synthesis of Styrene-Acrylonitrile Copolymers and Related Block Copolymers by Atom Transfer Radical Polymerization, *Macromolecules*, **35(16)**, 6142-6148.
- [155] **Ramakrishnan, A., Dhamodharan, R.**, 2003. Facile Synthesis of ABC and CBABC Multiblock Copolymers of Styrene, *tert*-Butyl Acrylate, and Methyl Methacrylate via Room Temperature ATRP of MMA, *Macromolecules*, **36(4)**, 1039-1046.
- [156] **Kotani, Y., Kato, M., Kamigaito, M., Sawamoto, M.**, 1996. Living Radical Polymerization of Alkyl Methacrylates with Ruthenium Complex and Synthesis of Their Block Copolymers¹, *Macromolecules*, **29(22)** 6979-6982
- [157] **Jo, S.M., Gaynor, S. G., Matyjaszewski, K.**, 1996. Homo and ABA block polymerizations of acrylonitrile, *n*-butyl acrylate, and 2-ethylhexyl acrylate using ATRP, *Polym. Prepr. (Am. Chem. Soc., Div. Polym. Chem.)*, **37(2)**, 272.
- [158] **Coca, S., Matyjaszewski, K.**, 1997. Block Copolymers by Transformation of "Living" Carbocationic into "Living" Radical Polymerization, *Macromolecules*, **30(9)**, 2808-2810.
- [159] **Coca, S., Matyjaszewski, K.**, 1997. Block Copolymers by Transformation of "Living" Carbocationic into "Living" Radical Polymerization. II. ABA-type Block Copolymers Comprising Rubbery Polyisobutene

Middle Segment, *J. Polym. Sci., Polym. Chem. Ed.*, **35(16)**, 3595-3601.

- [160] **Gaynor, S.G., Matyjaszewski, K.**, 1997. Step-Growth Polymers as Macroinitiators for "Living" Radical Polymerization: Synthesis of ABA Block Copolymers, *Macromolecules*, **30(14)**, 4241-4243.
- [161] **Leduc, M.R., Hawker, C.J., Dao, J., Frechet, J.M.J.**, 1996. Dendritic Initiators for "Living" Radical Polymerizations: A Versatile Approach to the Synthesis of Dendritic-Linear Block Copolymers, *J. Am. Chem. Soc.*, **118(45)**, 11111-11118.
- [162] **Matyjaszewski, K., Shigemoto, T., Frechet, J.M.J., Leduc, M.**, 1996. Controlled/"Living" Radical Polymerization with Dendrimers Containing Stable Radicals, *Macromolecules*, **29(12)**, 4167-4171.
- [163] **Coca, S., Paik, H. J., Matyjaszewski, K.**, 1997. Block Copolymers by Transformation of Living Ring-Opening Metathesis Polymerization into Controlled/"Living" Atom Transfer Radical Polymerization, *Macromolecules*, **30(21)**, 6513-6516.
- [164] **Eschwey, H., Hallensleben, M.L., and Burchard, W.**, 1973. Preparation and Some Properties of Star-Shaped Polymers with more than Hundred Side Chains, *Makromol. Chem.*, **173 (1)**, 235-239.
- [165] **Cloutet, E., Fillaut, J., Gnanou, Y., and Astruc, D.**, 1994. Hexaarm Star-Shaped Polystyrenes by Core-First Method, *J. Chem. Soc., Chem Commun.*, **21**, 2433-2434.
- [166] **Shohi, H., Sawamoto, M., and Higashimura, T.**, 1991. Tri-Armed Star Polymers by Living Cationic Polymerization. 1. Trifunctional Initiators for Living Polymerization of isobutyl vinyl ether, *Macromolecules*, **24(17)**, 4926-4931.
- [167] **Angot, S., Taton, D., and Gnanou, Y.**, 2000. Amphiphilic Stars and Dendrimer-Like Architectures Based on Poly(ethylene oxide) and Polystyrene, *Macromolecules*, **33(15)**, 5418-5426.
- [168] **Roovers, J., Zhou, L.L., Toporowski, P.M., Zwan, M., Iatrou, H., and Hadjichristidis N.**, 1993. Regular Star Polymers with 64 and 128 Arms. Models For Polymeric Micelles, *Macromolecules*, **26(16)**, 4324-4331.
- [169] **Sunder, A., Krämer, M., Hanselmann, R., Mülhaupt, R., and Frey, H.**, 1999. Molecular Nanocapsules Based on Amphiphilic Hyperbranched Polyglycerols, *Angew. Chem. Int. Ed.*, **38(23)**, 3552-3555.
- [170] **Claesson, H., Malstrom, E., Johansson, M., and Hult, A.**, 2002. Synthesis and Characterisation of Star Branched Polyesters with Dendritic Cores and The Effect of Structural Variations on Zero Shear Rate Viscosity, *Polymer* **43(12)**, 3511-3518.

- [171] **Gauthier, M., Tichagwa, L., Downey, J., and Gao, S.,** 1996. Arborescent Graft Copolymers: Highly Branched Macromolecules with a Core-Shell Morphology, *Macromolecules*, **29(2)**, 519-527.
- [172] **Kanaoka, S., Omura, T., Sawamoto, M., and Higashimura, T.,** 1992. Star-Shaped Polymers by Living Cationic Polymerization. 3. Synthesis of Heteroarm Amphiphilic Star-Shaped Polymers of Vinyl Ethers with Hydroxyl or Carboxyl Pendant Groups, *Macromolecules*, **25(24)**, 6407-6413.
- [173] **Okay, O., and Funke, W.,** 1990. Anionic Dispersion Polymerization of 1,4-divinylbenzene, *Macromolecules*, **23(10)**, 2623-2628.
- [174] **Wang, J.-S., Greszta, D., and Matyjaszewski, K.,** 1995. Atom Transfer Radical Polymerization (ATRP): A New Approach Towards Well-Defined (Co)Polymers, *Polym. Mater. Sci. Eng.*, **73**, 416.
- [175] **Gaynor, S. G., Edelman, S., and Matyjaszewski, K.,** 1996. Synthesis of Branched and Hyperbranched Polystyrenes, *Macromolecules*, **29(3)**, 1079-1081.
- [176] **Matyjaszewski, K., Miller, P.J., Pyun, J., Kickelbick, G., and Diamanti, S.,** 1999. Synthesis and Characterization of Star Polymers with Varying Arm Number, Length, and Composition from Organic and Hybrid Inorganic/Organic Multifunctional Initiators, *Macromolecules*, **32(20)**, 6526-6535.
- [177] **Matyjaszewski, K.,** 2003. The Synthesis of Functional Star Copolymers as an Illustration of the Importance of Controlling Polymer Structures in the Design of New Materials, *Polym. Intl.*, **52(10)**, 1559-1565.
- [178] **Angot, S., Murthy, K.S., Taton, D., and Gnanou, Y.,** 1998. Atom Transfer Radical Polymerization of Styrene Using A Novel Octafunctional Initiator: Synthesis of Well-Defined Polystyrene Stars, *Macromolecules*, **31(21)**, 7218-7225.
- [179] **Ueda, J., Kamigaito, M., and Sawamoto, M.,** 1998. Calixarene-Core Multifunctional Initiators for the Ruthenium-Mediated Living Radical Polymerization of Methacrylates, *Macromolecules*, **31(20)**, 6762-6768.
- [180] **Matyjaszewski, K., Gaynor, S.G., Kulfan, A., and Podwika, M.,** 1997. Preparation of Hyperbranched Polyacrylates by Atom Transfer Radical Polymerization. 1. Acrylic AB* Monomers in "Living" Radical Polymerizations, *Macromolecules*, **30(17)**, 5192-5194.
- [181] **Frechet, J.M.J., Henmi, M., Gitsov, I., Aoshima, S., Leduc, M., and Grubbs, R.B.,** 1995. Self-Condensing Vinyl Polymerization: An Approach to Dendritic Materials, *Science*, **269**, 1080-1083.
- [182] **Matyjaszewski K., and Gaynor S.G.,** 1997. Preparation of Hyperbranched Polyacrylates by Atom Transfer Radical Polymerization. 3. Effect of

Reaction Conditions on the Self-Condensing Vinyl Polymerization of 2-((2-Bromopropionyl)oxy)ethyl Acrylate, *Macromolecules*, **30(23)**, 7042-7049.

- [183] **Matyjaszewski K., Gaynor S.G., and Mueller, A.H.E.**, 1997. Preparation of Hyperbranched Polyacrylates by Atom Transfer Radical Polymerization. 2. Kinetics and Mechanism of Chain Growth for the Self-Condensing Vinyl Polymerization of 2-((2-Bromopropionyl)oxy)ethyl Acrylate, *Macromolecules*, **30(23)**, 7034-7041.
- [184] **Rein, D, Rempp, P., Lutz, P.J.**, 1993. Recent Developments in the Field of Star-Shaped Polymers, *Makromolekulare Chemie, Macromolecular Symposia*, **67**, 237-49.
- [185] **Xia, J., Zhang, X., and Matyjaszewski, K.**, 1999. Synthesis of Star-Shaped Polystyrene by Atom Transfer Radical Polymerization Using an "Arm First" Approach, *Macromolecules*, **32(13)**, 4482-4484.
- [186] **Zhang, X., Xia, J., and Matyjaszewski, K.**, 2000. End-Functional Poly(*tert*-butyl acrylate) Star Polymers by Controlled Radical Polymerization, *Macromolecules*, **33(7)**, 2340-2345.
- [187] **Baek, K.-Y., Kamigaito, M., and Sawamoto, M.**, 2002. Core-Functionalized Star Polymers by Transition Metal-Catalyzed Living Radical Polymerization. 2. Selective Interaction with Protic Guests via Core Functionalities, *Macromolecules*, **35(5)**, 1493-1498.
- [188] **Georgiades, S.N., Vamvakaki, M., and Patrickios, C.S.**, 2002. Synthesis and Characterization of Double-Hydrophilic Model Networks Based on Cross-linked Star Polymers of Poly(ethylene glycol) Methacrylate and Methacrylic Acid, *Macromolecules*, **35(13)**, 4903-4911.
- [189] **Du, J.Z., and Chen, Y.M.**, 2004. Star Polymer, PCL-PS Heteroarm Star Polymer by ATRP, and Core-Carboxylated PS Star Polymer Thereof, *Macromolecules*, **37(1)**, 3588-3594.
- [190] **Hadjichristidis, N.**, 1999. Synthesis of Miktoarm Star (μ -star) Polymers, *J. Polym. Sci. Pol. Chem.*, **37(7)**, 857-871.
- [191] **Gao, H., Tsarevsky, N.V., and Matyjaszewski, K.**, 2005. Synthesis of Degradable Miktoarm Star Copolymers via ATRP, *Macromolecules*, **38(14)**, 5995-6004.
- [192] **Hawker, C.J.**, 1995. Architectural Control in "Living" Free Radical Polymerizations: Preparation of Star and Graft Polymers, *Angew. Chem., Int. Ed. Engl.*, **34(13-14)**, 1456-1459.
- [193] **Hay, A.S.**, 1962. Polymerization by Oxidative Coupling, *Polymer Engineering & Science*, **2(2)**, 108-109,

- [194] **Hay, A.S.**, 1998. Polymerization by Oxidative Coupling: Discovery and Commercialization of PPO® and Noryl® Resins, *J. Polym. Sci., Part A: Polym. Chem.*, **36(4)**, 505-517.
- [195] **Dordick, J.S., Marletta, M.A., and Klibanov, A.M.**, 1987. Polymerization of Phenols Catalyzed by Peroxidase in Nonaqueous Media, *Biotechnol. Bioeng.*, **30(1)**, 31-36.
- [196] **Akkara, J.A., Senecal, K.J., Kaplan, D.K.**, 1991. Synthesis and Characterization of Polymers Produced by Horseradish Peroxidase in Dioxane, *J. Polym. Sci., Polym. Chem. Ed.*, **29(11)**, 1561-1574.
- [197] **Uyama, H., Kurioka, H., Kaneko, I., and Kobayashi, S.**, 1994. Synthesis of a New Family of Phenol Resin by Enzymatic Oxidative Polymerization, *Chem. Lett.*, **23(3)**, 423-426.
- [198] **Ikeda, R., Sugihara, J., Uyama, H., and Kobayashi, S.**, 1996. Enzymatic Oxidative Polymerization of 2,6-Dimethylphenol, *Macromolecules*, **29(27)**, 8702-8705.
- [199] **Aycock, D., Abolins, V., and White, D.M.**, 1986. Encyclopedia of Polymer Science and Engineering (13), 2nd ed. pp 1-30, John Wiley & Sons: New York.
- [200] **Mijs, W.J., van Lohuizen, O.E., Bussink, J., Vollbracht, L.**, 1967. The Catalytic Oxidation of 4-Aryloxyphenols, *Tetrahedron*, **23(5)**, 2253-2264.
- [201] **Higashimura, H., Fujisawa, K., Moro-oka, Y., Kubota, M., Shiga, A., Terahara, A., Uyama, H., and Kobayashi, S.**, 1998. Highly Regioselective Oxidative Polymerization of 4-Phenoxyphenol to Poly(1,4-phenylene oxide) Catalyzed by Tyrosinase Model Complexes, *J. Am. Chem. Soc.*, **120(33)**, 8529-8530.
- [202] **Higashimura, H., Kubota, M., Siga, A., Fujisawa, K., Morooka, Y., Uyama, H., and Kobayashi, S.**, 2000. Radical-Controlled" Oxidative Polymerization of 4-Phenoxyphenol by a Tyrosinase Model Complex Catalyst to Poly(1,4-phenylene oxide), *Macromolecules*, **33(6)**, 1986-1995.
- [203] **Halfen, J.A., Mahapatra, S., Wilkinson, E.C., Kaderli, S., Young Jr., V.G., Que Jr., L., Zuberbuhler, A.D., and Tolman, W.B.**, 1996. Reversible Cleavage and Formation of the Dioxygen O-O Bond Within a Dicopper Complex, *Science*, **271**, 1397-1400.
- [204] **Berces, A.**, 1997. Ligand Effects in the Models and Mimics of Oxyhemocyanin and Oxytyrosinase. A Density Functional Study of Reversible Dioxygen Binding and Reversible O-O Bond Cleavage, *Inorg. Chem.*, **36(21)**, 4831-4837.

- [205] **Hay, A.S.** 1977. Process for the Preparation of Polyphenylene Oxides with Hydrolytically Stable Copper Catalysts, *United States Patent*, No: 4028341 dated 07.6.1977
- [206] **Bennett, J.G., Cooper G.D.,** 1978. Method for Preparing Polyphenylene Ethers, *United States Patent*, No: 4092294 dated 30.5.1978
- [207] **Tsuchida, E., Nishide, H., and Nishiyama, T.,** 1972. The Kinetics of the Oxidative Polymerization of 2,6-xyleneol with a Copper–Amine Complex, *Makromol. Chem.*, **151**, 221-234.
- [208] **Tsuchida E.** New Frontiers in Organometallic and Inorganic Chemistry, 2nd Meeting, Science Press, Beijing, 1982, p.207 (Chem Abstr 1985, **102**, 185 554z)
- [209] **Nishide, H., Suzuki, Y., and Tsuchida, E.,** 1981. Oxidative Polymerization of 2,6-dimethylphenol Catalysed by Insoluble Polymer Copper Complexes, *Eur. Polym. J.*, **17 (5)**, 573-577.
- [210] **Yoshimura, T., Storck, W., and Manecke, G.,** 1977. New Catalysts for the Oxidative Polymerisation of 2,6-dimethylphenol, 2 Copper Complexes Containing the Dicyanoethenedithiolatocuprate Structure as the Ligand, *Makromol. Chem.*, **178**, 75-96.
- [211] **Paul, I.C.,** 1974. The Chemistry of the Thiol Group, Vol. 1, pp 111-149, Patai, S., Ed.; Wiley: London.
- [212] **Oae, S.,** 1991. Organic Sulfur Chemistry: Structure and Mechanism; CRC Press: Boca Raton.
- [213] **Shaw, R.,** 1974. The Chemistry of the Thiol Group, Vol. 1, pp 151-161, Patai, S., Ed.; Wiley: London.
- [214] **March, J.,** 1992. Advanced Organic Chemistry: Reactions, Mechanisms, and Structure; 4th ed.; Wiley: New York.
- [215] **Pearson, R.G.,** 1963. Hard and Soft Acids and Bases, *J. Am. Chem. Soc.*, **85(22)**, 3533-3539.
- [216] **Benson, S.W.,** 1978. Thermochemistry and Kinetics of Sulfur-Containing Molecules and Radicals, *Chem. Rev.*, **78(1)**, 23-43.
- [217] **Sonntag, C.V., and Schuchmann, H.P.,** 1980. The Chemistry of Ethers, Crown Ethers, Hydroxyl Groups and Their Sulfur Analogues, in The Chemistry of the Thiol Group, Vol. 2, pp 923-934, Patai, S., Ed.; Wiley: Chichester.
- [218] **Tsarevsky, N.V.,** 2005. Synthesis of Well-Defined Polymeric Materials with Polar Functional Groups by Atom Transfer Radical Polymerization, *PhD Thesis*, Carnegie Mellon University, Pittsburgh, PA.

- [219] **Bookwalter, C.W., Zoller, D.L., Ross, P.L., and Johnston, M.V.**, 1995. Bond-Selective Photodissociation of Aliphatic Disulfides, *J. Am. Soc. Mass Spectrom.*, **6(9)**, 872-876.
- [220] **Thyagarajan, B.S.**, 1958. Oxidations By Ferricyanide, *Chem. Rev.*, **58(3)**, 439-460,
- [221] **Wallace, T.J.**, 1966. Reactions of Thiols with Metals. II. Low-Temperature Oxidation by Soluble Metal Salts, *J. Org. Chem.*, **31(10)**, 3071-3074,
- [222] **Hill, J., and McAuley, A.**, 1968. Metal-Ion Oxidation in Solution. Part IV. The Oxidation of Thiomalic Acid by Cobalt(III) Ions, *J. Chem. Soc. A*, 2405-2408.
- [223] **Hill, J., and McAuley, A.**, 1968. Metal-Ion Oxidations in Solution. Part I. The Oxidation of Some α -Mercaptocarboxylic Acids by Cerium(IV), *J. Chem. Soc. A*, 156-159.
- [224] **Pickering, W.F., and Mcauley, A.**, 1968. Metal-Ion Oxidations in Solution. Part III. The Oxidation of 2-Mercaptosuccinic Acid by Vanadium(V), *J. Chem. Soc. A*, 1173-1176,.
- [225] **Lee, C.D.S., and Daly, W.H.**, 1974. Mercaptan-Containing Polymers, *Adv. Polym. Sci.*, **15**, 61-90.
- [226] **Duda, A., Penczek, S.**, 1989. Encyclopedia of Polymer Science and Engineering, Vol. 16, pp 246-368, Wiley: New York.
- [227] **Spassky, N.**, 1993. Polymers Containing Sulfur in the Main Chain Synthesis, Properties, Applications, Phosphorus, *Sulfur, Silicon Relat. Elem.*, **74(1-4)**, 71-92.
- [228] **Jorczak, J.S., Fettes, E.M.**, 1951. Polysulfide Liquid Polymers, *Ind. Eng. Chem.*, **43(2)**, 324-328.
- [229] **Panek, J.R. Polyethers, Gaylord, N.G.**, 1962. Polyalkylene Sulfides and Other Thioethers, Vol. III., pp 115-224, Ed. Wiley: New York, London.
- [230] **Wheaton, R.M.; Hatch, M.J.**, 1969. Ion Exchange, Vol. 2, pp 191-234, ed. Marinsky, J. A., Marcel Dekker: New York.
- [231] **Cassidy, H.G.**, 1949. Electron Exchange-Polymers., *J. Am. Chem. Soc.*, **71(2)**, 402-406.
- [232] **Gregor, H.P., Dolar, D., and Hoeschele, G.K.**, 1955. Polythiolstyrene- A New Oxidation-Reduction Ion Exchange Resin, *J. Am. Chem. Soc.*, **77(13)**, 3675.
- [233] **Rikukawa, M., and Sanui, K.**, 2000. Proton-Conducting Polymer Electrolyte Membranes Based on Hydrocarbon Polymers, *Prog. Polym. Sci.*, **25(10)**, 1463-1502.

- [234] **Andersson, M.R., Thomas, O., Mammo, W., Svensson, M., Theander, M., and Inganas, O.**, 1999. Substituted Polythiophenes Designed for Optoelectronic Devices and Conductors, *J. Mater. Chem.*, **9**, 1933-1940.
- [235] **Fichou, D.**, 1999. Handbook of Oligo- and Polythiophenes, Ed. Wiley-VCH: Weinheim.
- [236] **Berenbaum, M.B. Polyethers; Gaylord, N.G.**, 1962. Polyalkylene sulfides and other thioethers, Vol. III. pp 43-114, Ed.; Wiley: New York, London.
- [237] **Marvel, C.S., and Olson, L.E.**, 1957. Polyalkylene Disulfides, *J. Am. Chem. Soc.*, **79(12)**, 3089-3091.
- [238] **Brandrup, J., Immergut, E.H., Grulke, E.A.**, 1999. Eds. Polymer Handbook; 4th ed.; Wiley: New York.
- [239] **Coessens, V., Pintauer, T., and Matyjaszewski, K.**, 2001. Functional Polymers by Atom Transfer Radical Polymerization, *Prog. Polym. Sci.*, **26(3)**, 337-377.
- [240] **Wardell, J.L.**, 1974. in The Chemistry of the Thiol Group, Patai, S., Vol. 1, pp 163-269 Ed.; Wiley: London.
- [241] **Cossar, B.C., Fournier, J.O., Fields, D.L., and Reynolds, D.D.**, 1962. Preparation of Thiols, *J. Org. Chem.*, **27(1)**, 93-95.
- [242] **Garamszegi, L., Donzel, C., Carrot, G., Nguyen, T.Q., and Hilborn, J.**, 2003. Synthesis of Thiol End-Functional Polystyrene via Atom Transfer Radical Polymerization, *React., Funct. Polym.*, **55(2)**, 179-183.
- [243] **Yamashita, K., Kimura, Y., Saba, H., and Tsuda, K.**, 1991. Esterolysis of Active Esters by Soluble Thiol Polymer, *J. Polym. Sci.: Part A: Polym. Chem.*, **29(5)**, 777-779.
- [244] **Carrot, G., Hilborn, J., Hedrick, J.L., and Trollsas, M.**, 1999. Novel Initiators for Atom Transfer Radical and Ring-Opening Polymerization: A New General Method for the Preparation of Thiol-Functional Polymers, *Macromolecules*, **32(15)**, 5171-5173.
- [245] **Shah, R.R., Merreces, D., Husseman, M., Rees, I., Abbot, N.L., Hawker, C.J., and Hedrick, J.L.**, 2000. Using Atom Transfer Radical Polymerization To Amplify Monolayers of Initiators Patterned by Microcontact Printing into Polymer Brushes for Pattern Transfer, *Macromolecules*, **33(2)**, 597-605.
- [246] **Huang, W., Kim, J.B., Bruening, M.L., and Baker, G.L.**, 2002. Functionalization of Surfaces by Water-Accelerated Atom-Transfer Radical Polymerization of Hydroxyethyl Methacrylate and Subsequent Derivatization, *Macromolecules*, **35(4)**, 1175-1179.

- [247] **Tsarevsky, N.V., and Matyjaszewski, K.,** 2002. Reversible Redox Cleavage/Coupling of Polystyrene with Disulfide or Thiol Groups Prepared by Atom Transfer Radical Polymerization, *Macromolecules*, **35(24)**, 9009-9014.
- [248] **Tsarevsky, N.V., and Matyjaszewski, K.,** 2005. Combining Atom Transfer Radical Polymerization and Disulfide/Thiol Redox Chemistry: A Route to Well-Defined (Bio)degradable Polymeric Materials, *Macromolecules*, **38(8)**, 3087-3092.
- [249] **Li, C., Madsen, J., Armes, S.P., and Lewis, A.L.,** 2006. A New Class of Biochemically Degradable, Stimulus-Responsive Triblock Copolymer Gelators, *Angew. Chem. Int. Ed.*, **45(21)**, 3510 –3513
- [250] **Mert, H.,** 2001. The Effect of Thiophenol Derivatives on Atom Transfer Radical Polymerization of Styrene, *Master Thesis*, İ.T.Ü. Institute of Science and Technology, İstanbul.
- [251] **Nakagawa, Y., and Matyjaszewski, K.,** 1998. Synthesis of Well-Defined Allyl End-Functionalized Polystyrene by Atom Transfer Radical Polymerization with an Allyl Halide Initiator, *Polym. J.*, **30(2)**, 138-141.
- [252] **Zeng, F., Shen, Y., Zhu, S., and Pelton, R.,** 2000. Synthesis and Characterization of Comb-Branched Polyelectrolytes. 1. Preparation of Cationic Macromonomer of 2-(Dimethylamino)ethyl Methacrylate by Atom Transfer Radical Polymerization, *Macromolecules*, **33(5)**, 1628-1635.
- [253] **Matyjaszewski, K., Beers, K.L., Kern, A., and Gaynor, S.G.,** 1998. Hydrogels by Atom Transfer Radical Polymerization. I. Poly(N-vinylpyrrolidinone-g-styrene) via the Macromonomer Method, *J. Polym. Sci., Polym. Chem.*, **36(5)**, 823-830.
- [254] **Haddleton, D.M., Waterson, C., Derrick, P.J., Jasieczek, C.B., and Shooter, A.J.,** 1997. Monohydroxy Terminally Functionalised Poly(methyl methacrylate) from Atom Transfer Radical Polymerisation, *Chem. Commun.*, **7**, 683-684.
- [255] **Coessens, V., and Matyjaszewski, K.,** 1999. Synthesis of Polymers with Hydroxyl End Groups by Atom Transfer Radical Polymerization, *Macromol. Rapid Commun.*, **20(3)**, 127-134.
- [256] **Malz, H., Komber, H., Voigt, D., Hopfe, I., and Pionteck, J.,** 1999. Synthesis of Functional Polymers by Atom Transfer Radical Polymerization, *Macromol. Chem. Phys.*, **200(3)**, 642-651.
- [257] **Matyjaszewski, K., Pintauer, T., and Gaynor, S.,** 2000. Removal of Copper-Based Catalyst in Atom Transfer Radical Polymerization Using Ion Exchange Resins, *Macromolecules*, **33(4)**, 1476-1478

- [258] **Fields, G.B., Lauer-Fields, J.L., Liu, R.-q., Barany, G.**, 2002. Principles and Practice of Solid-Phase Peptide Synthesis, in *Synthetic Peptides*, pp 93–219.
- [259] **Merrifield, R.B.**, 1966. Solid Phase Peptide Synthesis. I. The Synthesis of a Tetrapeptide, *J. Am. Chem. Soc.*, **85(14)**, 2149-2154.
- [260] **Wang, S.-S.**, 1973. *p*-Alkoxybenzyl Alcohol Resin and *p*-alkoxybenzyloxycarbonylhydrazide Resin for Solid Phase Synthesis of Protected Peptide Fragments, *J. Am. Chem. Soc.*, **95(4)**, 1328-1333.
- [261] **Angot, S., Ayres, N., Bon, S.A.F., and Haddleton, D.M.**, 2001. Living Radical Polymerization Immobilized on Wang Resins: Synthesis and Harvest of Narrow Polydispersity Poly(methacrylate)s, *Macromolecules*, **34(4)**, 768-774.
- [262] **Von Werne, T., and Patten, T.E.**, 1999. Preparation of Structurally Well-Defined Polymer-Nanoparticle Hybrids with Controlled/Living Radical Polymerizations, *J. Am. Chem. Soc.*, **121(32)**, 7409-7410.
- [263] **Matyjaszewski, K., Miller, P.J., Shukla, N., Immaraporn, B., Gelman, A., Luokala, B.B., Siclovan, T.M., Kickelbick, G., Vallant, T., Hoffmann, H., and Pakula, T.**, 1999. Polymers at Interfaces: Using Atom Transfer Radical Polymerization in the Controlled Growth of Homopolymers and Block Copolymers from Silicon Surfaces in the Absence of Untethered Sacrificial Initiator, *Macromolecules*, **32(26)**, 8716-8724.
- [264] **Pyun, J., Jia, S., Kowalewski, T., Patterson, G.D., and Matyjaszewski, K.**, 2003. Synthesis and Characterization of Organic/ Inorganic Hybrid Nanoparticles: Kinetics of Surface-Initiated Atom Transfer Radical Polymerization and Morphology of Hybrid Nanoparticle Ultrathin Films, *Macromolecules*, **36(14)**, 5094–5104.
- [265] **Haddleton, D.M., Duncalf, D.J., Kukulj, D., and Radigue, A.P.**, 1999. 3-Aminopropyl Silica Supported Living Radical Polymerization of Methyl Methacrylate: Dichlorotris(triphenylphosphine)ruthenium(II) Mediated Atom Transfer Polymerization, *Macromolecules*, **32(15)**, 4769-4775.
- [266] **Shen, Y.**, 2001. Atom Transfer Radical Polymerization and Its Continuous Process, PhD Thesis, McMaster University, Canada.
- [267] **Shen, Y., Zhu, S., Zeng, F. and Pelton, R.H.**, 2000. Atom Transfer Radical Polymerization of Methyl Methacrylate by Silica Gel Supported Copper Bromide/Multidentate Amine, *Macromolecules*, **33(15)**, 5427-5431
- [268] **Shen, Y., Zhu, S., Zeng, F., and Pelton, R.**, 2000. Synthesis of Methacrylate Macromonomers Using Silica Gel Supported Atom Transfer Radical Polymerization, *Macromol. Chem. Phys.*, **201(13)**, 1387–94.

- [269] **Shen, Y., Zhu, S., and Pelton, R.,** 2000. Packed Column Reactor for Continuous Atom Transfer Radical Polymerization: Methyl Methacrylate Polymerization Using Silica Gel Supported Catalyst, *Macromol. Rapid Commun.*, **21(14)**, 956–959.
- [270] **Shen, Y., Zhu, S., and Pelton, R.,** 2002. Packed Column Reactor for the Continuous Atom Transfer Radical Polymerization of Methyl Methacrylate and Its Block Copolymerization, *AIChE J.*, **48(11)**, 2609–2619.
- [271] **Kickelbick, G., Paik, H., and Matyjaszewski, K.,** 1999. Immobilization of the Copper Catalyst in Atom Transfer Radical Polymerization, *Macromolecules*, **1999**, **32(9)**, 2941–2947.
- [272] **Shen, Y., Zhu, S., Zeng, F., and Pelton, R.,** 2001. Supported Atom Transfer Radical Polymerization of Methyl Methacrylate Mediated by CuBr–Tetraethyldiethylenetriamine Grafted onto Silica Gel, *Journal of Polymer Science: Part A: Polymer Chemistry*, **39(7)**, 1051–1059.
- [273] **Honigfort, M.E., and Brittain, W. J.,** 2003. Use of JandaJel Resins for Copper Removal in Atom Transfer Radical Polymerization, *Macromolecules*, **36(9)**, 3111–3114
- [274] **Liou, S., Rademacher, J.T., Malaba, D., Pallack, M.E., and Brittain, W.J.,** 2000. Atom Transfer Radical Polymerization of Methyl Methacrylate with Polyethylene-functionalized Ligands, *Macromolecules*, **33(12)**, 4295–4296.
- [275] **Shen, Y., Zhu, S., and Pelton, R.H.,** 2001. Effect of Ligand Spacer on Silica Gel Supported Atom Transfer Radical Polymerization of Methyl Methacrylate, *Macromolecules*, **34(17)**, 5812–5818.
- [276] **Ding, S., Yang, J., Radosz, M., and Shen, Y.,** 2004. Atom Transfer Radical Polymerization of Methyl Methacrylate via Reversibly Supported Catalysts on Silica Gel via Self-Assembly, *Journal of Polymer Science: Part A: Polymer Chemistry*, **42(1)**, 22–30.
- [277] **Shen, Z., Chen, Y., Frey, H., and Stiriba, S.-E.,** 2006. Complex of Hyperbranched Polyethylenimine with Cuprous Halide as Recoverable Homogeneous Catalyst for the Atom Transfer Radical Polymerization of Methyl Methacrylate, *Macromolecules*, **39(6)**, 2092–2099
- [278] **Shen, Y., and Zhu, S.,** 2001. Atom Transfer Radical Polymerization of Methyl Methacrylate Mediated by Copper Bromide–Tetraethyldiethylenetriamine Grafted on Soluble and Recoverable Poly(ethylene-*b*-ethylene glycol) Supports, *Macromolecules*, **34(25)**, 8603–8609
- [279] **Horvath, I.T., and Rabai, J.,** 1994. Facile Catalyst Separation Without Water: Fluorous Biphasic Hydroformylation of Olefins, *Science*, **266**, 72–75.

- [280] (a) **Pozzi, G., Cavazzini, M., Quici, S., and Fontana, S.**, 1997. Metal Complexes of a Tetraazacyclotetradecane Bearing Highly Fluorinated Tails: New Catalysts for the Oxidation of Hydrocarbons under Fluorous Biphasic Conditions, *Tetrahedron Lett.*, **38(43)**, 7605-7608.
 (b) **Klement, I., Lutjens, H., and Knochel, P.**, 1997. Transition Metal Catalyzed Oxidations in Perfluorinated Solvents, *Angew. Chem., Int. Ed. Engl.*, **36(13-14)**, 1454-1456.
- [281] **Betzemeier, B., Knochel, P.**, 1997. Palladium-Catalyzed Cross-Coupling of Organozinc Bromides with Aryl Iodides in Perfluorinated Solvents, *Angew. Chem., Int. Ed. Engl.*, **36(23)**, 2623-4.
- [282] **Betzemeier, B., Lhermitte, F., and Knochel, P.**, 1998. Wacker Oxidation of Alkenes Using a Fluorous Biphasic System. A mild Preparation of Polyfunctional Ketones, *Tetrahedron Lett.*, **39(37)**, 6667-70.
- [283] **Kleijn, H., Jastrzebski, J., Gossage, R. A., Kooijman, H., Spek, A.L., and vanKoten, G.**, 1998. Ortho-bis(amino)arylnickel(II) Halide Complexes Containing Perfluoroalkyl Chains as Model Catalyst Precursors for Use in Fluorous Biphasic Systems, *Tetrahedron*, **54(7)**, 1145-52.
- [284] **DeCampo, F., Lastecoueres, D., Vincent, J.M., and Verlhac, J.B.**, 1999. Copper(I) Complexes Mediated Cyclization Reaction of Unsaturated Ester under Fluoro Biphasic Procedure, *J. Org. Chem.*, **64(13)**, 4969-71.
- [285] **Haddleton, D.M., Jackson, S.G., and Bon, S.A.F.**, 2000. Copper(I)-Mediated Living Radical Polymerization under Fluorous Biphasic Conditions, *J. Am. Chem. Soc.*, **122(7)**, 1542-1543
- [286] **Bosanac, T., Yang, J., and Wilcox, C.S.**, 2001. Precipitons - Functional Protecting Groups to Facilitate Product Separation: Applications in Isoxazoline Synthesis, *Angew. Chem., Int. Ed.*, **40(10)**, 1875-1879.
- [287] **Bosanac, T., and Wilcox, C.S.**, 2001. A Novel Precipitating Auxiliary Approach to the Purification of Baylis–Hillman Adducts, *Chem. Commun.*, **17**, 1618-1619.
- [288] **Bosanac, T., and Wilcox, C.S.**, 2001. Precipiton Strategies Applied to the Isolation of α -Substituted β -Ketoesters, *Tetrahedron Lett.*, **42(26)**, 4309-4312.
- [289] **Honigfort, M.E., Brittain, W.J., Bosanac, T., and Wilcox, C.S.**, 2002. Use of Precipitation for Copper Removal in Atom Transfer Radical Polymerization, *Macromolecules*, **35(13)**, 4849–51.
- [290] **Bergbreiter, D.E., Chen, L., and Chandran, R.**, 1985. Recyclable Polymer-Bound Lanthanide Diene Polymerization Catalysts, *Macromolecules*, **18(6)**, 1055-1057.

- [291] **Shen, Y., Zhu, S., and Pelton, R.**, 2001. Soluble and Recoverable Support for Copper Bromide-Mediated Living Radical Polymerization, *Macromolecules*, **34**(10), 3182-3185
- [292] **Kumar, K.R., Kizhakkedathu, J.N., Brooks, D.E.**, 2004. Atom Transfer Radical Polymerization Using Multidentate Amine Ligands Supported on Soluble Hyperbranched Polyglycidol, *Macromol. Chem. Phys.*, **205**(5), 567-573.
- [293] **Boussif, O., Lezoualch, F., Zanta, M.A., Mergny, M.D., Scherman, D., Demeneix, B., and Behr, J.P.**, 1995. A Versatile Vector for Gene and Oligonucleotide Transfer into Cells in Culture and in vivo: Polyethylenimine, *Proc. Natl. Acad. Sci. U.S.A.*, **92**, 7297-7301.
- [294] **Godbey, W.T., Wu, K.K., and Mikos, A.G.**, 1999. Tracking the Intracellular Path of Poly(ethylenimine)/DNA Complexes for Gene Delivery, *Proc. Natl. Acad. Sci. U.S.A.*, **96**, 5177-5181.
- [295] **Godbey, W.T., Barry, M.A., Saggau, P., Wu, K.K., and Mikos, A.G.**, 2000. Poly(ethylenimine)-Mediated Transfection: A New Paradigm for Gene Delivery, *J. Biomed. Mater. Res.*, **51**(3), 321-328.
- [296] **Hong, S.C., Paik, H.J., and Matyjaszewski, K.**, 2001. An Immobilized/Soluble Hybrid Catalyst System for Atom Transfer Radical Polymerization, *Macromolecules*, **34**(15), 5099-5102
- [297] **Hong, S.C., Lutz, J.F., Inoue, Y., Strissel, C., Nuyken, O., and Matyjaszewski, K.**, 2003. Use of an Immobilized/Soluble Hybrid ATRP Catalyst System for the Preparation of Block Copolymers, Random Copolymers, and Polymers with High Degree of Chain End Functionality, *Macromolecules*, **36**(4), 1075-1082
- [298] **Ege S.**, 1999. In Organic Chemistry Structure and Reactivity 4th ed., p.959., Houghton Mifflin Company Boston.
- [299] **De Vries, A., Klumperman, B., De Wet-Roos, D., and Sanderson, R.D.**, 2001. The Effect of Reducing Monosaccharides on the Atom Transfer Radical Polymerization of Butyl Methacrylate, *Macromol. Chem. Phys.*, **202**(9), 1645-1648.
- [300] **Breeze, R.S., and Wang, S.**, 1996. Perturbation of the Electronic Structure of a Copper(II) ion by a Cu^ICl Moiety in a Class I Mixed Valence Copper Complex, Cu^{II}(Me₃dien)Cl₂(Cu^ICl), *Inorg. Chem.*, **35**(11), 3404-3408.
- [301] **Osako, T., Karlin, D.K., and Itoh, S.**, 2005. Carbon-Halogen Bond Activation Mechanism by Copper(I) Complexes of (2-Pyridyl)alkylamine Ligands, *Inorg. Chem.*, **44**(2), 410-415.
- [302] **Wei, M., Patten, T.E., Matyjaszewski, K.**, 1997. Model Studies of the Slow Termination Process in the Polymerization of Styrene by Atom

Transfer Radical Polymerization, *Polym. Prepr. (Am.Chem. Soc., Div. Polym. Chem.)*, **38(1)**, 683.

- [303] **Sawyer, D.T., Sobkowiak, A., Roberts, J.J.L.**, 1995. In *Electrochemistry for Chemists*, 2nd ed.; John Wiley & Sons: New York.
- [304] **Greszta, D., and Matyjaszewski, K.**, 1996. Mechanism of Controlled/"Living" Radical Polymerization of Styrene in the Presence of Nitroxyl Radicals. Kinetics and Simulations, *Macromolecules*, **29(24)**, 7661-7670.
- [305] **Veregin, R.P.N., Georges, M.K., Hamer, G.K., and Kazmaier, P.M.**, 1995. Mechanism of Living Free Radical Polymerizations with Narrow Polydispersity: Electron Spin Resonance and Kinetic Studies, *Macromolecules*, **28(13)**, 4391-4398.
- [306] **Cappozzi, G., Modena, G.**, 1974. In *The chemistry of Thiol Group (2)*, pp. 785- 839, Patai, S., Ed.; Wiley-Interscience, London.
- [307] **Tripathi, G.N.R., Sun, Q., Armstrong, D.A., Chipman, D.M., and Schuler, R.H.**, 1992. Resonance Raman-Spectra and Structure of Phenylthiyl Radical, *J. Phys. Chem.*, **96(13)**, 5344-5350.
- [308] **Anderson, C.H., and Holwerda, R.A.**, 1985. Mechanistic Flexibility in the Reduction of Copper(II) Complexes of Aliphatic Polyamines by Mercapto Amino-Acids, *J. Inorg. Biochem.*, **23(1)**, 29-41.
- [309] **Lappin, A.G., and McAuley, A.**, 1978. Reactions Between Copper(II) and 2-Mercaptosuccinic Acid in Aqueous Perchlorate Solution, *J. Chem. Soc. Dalton Trans.*, **12**, 1606-1609.
- [310] **Deutsch, E., Root, M.J., Nosco, D.L.**, 1982. In *Advances in Inorganic and Bioinorganic Reaction Mechanisms (1)*, pp. 269-389, Sykes, A. G., Ed.; Academic Press: London,.
- [311] **Baek, K.H., Cooper, R.L., and Holwerda, R.A.**, 1985. Stability of the Copper(II)-Sulfur Bond in Mercapto Amino Acid Complexes of [2,2',2''-tris(dimethylamino)triethylamine]copper(II) and [tris(2-pyridylmethyl)amine]copper(II), *Inorg. Chem.*, **24(7)**, 1077-1081.
- [312] **Que Jr., L., Tolman, W.B.**, 2002. Bis(μ -oxo)dimetal "Diamond" Cores in Copper and Iron Complexes Relevant to Biocatalysis, *Angew. Chem. Int. Ed.*, **41(7)**, 1114-1137.
- [313] **Ito, O., and Matsuda, M.**, 1979. Evaluation of Addition Rates of the Thiyl Radicals to Vinyl Monomers by Flash Photolysis. 2. Substituent Effect on Addition of Substituted Benzenethiyl Radicals to Methyl Methacrylate or Styrene, *J. Am. Chem. Soc.*, **101(19)**, 5732-5735.
- [314] **Ueda, A., Nagai, S.**, 1999. In *Polymer Handbook 4th Ed. Vol. 1*, P.II-97, Brandrup, J., Immergut, E. H., Grulke, E. A., Eds., Wiley-Interscience, New York.

- [315] **Ito, O., and Matsuda, M.**, 1979. Evaluation of Addition Rates of *p*-chlorobenzenethiyl Radical to Vinyl Monomers by Means of Flash Photolysis, *J. Am. Chem. Soc.*, **101(7)**, 1815-1819.
- [316] **Ito, O.**, 1999. S-Centred Radicals, in *The Chemistry of Free Radicals*, Ch 6, p 193, Ed. Alfassi, Z. B., Wiley-Interscience, New York.
- [317] **Nonaka H., Ouchi M., Kamigaito M., and Sawamoto M.**, 2001. MALDI-TOF-MS Analysis of Ruthenium(II)-Mediated Living Radical Polymerizations of Methyl Methacrylate, Methyl Acrylate, and Styrene¹, *Macromolecules*, **34(7)**, 2083-2088.
- [318] **Zammit M.D., Davis T. D., Haddleton D.M., and Suddaby K.G.**, 1997. Evaluation of the Mode of Termination for a Thermally Initiated Free-Radical Polymerization via Matrix-Assisted Laser Desorption Ionization Time-of-Flight Mass Spectrometry, *Macromolecules*, **30(7)**, 1915-1920.
- [319] **Kobayashi, S., and Higashimura, H.**, 2003. Oxidative Polymerization of Phenols Revisited, *Prog. Polym. Sci.*, **28(6)**, 1015-1048.
- [320] **Viersen, F.J., Challa, G., and Reedijk, J.**, 1990. Mechanistic Studies of the Oxidative Coupling Polymerization of 2,6-dimethylphenol: 1. Kinetics of Polymerization Catalysed by a Copper(II)-tmed Complex, *Polymer*, **31(7)**, 1361-1367.
- [321] **Demin, R.T., Swerdloff, M.D., and Rogic, M.M.**, 1981. Copper(II)-Induced Oxidations of Aromatic Substrates: Catalytic Conversion of Catechols to o-benzoquinones. Copper phenoxides as Intermediates in the Oxidation of Phenol, and a Single-Step Conversion of Phenol, Ammonia, and Oxygen into Muconic acid Mononitrile, *J. Am. Chem. Soc.*, **103(19)**, 5795-5804.
- [322] **Tkatchouk, E., Fomina, L., Rumsh, L., and Fomine, S.**, 2003. Role of (μ -Oxo)dicopper(III) Complexes in Oxidative Polymerization of Phenol. A DFT Study, *Macromolecules*, **36(15)**, 5607- 5612.
- [323] **Pintauer, T., Reinohl, U., Feth, M., Bertagnolli, H., and Matyjaszewski, K.**, 2003. Extended X-ray Absorption Fine Structure Study of Copper(I) and Copper(II) Complexes in Atom Transfer Radical Polymerization, *Eur. J. Inorg. Chem.*, **2003(11)**, 2082-2094,.
- [324] **Karlin, K.D., Wei, N., Jung, B., Kaderli, S., Niklaus, P., and Zuberbuehler, A.D.**, 1993. Kinetics and Thermodynamics of Formation of Copper-Dioxygen Adducts: Oxygenation of Mononuclear Copper(I) Complexes Containing Tripodal Tetradentate Ligands, *J. Am. Chem. Soc.*, **115(21)**, 9506-9514.
- [325] **Cheng, Z., Zhu. X., Zhou. N., and Lu. J.**, 2003. Living/Controlled Radical Autopolymerization of Styrene in the Presence of CuCl₂ and 2,2'-bipyridine, *J. Appl. Polym. Sci.*, **90(6)**, 1532-1538

- [326] **Berends, P.H., and Stephan, W. D.**, 1987. Toward Copper(II) Hemocyanin Models. 2. Synthesis and Characterization of Binuclear Copper(II) Complexes of a Heptadentate Ligand, *Inorg. Chem.*, **26(5)**, 749-754
- [327] **Faucher, S., and Zhu, S.**, 2004. Location of the Catalytic Site in Supported Atom Transfer Radical Polymerization, *Macromol. Rapid Commun.*, **25(10)**, 991–994.

AUTOBIOGRAPHY

Hümeýra Mert Balaban was born in Çorum in 1979. She graduated from Atatürk High School in 1997.

She graduated from Marmara University, Department of Chemistry Education Faculty in 2001 with a first degree. Then she was accepted as a M.Sc. student to İstanbul Technical University, Organic Chemistry, where she obtained M.Sc. degree in 2003.

She was registered as a Ph.D. student to Istanbul Technical University, Polymer Science and Technology Programme in 2003. During her Ph.D. studies she was supported by TUBITAK-BDP Programme through a doctoral fellowship. As part of this doctoral fellowship programme, she worked as a visiting Ph.D. student at the Polymer Chemistry Research Group, Department of Organic Chemistry in Carnegie Mellon University (U.S.A.) for 6 months.

She is co-author of the following 3 scientific papers published in international journals.

1. **H. Mert**, U. Tunca, G. Hızal Thiophenol derivatives as a reducing agent for in situ generation of Cu(I) species via electron transfer reaction in copper-catalyzed living/controlled radical polymerization of styrene, *Journal of Polymer Science: Part A: Polymer Chemistry*, 44, 5923-5932 (2006).
2. G. Hızal, U. Tunca, S. Aras, **H. Mert** Air-stable and recoverable catalyst for copper-catalyzed controlled/living radical polymerization of styrene; In situ generation of Cu(I) species via electron transfer reaction, *Journal of Polymer Science: Part A: Polymer Chemistry*, 44, 77-87 (2006).
3. A. Dağ, **H. Mert**, U. Tunca, G. Hızal Fructose as a reducing agent for in situ generation of Cu(I) species via electron transfer reaction in copper-catalyzed living/controlled radical polymerization of styrene, *IN PRESS*.

She has attended National and International Conferences with the following Proceedings.

- H. Mert, U. Tunca, G. Hızal “Tiyofenol ve Türevlerinin Stirenin Atom Transfer Radikal Polimerizasyonu Üzerine Etkisi” (Poster)

XVI. National Congress of Chemistry
Konya, Türkiye, Sept. 10-13, 2002

- H. Mert, U. Tunca, G. Hızal “The Effect of Thiophenol Derivatives on Atom Transfer Radical Polymerization (ATRP) of Styrene” (Poster)
The 5th International APME’5-2003 Conference,
Montreal, Canada, June 21-26, 2003
- H. Mert, U. Tunca, G. Hızal “‘*In situ*’ Cu (I) Formation in Atom Transfer Radical Polymerization (ATRP) by Phenol and Thiophenol Derivatives ” (Poster)
The 6th International APME’6-2005 Conference,
İstanbul, Türkiye, August 14-19, 2005
- H. Mert, U. Tunca, G. Hızal “Atom Transfer Radikal Polimerizasyon'da Fenol ve Tiyofenol Bileşikleri ile '*in situ*' Cu(I) Oluşumu” (Oral)
XIX. National Congress of Chemistry
Kuşadası, Türkiye, 30 Sept.- 4 Oct., 2005